The mechanism of action of novel therapies for use in Chronic Lymphocytic Leukaemia

Submission for the degree of Doctor of Philosophy

2007

Susan Louise Kohlhaas, BSc

The mechanism of action of novel therapies for use in Chronic Lymphocytic Leukaemia

Susan Kohlhaas, BSc

Chronic Lymphocytic Leukaemia (CLL) remains incurable and novel treatments are ugently required to combat this disease. The proteasome inhibitor bortezomib induces high levels of apoptosis *in vitro* in CLL patient samples, but clinical trials have been discouraging. In this study, bortezomib induced apoptosis in all CLL samples tested at nanomolar concentrations. However, incubation of CLL cells with red blood cells (RBCs) reduced the activity of bortezomib. These data imply that RBC uptake may reduce the activity of bortezomib *in vivo*.

TNF-related apoptosis inducing ligand (TRAIL) is an attractive cancer therapy because of its selectivity towards tumour cells. TRAIL and agonistic mAbs to two TRAIL receptors (TRAIL-R1 and TRAIL-R2) are in clinical trials. CLL cells are resistant to TRAIL but can be sensitised by pre-treatment with histone deacetylase inhibitors (HDACi). HDACi sensitised CLL cells to preparations of TRAIL that induce apoptosis through TRAIL-R1 but not through TRAIL-R2. In contrast, K562 cells, when pre-treated with HDACi, responded to preparations of TRAIL that induce apoptosis through TRAIL-R2. To confirm this, TRAIL receptor-selective mutants were generated and tested for specificity in cell lines. CLL cells, pre-treated with depsipeptide, responded only to the TRAIL-R1 mutant. These data confirm that CLL cells can be sensitised to TRAIL induced apoptosis primarily through TRAIL-R1 and that clinical trials in CLL should focus on HDACi in combination with preparations of TRAIL that induce apoptosis through TRAIL-R1.

Recent publications suggest that internalisation of CD95 and TNFR1 are required for induction of apoptosis. TRAIL-internalisation has not been widely studied. In this study, TRAIL-induced DISC formation was shown to occur at the plasma membrane, suggesting that TRAIL signalling is unlike other members of the TNF superfamily (CD95L and TNFα). Inhibiting TRAIL internalisation with hyperosmotic solution did not inhibit apoptosis induction, suggesting that internalisation is not important for TRAIL activity.

Acknowledgements

I would like to take this opportunity to thank my supervisors Gerry Cohen and Martin Dyer for their continued support and encouragement throughout my time at the MRC Toxicology Unit. I am incredibly grateful for the opportunities they have given me over the years to work on exciting projects. I would also like to thank Dr. Marion MacFarlane for her time, advice and assistance with all of my projects over the years. In addition, I would like to thank Luise Wheat for providing encouragement and advice whenever it was required. I would also like to thank Satoshi Inoue, Nick Harper, Andy Craxton, Xiao Ming Sun, Michelle Hughes, Mike Pinkoski, and Jim Embleton for discussions, advice and assistance.

I would like to thank Renata Walewska for collecting patient samples and data regarding patient samples, Aneela Majid for CLL mutation data, Mike Sutcliffe for molecular modelling, Johan Monbaliu and Roland DeCoster for kindly providing Figure A.2, Kul Sikand for assistance with confocal microscopy and Roger Snowden for assistance with flow cytometry. I would also like to thank those people who have made my time at the Unit more enjoyable, particularly, Clare Lawrence, Pauline Thornton, Theo Balasas, MartinaStagno d'Alcontres, Helen Barbour, Claudia Langlais, Davina Twiddy and Mike Butterworth.

I would like to thank my parents and family for their continued support and encouragement. I would like to thank Lizzie Butler for her patience during the time that I was writing up. I would also like to thank Matt Harris for his constant support during the time that I was in the lab and writing up.

Table of contents

List of Figures and Tables

Chapter 1

Chapter 2

Chapter 3

Abbreviations used in this thesis

AHP	autologous human plasma
ALT	alanine aminotransferase
ANOVA	Analysis of Variance
Apo2L	apoptosis inducing ligand 2
AST	aspartate aminotransferase
ATP	adenosine triphosphate
BSA	bovine serum albumin
CARD	caspase recruitment domain
Caspase	cystein aspartate protease
CD	cluster of differentiation
CD95L	CD95 ligand
c-FLIP	cellular FLICE-like inhibitory protein
CLL	Chronic Lymphocytic Leukaemia
DD	Death domain
DED	death effector domain
DISC	Death inducing signalling complex
DMEM	Dulbecco's Modified Eagle's Medium
DMSO	Dimethyl Sulphoxide
DNA	deoxyribose nucleic acid
dNTP	deoxyribose nucleotide triphosphate
DRs	Death receptors
E. coli	Escherichia coli
ECL	enhanced chemiluminesence
EDTA	ethylenediaminetetracetic acid
EEA-1	early endosomal antigen 1
ER	endoplasmic reticulum
FADD	Fas associated death domain containing protein
FCR	fludarabine, cyclophosphamide and rituximab in combination
FCS	Foetal Calf Serum
FITC	fluorescein
FSC	Forward Scatter
GTPase	guanine triphosphatase

HDADi	Histone Deacetylase inhibitor
HGS	Human Genome Sciences
HIS	Histidine-tagged TRAIL
HIS-LE	Histidine-tagged TRAIL with low levels of endotoxin
hrs	hours
IFN-γ	Interferon gamma
IKK	Ikappa B kinase
IL	Interleukin
IPTG	Isopropyl-D-thiogalactopyranoside
JNK	c Jun-NH2-terminal kinase
Li	Lithium
mAbs	monoclonal antibodies
mg	milligrams
MG132	z-leu-leu-leucinal
mins	minutes
Ml	millilitres
MRD	Minimal Residual Disease
NCI	National Cancer Institute
NEMO	NF-kappa B essential modulator
NF-κB	Nuclear Factor kappa B
Ng	nanogram
Ni-NTA	Nickel-NTA
NK	Natural Killer
OPG	osteoprotegrin
PAGE	polyacrylamide gel electrophoresis
PARP	poly-ADP-ribose protein
PBS	phosphate buffered saline solution
PCR	polymerase chain reaction
PE	phycoerythrin
PI	Propidium Iodide
PLADS	Pre-formed ligand assembly domains
PS	Phosphatidylserine
RBC	Red blood cell
RIP	receptor interacting protein

RNA	ribonucleic acid
ROS	reactive oxygen species
Rpm	revolutions per minute
RPMI	Roswell Park Memorial Institute
SDS	Sodium dodecyl sulphate
siRNAs	small interfering RNAs
SSC	Side Scatter
TBS	Tris Buffered Saline solution
TBS-Mt	TBS with 5% Marvel and 0.1% Tween 20
TBSt	TBS with 0.1% Tween20
TMRE	tetramethylethylester
TNF	Tumour Necrosis Factor
TNFR1	TNF Receptor 1
TNFR2	TNR Receptor 2
TNFα	TNF alpha
TRADD	TNFR1 associated Death Domain containing protein
TRAF-2	TNF receptor associated factor 2
TRAIL	TNF related apoptosis inducing ligand
TRAIL-R1	TRAIL receptor 1
TRAIL-R2	TRAIL receptor 2
TRAIL-R3	TRAIL receptor 3
TRAIL-R4	TRAIL receptor 4
u/s	unstimulated
WCC	White cell count
ZAP70	Zeta Associated protein 70
z-VAD.fmk	benzyloxycarbonyl-Val-Ala-Asp (OMe) fluoromethylketone
µg	micrograms
µM	micromolar
µm	micron

Chapter 1: Introduction

Chapter 1: Introduction

1.1 Chronic Lymphocytic Leukaemia

Chronic Lymphocytic Leukaemia (CLL) is the most common form of leukaemia in the western world. It is an incurable disease that affects more men than women. Like most other forms of cancer, it is a disease of the elderly with a median age at diagnosis of 65. There is a genetic element to the disease as it is common for siblings to present with CLL, but further studies are required to investigate what underlies this genetic pre-disposition (Yuille, Matutes et al. 2000; Sellick, Catovsky et al. 2006). Interestingly, CLL tends to affect western populations more than eastern societies. Environmental factors are thought to play a minimal role in disease formation (Brandt 1985).

In the absence of better prognostic markers, the prognosis of CLL is largely reliant on disease stage with early stage patients often not requiring treatment and living as long as age-matched controls, and late stage patients requiring urgent treatment with a life expectancy of as little as 18 months after disease presentation (Binet, Auquier et al. 1981). The characteristics of different disease stages according to the Rai (Rai and Montserrat 1987) and Binet (Binet, Auquier et al. 1981) staging systems are summarized in Table 1.1.

Table 1.1: Staging systems of CLL

Staging system	Stage	Risk	Clinical Features	Median Survival	Reference
Binet Stages	A	Good-prognosis	No anemia or thrombocytopenia, less than three involved lymphoid areas	12 yrs	Binet et al 1981
	B	Intermediate-prognosis	No anemia or thrombocytopenia, more than three involved lymphoid areas	5 yrs	Binet et al 1981
	C	Poor-prognosis	Anemia and low platelet count	2 yrs	Binet et al 1981
Rai Stages	0	Low-risk	Lymphocytosis in blood and marrow	10 yrs	Rai et al 1987
	I/II	Intermediate-risk	Lymphocytosis, lymphadenopathy, splenomegaly and/or hepatomegaly	7 yrs	Rai et al 1987
	III/IV	High-risk	Lymphocytosis , anaemia, thrombocytopenia	1.5 yrs	Rai et al 1987

The clinical course of CLL is staged according to the Rai or Binet system with earlier stages correlating with less progressive disease in most cases (Binet, Auquier et al. 1981; Rai and Montserrat 1987). The clinical characteristics of CLL include an elevated number of malignant lymphocytes sometimes accompanied by lymphadenopathy and splenomegaly, anaemia and thrombocytopenia (Binet, Auquier et al. 1981; Rai and Montserrat 1987). Most patients remain asymptomatic, even in cases with advanced diseases. Symptoms include

weakness, fatigue, night sweats and fever as well as autoimmune diseases and an increase in infections, which become difficult to manage and are often the cause of death. In late stages of the disease, therapy is essential to manage many of the recurring symptoms associated with CLL.

There are currently limited treatment options available to patients with CLL. Purine nucleoside analogues such as fludarabine or fludarabine in combination with cyclophosphamide tend to be first line therapy agents in the UK and response rates are generally favourable with approximately 95% overall response rates (Elter, Hallek et al. 2006). Despite a good response to fludarabine as a first line treatment in CLL, there is no difference in survival of patients that have received fludarabine compared with patients that have remained untreated. Increasingly, combination regimens such as FCR (fludarabine, cyclophosphamide and rituximab) are being used and have shown promise in CLL (Keating, O'Brien et al. 2005). For refractory CLL, alemtuzumab/CAMPATH-1H (a monoclonal antibody to CD52) or allogenic bone marrow transplantation has shown some promise (Dreger and Montserrat 2002; Fiegl, Falkner et al. 2006). However, relapse is always incurable and acquired resistance to fludarabine is an issue that has not been overcome. Therefore, novel therapies are required to achieve prolonged survival after relapse.

CLL is characterised by the clonal expansion of an abnormal population of B-lymphocytes that display an unusual range of molecules on the cell surface including co-expression of CD5, CD23, CD19, CD20 and low surface IgM (Caligaris-Cappio and Hamblin 1999). Accumulation of CLL cells occurs primarily in the peripheral blood and bone marrow but also secondary lymphoid organs such as the spleen and lymph nodes.

As CLL cells are arrested in the G_0 phase of the cell cycle, they were originally thought to accumulate as a result of failure to undergo apoptosis rather than excessive proliferation. This is demonstrated by their high protein expression levels of Mcl-1 and Bcl-2 (Packham and Stevenson 2005). CLL cells rapidly undergo spontaneous apoptosis when purified from whole blood and cultured in media suggesting strong environmental influences in its progression and survival (Collins, Verschuer et al. 1989). The level of spontaneous apoptosis is patient

dependent and low spontaneous apoptosis has been associated with good prognosis cytogenetics (Jahrsdorfer, Wooldridge et al. 2005). Interestingly, the presence of defined "proliferation" centres in the bone marrow suggests that CLL cells can rapidly proliferate under certain circumstances, most likely due to unknown environmental factors within the bone marrow microenvironment (Schmid and Isaacson 1994). This is supported by data showing that increased survival of CLL cells occurs when they are cultured in contact with bone marrow stromal layers, in the presence of "nurse" cells or treated with a range of cytokines (IL-4, IFNα, IFNγ, IL-8 or IL-13) (Jewell, Lydyard et al. 1995; Panayiotidis, Jones et al. 1996; Burger, Tsukada et al. 2000).

In the past CLL has been considered as one disease by morphology and immunophenotype but it has extremely heterogeneous outcomes associated largely with mutational status as defined by the presence of *IGHV* mutations and other prognostic factors such as CD38 or ZAP70 expression (Damle, Wasil et al. 1999; Oscier, Gardiner et al. 2002; Wiestner, Rosenwald et al. 2003). Table 1.2 shows some common prognostic markers that are used in CLL. In recent years, much effort has been placed on determining new prognostic factors that are relatively easy to assess diagnostically in CLL patient samples, but the most common ones used are in Table 1.2.

Table 1.2: Common prognostic markers used in CLL.

Prognostic Factors	% of all CLL	Prognosis	Reference
VH mutated	60	Associated with increased survival	Oscier et al 2002
VH unmutated	40	Associated with decreased survival	Oscier et al 2002
del 17q	7	Associated with poor survival and drug resistance	Carter et al 2006
trisomy 12	20	Associated with aggressive disease and atypical morphology	Merup et at 1997
del 11q	13-20	Associated with advanced clinical stage	Fegan et al 1995
del 13q	50	Associated with decreased survival	Starostik et al 1999
>30% CD38+ cells	correlates with high disease stage	Associated with requirement for continuous chemotherapy	Damle et al 1999
high ZAP70 expression	correlates with unmutated *IGHV* genes	Associated with inferior clinical outcome	Weistner et al 2003

The origin of CLL cells with unmutated *IGHV* genes are generally thought to be pre-germinal naïve B cells following an aggressive course, whereas mutations in *IGHV* gene segments would suggest that these CLL cells stem from the memory germinal centre and are antigen experienced, more mature and follow a benign course (Chiorazzi, Rai et al. 2005). Gene

expression microarray studies have suggested that the two classes (unmutated and mutated *IGHV* genes) of CLL should be categorised as one disease with two separate entities (Rosenwald, Alizadeh et al. 2001), but many feel that with two different cells of origin, CLL should be classed as two separate diseases and treated differently (Hamblin 2002; Chiorazzi, Rai et al. 2005).

The presence of cytogentic abnormalities is not uniform in CLL but there are several common abnormalities that are associated with the disease, the most common being the 13q14 deletion present in about 55 % of all cases. This abnormality is associated with a good prognosis (Starostik, Manshouri et al. 1998; Starostik, O'Brien et al. 1999; Dohner, Stilgenbauer et al. 2000). Other common abnormalities include deletion of 11q22-23 (18 % of all cases) affecting the *ATM* gene and associated with an unfavourable prognosis (Starostik, Manshouri et al. 1998; Dohner, Stilgenbauer et al. 2000; Austen, Powell et al. 2005), deletion of 17p13 (Dohner, Stilgenbauer et al. 2000)(7 % of all cases) affecting the p53 gene and associated with a poor prognosis and resistance to chemotherapeutic drugs (Carter, Lin et al. 2006) and trisomy 12 (16 % of all cases) associated with a poor prognosis (Juliusson and Gahrton 1987; Krober, Seiler et al. 2002).

Patients with unmutated *IGHV* genes have a much worse prognosis than those with mutated *IGHV* genes. As most cases of CLL can remain asymptomatic and stable there is a general attitude of "wait and see" when it comes to the treatment of CLL. However with an increasing number of less toxic and possibly more effective treatments, this idea is starting to waver. Current treatment strategies in CLL depend upon disease stage and prognosis and aim at achieving minimal residual disease (MRD), but new treatment options are urgently required to combat acquired resistance to existing therapies.

1.2 Apoptosis and Cancer

Apoptosis or programmed cell death is essential for an organism to undergo normal development and to remove damaged cells. It was originally characterised by observations in morphological changes which entailed nuclear condensation and membrane blebbing into

apoptotic bodies that allowed surrounding macrophages and NK cells to engulf the apoptotic cell, thus avoiding inflammation (Kerr, Wyllie et al. 1972).

Problems occur when the process of apoptosis is dysregulated. Apoptosis that occurs too frequently can lead to neurological disorders such as Huntington's disease. In contrast, the accumulation of damaged cells due to a failure to undergo apoptosis can lead to certain types of cancer, including CLL. Therefore, much effort is placed on understanding the process of apoptosis and its relation to disease. In the last decade notable progress has been made in identifying molecular changes that occur within a cell during the process of apoptosis.

1.3 Cysteine aspartate proteases (caspases)

Caspases are a highly conserved family of proteins that are essential to orchestrate apoptosis. They were originally identified because of their high sequence homology to the ced3 gene, known to orchestrate cell death in *C. elegans* (Yuan, Shaham et al. 1993). Under normal non-apoptotic conditions, caspases are synthesised and maintained in their inactive states (unprocessed zymogens). All caspases contain an N-terminal pro-domain, a large subunit and a small subunit. Once an apoptotic signal is initiated caspases can be activated by processing of their inactive zymogens to enzymatically active heterotetrameric fragments, containing 2 large and 2 small subunits (Nicholson 1999; Fuentes-Prior and Salvesen 2004).

There are currently 14 mammalian caspases that have been identified and the structures of each caspase is shown in Figure 1.1 and they can be divided into 3 groups, the initiator caspases (containing a large pro-domain often with a caspase recruitment domain (CARD) or death effector domain (DED)), the executioner caspases (containing a small pro-domain) and the caspases that are thought to play a role in inflammation (Nicholson 1999; Fuentes-Prior and Salvesen 2004). Caspases recognise and cleave tetrapeptide motifs with high specificity within their substrates and have high specificity for aspartic acid residues in the P1 position although specificity at other positions can vary (Nicholson 1999; Fuentes-Prior and Salvesen 2004). After activation they can go on to cleave other caspases and caspase-substrates and eventually induce membrane blebbing and apoptosis (Nicholson 1999; Slee, Adrain et al. 1999; Fuentes-Prior and Salvesen 2004).

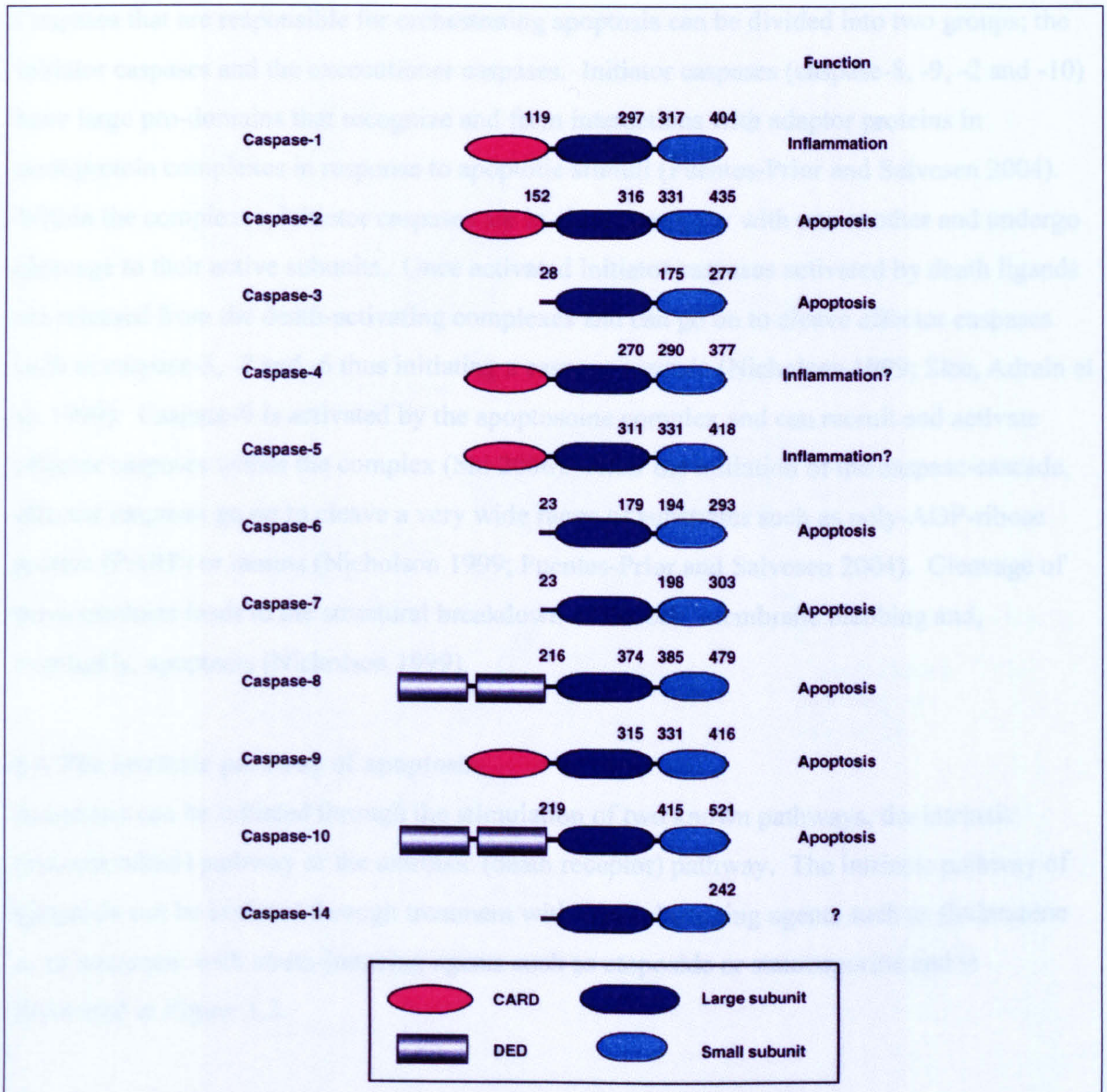

Figure 1.1: The structure of the caspase family. All caspases contain a C-terminal small catalytic subunit (light blue) and a large subunit (dark blue), however caspases can be split into three groups. Group I represents caspases that are thought to play a role in immune function, while Group II contains initiator caspases and Group III contains excecutioner caspases. Initiator caspases can bind to Death Signalling structures through their CARD shown in pink or their DED shown in grey and initiate apoptosis. In contrast, excecutioner caspases are cleaved by activated initiator caspases and go on to cleave important structural molecules that lead to the breakdown of the cell. This figure was taken from Creagh, Conroy, Martin, 2003.

Caspases that are responsible for orchestrating apoptosis can be divided into two groups; the initiator caspases and the excecutioner caspases. Initiator caspases (caspase-8, -9, -2 and -10) have large pro-domains that recognize and form interactions with adaptor proteins in multiprotein complexes in response to apoptotic stimuli (Fuentes-Prior and Salvesen 2004). Within the complexes, initiator caspases are in close proximity with one another and undergo cleavage to their active subunits. Once activated initiator caspases activated by death ligands are released from the death-activating complexes and can go on to cleave effector caspases such as caspase-3, -7 and -6 thus initiating a caspase-cascade (Nicholson 1999; Slee, Adrain et al. 1999). Caspase-9 is activated by the apoptosome complex and can recruit and activate effector caspases within the complex (Shi 2006). After the initiation of the caspase-cascade, effector caspases go on to cleave a very wide range of substrates such as poly-ADP-ribose protein (PARP) or lamins (Nicholson 1999; Fuentes-Prior and Salvesen 2004). Cleavage of these products leads to the structural breakdown of the cell, membrane blebbing and, eventually, apoptosis (Nicholson 1999).

1.4 The intrinsic pathway of apoptosis

Apoptosis can be initiated through the stimulation of two known pathways, the intrinsic (mitochondrial) pathway or the extrinsic (death receptor) pathway. The intrinsic pathway of apoptosis can be initiated through treatment with DNA damaging agents such as fludarabine or by treatment with stress-inducing agents such as etoposide or staurosporine and is illustrated in Figure 1.2.

The intrinsic pathway of apoptosis is regulated by the Bcl-2 family of proteins. This family of proteins is made up of pro- and anti-apoptotic proteins and can be divided into three groups. The anti-apoptotic proteins consist of Bcl-2, Bcl-X_L, A1/Bfl-1, Bcl-w, Boo/Diva/Bcl-B and Mcl-1 and they contain BH1-4 domains as well as a transmembrane domain (Marsden and Strasser 2003). CLL cells do not express high levels of the Bcl-X_L protein, but express high levels of Mcl-1 and Bcl-2, thus providing a possible mechanism for their failure to undergo apoptosis *in vivo* (Hanada, Delia et al. 1993; Kitada and Reed 2004; Packham and Stevenson 2005).

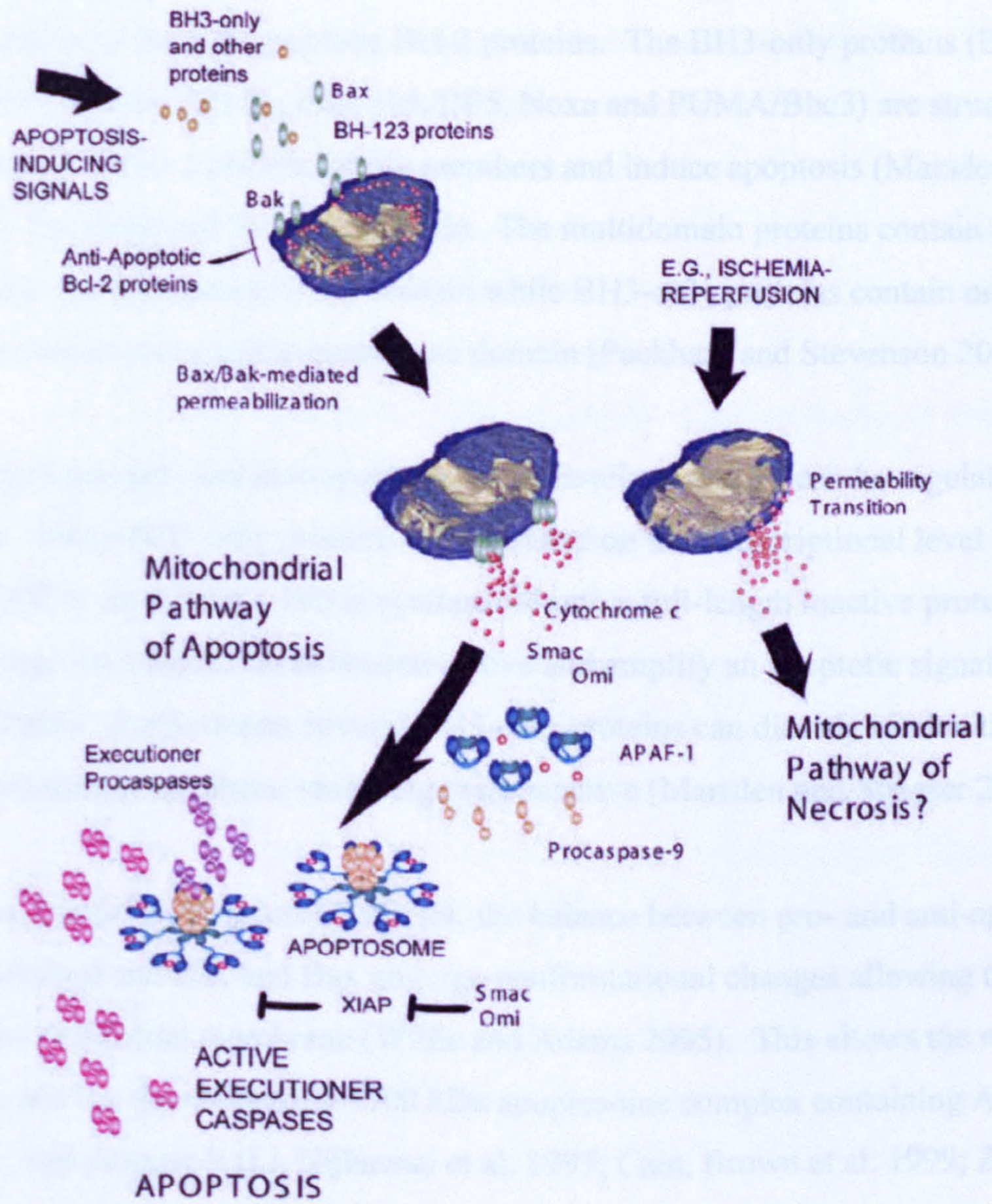

Figure 1.2: The mitochondrial pathway to apoptosis. Upon stimulation with an apoptosis inducing signal, the balance between pro- and anti-apoptotic mitochondrial proteins is shifted in the favour of apoptosis and Bak and Bax form pores in the mitochondrial membrane. This causes the release of cytochrome c which then interacts with APAF-1 and procaspase-9 to form an apoptosome complex. Within the apoptosome, caspase-9 is cleaved and released to cleave effector caspases which then go on to induce apoptosis. This figure was taken from Green 2005.

Pro-apoptotic Bcl-2 protein family members can be further divided into two subgroups; the multi-domain proteins (Bax, Bak, Bok/Mtd, Bcl-x_S and Bcl-G_L) are pro-apoptotic and are structurally similar to the anti-apoptotic Bcl-2 proteins. The BH3-only proteins (Bim/Bod, Bad, Bid, Bik/Nbk, Bmf, Bcl-G_S, Blk, Hrk/DP5, Noxa and PUMA/Bbc3) are structurally divergent from other Bcl-2 protein family members and induce apoptosis (Marsden and Strasser 2003; Packham and Stevenson 2005). The multidomain proteins contain several BH1-3 domains and a transmembrane domain while BH3-only proteins contain only a BH3 domain and, in some cases, a transmembrane domain (Packham and Stevenson 2005).

The balance between pro- and anti-apoptotic Bcl-2 family members can be regulated on several levels. Many BH3-only proteins are regulated on the transcriptional level (Marsden and Strasser 2003). In addition, Bid is synthesised into a full-length inactive protein that requires cleavage (by caspase-8) to become active and amplify an apoptotic signal (Marsden and Strasser 2003). Furthermore, several BH3-only proteins can directly bind with pro-apoptotic Bcl-2 family members, rendering them inactive (Marsden and Strasser 2003).

When cells are treated with apoptotic stimuli, the balance between pro- and anti-apoptotic proteins is disturbed and Bak and Bax undergo conformational changes allowing them to form pores in the mitochondrial membrane (Willis and Adams 2005). This allows the release of cytochrome c and the formation of a ~700 kDa apoptosome complex containing Apaf-1, cytochrome c, and caspase-9 (Li, Nijhawan et al. 1997; Cain, Brown et al. 1999; Zou, Li et al. 1999; Waterhouse, Ricci et al. 2002; Shi 2006). The enzymatic activity of caspase-9 is greatly increased within the apoptosome complex and this allows caspase-9 to be cleaved to its p35 form. Once activated, caspase-9 is able to recruit other caspases (caspase-3 and -7) into the apoptosome complex and activate and release them from the complex thus initiating a caspase cascade (Shi 2006). Once activated, caspase-3 is believed to cleave caspase-9 to its p37 form. Once the mitochondrial membrane is no longer intact, the cell is committed to undergo apoptosis.

1.5 The extrinsic pathway of apoptosis

The extrinsic pathway of apoptosis can be initiated by ligands (CD95/CD95L, Tumour Necrosis Factor (TNF) and TNF-Related Apoptosis-Inducing Ligand (TRAIL)) and monoclonal antibodies (mAbs) that bind to members of the death receptor family (CD95/Fas, TNF-R1, TRAIL-R1 or TRAIL-R2). A model of this pathway is shown in Figure 1.3. In the extrinsic pathway of apoptosis, antibody or trimeric ligand binds to a trimeric receptor complex thus exposing the Death Domain (DD) of the receptor (Chan, Chun et al. 2000; Sartorius, Schmitz et al. 2001; Clancy, Mruk et al. 2005). FADD is recruited to the DD of the ligand-receptor complex thus exposing the DED of FADD. Caspase-8 and, in some circumstances, caspase-10 has been shown to be recruited to the ligand-receptor DISC complex through binding of the FADD DED with the caspase DED (Boldin, Goncharov et al. 1996; Muzio, Chinnaiyan et al. 1996; Ashkenazi and Dixit 1999). This step can be inhibited by the presence of c-FLIP, which can bind to FADD through its DED but does not have proteolytic activity and cannot induce apoptosis (Hu, Vincenz et al. 1997; Irmler, Thome et al. 1997; Srinivasula, Ahmad et al. 1997). Some groups have suggested that c-FLIP is an activator of the DISC, but this has only been shown by overexpression (Han, Chaudhary et al. 1997; Shu, Halpin et al. 1997; Chang, Xing et al. 2002).

Once caspase-8 is bound to FADD within the DISC, it can activate itself through an induced proximity model (Ashkenazi and Dixit 1999; Sartorius, Schmitz et al. 2001). Caspase-8 is cleaved to its catalytically active p18 form and released from the DISC. Once activated, caspase-8 can cleave and activate caspase-3, -9, -6 and -7 thus initiating a caspase-cascade and ultimately induce apoptosis.

In some cell types, the extrinsic apoptotic pathway may activate the intrinsic pathway and create an amplification loop (Scaffidi, Schmitz et al. 1999). These cell types are known as Type II cells and require the cleavage of the BH3-only protein Bid to its truncated form tBid which then initiates the mitochondrial apoptotic pathway.

The distinction between Type I (that do not require the cleavage of Bid to tBid to undergo apoptosis) and Type II cells (that require Bid cleavage to tBid to undergo apoptosis) has

primarily been made using CD95L and needs to be further characterised with other death receptor ligands such as TNF and TRAIL. CLL cells appear to display characteristics similar to those of Type II cells such as, less extensive and less rapid DISC formation although this has not been extensively shown.

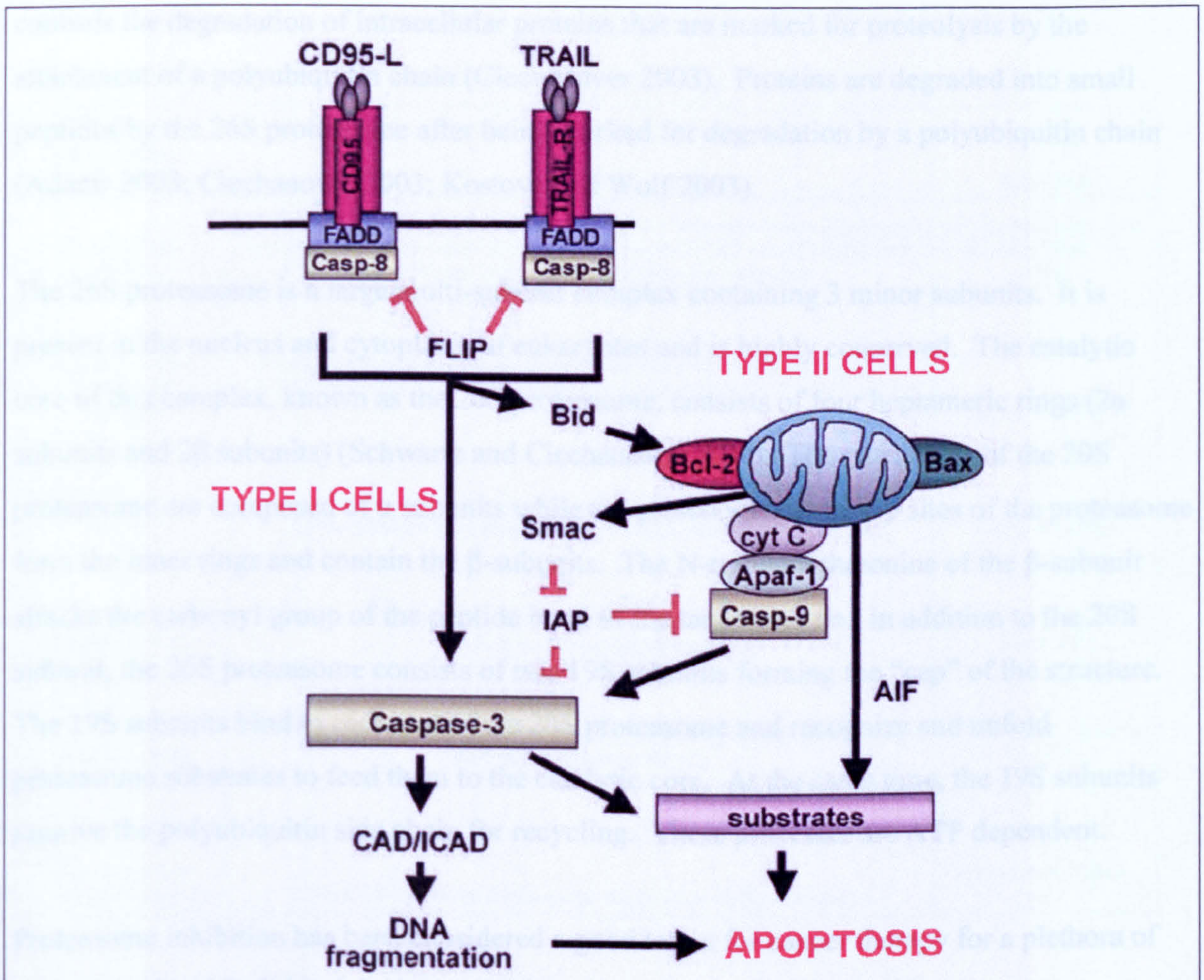

Figure 1.3: The Death Receptor pathway to apoptosis. TRAIL or CD95L bind to their respective receptors in the form of a trimer causing the DD of the cytoplasmic end of the receptor to become exposed. As a result the DD of FADD allows recruitment of FADD into the DISC to form a complex with the receptors. Through FADD homology domains or DEDs procaspase-8 is recruited into the DISC and activated, a step that c-FLIP can inhibit. Caspase-8 is released from the DISC and can cleave caspase-3 to initiate a caspase cascade. In Type II cells Bid cleavage to tBid by caspase-8 is a requisite step to initiate a mitochondrial amplification loop to release cytochrome c and activate the intrinsic apoptotic pathway. This figure was adapted from Fulda and Debatin, 2006.

1.6 The proteasome as a target for cancer therapy

The function of the ubiquitin-proteasome pathway is to monitor protein quality and control the degradation of misfolded and unfolded proteins (Ciechanover 2003). Therefore, proteasome integrity is essential for the maintenance of the cell. Under normal conditions, the proteasome controls the degradation of intracellular proteins that are marked for proteolysis by the attachment of a polyubiquitin chain (Ciechanover 2003). Proteins are degraded into small peptides by the 26S proteasome after being marked for degradation by a polyubiquitin chain (Adams 2003; Ciechanover 2003; Kostova and Wolf 2003).

The 26S proteasome is a large multi-subunit complex containing 3 minor subunits. It is present in the nucleus and cytoplasm of eukaryotes and is highly conserved. The catalytic core of this complex, known as the 20S proteasome, consists of four heptameric rings (2α subunits and 2β subunits) (Schwartz and Ciechanover 1999). The outer rings of the 20S proteasome are composed of α subunits while the proteolytically active sites of the proteasome form the inner rings and contain the β-subunits. The N-terminal threonine of the β-subunit attacks the carbonyl group of the peptide bond of the target protein. In addition to the 20S subunit, the 26S proteasome consists of two 19S subunits forming the "cap" of the structure. The 19S subunits bind to each end of the 20S proteasome and recognize and unfold proteasome substrates to feed them to the catalytic core. At the same time, the 19S subunits remove the polyubiquitin side chain for recycling. These processes are ATP dependent.

Proteasome inhibition has been considered a good target for cancer therapy for a plethora of reasons outlined in Table 1.3 (Adams 2004). There are many reasons why proteasome inhibitors may be selective to transformed cells compared with normal cells. For example, many transformed cell types have a high proliferative index and therefore a high protein turnover, as more than 80 % of the cells proteins are degraded by the proteasome, proteasome inhibitors may target these cells to a greater extent than normal cells (Adams 2004; Adams 2004). In addition, many cancer cells have constitutive NF-kB activation (Keutgens, Robert et al. 2006; Pacifico and Leonardi 2006) and by targeting the NF-kB pathway, proteasome inhibitors induce apoptosis in tumour cells selectively (Luo, Kamata et al. 2005). Moreover,

many transformed cells, such as CLL, have high levels of anti-apoptotic Bcl-2 proteins such as Mcl-1 or Bcl-2 (Packham and Stevenson 2005). Proteasome inhibitors can disrupt the balance between the pro- and anti- apoptotic proteins by inducing upregulation (either through transcription or stabilisation) of BH3-only proteins, such as Noxa or Bik/NBK (Qin, Ziffra et al. 2005; Zhu, Zhang et al. 2005; Perez-Galan, Roue et al. 2006).

Table 1.3: Anti-tumour effects of proteasome inhibitors.

General Mechanisms of Action	Evidence	Reference
Blocks NF-kB activation	bortezomib inhibited NF-kB reporter activity at low concentrations in Squamous cell carcinoma, expression of NF-kB family members p65 and p50 decreased after treatment with bortezomib in renal cell carcinoma	An, Sun et al 2004 and Sunwoo, Chen et al 2001
Upregulate BH3-only pro-apoptotic proteins	Proteasome inhibitors induce Noxa transcription in melanoma and myeloma cell lines and RNAi against Noxa blocks the apoptotic activity of bortezomib by up to 50 %	Qin, Ziffra et al 2005
Cause cell cycle arrest	bortezomib induces cell cycle arrest in Hodgkin lymphoma cell lines	Zheng et al 2004
Induces ER stress	proteasome inhibitors induce a misfolded protein response and ROS through ER stress, mechanism not clear	Fribley, Zeng and Wang 2004
Generates ROS	bortezomib induced ROS generation in primary mantle cell lymphoma cells that pre-ceded apoptosis induction	Perez-Galan, Rone et al 2006
targets cells with high protein turnover	80 % of proteins in the cells undergo degradation via the proteasome	Adams 2002, Adams 2004

In general proteasome inhibitors have been found to upregulate or stabilise several pro-apoptotic molecules such as Bax, Noxa and Bim and downregulate anti-apoptotic pathways such as NFκB (Almond and Cohen 2002; Voorhees, Dees et al. 2003; Qin, Ziffra et al. 2005; Fribley, Evenchik et al. 2006; Mitsiades, Mitsiades et al. 2006; Perez-Galan, Roue et al. 2006). In addition, the inhibition of the proteasome may activate Endoplamic Reticulum (ER) stress pathways that, for unknown reasons, activate the intrinsic apoptotic pathway (Fribley and Wang 2006). However, the mechanisms of proteasome inhibition-induced apoptosis are cell-

type dependent and due to the general importance of the proteasome in maintaining healthy cells, may effect apoptotic and stress pathways on many levels.

1.7 Bortezomib/PS-341/Velcade as a therapeutic agent in cancer

There are several classes of proteasome inhibitors that have different effects on proteasome inhibition. However, many proteasome inhibitors are not suitable for clinical use because they are either irreversible or inhibit calpains and cathepsins (Tsubuki, Saito et al. 1996). One proteasome inhibitor that was originally identified as a good potential therapy by a screen of 60 cell lines at the NCI is bortezomib (Adams 2002). It has shown promise as a therapeutic agent against many types of primary tumour cells including CLL *in vitro*. Bortezomib is a peptide boronic acid proteasome inhibitor that specifically, but reversibly, inhibits the chymotryptic site of the 20S proteasome.

The specific role of proteasome inhibitors as therapeutic agents in CLL is still unknown, although there are many studies that document the activity of proteasome inhibitors as apoptotic agents. Work with the apoptosome and Bax have suggested that proteasome inhibitors induce apoptosis through the mitochondrial apoptotic pathway in CLL (Almond, Snowden et al. 2001; Dewson, Snowden et al. 2003); however, this has not been documented with bortezomib. Bortezomib has been widely tested on various tumour cells and is found to be effective in most (Adams 2002). Although the exact mechanism of action of bortezomib is unclear, several recent publications have defined its mechanism in various cell types.

Pre-clinical studies have found bortezomib and other proteasome inhibitors to be very effective at killing CLL cells *in vitro*. Despite numerous studies investigating the efficacy of bortezomib in CLL (Pahler, Ruiz et al. 2003; Kelley, Alkan et al. 2004), very little work has been done on its specific mechanism of action. Although proteasome inhibitors, including bortezomib, are thought to be selective towards transformed cells, the mechanism of this selectivity is not entirely clear. It is thought to arise because transformed cells tend to proliferate at a higher rate than normal cells thus turning over proteins more rapidly. However *in vitro* results of bortezomib activity in CLL would suggest that this is not necessarily the case. CLL cells were found to be 10 times more sensitive to proteasome inhibitors than

normal lymphocytes (Chandra, Niemer et al. 1998), suggesting a degree of selectivity towards transformed cells, but independent of their proliferative index.

Several studies have suggested that the stabilisation of BH3 only proteins, such as Bik or Bim, is a requirement for bortezomib induced apoptosis (Nikrad, Johnson et al. 2005). However it is difficult to attribute bortezomib-induced apoptosis to stabilisation of a specific protein without using siRNAs, which is not very effective in primary cells. Thus, a major difficulty in studying CLL concerns the lack of a good *in vitro* model that allows manipulation of specific genes. As yet there is no good mouse model for this disease.

Another study suggested that generation of reactive oxygen species (ROS) could contribute to bortezomib-induced apoptosis in primary mantle cell lymphoma cells (Perez-Galan, Roue et al. 2006). However ROS generation occurred at least 4 hours after treatment with bortezomib and this group did not suggest a mechanism for ROS generation or a link of generation of ROS to apoptosis induction through the mitochondrial pathway of apoptosis. There have also been suggestions of a role for ER stress, causing an unfolded protein response, in bortezomib-induced apoptosis in pancreatic cancer, multiple myeloma and head and neck squamous cell carcinoma cells and that caspase-9 and -2 and possibly caspase-4 is involved in this pathway (Fribley, Zeng et al. 2004; Hitomi, Katayama et al. 2004; Nawrocki, Carew et al. 2005; Cheung, Lynn Kelly et al. 2006; Obeng, Carlson et al. 2006). However, this pathway has not been well characterised and has not been identified in CLL as a mechanism for bortezomib-induced apoptosis.

In clinical trials, bortezomib has shown most promise in multiple myeloma and has been approved for use by the U.S. Food and Drug Administration (Kane, Farrell et al. 2006). It is also in clinical trials for use in many solid tumour malignancies and mantle cell lymphoma, follicular lymphoma and CLL. Toxicity has been severe in some cases, the most severe toxicity being; cardiac failure, peripheral neuropathy, neurotoxicity, thrombocytopenia, and tumour lysis syndrome (Agterof and Biesma 2005; Jaskiewicz, Herrington et al. 2005; Lonial, Waller et al. 2005; Van Regenmortel, Van de Voorde et al. 2005; Caravita, de Fabritiis et al. 2006; Faderl, Rai et al. 2006; Richardson, Briemberg et al. 2006; Richardson, Mitsiades et al.

2006; Voortman and Giaccone 2006). Only one large study has been reported in CLL and toxicity was manageable in the majority of patients. However clinical responses were discouraging (Faderl, Rai et al. 2006). No complete or partial responses were reported. However biological activity of the drug was observed and manifested itself in the form of reduced WCC and lymph node sizes (Faderl, Rai et al. 2006). No work has currently been undertaken to investigate why bortezomib is unsuccessful in clinical trials in CLL but effective at killing the cells at low concentrations *in vitro*.

1.8 The TNF superfamily

The TNF superfamily is a growing family of cytokines that initiate survival, differentiation and apoptotic signals within a cell through binding to their respective receptors and activating specific pathways (Hehlgans and Pfeffer 2005). Members of the TNF superfamily often have more than one receptor and, upon ligand-receptor binding, can recruit adaptor proteins to specific complexes within the cell and initiate survival signals, via the NF-κB pathway (Gaur and Aggarwal 2003), or death signals via the extrinsic apoptotic pathway (Gaur and Aggarwal 2003). Figure 1.4 depicts the currently known members of the TNF superfamily of ligands and their respective receptors.

TNF superfamily receptors vary structurally depending on their functions. For example, Death Receptors (DRs) contain functioning DDs that, once stimulated with ligand, can recruit and bind DD containing adaptor molecules such as TRADD or FADD (Chinnaiyan, O'Rourke et al. 1996; Kischkel, Lawrence et al. 2000), thus forming an apoptosis-initiating DISC (Kischkel, Hellbardt et al. 1995; Boldin, Goncharov et al. 1996; Muzio, Chinnaiyan et al. 1996; Medema, Scaffidi et al. 1997). TNFR1, CD95, TRAIL-R1 and TRAIL-R2 are the most well characterised DRs and have been implicated as potential therapeutic agents. However, because of problems with toxicity (Feinberg, Kurzrock et al. 1988; Ogasawara, Watanabe-Fukunaga et al. 1993), TRAIL is the only of these family members that remains viable for therapeutic exploitation (Ashkenazi, Pai et al. 1999).

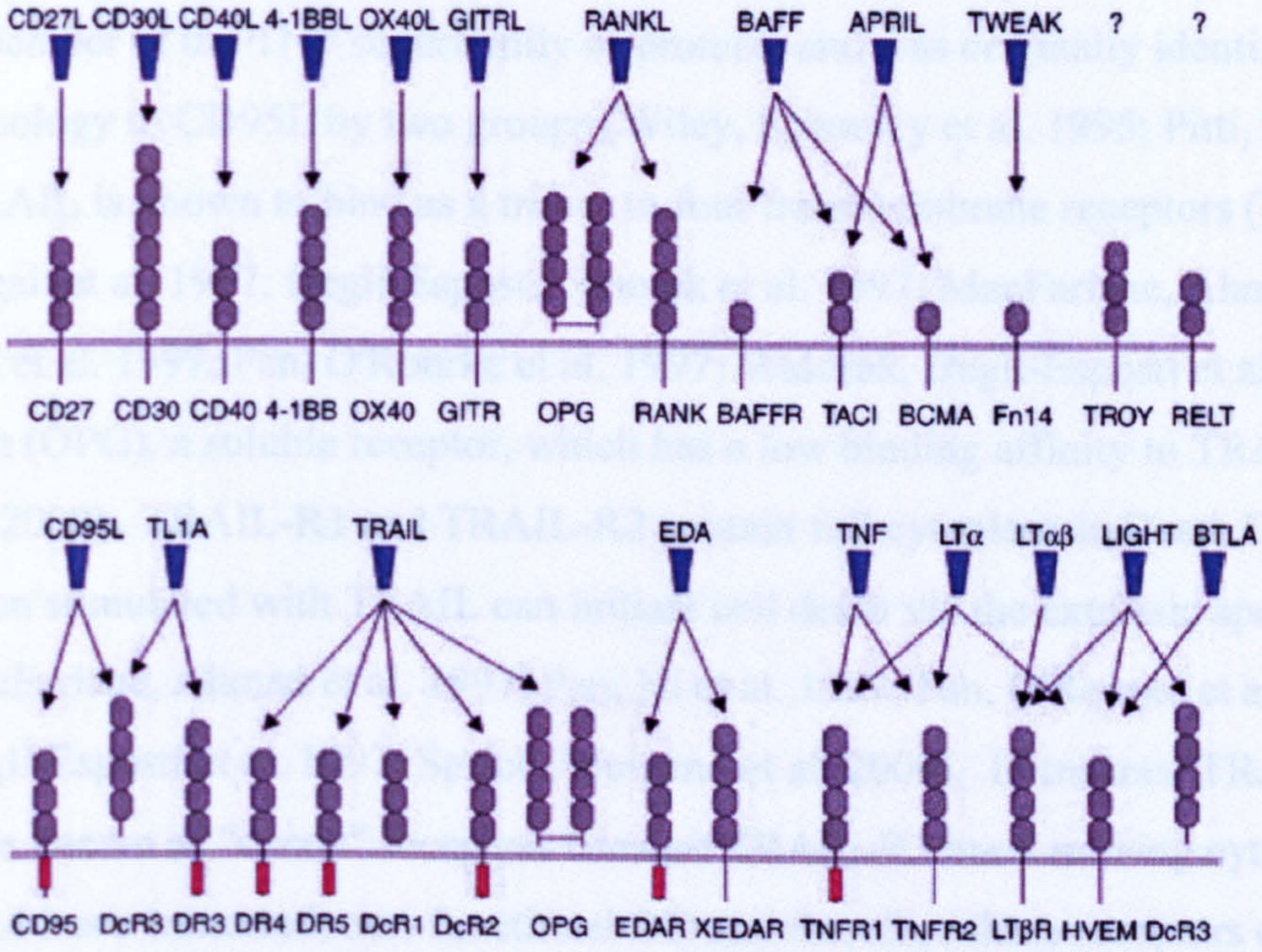

Figure 1.4: Members of the TNF superfamily. TNF family members are shown ranked by chromosomal position. Arrows indicate which receptor each family member can bind. The red cylinder indicates the presence of a death domain. Some common survival and apoptotic pathways that are activated by binding to adaptor molecules are also shown. This figure was taken from Hehlgans and Pfeffer, 2005.

In contrast to DD containing TNF family members, many members of the TNF superfamily can bind to their respective receptors to induce cell survival and proliferation through activation of the NF-kB pathway. In the case of TNFR2, the adaptor protein RIP is recruited to the NF-kB activating complex and the NF-kB regulatory protein NEMO is recruited into the complex (Kovalenko and Wallach 2006). Upon binding of NEMO to RIP the IKK signalling complex is activated thus inducing NF-kB activation and survival signals (Kovalenko and Wallach 2006). It is important to note that proteins that do not contain a DD have not been shown to induce apoptosis, in contrast, DD containing proteins have been shown to signal to and activate the NF-kB pathway upon stimulation with their respective ligand (Harper, Farrow et al. 2001; Ehrhardt, Fulda et al. 2003; Peter, Legembre et al. 2005).

1.9 TRAIL as a therapeutic agent in cancers

TRAIL is a member of the TNF superfamily of proteins and was originally identified by its sequence homology to CD95L by two groups (Wiley, Schooley et al. 1995; Pitti, Marsters et al. 1996). TRAIL is known to bind as a trimer to four transmembrane receptors (Degli-Esposti, Dougall et al. 1997; Degli-Esposti, Smolak et al. 1997; MacFarlane, Ahmad et al. 1997; Pan, Ni et al. 1997; Pan, O'Rourke et al. 1997; Walczak, Degli-Esposti et al. 1997) and osteoprotegrin (OPG), a soluble receptor, which has a low binding affinity to TRAIL (Truneh, Sharma et al. 2000). TRAIL-R1 and TRAIL-R2 contain full cytoplasmic Death Domains (DD) and when stimulated with TRAIL can initiate cell death via the extrinsic apoptotic pathway (MacFarlane, Ahmad et al. 1997; Pan, Ni et al. 1997; Pan, O'Rourke et al. 1997; Walczak, Degli-Esposti et al. 1997; Sprick, Weigand et al. 2000). In contrast TRAIL-R3 and TRAIL-R4 are known as "decoy" receptors because TRAIL-R3 has a missing cytoplasmic DD and TRAIL-R4 has a truncated, non-functional DD and therefore these receptors cannot initiate apoptosis (Degli-Esposti, Dougall et al. 1997; Degli-Esposti, Smolak et al. 1997; MacFarlane, Ahmad et al. 1997; Pan, Ni et al. 1997).

TRAIL-R3 and TRAIL-R4 were originally termed "decoy" receptors because of their high surface expression levels on normal cells, which are resistant to TRAIL (Sheridan, Marsters et al. 1997). In addition, one study found evidence suggesting that "decoy" receptors can form a stable DISC with TRAIL-R2 prior to stimulation with ligand, thus preventing TRAIL-induced apoptosis, which would support their status as "decoy" receptors (Clancy, Mruk et al. 2005). However, there has been some dispute as to whether they are true "decoy" receptors as surface expression of TRAIL receptors does not necessarily correlate with sensitivity to TRAIL and "decoy" receptor expression is present on transformed cells (Held and Schulze-Osthoff 2001).

TRAIL is thought to bind pure TRAIL-R1 and TRAIL-R2 homocomplexes in the form of a trimer. There is evidence that TRAIL can bind to TRAIL-R1/TRAIL-R2 heterocomplexes, but the existence of these complexes has only been identified in one study using overexpressed proteins and not endogenous receptors (Kischkel, Lawrence et al. 2001). There has also been some evidence of preformed ligand assembly domains (PLADS) that are thought to exist prior to TRAIL-receptor binding (Clancy, Mruk et al. 2005). In that study, TRAIL-R2 and TRAIL-

R4 were thought to exist in a complex prior to ligand binding and this was thought to be a mechanism of TRAIL-R4-mediated resistance (Clancy, Mruk et al. 2005). However, this study suggests the existence of hetercomplexes between death and "decoy" receptors independent of ligand binding.

TRAIL has been thought to be a good candidate for tumour therapy because it induces apoptosis in many tumour types but, unlike its family members CD95L, which causes severe liver toxicity (Ogasawara, Watanabe-Fukunaga et al. 1993), and TNF, which induces a sepsis-like syndrome (Feinberg, Kurzrock et al. 1988), it does not appear to be toxic to most normal cell types (Wiley, Schooley et al. 1995; Pitti, Marsters et al. 1996). Despite its discovery in 1995, TRAIL and mAbs to TRAIL have only recently been admitted into clinical trials because of a concern that it may be toxic to normal human hepatocytes (Jo, Kim et al. 2000).

Although the issue of whether TRAIL is toxic to hepatocytes is not yet clear, several groups have suggested that primary human hepatocytes only undergo apoptosis when stimulated with certain preparations of TRAIL and that untagged TRAIL does not induce hepatocyte toxicity (Lawrence, Shahrokh et al. 2001; Ganten, Koschny et al. 2006). In addition, several studies using blocking antibodies to TRAIL-R1 and TRAIL-R2 suggest that hepatocytes undergo TRAIL-induced apoptosis through both TRAIL-R1 and TRAIL-R2 in equal amounts (Mori, Thomas et al. 2004; Ganten, Koschny et al. 2006). Therefore, using preparations of TRAIL that can target one receptor type such as receptor-selective mutant ligands or antibodies may reduce hepatocyte toxicity and prove TRAIL to be an appropriate treatment in many tumour types.

1.10 Versions of TRAIL in clinical trials

There are currently several forms of TRAIL, including agonistic mAbs to TRAIL-R1 and TRAIL-R2 that are in clinical trials. The mechanism of TRAIL induced apoptosis is well characterised, but the mechanism of mAb induced apoptosis is less well characterised. Lexatumumab (ETR2, Human Genome Sciences) and Mapatumumab (ETR1, Human Genome Sciences) are two mAbs that induce apoptosis *in vitro* without crosslinking however, most commercial antibodies for therapy require crosslinking to induce apoptosis *in vitro* (Ludwig,

Pereira et al. 2003; Georgakis, Li et al. 2005; Pukac, Kanakaraj et al. 2005; Zeng, Wu et al. 2006). The two Human Genome Sciences (HGS) mAbs will be referred to as ETR1 and ETR2 throughout the rest of this thesis. ETR1 and ETR2 were shown to bind and induce apoptosis specifically through their respective receptors. Crosslinking has been shown to enhance apoptosis but is not essential to induce apoptosis, suggesting that higher order structures may need to be formed in order to induce apoptosis in some cell types but, importantly, not all cell types (Georgakis, Li et al. 2005; Pukac, Kanakaraj et al. 2005).

Recombinant Human TRAIL/Apo2L is currently in a phase I/II clinical trials. Results of this study are not yet published (Duiker, Mom et al. 2006). Non-human primates were used in pre-clinical evaluation studies because of high sequence homology of their TRAIL receptors to human receptors (Duiker, Mom et al. 2006). Pre-clinical studies indicated that untagged TRAIL (Apo2L) showed significant anti-tumour activity and suppressed tumour activity *in vivo* in colon cancer models (Ashkenazi, Pai et al. 1999; Kelley, Harris et al. 2001). Apo2L was also found to be safe with few toxic side effects in non-human primates, however, this may not be the case with humans (Kelley, Harris et al. 2001).

ETR1 and ETR2 are currently in phase II and phase I clinical trials, respectively (Duiker, Mom et al. 2006). ETR1 has shown some promise as a therapeutic agent particularly in follicular lymphoma with 8% of patients yielding a complete or partial response and 30% of patients with stable disease (Georgakis, Li et al. 2005). ETR1 has been well tolerated with a maximum tolerated dose yet to be reached (Georgakis, Li et al. 2005). ETR2 has also shown promise with 32% of patients with stable disease after treatment and minimal toxicity. One patient out of 20 died of renal failure, possibly associated with hepatotoxicity and maximum tolerated dose was reported to be 10 mg/kg. Three patients were reported to have minor toxicity in the form of hyperamylasemia (increased levels of the amylase enzyme) and increased alanine aminotransferase (AST) and aspartate aminotransferase (ALT) levels, suggesting the presence of damaged hepatocytes.

Overall, Apo2L and mAbs appear to be safe as single agents although efficacy is not as high as expected as there was only one complete remission in response to ETR1 in follicular

lymphoma. ETR2 induced renal failure in one patient that may be related to hepatotoxicity and this is cause for concern. Little has been done to determine the safety and efficacy of TRAIL or mAbs in combination with other therapeutic agents that may sensitise tumour cells to TRAIL-induced apoptosis and further studies need to be carried out to determine safety of combination therapies.

1.11 Sensitisation of CLL cells to TRAIL-induced apoptosis

CLL cells are resistant to TRAIL (MacFarlane, Harper et al. 2002). MacFarlane et al 2002 showed that the block in TRAIL sensitivity is at the level of the DISC, not at the level of surface expression (MacFarlane, Harper et al. 2002). More recent studies have focussed on sensitising CLL cells to TRAIL induced apoptosis by pre-treatment or co-treatment with subtoxic doses of sensitising agents and therefore induce apoptosis in CLL cells without inducing toxicity in normal tissues.

Inoue et al 2004 showed that pre-treatment of primary CLL cells with low non-toxic concentrations of the histone deacetylase (HDAC) inhibitors depsipeptide or valproate sensitised most patient samples to TRAIL-induced apoptosis (Inoue, MacFarlane et al. 2004). The proposed mechanism of sensitisation to TRAIL was through facilitation of FADD recruitment to the DISC but this was independent of *de novo* protein synthesis (Inoue, MacFarlane et al. 2004). Two subsequent publications have shown that HDAC 1 and 2 are involved in HDAC inhibitor sensitisation of TRAIL in CLL cells and that sensitisation of CLL cells to TRAIL is independent of upregulation of TRAIL-R2 (Inoue, Mai et al. 2006; Inoue, Twiddy et al. 2006). HDAC inhibitors are also known to sensitise other tumour cell types to TRAIL-induced apoptosis through various mechanisms that involve both the intrinsic and extrinsic pathways to apoptosis including; 1) redistribution of TRAIL and its receptors to lipid raft compartments, 2) downregulation of Bcl-xL, 3) upregulation of Bim and 4) increases in Bax and TRAIL-R2 (Neuzil, Swettenham et al. 2004; Shankar, Singh et al. 2005; Vanoosten, Moore et al. 2005; Butler, Liapis et al. 2006; Gillespie, Borrow et al. 2006).

HDAC inhibitors are currently undergoing evaluation for use as a single agent in tumour therapies (Bolden, Peart et al. 2006). Depsipeptide and valproate have been evaluated most

thoroughly in terms of use as a combination therapy with TRAIL and are currently in phase III clinical trials for use as single agents in tumours including T-cell lymphoma, myelodysplastic syndromes and diffuse B-cell lymphoma (Bolden, Peart et al. 2006). Depsipeptide has shown significant cardiotoxicity (Shah, Binkley et al. 2006) and valproate has shown hepatotoxicity (Bottom, Adams et al. 1997; Yao, Mather et al. 1999). However this may not be an issue with TRAIL combination therapy because, in the case of depsipeptide, the doses required to sensitise are much lower than doses required to make an impact as a single agent (Inoue, MacFarlane et al. 2004).

1.12 Mechanisms of resistance to TRAIL

In recent years, much attention has been placed on understanding the mechanisms of resistance to TRAIL-induced apoptosis. Table 1.4 shows a list of possible mechanisms of resistance to TRAIL however, several factors that may be important in CLL resistance to TRAIL are discussed below.

The study by MacFarlane et al 2002, emphasised the importance of relative levels of DISC proteins in CLL as a factor in determining resistance to TRAIL (MacFarlane, Harper et al. 2002). In particular, they indicated the low ratio of caspase-8 to c-FLIP as a possible mechanism of resistance in CLL (MacFarlane, Harper et al. 2002). This could be relevant to other tumours and cell types that are resistant to TRAIL. However in a subsequent study, FADD recruitment to the DISC was shown to be the important step in determining sensitivity of CLL cells to TRAIL when pre-treated with an HDAC inhibitor, and increases in protein levels did not appear to play a role in CLL cell resistance to TRAIL (Inoue, MacFarlane et al. 2004).

In addition, different death receptor ligands are known to have different signalling capabilities. For example, TNFα is known to signal to and activate the NF-κB and c-Jun NH2 terminal kinase (JNK) pathways and promote cell survival through TNF-R1 recruitment of TRAF2 and RIP (Wallach, Varfolomeev et al. 1999). Alternatively, TNFα can also signal to apoptosis by recruiting FADD through the DD of TRADD, but TNF receptors cannot bind FADD directly (Wallach, Varfolomeev et al. 1999). In contrast, CD95L and TRAIL can stimulate their

respective death receptors and recruit and bind FADD and caspase-8 (Boldin, Goncharov et al. 1996; Muzio, Chinnaiyan et al. 1996; Ashkenazi and Dixit 1999; Sprick, Weigand et al. 2000).

Table 1.4: Mechanisms of Resistance to TRAIL.

Mechanism of Resistance	Evidence	Reference
Down regulation of TRAIL Death Receptors	Loss of heterozygosity 8p deletions prevelent in B cell lymphomas	Shin et al 2001, Pai et al 1998
High levels of "decoy" receptors	PLADS found to contain TRAIL-R2 and TRAIL-R4 High levels of Decoy receptors expressed in TRAIL resistant cells	Clancy et al 2005 Sanlioglu et al 2005
Low caspase-8 to c-FLIP ratio	Inducible degradation of c-FLIP sensitised tumour cells to TRAIL	Kim et al 2002
High levels of IAP family proteins	Anti-cancer therapeutics can sensitise osteosarcoma cells to TRAIL by downregulation of IAPs RNAi to XIAP and survivin sensitises cells to TRAIL-induced apoptosis	Mirandola et al 2006 Chawla-Sarkar et al 2005
constitutive NF-kappaB activation	NF-kB activity constitutive in many TRAIL-resistant tumour types including CLL Block of NF-kB activity can sensitise tumour cells to TRAIL-induced apoptosis	Furman et al 2000 Lou et al 2004
Deficiency in Bax or other BH3 only proteins	Mutations or inactivation of Bax leads to TRAIL resistance	LeBlanc et al 2002
Death receptor ligands can induce survival signals	TNF and CD95 have been shown to activate the NF-kB survival pathway TRAIL has been reported to induce proliferation in tumour cells TRAIL can activate the NF-kB and JNK survival pathways in a secondary signalling complex	Peter et al 2005, Wallach et al 1999 Ehrhardt et al 2003 Varfolomeev et al 2005
Deficiency in endocytosis machinery	CD95-induced DISC internalisation is required for CD95L-induced apoptosis in Type I cells TNF receptor signalling is a two step process requiring internalisation for DISC activation	Lee et al 2006 Schneider-Brachert et al 2004

Recruitment of the DISC components and signalling to apoptosis is thought to play a major role in CD95L and TRAIL signalling, but not TNF signalling, however there are several reports suggesting the TRAIL and, in particular, CD95L can induce anti-apoptotic signals in various cell types (Ehrhardt, Fulda et al. 2003; Peter, Legembre et al. 2005). More specifically, TRAIL has been shown to induce proliferation in the 293 tumour cell line in the absence of caspase activity and it can activate the NF-κB pathway through RIP recruitment to the DISC (Jeremias and Debatin 1998; Harper, Farrow et al. 2001; Ehrhardt, Fulda et al. 2003). It is not yet clear what determines the amplification of pro- or anti-apoptotic signals by death receptor ligands but the mechanisms of NF-κB activation and apoptosis activation by death ligand needs further investigation.

Several recent reports have suggested that apoptotic signals are initiated upon receptor complex endocytosis and that survival signals are initiated at the plasma membrane (Schneider-Brachert, Tchikov et al. 2004; Lee, Feig et al. 2006). This is surprising given a previous report suggesting that CD95 DISC formation occurred at the plasma membrane and that internalisation of DISC complexes was dependent on caspase-8 activation (Algeciras-Schimnich, Shen et al. 2002).

Several groups have published studies on endocytosis of death receptors and their components and proposed possible mechanisms of resistance to apoptosis in certain cell types. A recent report showed that, in Type I cells, clathrin-dependent internalisation was most likely required for CD95L-mediated DISC formation and apoptosis (Lee, Feig et al. 2006). They also showed that when CD95 internalisation was blocked, activation of non-apoptotic signalling pathways was induced. This phenomenon was not extended to Type II cells and was surprising given the same groups previous report suggesting that CD95 DISC formation occurred at the plasma membrane and caspase activation was required for internalization (Algeciras-Schimnich, Shen et al. 2002).

Nevertheless, these results are fascinating given less recent findings that TNF-induced apoptosis is part of a two-step process and that DISC formation and activation is dependent on internalisation (Schneider-Brachert, Tchikov et al. 2004). However this study found that non-apoptotic functions of TNF-R1 were mediated at the plasma membrane further suggesting the importance of endocytosis in death receptor-mediated apoptosis (Schneider-Brachert, Tchikov et al. 2004).

Although the importance of TRAIL and TRAIL-receptor internalisation has not been definitively studied, it is intriguing to speculate that defective internalisation may be a mechanism of resistance to TRAIL-induced apoptosis or even produce anti-apoptotic signals. One study on TRAIL-internalisation suggested that death receptor activation by TRAIL led to caspase-mediated cleavage of important clathrin adaptor molecules and aided in halting clathrin-mediated endocytosis, thus providing amplification of apoptosis (Austin, Lawrence et

al. 2006). Although this group did not study the effects of defective internalisation on TRAIL-mediated apoptosis, they suggested that internalisation may be important to amplify a TRAIL-induced cell death signal.

1.13 Clathrin-mediated endocytosis

Many important discoveries have been made in the field of endocytosis in recent years, however relatively little has been achieved in looking at endocytosis and its effects on apoptosis, particularly in relation to TRAIL. It is possible that defects in internalisation may be the cause of TRAIL-resistance in many tumour cells. Therefore, it is important to investigate the role of internalisation in TRAIL-induced apoptosis.

Clathrin-mediated endocytosis is the best characterized and most common pathway for proteins to undergo endocytosis (Polo and Di Fiore 2006). It is orchestrated by interactions with a series of adaptor proteins whose role has been well characterized. Interestingly, many death receptors and their ligands, including TRAIL, are thought to undergo endocytosis through the clathrin-mediated endocytic pathway (Schneider-Brachert, Tchikov et al. 2004; Austin, Lawrence et al. 2006; Lee, Feig et al. 2006). However it is important to note that ligands and receptors may undergo endocytosis through a range of different pathways, and that in the absence of one pathway, compensatory pathways may be employed (Polo and Di Fiore 2006). Moreover, alternative endocytic pathways are rapidly being defined and some of these pathways have similar characteristics to already defined pathways (Kirkham and Parton 2005). A scheme of clathrin-mediated endocytosis is shown in Figure 1.5.

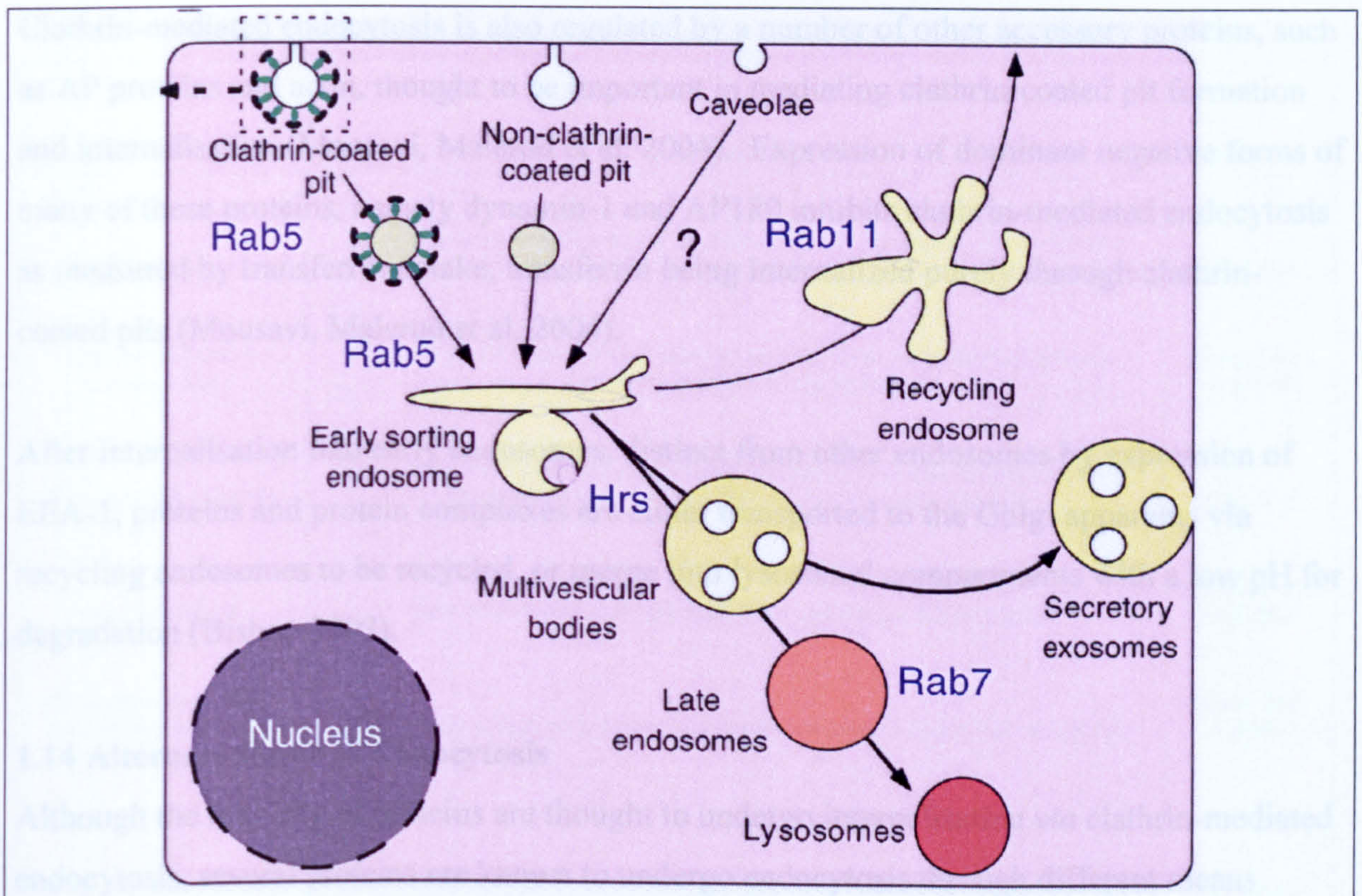

Figure 1.5: A scheme of ligand-induced receptor internalisation. Receptor synthesis occurs in recycling centres in the golgi apparatus and transferred in vesicles to the cell surface. Upon ligand binding receptors are clustered and formed into coated pits by a series of adaptor molecules. The coated pits bud off the cell surface to form coated vesicles into early endosomes that can be recycled or transported within the cell. This figure was taken from Le Borgne, Bardin, and Schwelsguth, 2005.

Clathrin-mediated endocytosis is initiated when clathrin coat components are recruited to the plasma membrane. The membrane is subsequently invaginated to form a clathrin-coated pit followed by a fission reaction into an endocytic vesicle. During the process of clathrin-mediated endocytosis, the small GTPase dynamin-1 has been shown to polymerise and form tubular structures around the neck of the pits augmenting fragmentation of the tubules and internalisation of the clathrin-coated pits (Takei, Haucke et al. 1998). Dynamin-1 is required for clathrin-mediated endocytosis, but is not necessarily required for other forms of endocytosis (Takei, Yoshida et al. 2005).

Clathrin-mediated endocytosis is also regulated by a number of other accessory proteins, such as AP proteins and actin, thought to be important in mediating clathrin-coated pit formation and internalisation (Mousavi, Malerod et al. 2004). Expression of dominant negative forms of many of these proteins, namely dynamin-1 and AP180 inhibits clathrin-mediated endocytosis as measured by transferrin uptake, transferrin being internalized purely through clathrin-coated pits (Mousavi, Malerod et al. 2004).

After internalisation into early endosomes, distinct from other endosomes by expression of EEA-1, proteins and protein complexes are either transported to the Golgi apparatus via recycling endosomes to be recycled, or merge into lysosomal compartments with a low pH for degradation (Bishop 2003).

1.14 Alternate forms of Endocytosis

Although the majority of proteins are thought to undergo internalisation *via* clathrin-mediated endocytosis, several proteins are known to undergo endocytosis through different means including internalisation by lipid rafts, macropinocytosis, caveolin-induced internalisation, and a novel pathway recently described dependent on flotillin-1 (Amyere, Mettlen et al. 2002; Sigismund, Woelk et al. 2005; Cheng, Singh et al. 2006; Glebov, Bright et al. 2006; Orth, Krueger et al. 2006; Shaw 2006). Table 1.5 describes other pathways that have been identified as important in endocytosis.

Table 1.5: Endocytic pathways.

Mechanism of endocytosis	Characteristics	Reference
Clathrin-dependent	Involves formation of clathrin-coated pits that bud off from the plasma membrane to form vesicles	Takei, 1998
Caveolin-dependent endocytosis	The coat protein caveolin forms a flask-like structure at the cell surface that bind and internalise proteins into endosomes	Cheng, Singh et al 2006
Endocytosis into lipid rafts	Involves cholesterol enriched membrane domains that are detergent-resistant that rapidly internalise proteins, their biological significance is being disputed	Shaw, 2006
Macropinocytosis	Form actin-dependent exvaginations that engulf proteins into endosomes	Amyere, Mellen et al 2002
Flotillin-dependent clathrin-independent endocytosis	Not well characterised, but is dependent on flotillin and does not involve the use of clathrin	Glebov, Bright et al 2006
Endocytosis through Dorsal Ruffles	Restructuring of the actin-cytoskeleton causes ruffles at the cell surface that progress inwards to form a compact mass of tubules that generate large numbers of endosomes	Orth, Krueger et al 2006
Ubiquitin-dependent endocytosis	Proteins are marked for internalisation by a Ubiquitin (sometimes one Ubiquitin is sufficient) and internalised into endosomes	Sigismund, Woelk et al 2005
Other forms of clatrhin-independent endocytosis	Not well characterised	No reference

1.15 Aims

The aims of this thesis are outlined as follows:

1) Evaluate bortezomib for use as a single agent in CLL
2) Evaluate and TRAIL mAbs for use as a single agent in CLL
3) Determine the potential of sensitising agents to TRAIL-induced apoptosis in CLL with various preparations of TRAIL
4) Generate and characterise receptor-selective mutants to TRAIL-R1 and TRAIL-R2
5) Further characterise the general mechanism of action of TRAIL induced apoptosis

Chapter 2: Materials and Methods

2.1 Materials

Unless otherwise stated all chemicals were from Fisher Scientific (Loughborough, UK). Bortezomib was from Millenium Pharmaceuticals (London, UK) and Fludarabine was from Shering Healthcare (Burgess Hill, UK). Depsipeptide was kindly provided by Dr. E. Sausville (National Cancer Institute, Bethseda, MD) and Valproic Acid was purchased from Calbiochem (La Jolla, CA). MG132 was purchased from Affiniti Research Products (Exeter, UK). ETR1 and ETR2 were kind gifts from Human Genome Sciences (Bethseda, MD). Apo2L was a kind gift from Genentech (South San Fransico, CA). His-tagged TRAIL further purified for low endotoxin and the blocking antibody HS101 for TRAIL-R1 were purchased from Alexis Biochemicals (Nottingham, UK). Propidium Iodide (PI), Imadazole, ETDA, Histopaque, kanamycin-sulphate, ethidium bromide, Lb broth, Lb agar, IPTG, Agarose, Bromophenol Blue, Amonium Persulphate, Saponin, Glycerol, Hepes, Paraformaldehyde and Formaldehyde were purchased from Sigma (Poole, UK). PE-conjugated CD19 and Anti-Mouse Bax Clone-3 Antibody were from Becton Dickenson (Oxford, UK). SOC buffer, Hoechst-33342, Streptavidin labelled Alexa-568, cholera toxin B directly conjugated with Alexa-488, Goat-anti-Mouse Alexa-488 Antibody, RPMI, DMEM, Foetal Calf Serum (FCS) and Glutamax were purchased from Invitrogen and primers for site directed mutagenesis were designed in collaboration with Marion MacFarlane and purchased from Invitrogen (Paisley, UK). FITC-conjugated Annexin V and CD19-FITC combined with CD-5 PE were from Caltag Medsystems (Buckingham, UK). PE-conjugated Antibodies to TRAIL-R1 and TRAIL-R2 (clones DJR1 and DJR2, respectively) and anti-mouse PE-conjugated IgG1 κ light chain isotype control antibody (clone P3) was purchased from eBiosciences (San Diego, CA). Bradford protein assay reagent and ECL were from Pierce (Cramlington, UK). Acrylamide and Triton X were from National Diagnostics and BDH, respectively (Atlanta, GA and Auckland, New Zealand, respectively). Streptavidin-labelled Sepharose beads and Nickel-labelled Agarose beads were from Amersham Biosciences (Little Chalfort, UK). Complete Mini Protease inhibitor tablets and EDTA-Free mini-protease inhibitor tablets were from Roche (Burgess Hill, UK). Site Directed Mutagenesis kits were from Stratagene (Basingstoke, UK). Quiaspin® Miniprep kit and Dyex 2.0 Spin Columns were from Quiagen (Crawley, UK). Neutralising Antibody to TRAIL-R2 (Recombinant Human TRAIL-R2/Fc) and z-VAD.fmk were from R&D Systems and Enzyme Systems, respectively (Abingdon and

Newbury, UK, respectively). Anti-mouse caspase-9 Antibody was purchased from Marine Biological Laboratory (Woods Hole, MA). Hyperladder I was from Bioline (London, UK) and Protein Assay Reagent was from BioRad (Hemel Hempstead, UK). HeLa cells inducibly expressing the K44A mutant of dynamin and wt dynamin were kindly provided by Dr. Chris Bleackley (University of Alberta, Edmonton, Canada) with permission from Dr. Sandra Schmid (Scripps Research Institute, La Jolla, CA). BJAB cells were kindly provided by Dr. Andrew Thorburn (University of Colorado Health Sciences Center, Aurora, CO).

A list of recipes for solutions used in this thesis is provided in the Appendix, Figure A.1.

2.2 Cell Lines and Cell Culture

A list of cell lines used with culture conditions and origins are shown in Table 2.1. All cell lines were determined to be mycoplasma negative by PCR with the exception of K562 cells that tested mycoplasma positive. Cells were cultured in Medium (specified in Table 2.1) supplemented with 10% FCS and glutamax.

Table 2.1: Cell lines and culture conditions

Cell Line	Origin	Doubling Time (hours)	Culture Conditions	Reference
BJAB	Burkitt Lymphoma	20	RPMI	Menezes et al 1975
Elijah	Burkitt Lymphoma	36	RPMI	Rowe et al 1985
HeLa wt dynamin	Human Cervical Carcinoma transfected with wt dynamin-1	24	DMEM with puromycin (25 µg/ml), tetracycline (1 mg/ml) and geneticin (400 µg/ml)	Damke et al 1994
HeLa dynamin-1 dominant negative	Human Cervical Carcinoma transfected with K44A mutant dynamin-1	24	same as HeLa with wt dynamin	Damke et al 1994
Jurkat clone E6.1	Human leukemic T cell lymphoblast	24	RPMI	Weiss et al 1984
K562	Human Chronic Myeloid Leukemia	24	RPMI	Lozzio et al 1977
Z-138	Human B-cell Acute Lymphoblastic Leukemia	24	RPMI	Estrov et al 1998
Ramos	Human Burkitt's Lymphoma	36	RPMI	Klein et al 1975

HeLa cells were grown in the presence of tetracycline unless otherwise stated.

2.3 Purification of CLL cells from whole blood

Peripheral blood was collected into Li-Heparin tubes from patients diagnosed with CLL staged according to the Binet system. Blood was diluted 1:2 in RPMI and loaded on a Ficol density

gradient (Histopaque) in a 1:2 ratio. The gradients were centrifuged at 1600 rpm for 30 minutes at room temperature and the lymphocyte fraction was collected. Figure 2.1 shows fractions that are separated by the ficol density gradient. After collection, cells were washed in RPMI and centrifuged at 1200 rpm for 10 minutes and resuspended in RPMI containing 10% FCS and 2 mM glutamax. Cells were counted on a Sharfe Coulter cell counter and resuspended to 5 x 10^6 per ml.

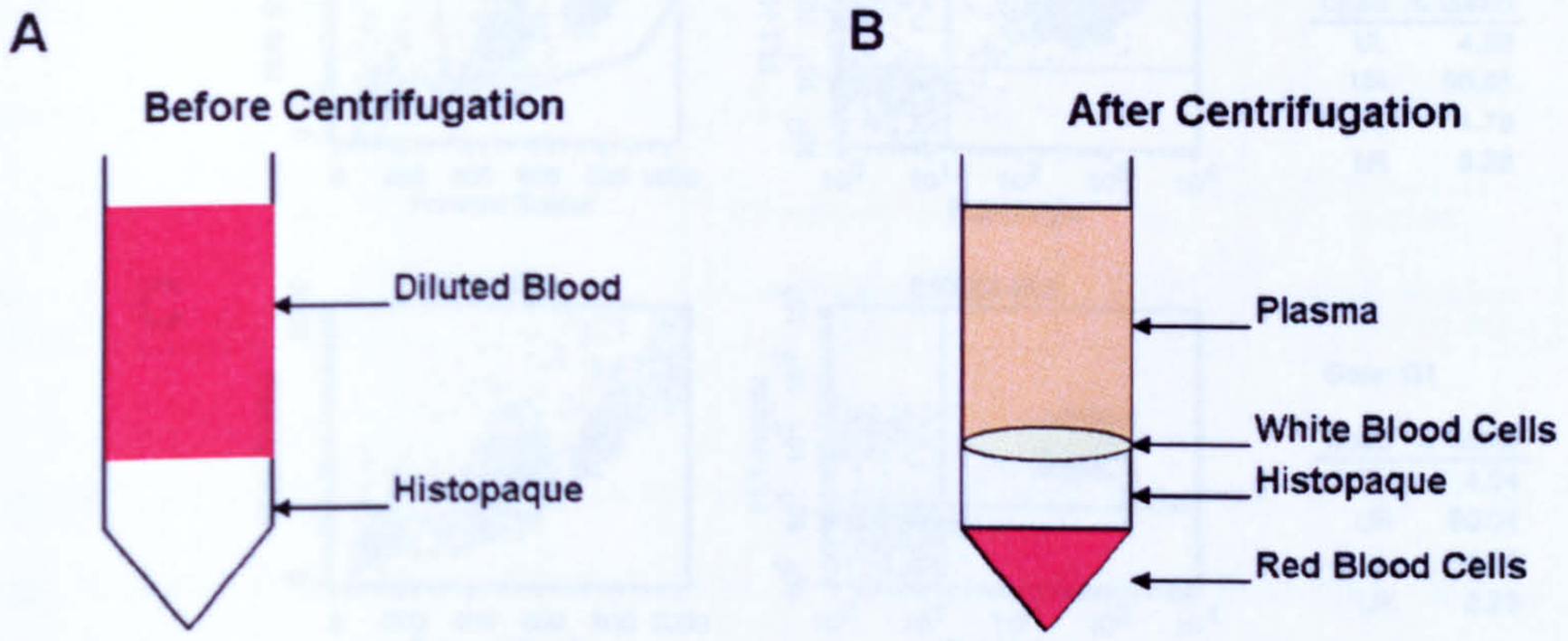

Figure 2.1: Purifying CLL cells on a ficol density gradient. Whole blood from CLL patients was diluted 1:1 in RPMI and loaded onto a ficol density gradient in a 2:1 ratio as shown in part A. After centrifugation at 1600 rpm for 30 minutes at room temperature, whole blood was separated by density with RBCs on the bottom of the gradient and plasma on the top. White blood cells (including CLL cells) formed a buffy coat in the middle of the gradient as shown in part B.

Purity of CLL cells was determined by the percentage of CD19/CD5 positive cells on the flow cytometer. 1 x 10^6 cells were pelleted at 1000 rpm for 5 minutes and resuspended in 2% BSA on ice in the presence of CD19-PE and CD5-FITC for 20 minutes, washed three times in ice-cold PBS and resuspended in cold PBS. Cells were analysed on a Becton Dickenson Flow Cytometer and cells that were stained for both CD19 and CD5 were counted as CLL cells. An example of a typical cell count and measurement of CLL cell purity are shown in Figure 2.2. As a result of stimulating the cells with antibody, a small population of "activated" cells appeared to be larger than the normal population as determined by the Forward Scatter/Side Scatter profile. It appeared that these cells were brightly stained for CD19/5, but did not represent a larger portion of the total population of CD19/5 positive cells.

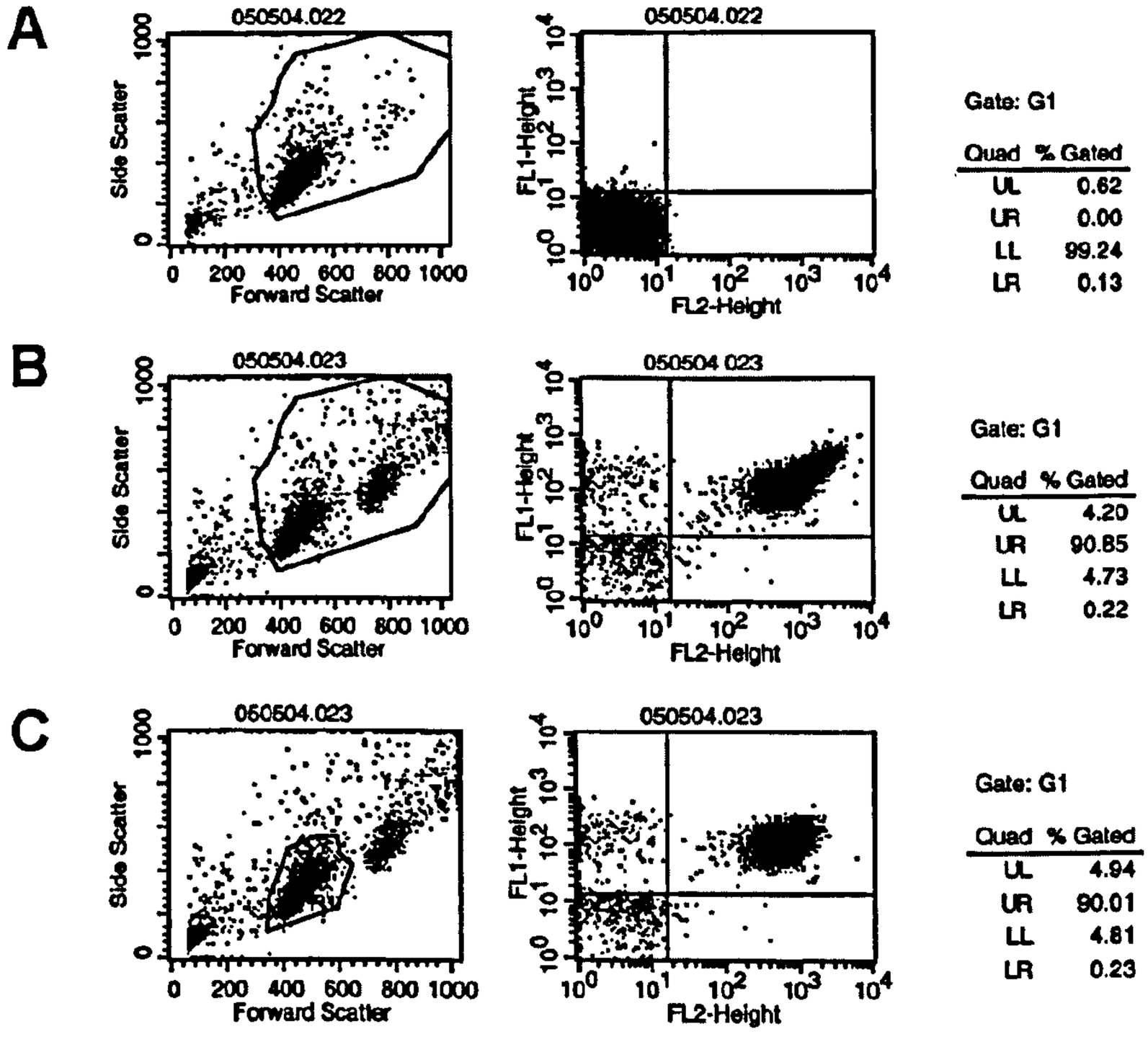

Figure 2.2: Assessing the purity of CLL cells separated from whole blood components by a ficol density gradient. 1 x 106 cells were stained for CD19/5 purity as described in section 2.3. A) Unstained cells were set in the first quadrant of FL-1 and FL-2. B) The percentage of CD19/5 cells was determined by counting all cells that were positive for FL-1 (CD5) and FL-2 (CD19). In this case, CLL cells are in the upper right quadrant and make up 90% of the entire white cell population. C) Cells were gated to prevent acquisition of "activated" cells. No difference to the total %CD19/5 cells was observed, however the cells were less brightly stained.

2.4 Culture and treatment of CLL cells

Purified CLL cells were cultured at a density of 5 x 10^6 per ml in RPMI containing 10% FCS and 2 mM glutamax for up to 24 hours. In Chapter 3 CLL cells were either treated with up to 20% FCS or the serum layer containing plasma was removed from the ficol preparation and cells were treated in RPMI containing autologous plasma (up to 20%) during treatment with proteasome inhibitors. In addition in Chapter 3, purified CLL cells were treated in increasing concentrations of RBCs (0-50%) recovered from the ficol gradient. Unpurified CLL cells were treated in whole blood with bortezomib, MG132 or vehicle alone (0.1% DMSO) as indicated in Chapter 3 for 6 or 24 hours. Cells were treated with various agents at a density of 5 x 10^6 per ml as described in Table 2.2.

Table 2.2: Agents used to treat CLL and cell lines in this thesis.

Compound	Concentration	Length of time used (hours)	Cell lines treated	Used as a single agent	Used to sensitise
Bortezomib	1-100 nM	2 to 24	CLL cells	Yes	To TRAIL induced apoptosis (1 nM for 16 hours)
MG132	1 μM	2 to 24	CLL cells	Yes	No
Fludarabine	10 μM	16	CLL cells	No	To TRAIL-induced apoptosis
Depsipeptide	10 nM	16	CLL cells and K562 cells	No	To TRAIL-induced apoptosis
Valproic Acid	2 mM	16	CLL cells and K562 cells	No	To TRAIL-induced apoptosis
TRAIL (various preparations)	100-1000 ng/ml	1 to 8	CLL cells and all cell lines in Table 2.1	Yes	After treatment with other sensitising agents

To sensitise CLL cells to TRAIL-induced apoptosis, cells were treated for 16 hours with the indicated concentrations of sensitising agent and assessed for spontaneous apoptosis and receptor surface expression. Cells were subsequently treated with the indicated preparation of TRAIL for a further 6 hours and assessed for apoptosis induction by Annexin V/PI staining. Lysates were made and stored on selected treatments to assess apoptosis induction by measuring caspase-processing on a western blot.

Where indicated, a blocking antibody to TRAIL-R1 (HS101) and a neutralising antibody to TRAIL-R2 were used to determine the specificity of TRAIL mutants. To block TRAIL activity, cells were pre-treated with the TRAIL-R1 blocking antibody (1 μg/ml) or the TRAIL-R2 neutralising antibody (5 μg/ml) for 30 minutes at 37oC. After treatment, TRAIL was added to the cells at the indicated concentrations and apoptosis assessed 4 hours later.

2.5 Measurement of apoptosis induction by AnnexinV/PI binding

In non-apoptotic cells, phosphatidylserine (PS) is localised to the inner side of the plasma membrane. When apoptosis is induced, PS is externalised to the outer surface of the plasma membrane and provides an engulfment signal to macrophages and NK cells (Fadok, Bratton et al. 1998). In 1995, Annexin V was discovered to preferentially bind to PS and therefore can mark apoptotic cells (Vermes, Haanen et al. 1995). Fluorescently-tagged Annexin V

(conjugated with FITC) can measure the extent of apoptosis in a given population (Vermes, Haanen et al. 1995). In conjunction with Propidium iodide (PI), to establish membrane integrity, apoptotic cells can be identified by flow cytometry.

For each measurement, 1 x 10^6 cells were collected and washed. Cells were resuspended in Annexin Buffer and 1.5 µl of FITC conjugated Annexin V was added to each sample. Cells were incubated for 10 mins at room temperature. After incubation, cells were placed on ice and 250 ng of PI was added to each sample. Samples were read on a Becton Dickenson FacsScan flow cytometer immediately. Figure 2.3 shows an example of a non-apoptotic Annexin V/PI profile and an apoptotic Annexin V/PI profile.

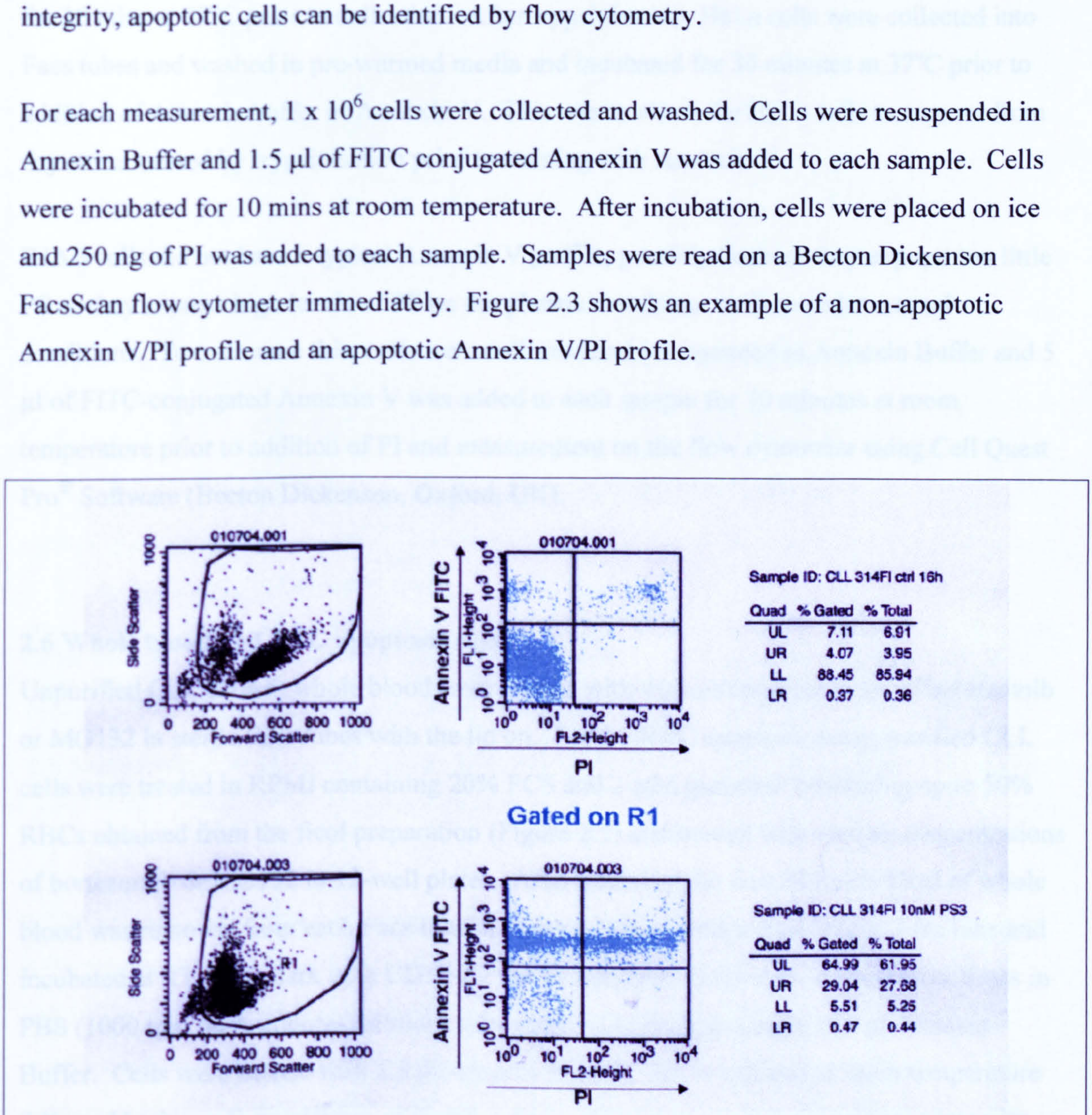

Figure 2.3: Apoptotic cells as measured by AnnexinV/PI positivity. CLL cells were treated with vehicle alone (0.1% DMSO, top row) or 10 nM bortezomib (bottom row) for 16 hours. After treatment cells were stained for AnnexinV/PI as described in section 2.5. Apoptotic cells are stained positive on FL-1 (Annexin V) and FL-1 and FL-2 (Annexin V and PI). The top row shows a non-apoptotic population (11% apoptosis) and the bottom row shows an apoptotic population (94% apoptosis). Changes in Forward Scatter and Side Scatter profiles reflect this.

HeLa cells were seeded at a density of 0.25 x 10^5 cells per ml in 6-well plates 48 hrs prior to treatment with TRAIL. After treatment, HeLa cells were trypsinised in 0.25 x trypsin/EDTA for 30 mins at 37°C prior to collection. After trypsinisation, HeLa cells were collected into Facs tubes and washed in pre-warmed media and incubated for 30 minutes at 37°C prior to addition of Annexin buffer or Annexin V. This was to allow the HeLa cells to recover from any stress caused by trypsinisation prior to staining with Annexin V.

BJAB cells did not have a typical Annexin V profile, possibly because they express too little PS or they express high levels of PS on the plasma membrane surface under normal conditions. To overcome this, cells were collected and resuspended in Annexin Buffer and 5 µl of FITC-conjugated Annexin V was added to each sample for 30 minutes at room temperature prior to addition of PI and measurement on the flow cytometer using Cell Quest Pro® Software (Becton Dickenson, Oxford, UK).

2.6 Whole blood and RBC apoptosis assay

Unpurified CLL cells in whole blood were treated with various concentrations of bortezomib or MG132 in sterile Facs tubes with the lid on. For the RBC apoptosis assay, purified CLL cells were treated in RPMI containing 20% FCS and 2 mM glutamax containing up to 50% RBCs obtained from the ficol preparation (Figure 2.1) and treated with various concentrations of bortezomib or MG132 in 12-well plates. After treatment for 6 or 24 hours 50 µl of whole blood was removed from each Facs tube or well and placed into a fresh sterile Facs tube and incubated at RT in the dark with CD19-PE for 15 minutes. Cells were washed three times in PBS (1000 rpm for 5 minutes) at room temperature and resuspended in 500 µl Annexin Buffer. Cells were treated with 1.5 µl Annexin V-FITC for 15 minutes at room temperature followed by immediate addition of 5 µl 7-AAD to discriminate plasma membrane integrity. Cells were placed on ice and CLL cells considered to be apoptotic were CD19 positive and Annexin V positive. Results were analysed using Cell Quest Pro® Software. A typical example of how CLL cells were measured is shown in Figure 2.4.

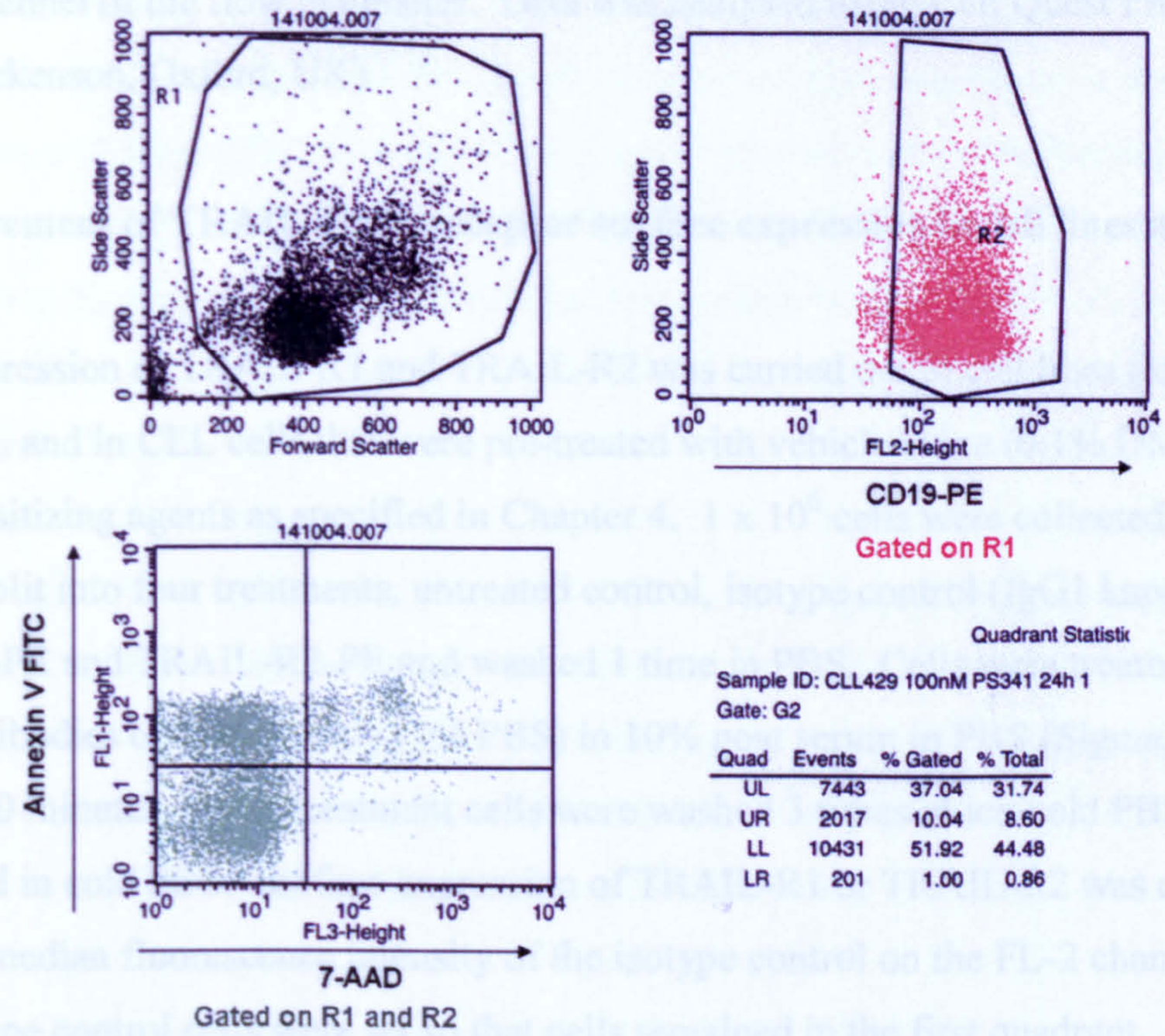

Figure 2.4: Red Blood cell and Whole blood apoptosis assay. Whole blood from CLL patients, or CLL cells treated in combination with RBCs were treated with an apoptosis-inducing agent. After treatment cells were stained for CD19-PE (FL-2), Annexin V-FITC (FL-1) and 7-AAD (FL-3) as described in section 2.6. Cells shown in red were gated on R1 (Forward Scatter, Side Scatter profiles) and represent the CD19 positive population. Cells shown in green were gated on R1 and R2 (Forward Scatter, Side Scatter profile and CD19, Side Scatter profile). Apoptotic CLL cells are positive for Annexin V and CD19 and represent approximately 50% of the gated population.

2.7 Measurement of Bax conformational changes in CLL cells treated with bortezomib

After treatment of CLL cells with increasing concentrations of bortezomib (1-100 nM), MG132 (1 μM) or vehicle alone (0.1% DMSO) cells were centrifuged at 1600 rpm for 3 minutes and fixed in 2% formaldehyde for 10 mins at room temperature. Following fixation, cells were washed 1 time in PBS spun at 3000 rpm for 3 mins followed by incubation with 1 μg/ml Bax Clone 3 antibody in permeabilisation buffer (0.1% saponin, 0.5% BSA in PBS) for 45 mins at 4°C. Cells were washed in permeabilisation buffer spun at 3000 rpm for 3 mins. Cells were incubated in Goat-anti-Mouse directly labelled with Alexa-488 for 45 mins in the dark at 4°C. Cells were washed 1 time in permeabilisation buffer at 3000 rpm for 3 mins and resuspended in 500 μl of PBS. Positive cells were considered those in the second quadrant of

the FL-1 channel of the flow cytometer. Data was analysed using Cell Quest Pro® Software (Becton Dickenson, Oxford, UK)

2.8 Measurement of TRAIL death receptor surface expression in cell lines and CLL samples

Surface expression of TRAIL-R1 and TRAIL-R2 was carried out in cell lines that were treated with TRAIL and in CLL cells that were pre-treated with vehicle alone (0.1% DMSO) or various sensitizing agents as specified in Chapter 4. 1×10^6 cells were collected into Facs tubes and split into four treatments, untreated control, isotype control (IgG1 kappa-PE), TRAIL-R1-PE and TRAIL-R2-PE and washed 1 time in PBS. Cells were treated with PE-labelled antibodies or vehicle only (1% PBS) in 10% goat serum in PBS (Sigma, Poole UK) on ice for 30 minutes. After treatment cells were washed 3 times in ice-cold PBS and resuspended in cold PBS. Surface expression of TRAIL-R1 or TRAIL-R2 was determined by setting the median fluorescence intensity of the isotype control on the FL-2 channel on a log scale. Isotype control cells were set so that cells remained in the first quadrant. The median-fluorescence intensity of cells stained with TRAIL-R1-PE and TRAIL-R2-PE were compared with isotype control-stained cells using Cell Quest Pro® software (Becton Dickenson, Oxford, UK).

2.9 Preparation of CLL cell lysates

5×10^6 CLL cells were harvested after treatment with varying agents and centrifuged at 13000 rpm for 1 minute. Cells were washed in ice cold PBS three times and liquid was removed from the pellet. Cells were snap frozen in liquid nitrogen. After freezing, lysates were thawed on ice and resuspended in 200 µl of 1 x sample buffer. Lysates were sonicated at an amplitude of 10 microns for 10 seconds on ice and boiled for 5 minutes. Lysates were stored in SDS sample buffer long term at -80°C.

2.10 Preparation of cell line lysates

After treatment, 1×10^6 cells of various cell lines were centrifuged at 13000 rpm for 1 minute. Cells were washed three times in ice cold PBS and liquid was removed from the pellet. Further treatment of cell lysates was carried out as described in section 2.9.

2.11 Western blotting

Western blotting is a technique used to fractionate and identify proteins on a membrane by their reaction with a specific antibody. Unlike flow cytometry, western blotting can compare protein levels between several populations of cells, but cannot detect differences in individual cells. Western blotting works on the principle that proteins can be fractionated according to their various sizes by an applied current through a gelated matrix (poly acrylamide gel electrophoresis, PAGE). A visible protein marker is used to detect relative sizes of proteins in the gel. After fractionation, proteins are transferred to a membrane by an applied current and detected using antibody. Primary antibody is used to recognise a specific protein of interest on the membrane. After the primary antibody binds to this protein, secondary antibody that recognises the host protein from the primary antibody on the membrane (directly conjugated to horseradish peroxidise) is bound on to the primary antibody and ECL is used to visualise the proteins on the membrane. Lists of primary and secondary antibodies used are in Tables 2.3 and 2.4, respectively.

Table 2.3: Primary antibodies used in western blotting.

Antibody	Host	Source	Concentration
Caspase-3	Rabbit	In House	1 in 3000
Caspase-9	Mouse	MBL	1 in 2000
Caspase-8	Rabbit	In House	1 in 3000
TRAIL-R1	Mouse	ProSci	1 in 1000
TRAIL-R2	Mouse	ProSci	1 in 1000
FADD	Mouse	BD Transduction laboratories	1 in 250
Poly-Ubiquitin	Mouse	Affiniti Research	1 in 2000

Table 2.4: Secondary antibodies used for western blotting.

Antibody	Host	Source	Concentration
Anti-Mouse HRP	Goat	Sigma	1 in 3000
Anti-Rabbit HRP	Goat	Dako	1 in 3000

Protein lysates were made as described in sections 2.9 and 2.10. Lysates were run on a stacking gel containing 4% acrylamide followed by a running gel containing 13% acrylamide with the exception of detection of poly-ubiquitin (run on a 10% gel). 10 µl of protein lysate was run for each sample and gels were run until the dye front reached the bottom of the gel. Gels were run in SDS running buffer on a 40 milliAmp current.

Proteins from the gel were transferred onto a nitrocellulose membrane that was hydrated in water and transfer buffer. Gels were washed in transfer buffer and stacked into a sandwich directly against the membrane. Filter paper and sponges were soaked in transfer buffer and stacked on both sides of the membrane/gel complex and placed into the cassette. The current was run so the charged proteins were transferred from the gel to the membrane. The transfer was run overnight in transfer buffer at 25 volts.

After transfer, the membrane was removed, washed in TBSt and blocked for 1 hour in TBSt containing 5% Marvel (TBS-Mt) at room temperature with shaking. The membrane was washed 2 times for 5 mins with shaking in TBSt to remove traces of TBS-Mt. Primary antibody, diluted in TBSt, was applied for 1 hour at room temperature with shaking. To remove unbound antibody, the membrane was washed 2 times for 5 mins in TBS-Mt followed by 2 times for 5 mins in TBSt. Secondary antibody was diluted in TBSt and applied for 1 hour at room temperature with shaking. The membrane was washed 2 times for 5 mins in TBS-Mt, followed by 2 times 5 mins of TBSt and 2 times 5 mins in TBS. Proteins were visualised using Peirce ECL Western Blotting Substrate according to the manufacturer's instructions. Multiple exposures of each membrane were taken on Kodak film and developed using a Compact X4 developer from Xograph Imaging systems.

2.12 Analysis of DISC proteins in cell lines

The number of cells required for each DISC sample is indicated in the relevant figure legends. Cells were treated at a density of 2 x 10^6 per ml at 37°C for the indicated times with the indicated concentrations of biotinylated TRAIL. After treatment, cells were washed in ice cold PBS three times at 1000 rpm for 5 minutes. Cells were lysed in DISC lysis buffer (30 mM Tris/HCl pH 7.5, 150 mM NaCl, 10% Glycerol, 1% Triton X-100, 1 pellet of complete mini-protease inhibitors per 10 ml) for 30 mins at 4°C. Lysates were cleared in a centrifuge at 13000 rpm for 30 mins at 4°C and placed in a 15 ml tube with 30 µl pre-washed streptavidin coupled to agarose beads (Sigma, Poole, UK). Lysates were rotated on an end-to-end shaker overnight. The unstimulated control (u/s) for each experiment comprised of cells being lysed and cleared and then treated with biotinylated TRAIL.

After incubation with streptavidin-beads, lysates were centrifuged at 1000 rpm for 5 mins and supernatant was removed. Beads were washed 6 times in 0.5 ml lysis buffer and complexes were eluted from the beads in SDS sample buffer and boiled for 5 mins. Samples were loaded on an SDS-PAGE gel and proteins were detected using western blotting.

To measure DISC formation at 4°C, or to synchronise DISC complexes on the cell surface prior to releasing to 4°C, cells were pre-loaded with biotinylated TRAIL. Where indicated, biotinylated TRAIL was pre-loaded onto pre-chilled BJAB or HeLa cells at 4°C. Unbound TRAIL was washed 3 times in ice cold PBS from the cells and cells were either lysed, or released to 37°C for up to 1 hr followed by lysis.

2.13 Site Directed Mutagenesis of TRAIL

Site Directed Mutagenesis is a useful tool for determining the functions of proteins and, more specifically, the function of specific amino acid residues within a protein. Stratagene's Quick Change® Mutagenesis Kit allows specific amino acid residue changes using double stranded DNA and was used to mutate specific residues of wt TRAIL in Chapter 5 of this thesis. Mutagenic primers were designed in collaboration with Dr. Marion MacFarlane according to

the manufacturer's instructions and determined to have a $T_m \geq 78°C$ as determined by the following formula:

$$T_m = 81.5 + 0.41\ (\%GC) - 675/N - \%\ mismatch$$

Where N is the primer length in base pairs and values for % GC and % mismatch are whole numbers. Primers were from Invitrogen and purified by high performance liquid chromatography by Invitrogen. A list of primers used is shown in Figure 2.5.

TRAIL-R2 mutant Change 1:
His264Arg/Ile266Leu/Asp267Gln
-For:
ctgtaacaaatgagcgcttgctacgaatggaccatgaagcc

-Rev:
ggcttcatggtccattcgtagcaagcgctcatttgttacag

TRAIL-R2 mutant Change 2: Arg191Lys/Gln193Arg
-For:
cccaaacatactttaaaattttcgggaggaaataaaag

-Rev:
cttttatttcctcccgaaaattaaagtatgtttggg

TRAIL-R2 mutant Change 3: Tyr189Gln
-For:
catctattcccaaacacagtttaaatttcgggag

-Rev:
ctcccgaaatttaaactgtgtttgggaatagatg

TRAIL-R1 mutant Change 1: Tyr213Trp/Ser215Asp
-For:
ccaatatatttacaaatggacagattatcctgaccctatattg

-Rev:
caatatagggtcaggataatctgtccatttgtaaatatattgg

TRAIL-R1 mutant Change 2: Asn199Val/Lys201Arg
-For:
gaggaaataaaagaagtcacaaggaacgacaaacaaatgg

-Rev:
ccatttgtttgtcgttccttgtgacttcttttatttcctc

TRAIL-R1 mutant Change 3: Gln193Ser
-For:
catactttcgattttcggaggaaataaaagaag

-Rev:
cttcttttatttcctccgaaaatcgaaagtatg

TRAIL-R1 mutant Change 4: Tyr189Ala
-For:
catctattcccaaacagcctttcgattttcgg

-Rev:
ccgaaaatcgaaaggctgtttgggaatagatg

TRAIL-R1 mutant Change 5: Arg191Leu
-For:
cccaaacatactttctatttcaggaggaaataaaag

-Rev:
cttttatttcctcctgaaatagaaagtatgtttggg

TRAIL-R1 mutants Change 6: Asn199Val
-For:
ggaggaaataaaagaagtcacaaagaacgacaaac

-Rev:
gtttgtcgttctttgtgacttcttttatttcctcc

Figure 2.5: Primers for site directed mutagenesis. Amino Acid changes for TRAIL.R2-6 are highlighted in red. Amino Acid changes for TRAIL.R1 mutants are highlighted in blue. Specific residues to be mutated are underlined and in bold font. Primers were designed in collaboration with Dr. Marion MacFarlane.

Wild type TRAIL (residues 95-281) was cloned into a pet28 vector as previously described (MacFarlane, Ahmad et al. 1997). Primers were resuspended in ultrapure water and diluted to a final concentration of 100 µg/ml and 1.25 µl of each primer (forward and reverse) were used in the reaction mixture that contained 5 µl 10 x buffer, 50 ng TRAIL DNA, 1 µl dNTP, 1 µl Turbo enzyme made up to a final volume of 50 µl. All reagents apart from TRAIL DNA and each primer were supplied by Stratagene. Reaction mixtures were placed into a thermal cycler and run at the temperatures shown below. Between 12 and 18 cycles were repeated according to the manufacturer's instructions.

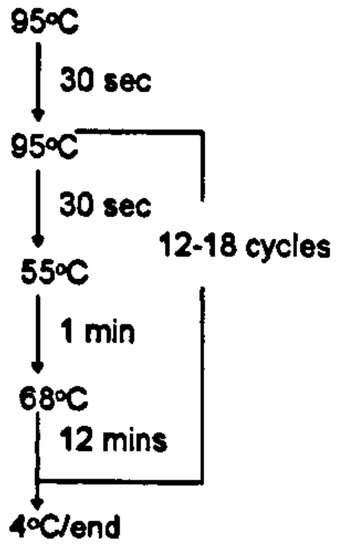

After the PCR reaction was finished, 10 µl of product was run on a 1% agar gel using hyperladder I as a marker to confirm the size of the product. The rest of the PCR product (40 µl) was digested using 1 µl DNP1 (provided by Stratagene) at 37°C for 1 hour. Following digestion, 1 µl of each product was transformed into 50 µl XL1 Blue competent cells (provided by Stratagene). Cells were mixed with PCR product and incubated on ice for 30 mins. Heat shock was carried out for 45 seconds at 42°C and cells were placed back on ice for a further 2 mins. SOC media (200 µl at room temperature) was added to the mixture and cells were incubated at 37°C for 30 mins shaking at 300 rpm. Cells were plated on agar plates containing 50 µg/ml kanamycin-sulphate and left at 37°C for at least 16 hours.

Colonies were visible after 16 hours of incubation at 37°C and at least 3 colonies of competent cells were picked into LB broth containing 50 µg/ml kanamycin-sulphate and 2 x NaCl. Cells were incubated for at least 16 hours at 37°C with shaking at 250 rpm. After incubation, cells were spun and minipreps were carried out to purify the plasmid using a DNAeasy miniprep spin kit according to the manufacturer's instructions (Quiagen).

Product from each miniprep (2 µl) was run on a 1% agarose gel containing ethidium bromide to visualise product. Concentration of each product was measured on a spectrophotometer measuring 260 and 280 wavelengths. Concentration of DNA was calculated by the following formula.

Concentration = 260 reading x 50 x dilution factor

After measuring the concentration of each sample, 500 ng of DNA was added to a sequencing reaction containing 8 µl Big Dye and 1.5 µl of either the reverse primer pet DS (100 µM stock solution) or the forward primer T7 (100 µM stock solution) and the reaction mixture was made up with ultrapure water to a total of 20 µl. A sequencing reaction was run in a thermal cycler as follows.

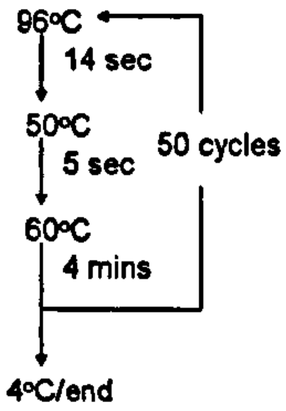

After the reaction was complete, dye was removed from the product using DyeEx columns according to the manufacturer's instructions (Quiagen). Samples were run on a sequencing gel overnight and the sequence was checked using Genetool software to confirm incorporation of the selected mutations.

2.14 Synthesis of TRAIL

After the required mutations were incorporated into TRAIL plasmid, 50 µl of E. coli (BL21-DE3) were transformed with 200 ng of pET28b-TRAIL by ligating the mixture on ice for 30 minutes followed by heat shock treatment at 42°C for 45 seconds followed by treatment on ice for 2 minutes. 200 µl SOC media (Sigma) was added and the culture was incubated for 1 hour at 37°C with shaking at 300 rpm. 100 µl of the culture was plated on Lb Agar plates containing 50 µg/ml kanamycin-sulphate and incubated at 37°C overnight. Single colonies were picked and used to inoculate a 10 ml Lb culture containing 25 µg/ml kanamycin-sulphate

at 37°C with shaking at 300 rpm for at least 16 hours. Cultures were sub-cultured (4mls) into 400 ml of Lb broth containing 25 µg/ml kanamycin-sulphate and grown at 37°C and 300 rpm for 3 hours until cultures reached an OD 600 nm reading of between 0.6 and 0.8. Cultures were then induced with 1 mM IPTG for a further 3 hours at 37°C and 300 rpm. After induction with IPTG, cultures were centrifuged for 10 minutes at 6000 rpm, washed one time in ice cold PBS and snap frozen on dry ice and stored at -80°C until required.

1ml of culture was removed before and after induction and spun at 13000 rpm for 1 minute, washed in ice cold PBS and snap frozen on dry ice. The pellets were resuspended in 100 µl sample buffer, sonicated at an amplitude of 10 microns for 10 seconds and boiled for 5 minutes. 5 µl of each sample was run on a SDS-PAGE gel and Coomasie stained and destained gel to check for induction before purification was carried out. Coomasie staining was carried out by staining the gel in coomasie stain for 1 hour shaking at room temperature followed by 2 washes in destain for 1 hour per wash. Figure 2.6 shows an example of a PAGE gel coomasie stained showing TRAIL protein before and after induction.

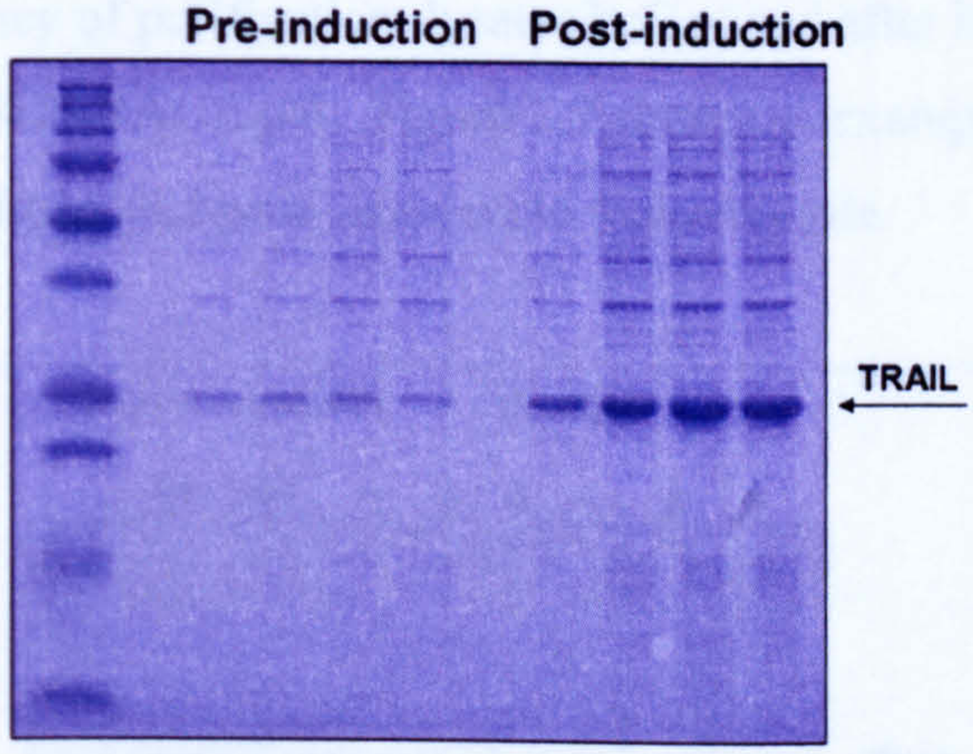

Figure 2.6: TRAIL protein before and after induction. TRAIL was induced with IPTG in 4 bacterial cultures as described in section 2.14. After induction of bacteria, lysates of cell pellets were made and run on a SDS-PAGE gel. The gel was coomasie stained and destained and TRAIL protein was visible in the post-induction samples at 27kDa.

2.15 Purification of TRAIL

E. coli pellets from 400 ml cultures were resuspended in 10 ml lysis buffer (30mM Tris-HCl, pH 7.5, 150 mM NaCl, 10 % Glycerol (w/v), 1 % Triton X-100 (v/v), containing Complete EDTA-free protease inhibitors, 1 pellet per 10 mls) and sonicated on ice 10 seconds at an

amplitude of 10 microns and 5 seconds off for 15 cycles. Lysates were incubated on ice for 30 mins and sonication was repeated.

Lysates were centrifuged at 15000 g for 30 mins at 4°C and the supernatants were collected and supplemented with 500 mM imadazole to a final concentration of 20 mM. 400 µl of Ni-NTA Agarose beads were washed 5 times in lysis buffer (2000 rpm for 1 min) and added to the lysates. Lysates were incubated for 2 hrs on an end-to-end shaker at 4°C. Beads were pelleted at 1000 rpm for 3 min and washed with lysis buffer (6 x 800 µl).

Bound TRAIL was eluted off the beads with 6 washes in 150 mM EDTA in PBS (800 µl) in the absence of protease inhibitors. Fractions 1-6 were collected and 5 µl of each fraction was resuspended in 2 x SDS sample buffer, boiled and run on an SDS-PAGE gel. Gels were stained and de-stained with Coomassie stain and fractions containing significant amounts of purified TRIAL were pooled and assay for protein content by Bradford assay, aliquoted and stored at -80°C until required.

To determine the efficiency of purification, lysates before and after imadazole treatment were collected and run on an SDS-PAGE gel. Figure 2.7 shows an example of purified TRAIL protein Fractions 1-6 and pre- and post- imadazole treated lysate.

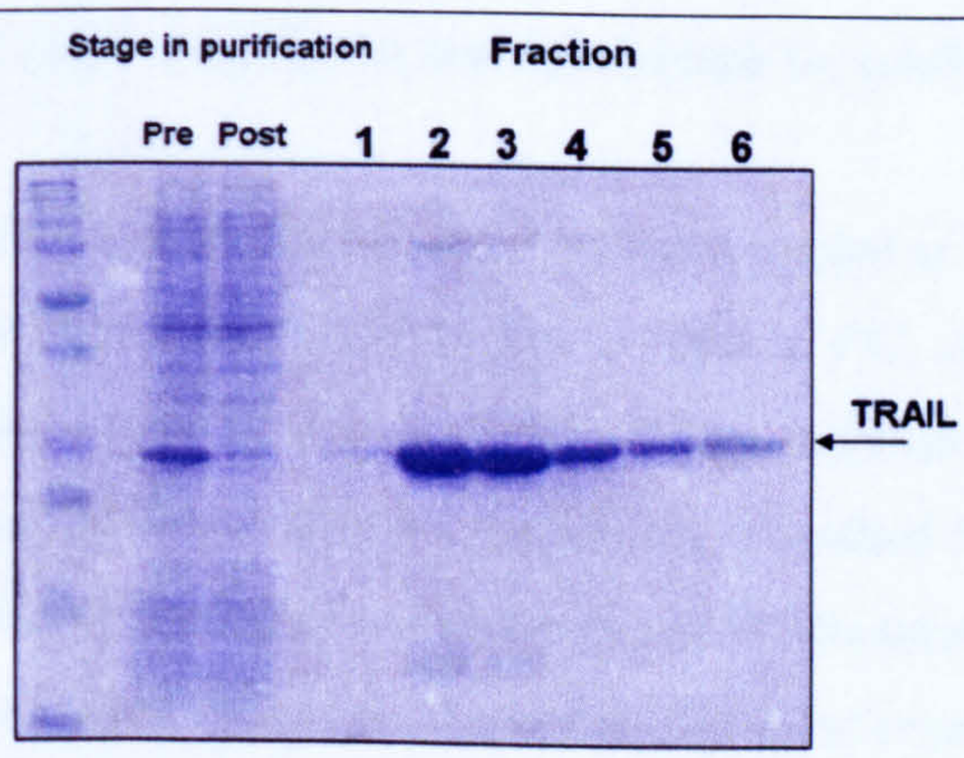

Figure 2.7: Assessment of TRAIL purity. TRAIL was purified as described in section 2.15. Samples of supernatant were taken pre- and post-purification. In addition 6 Fractions were run on a SDS-PAGE gel and TRAIL purity was assessed. Fractions 2 and 3 contain the highest levels of TRAIL protein. In this purification, Fractions 2-6 were pooled and assessed for protein concentration. Post induction pellets show that most of the TRAIL was purified.

2.16 Biotinylation of TRAIL

Biotinylation of TRAIL was performed during purification by Dr. Marion MacFarlane as previously described (Harper, Farrow et al. 2001). After biotin incorporation was determined (Harper, Farrow et al. 2001), protein content was measured by a Bradford assay, proteins were aliquoted and stored at -80°C until further required. To ensure that the biotin had no effect on the apoptotic activity of TRAIL, Ramos or Jurkat cells were treated with 500 ng/ml of biotin-labelled TRAIL for 4 hours and apoptosis was measured by staining with Annexin V/PI. Biotin-labelled TRAIL induced comparable levels of apoptosis in Ramos cells compared with unlabelled TRAIL purified in a similar manner.

2.17 Bradford assay to measure protein concentration

The Biorad method of measuring protein concentration is based on the Bradford method (Bradford 1976). To measure protein concentration of TRAIL mutants, a serial dilution was carried out of BSA protein (1 µg/ml) diluted 1:2 five times to make concentrations of 1 µg/ml, 0.5 µg/ml, 0.25 µg/ml, 0.125 µg/ml, 0.065 µg/ml and 0.0325 µg/ml for each of the 6 protein standards. Protein standards were diluted (5 µl into 1 ml) into 1 x Protein Assay Reagent (Biorad, Hemel Hempstead, UK) and protein concentration was confirmed by taking an OD reading at 595 on a spectrophotometer. TRAIL protein was diluted (2 µl in 1 ml) and the concentration was calculated using a standard curve.

2.18 Analysis of TRAIL and transferrin internalisation by confocal microscopy in BJAB and HeLa cells

To visualise TRAIL internalisation, BJAB cells were pre-cooled at 4°C for 1 hr followed by treatment with 500 ng/ml biotinylated TRAIL for 45 mins at 4°C. After treatment with TRAIL, cells were washed 3 times in ice cold PBS and treated with Streptavidin directly conjugated to Alexa Flour-568 for 1 hr at 4°C. Cells were washed 3 times in ice cold PBS to remove residual Streptavidin. Unstained control cells and cells treated at 4°C only were attached to poly-L-lysine coated slides and fixed with 4% paraformaldehyde at room temperature for 10 mins. The remaining samples were released up to 37°C for the indicated times, resuspended in cold PBS, and attached to poly-L-lysine coated slides followed by fixation as described above.

After fixation, cells were washed 3 times for 5 minutes in PBS and counterstained with the DNA dye Hoechst-33342. Cells were washed again in PBS and mounted with coverslips and stored at 4°C in the dark until images were taken. Z-stack images were collected using a Zeiss Axiovert LSM510 microscope equipped with a confocal microscope. Images were analysed with ImageJ software. Each cell shown is representative of more that 50 cells examined between three individual experiments.

To visualise internalisation of TRAIL and transferrin in HeLa cells expressing wt dynamin and K44A dominant negative dynamin, cells were washed 48 hour prior to staining to remove residual traces of tetracycline. The cells were seeded at a density of 0.25 x 10^6 per ml onto glass coverslips in 6-well plates and grown in the absence of tetracycline.

On the day of staining, cells were pre-cooled to 4°C as described above. To visualise TRAIL internalisation cells were stained with biotinylated TRAIL (500 ng/ml) and streptavidin directly conjugated to Alexa-568 as described above. Cells were washed and fixed, or TRAIL was allowed to internalise for 15 mins at 37°C followed by fixation. After fixation, cells were washed 3 times in PBS and counterstained with the DNA dye Hoechst-33342 (1 μg/ml for 10 minutes at room temperature) and cholera toxin B (5 μg/ml for 10 minutes at room temperature) to stain the nucleus and plasma membrane, respectively. Cells were mounted onto glass slides and images were collected as described above.

To visualise transferrin internalisation, HeLa cells expressing wt and dominant negative dynamin were pre-cooled to 4°C for 1 hour, washed in PBS and stained with 5 μg/ml transferrin directly conjugated with Alexa Flour-633 (Molecular Probes) for 1 hour at 4°C. Cells were washed 3 times in PBS to remove unbound transferrin and either fixed in 4% paraformaldehyde as described above, or transferrin was allowed to internalise by releasing cells up to 37°C for 30 mins followed by fixation. After fixation, cells were washed as described above and counterstained with the DNA dye Hoechst-33342 as described above. Cells were mounted onto glass slides and images were collected as described above.

2.19 Statistical Analysis

A One Way ANOVA followed by a Dunnett's test was used to compare 2 or more than 2 groups against vehicle control. Where indicated, a student's t-test was used to compare one group against vehicle control. $P < 0.05$ was considered statistically significant.

Chapter 3: An Evaluation of bortezomib for use in CLL

3.1 Introduction: An evaluation of bortezomib for use as a single agent in CLL.

The proteasome has been suggested as a suitable target for cancer therapy (Almond and Cohen 2002; Voorhees, Dees et al. 2003; Adams 2004; Jackson, Einsele et al. 2005; Richardson, Mitsiades et al. 2006). Proteasome inhibitors target the proteasome by blocking its activity and have been shown to induce apoptosis in several tumour models, including primary CLL cells (Chandra, Niemer et al. 1998; Adams, Palombella et al. 1999; Masdehors, Omura et al. 1999; Masdehors, Merle-Beral et al. 2000; Almond, Snowden et al. 2001; Adams 2002; Bogner, Schneller et al. 2003; Dewson, Snowden et al. 2003; Pahler, Ruiz et al. 2003; Kelley, Alkan et al. 2004). Although the specific mechanism of action of proteasome inhibitors is yet to be determined, in each tumour model they have been shown to generally increase activity of pro-apoptotic molecules such as Bax, and also to suppress anti-apoptotic molecules such as NF-κB, thus disrupting the balance of pro-apoptotic and anti-apoptotic proteins within a cell (Almond and Cohen 2002; Voorhees, Dees et al. 2003).

Bortezomib is a reversible peptide boronic acid inhibitor that is currently in Phase II/III clinical trials for multiple myeloma and several other haematological malignancies including CLL (Aghajanian, Soignet et al. 2002; Richardson, Barlogie et al. 2003; Berenson, Jagannath et al. 2005; Goy, Younes et al. 2005; O'Connor, Wright et al. 2005; Faderl, Rai et al. 2006). In 2003, it was approved by the US Food and Drug Administration for use in multiple myeloma (Kane, Farrell et al. 2006). It has been reported to induce apoptosis as a single agent in CLL *in vitro* (Pahler, Ruiz et al. 2003; Kelley, Alkan et al. 2004). These data suggested that bortezomib might have significant activity as a single agent therapy in CLL.

However, one recent clinical trial of 23 patients treated with varying doses of bortezomib found no partial or complete responses to the drug, although the study did report biological activity of the drug as manifested by a decrease in lymph node size and white blood cell count (Faderl, Rai et al. 2006). Five patients were removed from the study for unmanageable toxicity. Several other patients experienced severe toxicity (Faderl, Rai et al. 2006). The study concluded that bortezomib may not be ideal for treatment in CLL as a single agent, but may be active when used in combination with other drugs. However, it is not clear why bortezomib is reported to be extremely active *in vitro* but shows such discouraging activity *in vivo*.

The aims of this study were to investigate the mechanism of cell death caused by bortezomib *in vitro* in CLL and also to investigate possible reasons for the reported lack of activity of bortezomib in CLL *in vivo*. In this study bortezomib was found to induce high levels of apoptosis in all CLL patients regardless of mutation status or disease stage *in vitro*. However, despite this marked activity of bortezomib in purified lymphocytes; co-incubation of lymphocytes with the patient's own red blood cells (RBCs) markedly reduced the activity of bortezomib. In addition, *in vivo* data in monkeys completed by collaborators suggests that bortezomib is preferentially distributed to and retained in RBCs. Taken together, these data suggest that RBCs interfere with the activity of bortezomib *in vivo* thus causing the drug to be ineffective in CLL.

3.2 Results

Bortezomib treatment is accompanied by an increase in poly-ubiquitinated proteins in CLL cells.

The detection of ubiquitinated proteins was used to assess the degree of proteasomal inhibition because the proteasome is responsible for the degradation of poly-ubiquitinated proteins (Glickman and Ciechanover 2002). CLL cells were treated with increasing concentrations of bortezomib or MG132 for 2-16 hours and then assessed for the presence of poly-ubiquitinated proteins by western blotting.

Ubiquitinated proteins increased in a time- and concentration-dependent manner and preceded apoptosis (Figure 3.1). There was no visible build-up of ubiquitinated proteins in control samples (Figure 3.1, Lanes 1-5). At the lowest concentration of bortezomib (1 nM), build-up of ubiquitinated proteins was time-dependent only reaching high levels at 16 hours (Figure 3.1, Lanes 11-15). In comparison, the build-up of ubiquitinated proteins in cells treated with higher concentrations of bortezomib (10 and 100 nM) and with MG132 was much more rapid (Figure 3.1, Lanes 6-10 and 16-25). Ubiquitinated proteins were visible at 2 hours and reached a plateau between 4 and 8 hours, and decreased by 16 hours. The unexpected decrease in ubiquitinated proteins could be due to the high number of apoptotic cells in the lysates at that time. These data suggest that proteasome activity is maximally blocked within 16 hours at 1 nM of bortezomib and within 2 hours at higher

concentrations of bortezomib (10 and 100 nM) and within 2 hours when the cells are treated with MG132.

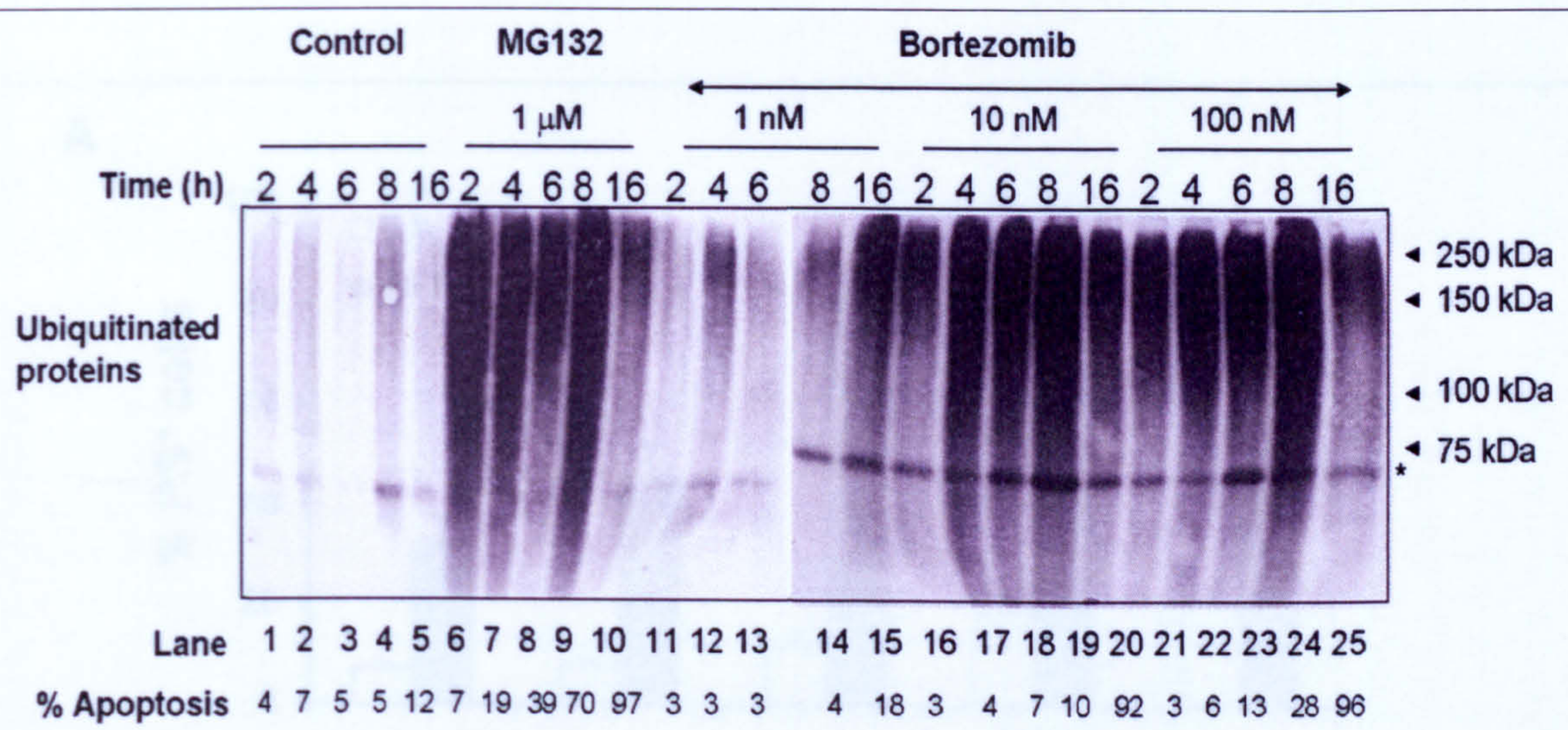

Figure 3.1: Bortezomib inhibits the proteasome in CLL cells as shown by an increase in poly-ubiquitinated proteins. CLL cells from three patients were treated with increasing concentrations of bortezomib (1-100 nM) or MG132 (1 μM) over a time course of 2-16 hours. Control cells were treated with 0.1% DMSO. 5×10^6 cells were collected from each treatment, cell lysates were prepared and the presence of poly-ubiquitinated proteins was assessed by western blotting. Results shown are from one representative patient. Accumulation of poly-ubiquitinated proteins is viewed as a smear. The percentage of PS^+ cells is shown below as a measure of cell death. * is likely to be a non-specific band.

Bortezomib induces apoptosis in all CLL patient samples in a concentration- and time- dependent manner.

Mononuclear cells from CLL patients (n=43) were purified and treated with various concentrations of bortezomib (1-100 nM), MG132 (1 μM), or vehicle only (0.1% DMSO) for up to 24 hours (Figure 3.2 and Table 3.1). Cells from all patients underwent apoptosis in a concentration and time dependent manner. Interestingly, induction of apoptosis was independent of *IGHV* mutational status or acquired resistance to fludarabine (Figure 3.2 and Table 3.1).

Bortezomib induced apoptosis in a concentration-dependent manner in 43 CLL patient samples (Figure 3.2 A and Table 3.1). At 24 hours, 10 and 100 nM bortezomib induced 88 ± 3% and 92 ± 1% apoptosis, respectively. MG132 (1 μM) also induced comparably high

levels of apoptosis (82 ± 5%) at 24 hours. In contrast, 1 nM bortezomib was unable to induce cell death significantly above spontaneous apoptosis (0.1% DMSO only) levels which were 32 ± 4% despite high levels of poly-ubiquitinated proteins.

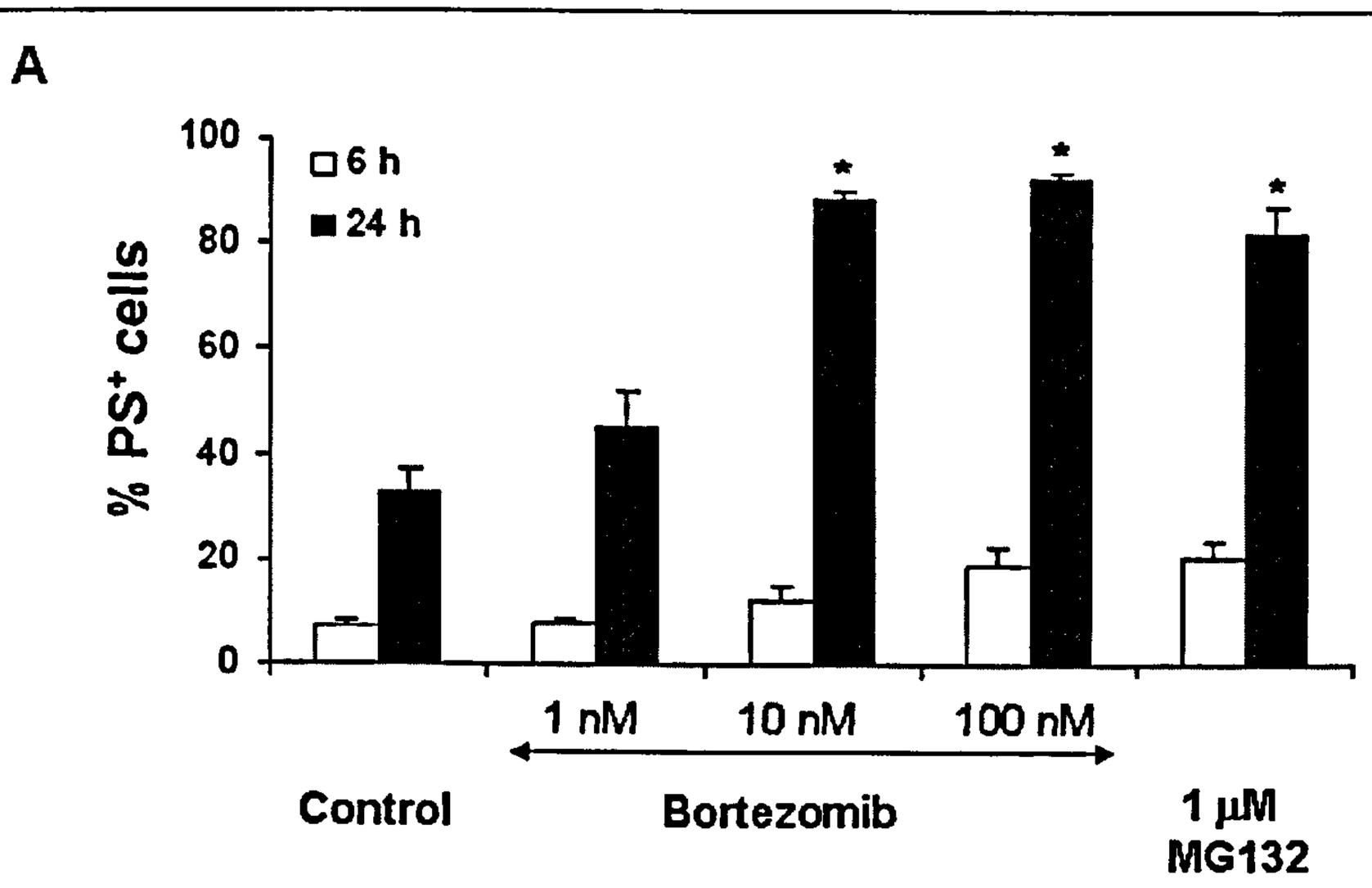

Figure 3.2: Bortezomib induces cell death in CLL cells as shown by % PS^+ cells. A) Purified lymphocytes from 47 CLL patients were treated with increasing concentrations of bortezomib (1-100 nM), 1 µM MG132 as a positive control, or vehicle alone (0.1% DMSO) for 6 and 24 hours. Quantification of cell death was measured by calculating the percent of PS positive cells. Results show % PS^+ cells as a mean value ± SEM for each dose. * denotes a p-value <0.05 as measured by a One Way ANOVA followed by the Dunnett's test. B) A representative patient was treated with increasing concentrations of bortezomib or MG132 over time from 2-24 hours and % PS^+ cells were measured. This figure was completed in collaboration with Dr. Luise Wheat.

Table 3.1: Summary of data from 47 patients with CLL.

Patient	Age/ Sex	Binet stage	Prior therapy	FAMP resistance	WCC x10^9/l	% *IGHV* homology	*IGHV* gene family	% CD 19/5	% PS+ cells
1	76/M	A	NIL		13	95	3 09	61	82
2	60/F	A(P)	NIL		102	88	3 64	75	65
3	90/F	C	CLB, Cyclophosphamide		40	95	3 21	79	88
4	78/F	A	NIL		12	92	4 34	94	83
5	59/M	B	NIL		77	91	4 59	89	87
6	85/F	A(P)	CLB, FAMP		108	100	3 09	84	95
7	76/M	B	FAMP+ Cyclophosphamide	Yes	103	100	3 09	90	91
8	50/F	A	NIL		35	95	3 30	92	81
9	90/M	B	CLB		152	93	1 18	94	95
10	66/M	A	CLB (x 2 courses)		55	86	4 34	88	85
11	87/M	A	NIL		18	97	3 30	78	81
12	85/M	A(0)	CLB		26	99	1 18	85	90
13	61/M	A(0)	NIL		19	94	3 21	77	91
14	72/M	A	FAMP		16	97	3 53	74	94
15	74/M	A	NIL		33	96	4 34	88	87
16	68/M	A(0)	FAMP		21	100	4 59	94	85
17	78/M	A(0)	CLB (x 2 courses)		19	92	1 69	88	96
18	83/F	A(P)	CLB		193	88	3 30	91	92
19	81/F	A	NIL		53	91	3 23	76	95
20	61/M	A	NIL		35	98	3 11	82	95
21	54/M	A	NIL		93	90	3 30	82	91
22	73/F	A(0)	NIL		18	95	4 31	78	84
23	68/M	A(0)	NIL		18	93	4 34	87	90
24	65/M	A	NIL		43	98	3 30	82	97
25	70/M	A(0)	NIL		27	98	3 33	81	96
26	93/M	A	NIL		96	94	3 07	78	86
27	59/M	A	NIL		18	94	3 66	70	66
28	70/M	C	CLB (x2 courses), FAMP, MP, FAMP+Cyclophosphamide	Yes	83	99	3 53	73	88
29	78/M	B	NIL		79	98/94	1 69 /3 07	64	91
30	49/M	A	NIL		75	98	1 69	88	93
31	87/F	A	CLB (x2 courses)		8	98	1 02	93	95
32	66/F	C	CLB, MP, FAMP		350	98	3 74	7	28
33	48/M	A	FAMP		95	99	1 02	68	87
34	70/M	B	CLB (x2 courses), FAMP, Campath		135	95	1 08	76	87
35	75/M	A(0)	NIL		26	93	3 30	82	90
36	80/M	A(0)	NIL		36	96	4 34	86	92
37	56/M	B	CLB, FAMP	Yes	102	96	1 69	76	78
38	79/M	B	CLB (x2 courses)		143	96	2 05	95	93
39	81/M	A(0)	NIL		47	98	3 23	87	84
40	72/M	C	CLB (x3 courses), FAMP, FAMP+Cyclophosphamide	Yes	33	97	4 59	79	82
41	61/F	C	CLB, FAMP, FAMP+Cyclophosphamide, R-CHOP	Yes	517	98	4 59	37	90
42	81/M	A	NIL		82	100	3 23	87	79
43	57/M	A	FAMP, CLB (x 3 courses)		12	94	1 03	77	70
44	45/F	A	NIL		34	96	3 48	65	67
45	67/M	A(0)	NIL		38	99	4 61	82	74
46	76/F	A	NIL		37	90	2 05	87	82
47	65/M	A(0)	NIL		33	86	4 59	72	93

Abbreviations: A(P) denotes progressive Stage A CLL; A(0) denotes Stage A CLL without lymphoadenopathy; FAMP denotes fludarabine; CLB denotes chlorambucil; MP denotes methylprednisolone; NIL indicates no prior therapy; WCC denotes white cell count at diagnosis. Patients # 6-

41 correspond with the patient data shown in figure 1A. We define ≥ 98 % homology of the *IGVH* gene to its germ line sequence as unmutated. % PS^+ cells denotes the % phosphatidyl serine externalisation in PBMCs isolated from each patient after incubation with 100 nM bortezomib for 16 or 24 hours. Clinical data was collected by Dr. Renata Walewska and IGHV mutation status was determined by Dr. Aneela Majid. Response to bortezomib and % CD 19/5 cells was completed in collaboration with Dr. Luise Wheat.

Bortezomib treatment was accompanied by a time-dependent induction of apoptosis as assessed by percentage of PS^+/PI^+ cells (n=10) (Figure 3.2 B). At 10 and 100 nM bortezomib, cells underwent apoptosis between 16 and 24 hours. In contrast, 1 nM bortezomib failed to induce apoptosis at any time point measured. MG132 induced apoptosis more rapidly than bortezomib with apoptosis starting within 4 hours and reaching maximum levels within 12 hours (Figure 3.2 B).

Bortezomib-induced apoptosis correlates with conformational changes of Bax.

Bax activation is important for the induction of spontaneous and drug-induced apoptosis in CLL cells (Bellosillo, Villamor et al. 2002). Furthermore, Bax conformational changes have been associated with proteasome inhibitor-induced apoptosis in CLL cells (Dewson, Snowden et al. 2003). Bax activation is also required for apoptosis induction *via* the intrinsic pathway of apoptosis (Packham and Stevenson 2005). Therefore, conformational changes in Bax were assessed as previously described (Dewson, Snowden et al. 2003). CLL cells were treated with increasing concentrations of bortezomib (1-100 nM) for 2-16 hours (Figure 3.3). A time course of CLL cells treated at 100 nM bortezomib from one representative patient of three is shown (Figure 3.3).

Conformational changes in Bax were observed with increasing time beginning at 4 and 8 hours onwards for 100 and 10 nM, respectively (Figure 3.3 A-C and data not shown). There was no observed change in Bax conformation in cells treated with 1 nM bortezomib, consistent with observations in apoptosis induction (data not shown). Conformational changes in Bax were time-dependent and reached a maximum of 91% at 16 hours (Figure 3.3 A).

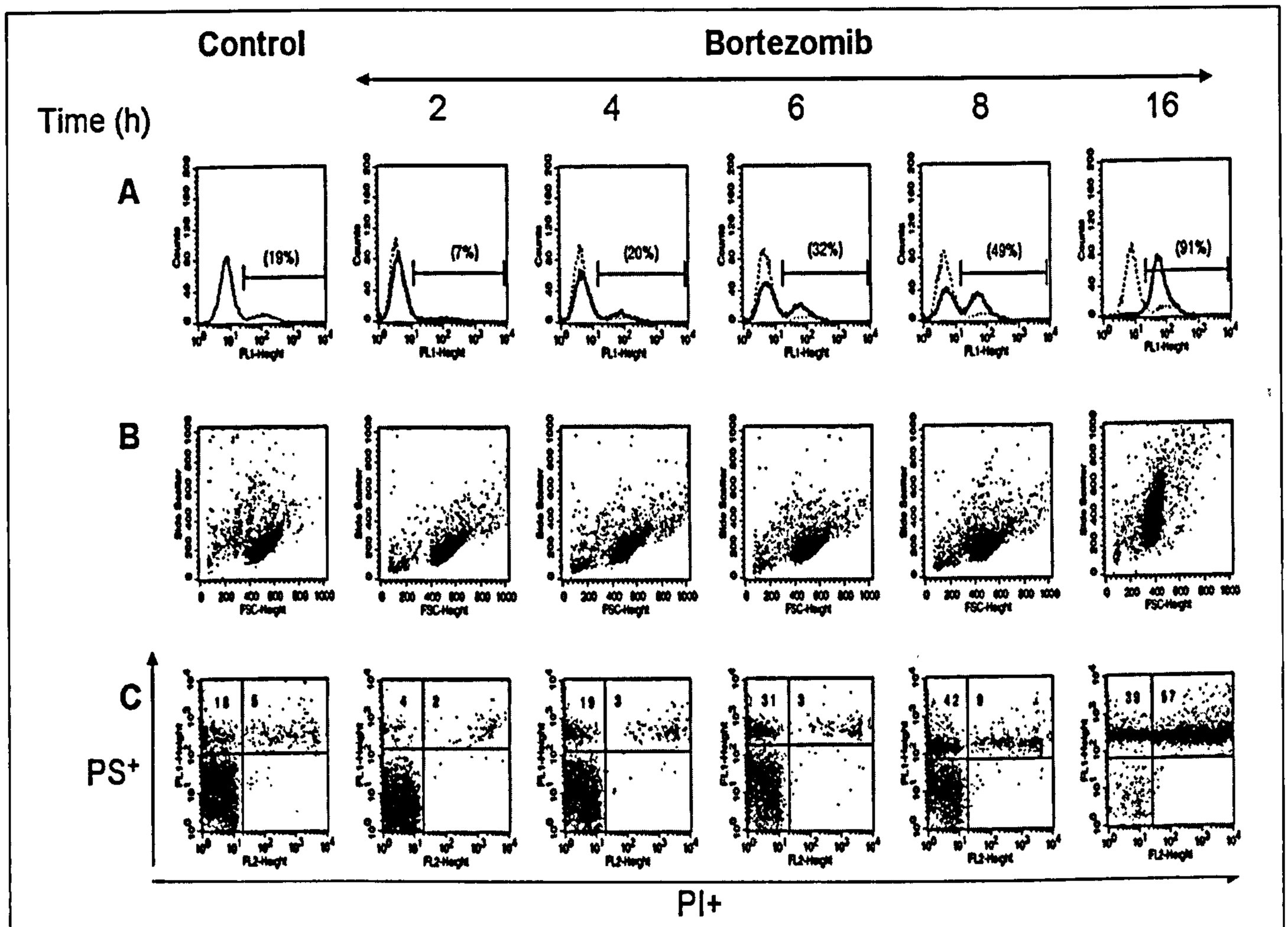

Figure 3.3: An increase in cell death is accompanied by conformational changes in Bax in CLL cells. A) 1 x 10^6 CLL cells were incubated with 100 nM Bortezomib for 2-16 hours fixed, permeabilised and stained with anti-Bax monoclonal antibody Clone 3 (FL1, solid line), or secondary antibody alone for each time point as a negative control (dashed line) for 1 hour on ice. Cells were washed in ice cold PBS and stained with secondary antibody. Conformational changes in Bax were detected by flow cytometry. Figures in brackets indicate geometric mean of the solid line and median of the negative control, respectively. B) Change in forward (FSC) and side (SSC) profiles of CLL cells treated with 100 nM bortezomib for 2-16 hours. C) Corresponding profiles of Annexin V/PI profiles are shown as a reference for quantification of cell death for cells treated with 100 nM bortezomib for 2-16 hours. Numbers in the upper left and upper right quadrants indicate % PS^+ cells and % PS/PI^+ cells, respectively.

Bortezomib-induced apoptosis in CLL cells is accompanied by caspase activation. Caspase activation was measured in CLL cells after treatment with bortezomib (1-100 nM) or MG132 for 2-16 hours (Figure 3.4) to confirm that bortezomib was inducing cell death by apoptosis. Processing of caspase-9, -3, and -8 was observed in a time- and concentration-dependent manner.

Caspase-9 was present in its unprocessed zymogen form in all control samples (Fig. 3.4, Lanes 1-5). However, treatment of CLL cells with all concentrations of bortezomib or MG132 led to the processing of procaspase-9 to its active forms. This was demonstrated by the accumulation of the catalytically active p35 and p37 forms as well as the disappearance of the proform. This was particularly evident when higher concentrations of bortezomib were used (10 and 100 nM) and when MG132 was used (Figure 3.4, Lanes 6-10 and 16-25). Processing began as early as 2 hours with the appearance of the p35 fragment followed by the caspase-3 dependent appearance of the p37 fragment by 16 hours with both 10 and 100 nM bortezomib (Figure 3.4, Lanes 16-25). The p37 fragment appeared at 4 hours in MG132-treated cells; compared with 16 hours in bortezomib-treated cells (Figure 3.4, Lanes 7-10 and Lanes 15 and 25). This is probably because MG132-induced apoptosis occured more rapidly than bortezomib-induced apoptosis. In samples treated with 1 nM bortezomib, caspase-9 processing was evident at 2 hours, most likely due to stabilisation of active caspase-9 within the cells (Figure 3.4, Lane 11). However, only the p35 fragment was observed until 16 hours (Figure 3.4, Lanes 11-14). At 16 hours, p35, low levels of p37, and the p20 fragments were observed (Figure 3.4, Lane 15).

At later times, particularly with higher concentrations of bortezomib (10 and 100 nM) and MG132, the accumulation of two uncharacterised bands of caspase-9 appeared (Figure 3.4, Lanes 9, 10, 15, 20, and 25). They were approximately of sizes p20 and p22 and have been described in CLL before upon treatment with CDDO (Inoue, Snowden et al. 2004). They are likely to be caused by further processing of the p35 and p37 fragments.

Caspase-3 was present as an unprocessed zymogen in control samples that had been treated with 0.1% DMSO (Figure 3.4, Lanes 1-5). Caspase-3 processing from the pro-form to the processed p20, -19, and -17 fragments was time and concentration-dependent. At 1 nM bortezomib treatment, no processing of caspase-3 was visible (Figure 3.4, Lanes 11-15). At 10 nM bortezomib processing of caspase-3 into its p20, -19 and low levels of p17 fragments was visible at 16 hours only (Figure 3.4, Lane 20). The decreasing level of the proform of caspase-3 accompanied the build-up of processed caspase-3, particularly the p19 and p20 forms. The activation of caspase-3 was more rapid in CLL cells treated with the highest concentration of bortezomib (100 nM) and with MG132 (Figure 3.4, Lanes 21-25 and 6-10, respectively). Processing of the proform of caspase-3 was observed starting at 6 and 4 hours, respectively. In both cases, levels of the processed forms increased up

until 8 hours (Figure 3.4, Lanes 6-9 and 21-24). At 16 hours, the processed versions of caspase-3 appeared to decrease slightly. This is likely to be caused by a decrease in loading.

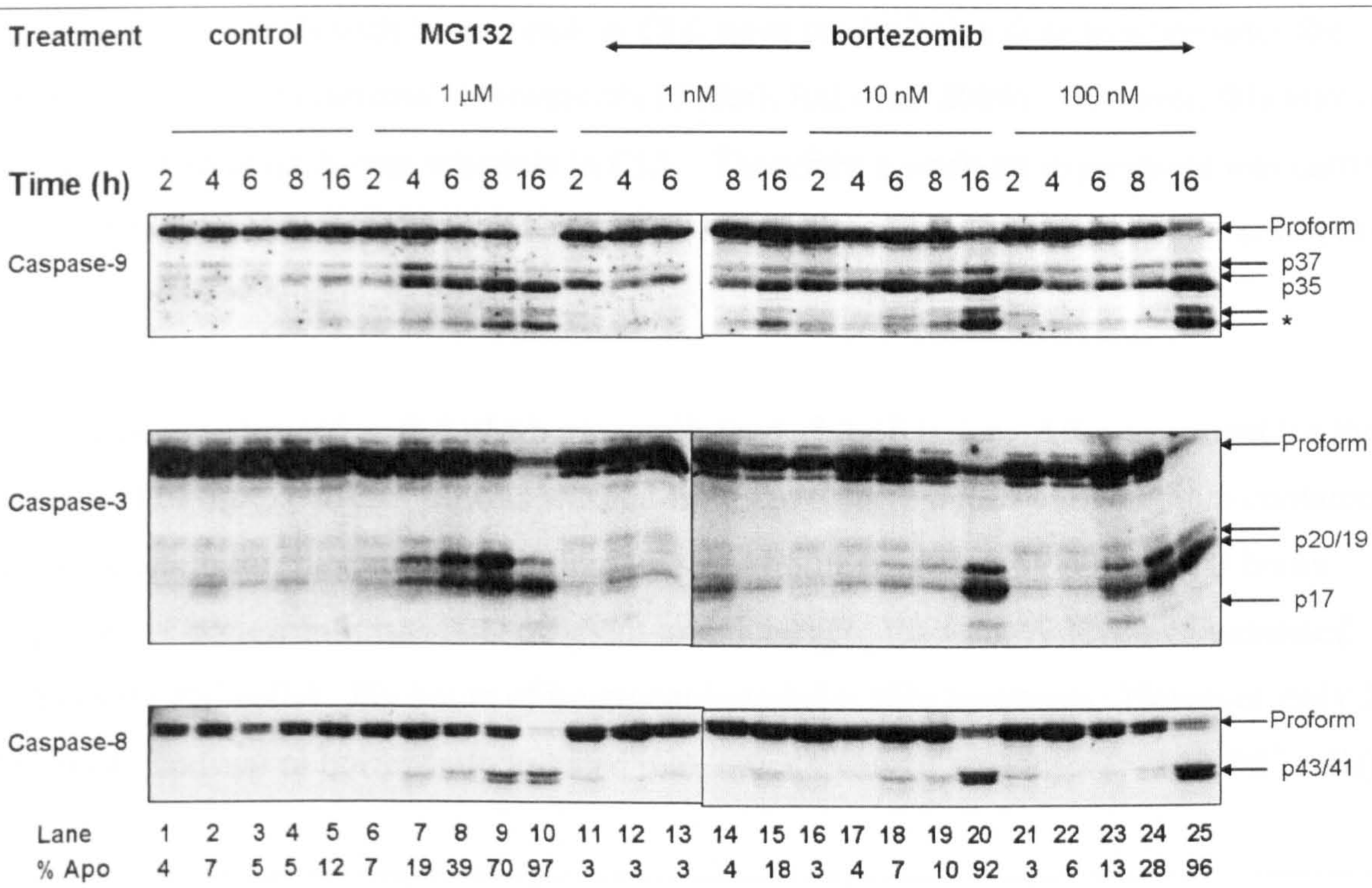

Figure 3.4: Bortezomib induces apoptosis in CLL as shown by activation of caspases -9, -3, and -8. CLL cells were treated with increasing concentrations of bortezomib (1-100 nM), MG132 (1 μM), or vehicle only (0.1% DMSO) over a time course of 2-16 hours. Cell lysates were prepared after treatment for various times and processing of caspases -9, -3, and -8 were examined by Western blotting. The result shown is from one representative patient of three and percentage cell death is shown on the bottom of the figure as measured by % PS^+ cells.

Caspase-8 activation appeared to occur late compared with caspase-3 and, particularly, caspase-9 activation. As with caspase-9 and -3, bortezomib-induced caspase-8 activation appeared to be time and concentration-dependent (Figure 3.4). Caspase-8 processing into its processed p43 and p41 forms was only observed when cells were treated with the highest concentrations of bortezomib and a high percentage of cell death was observed (10 and 100 nM at 16 hours only Figure 3.4, Lanes 20 and 25). Caspase-8 processing was accompanied by the decrease in the pro-form of caspase-8. In MG132 treated CLL cells,

caspase-8 processing occurred as early as 8 hours and increased at 16 hours (Figure 3.4, Lanes 9 and 10).

Bortezomib activity in CLL is dependent on time of exposure to the drug.

Current clinical trials with bortezomib in CLL have used a bolus dose to administer the drug even though bortezomib is reversible (Faderl, Rai et al. 2006). However, this may not be the most suitable dosing schedule in CLL. Therefore a washout experiment was carried out to determine whether CLL cells require a long exposure to bortezomib to be committed to undergo apoptosis.

CLL cells were treated with 5 nM bortezomib for 1, 3, or 6 hours. After treatment for the set period of time, bortezomib was washed from the cells replaced with medium containing no bortezomib for the remainder of time up to 24 hours (Figure 3.5). One and 3 hours exposure of bortezomib was not sufficient to induce apoptosis above levels of untreated cells (35% PS^+ cells). Six hours of treatment induced > 50% apoptosis. However, only 24 hours of exposure to bortezomib induced maximum levels of apoptosis (> 90% PS^+ cells).

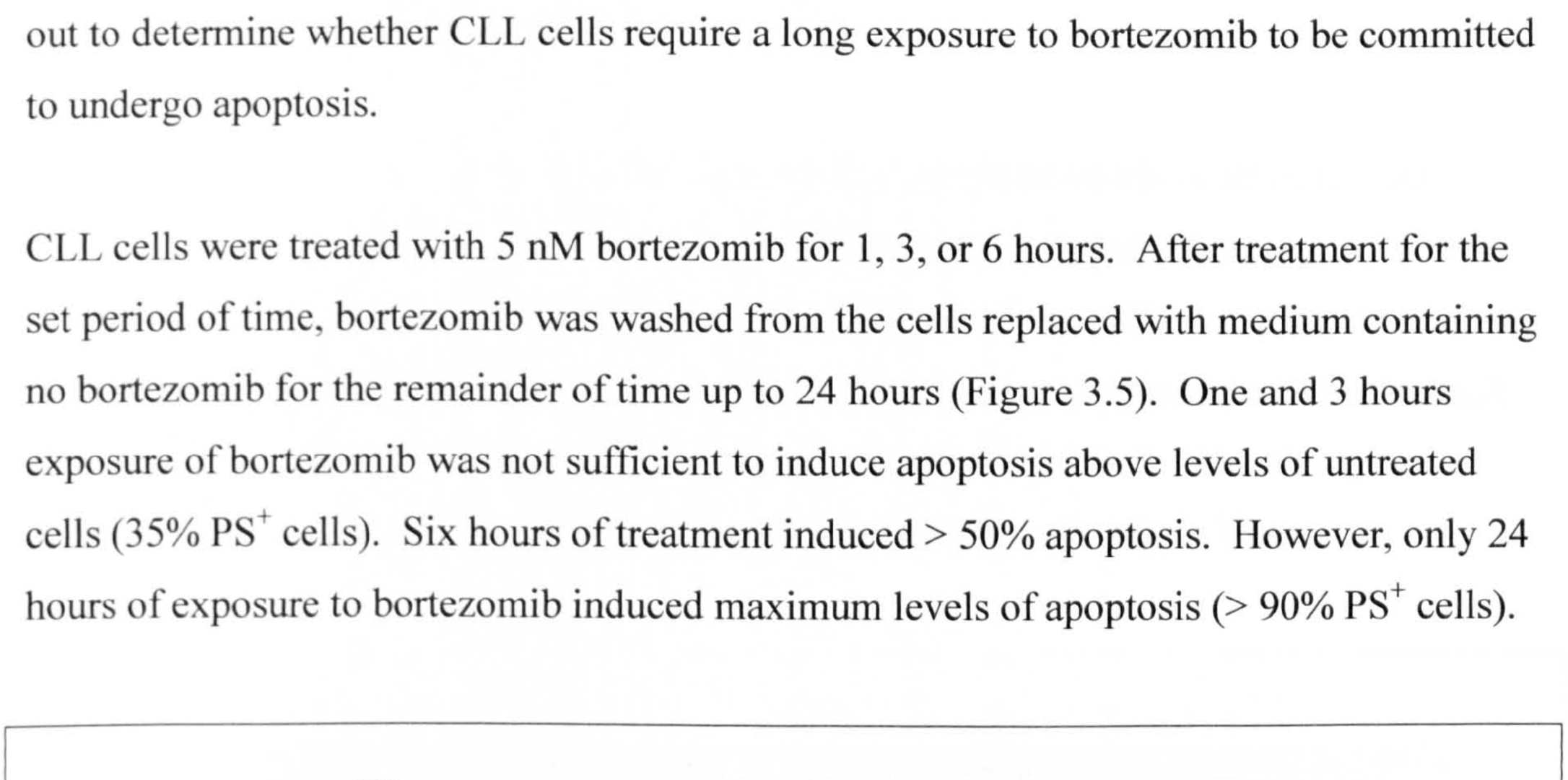

Figure 3.5: Bortezomib activity in CLL is dependent on time of exposure to the drug. CLL cells from one patient were treated with bortezomib (5 nM) for 1, 3, 6, or 24 hours. After treatment, bortezomib was washed out and cells were given fresh media. The cells were left for the remainder of time up to 24 hours. Cell death was then measured by quantification of % PS^+ cells after a total incubation time of 24 hours.

Bortezomib activity is reduced by co-culture of CLL cells with whole blood.

To determine whether components of whole blood could reduce activity of bortezomib in CLL *in vivo*, a whole blood apoptosis assay was developed to mimic *in vivo* conditions. CLL cells from 13 patients were either purified as previously described, or incubated in whole blood. Cells were treated with increasing concentrations of bortezomib (1-100 nM) or MG132 for 24 hours. The percentage of $PS^+/PI^+/CD19^+$ cells was used to determine cell death in B cells only (Figure 3.6).

Incubation with whole blood increased spontaneous apoptosis levels in all cases. As expected, treatment of purified CLL cells with bortezomib (10 and 100 nM) and MG132 induced high levels of apoptosis (> 90% PS^+ cells) in all 13 cases (Figure 3.6). In contrast, incubation of CLL cells in whole blood with corresponding concentrations of bortezomib reduced bortezomib-induced apoptosis to control levels (Figure 3.6). The ability of MG132 to induce apoptosis was not affected by incubation with whole blood.

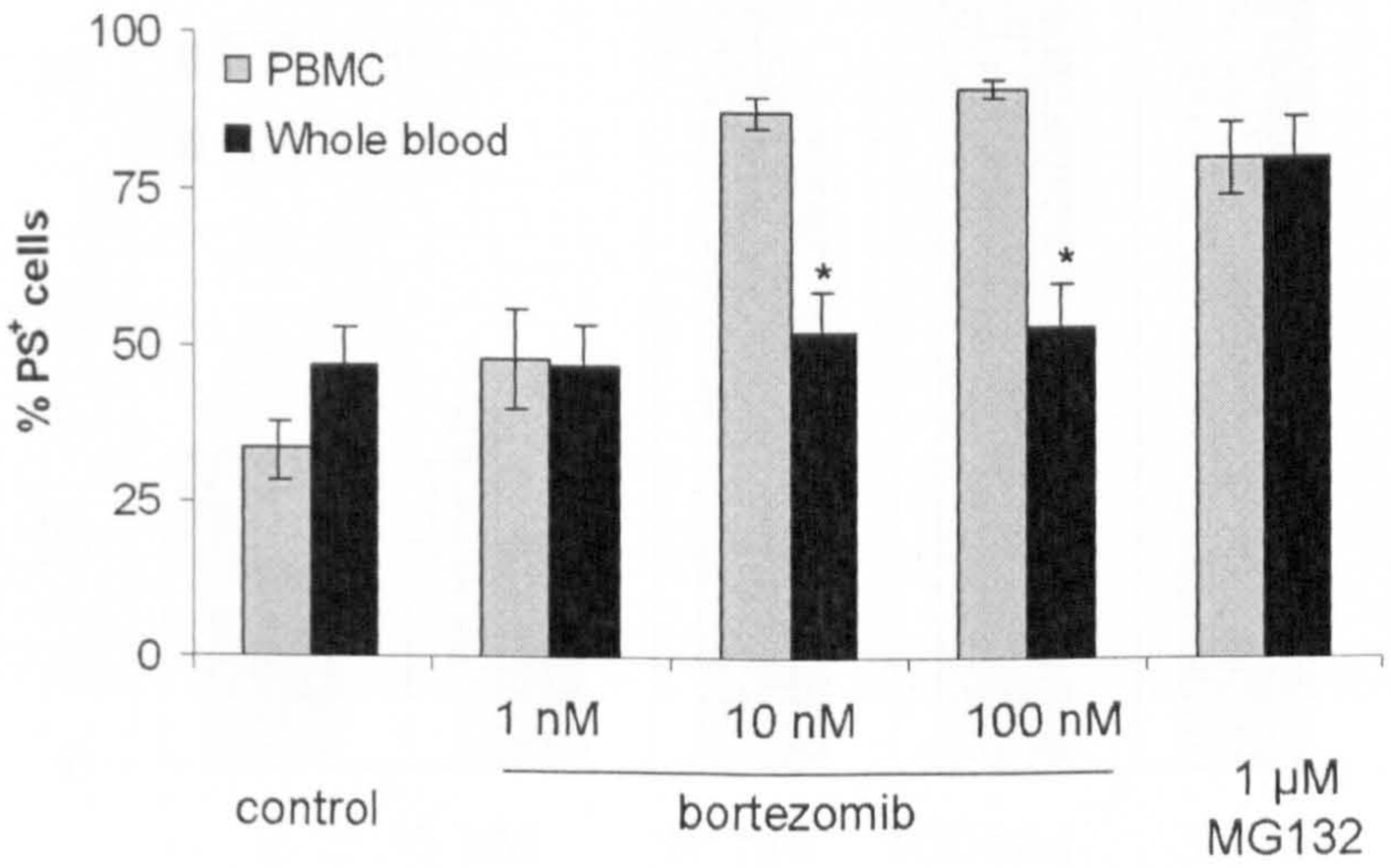

Fig 3.6: The activity of bortezomib is reduced in the presence of CLL whole blood compared with purified CLL lymphocytes in cell culture media. Isolated CLL cells (grey bars) or CLL cells in whole blood (black bars) from 13 patients were treated for 24 hours with increasing concentrations of bortezomib (1-100 nM), MG132 (1 μM), or vehicle alone (0.1 % DMSO). Cell death was measured by flow cytometry using Annexin V/7AAD staining. In all samples, cell death was measured by gating on $CD19^+$ cells. Data are presented as a mean ± SEM. * indicates a p value < 0.05 in samples treated in whole blood compared to those treated as purified cells as measured by the student's t-test. This figure was completed in collaboration with Dr. Luise Wheat.

Plasma does not affect the activity of bortezomib in CLL cells.

Plasma may affect the activity of bortezomib *in vivo*, by either binding to it, or activating a survival pathway (Jones, Ganeshaguru et al. 2003; Flinn, Byrd et al. 2005). CLL lymphocytes from 7 patients were purified as previously described and treated in 10% Foetal Calf Serum (FCS) or 10 to 100% of the patients own plasma (AHP) and treated with increasing concentrations of bortezomib (10 and 100 nM) or MG132 for 24 hours (Figure 3.7). The percentage of PS^+/PI^+ cells was used to determine apoptosis. As expected, both concentrations of bortezomib and MG132 induced > 80% apoptosis at 24 hours in all patients tested compared with control levels (~ 35% PS^+ cells). There was no statistical difference between treatment of CLL cells in FCS or AHP as measured by the a One Way ANOVA followed by the Dunnett's test (Figure 3.7). Therefore AHP did not interfere with bortezomib activity *in vitro*.

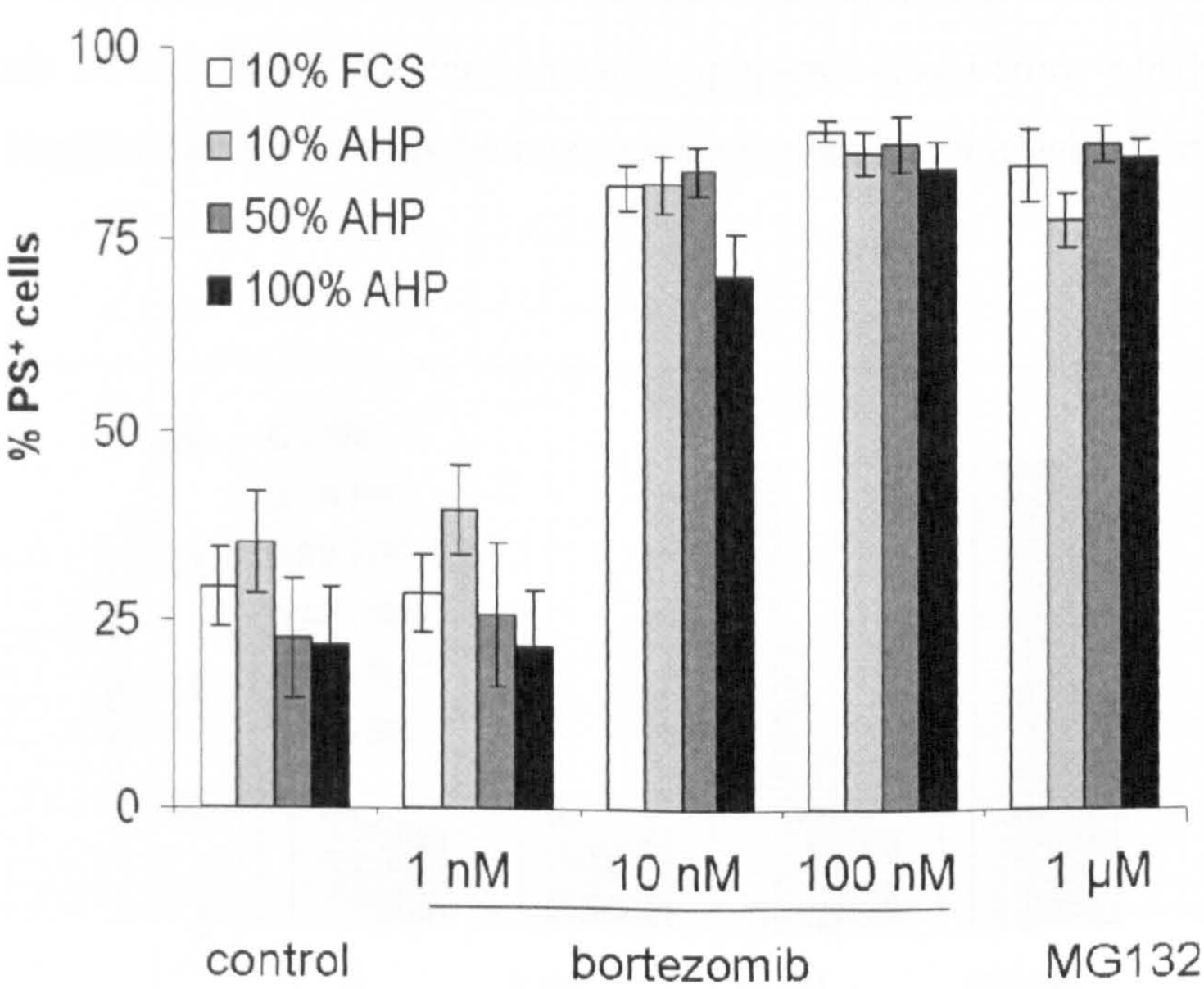

Figure 3.7: Plasma does not have an effect on bortezomib-induced apoptosis in CLL cells. Cells from seven patients with CLL were treated in duplicate with increasing concentrations of bortezomib (1-100 nM), MG132 (1 µM), or vehicle only (0.1% DMSO) 24 hours. Cultures were either supplemented with 10% FCS or 10 to 100% of autologous human plasma (AHP). Cell death was assessed by % PS^+ cells and presented as a mean ± SEM. This figure was provided by Dr. Luise Wheat.

Co-incubation of RBCs with purified CLL cells decreases the apoptosis-inducing activity of bortezomib *in vitro*.

It remained a possibility that RBCs were interfering with the ability of bortezomib to induce apoptosis in CLL. Therefore, purified CLL cells from 5 patients were incubated with increasing levels of RBCs (0-50% RBC) and treated with increasing concentrations of bortezomib (1-100 nM) for 24 hours and cell death in B cells was determined by measuring the percentage of $PS^+/PI^+/CD19^+$ cells (Figure 3.8). In control cells and 1 nM bortezomib-treated cells the RBCs appeared to decrease spontaneous apoptosis by up to 15% (Figure 3.8). When cells were treated with 10 nM bortezomib (without RBCs), apoptosis was induced (> 90% PS^+ cells) (Figure 3.8). However, apoptosis was inhibited by RBCs in a concentration-dependent manner. Five percent RBC inhibited apoptosis from > 90% to 60%. Inhibition of apoptosis increased with increasing RBC levels. The highest level of RBC (50%) reduced apoptosis to control levels. When cells were treated with 100 nM bortezomib, higher levels of RBCs were required to inhibit bortezomib activity. Only 50 % RBCs were able to reduce apoptosis levels from > 90% to 50%. These data suggest that RBCs may be responsible for interfereing with bortezomib activity *in vivo*.

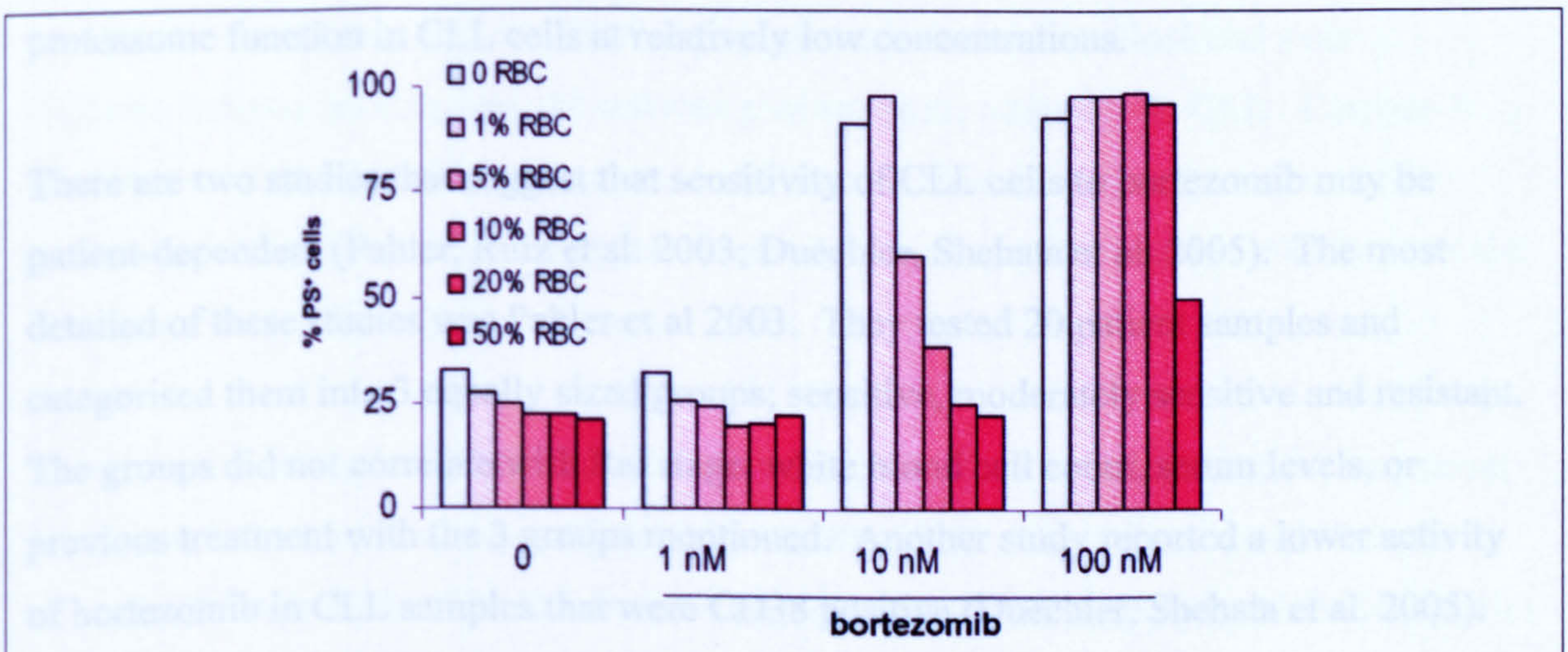

Figure 3.8: Incubation of purified CLL cells with red blood cells (RBC) decreased apoptosis-inducing activity of bortezomib *in vitro*. Isolated lymphocytes from six patients were treated with increasing concentrations of bortezomib (1-100 nM) or vehicle only (0.1% DMSO) for 24h in the presence or absence of 1, 5, 10, 20, or 50 % autologous RBC recovered from the lymphocyte preparation. Cell death was measured in $CD19^+$ cells by Annexin V/7AAD staining. Results are shown from one representative patient. This figure was completed in collaboration with Dr. Luise Wheat.

3.3 Discussion

Bortezomib is currently in Phase II/III clinical trials for several haematological malignancies including multiple myeloma, where it has been shown to be particularly effective (Cavo 2006; Popat, Joel et al. 2006). However, not all patients respond to bortezomib and some can develop resistance (Wu, van Wieringen et al. 2005). Interestingly, clinical trials with CLL using the same dosing regimen have been particularly discouraging, showing little efficacy (O'Connor 2005; Faderl, Rai et al. 2006). This is surprising given the promising *in vitro* data (Pahler, Ruiz et al. 2003; Kelley, Alkan et al. 2004). The discrepancy between *in vitro* and *in vivo* data in CLL was addressed in this study. This first part of this study aimed at characterising the activity and mechanism of action of bortezomib *in vitro* in CLL and the second part of this study was to address possible mechanisms of resistance of CLL to bortezomib that may occur *in vivo*.

Bortezomib has been shown to specifically and reversibly block the function of the 26S proteasome (Adams 2001; Adams 2002). This causes an accumulation of ubiquitinated proteins. The accumulation of ubiquitinated proteins occurred in a concentration- and time- dependent manner and occurred rapidly when bortezomib was used at high concentrations (Figure 3.1). Taken together, these data suggests that bortezomib inhibited proteasome function in CLL cells at relatively low concentrations.

There are two studies that suggest that sensitivity of CLL cells to bortezomib may be patient-dependent (Pahler, Ruiz et al. 2003; Duechler, Shehata et al. 2005). The most detailed of these studies was Pahler et al 2003. They tested 20 patient samples and categorised them into 3 equally sized groups; sensitive, moderately sensitive and resistant. The groups did not correlate with Rai stage, white blood cell count, serum levels, or previous treatment with the 3 groups mentioned. Another study reported a lower activity of bortezomib in CLL samples that were CD38 positive (Duechler, Shehata et al. 2005). One other less extensive study using bortezomib in CLL reported no patient variation in response to bortezomib, however, the sample size was small (n=10) (Kelley, Alkan et al. 2004). This was the first study with a large sample size to see no variation in response to bortezomib treatment. Because there was no variation in response to bortezomib treatment, there was also no observed correlation between response to bortezomib and *IGHV* gene mutation status and acquired resistance to fludarabine (Figure 3.2 and Table

3.1). It is worth mentioning that no variation in CLL patient samples has been reported in studies using lactacystin or MG132 (Chandra, Niemer et al. 1998; Masdehors, Omura et al. 1999; Masdehors, Merle-Beral et al. 2000; Almond, Snowden et al. 2001; Dewson, Snowden et al. 2003).

MG132 and lactacystin have induce a Bax conformational change in CLL cells (Almond, Snowden et al. 2001; Dewson, Snowden et al. 2003). In this study, conformational changes in Bax, due to bortezomib treatment, correlated well with apoptosis induction as measured by % AnnexinV/PI positive cells. It was expected for Bax conformational changes to precede late stage apoptotic markers such as AnnexinV binding and PI uptake and changes in cell size. As expected, Bax conformational change preceded changes in the forward scatter/side scatter profile, which measures the size of the cells (Figure 3.3 A and B). This difference in timing was most evident at 8 hours. Surprisingly, Bax conformational change did not appear to precede Annexin V/PI staining (Figure 3.3 A and C). Bax conformational change may be a late apoptotic event in response to bortezomib treatment however a more detailed time course is necessary to address this issue.

Proteasome inhibitors have been shown to initiate a caspase cascade in CLL cells (Almond, Snowden et al. 2001; Dewson, Snowden et al. 2003). As expected, bortezomib treatment initiated caspases-9, -3 and -8 processing in a concentration- and time-dependent manner confirming the activation of apoptotic pathways in CLL. Caspase-9 appeared to be the first caspase activated and thus the apical caspase, however, further studies including a more extensive time course or use of specific caspase-inhibitors would be required to confirm this.

These studies indicate that bortezomib induces high levels of apoptosis in all CLL patient samples *in vitro*; however why no such activity was observed *in vivo* was not clear (Jackson, Einsele et al. 2005; O'Connor 2005; Caravita, de Fabritiis et al. 2006; Faderl, Rai et al. 2006). One possible reason for the apparent lack of activity was current dosing schedules used in CLL. A bolus dose has been used in clinical trials (Jackson, Einsele et al. 2005; O'Connor 2005; Caravita, de Fabritiis et al. 2006; Faderl, Rai et al. 2006). However, a bolus dose does not maintain serum levels for extended periods of time and this may be detrimental for therapy because bortezomib is a reversible inhibitor (Figure A.2). Figure 3.5 shows that CLL cells require contact with bortezomib for at least 6 hours

for the drug to induce high levels of apoptosis. These data suggest that an infusional dose of bortezomib over an extended period of time may improve clinical responses in CLL patients.

It was also possible that a component of whole blood was blocking the activity of bortezomib *in vivo*. Incubation of CLL cells with whole blood completely inhibited bortezomib-induced apoptosis (Figure 3.6). Interestingly, it did not block MG132-induced apoptosis suggesting that a component of whole blood specifically blocks bortezomib activity, but not activity of other proteasome inhibitors.

It has been previously reported that autologous plasma can interfere with activity of flavopiridol by binding to it *in vivo*, thus limiting its activity in CLL (Flinn, Byrd et al. 2005). Different dosing schedules have been successful in resolving this problem (Rudek, Bauer et al. 2003). In addition, albumin in plasma has been shown to activate the AKT survival pathway in CLL, thus affecting fludarabine activity (Jones, Ganeshaguru et al. 2003). However, incubation with increasing concentrations of plasma had a minimal effect on the apoptotic activity of bortezomib suggesting that plasma has little to do with the lack of clinical response seen in CLL patients (Figure 3.7).

RBCs blocked bortezomib-induced apoptosis in a concentration-dependent manner (Figure 3.8). This suggested that RBCs may have been taking up bortezomib *in vivo*, thus causing inactivity of the drug. Therefore *in vivo* monkey models were set up by collaborators at Johnson and Johnson to test this hypothesis and the details of these experiments are shown in the Appendix (Figure A.2). Bortezomib concentration in the plasma and whole blood fractions were measured before and after 4 bolus doses of bortezomib. The whole blood fraction (containing RBCs) maintained the highest concentration of bortezomib for the longest period of time confirming that RBCs were taking up bortezomib preferentially to plasma. Taken together with data from Figure 3.8, these data suggest that RBCs are, at least in part, responsible for the poor clinical activity of bortezomib observed in CLL.

Interestingly, MG132 was not affected by incubation with whole blood. Although its non-specific nature renders it unsuitable for clincal trials (Tsubuki, Saito et al. 1996), MG132 is very useful as a postive control in this case. This result suggests that a structural difference in MG132 and bortezomib is the key to preferential RBC uptake. This structural

difference may lie in the fact that MG132 is a peptide aldehyde, while bortezomib is a peptide boronic acid. Further studies with different classes of proteasome inhibitors should be completed to determine what structural difference is responsible for the preferential uptake by RBCs.

Given that bortezomib uptake by RBCs appears to be a problem in CLL, it is surprising that reports are not made of poor responses in other malignancies such as mantle cell lymphoma, multiple myeloma and solid tumours. Reasons for this are not clear but there are several possibilities. First, multiple myeloma is a disease that infiltrates the bone and tissue. Therefore, bortezomib may have good activity when taken up very rapidly by tissue. In this model, and in solid tumour malignancies, bortezomib may be able to reach areas with fewer RBCs and therefore maintain its activity. Second, Figure 3.8 suggests that preferential bortezomib uptake by RBCs may be dependent on the ratio of lymphocytes to RBCs. Therefore, patients with a high WBC count and therefore a high WBC to RBC ratio may have a more promising outcome with bortezomib treatment. This may explain some of the activity of bortezomib in mantle cell lymphoma and also some of the moderate activity in CLL. However, this also suggests that bortezomib may only be effective when the WBC to RBC ratio is high.

Finally, bortezomib has been reported to induce apoptosis at lower concentrations in cycling B-CLL cells (Bogner, Schneller et al. 2003). In addition, resting B cells were shown to be less sensitive to proteasomal inhibition than stem cells (Chandra, Niemer et al. 1998). CLL is a disease that is characterised by the slow accumulation of B cells and their failure to undergo apopotosis (Caligaris-Cappio and Hamblin 1999). The majority of CLL cells do not proliferate rapidly (Caligaris-Cappio and Hamblin 1999). In contrast, mantle cell lymphoma is characterised by a rapid proliferation of B cells (Fernandez, Hartmann et al. 2005). Therefore in clinical trials, bortezomib may be more effective in mantle cell lymphoma because these cells are more sensitive to bortezomib than CLL cells due to their high proliferative index. This could also be the case with multiple myeloma and solid tumours where bortezomib has been shown to be a promising therapeutic agent *in vivo*. There is currently no study comparing the relative responses and sensitivities to bortezomib in many different primary tumour types and these data warrant such a study.

Although bortezomib has been reported to be effective as an anti-cancer agent in numerous diseases in clinical trials, treatment with bortezomib is associated with significant toxicities (Agterof and Biesma 2005; Chim, Ooi et al. 2005; Engelhardt, Muller et al. 2005; Jaskiewicz, Herrington et al. 2005; Knoops, Jacquemain et al. 2005; Lonial, Waller et al. 2005; Pour, Hajek et al. 2005; Van Regenmortel, Van de Voorde et al. 2005; Caravita, de Fabritiis et al. 2006; Faderl, Rai et al. 2006; Gupta, Pagliuca et al. 2006; Miyakoshi, Kami et al. 2006; Richardson, Briemberg et al. 2006; Richardson, Mitsiades et al. 2006; Stubblefield, Slovin et al. 2006; Voortman and Giaccone 2006). Because RBCs are effectively lowering the concentration of bortezomib available to the target cells, an increase in the dose of bortezomib may be required to combat RBC uptake. However this leaves a small therapeutic window in which to treat CLL, or other malignancies, whilst avoiding dangerous and unwanted toxicity. In addition, the uptake of bortezomib by RBCs could be exacerbating the unwanted side effects that have been reported in the literature.

The data in this chapter would suggest that bortezomib is not an ideal single agent therapy for use in CLL however structurally different proteasome inhibitors may show some promise (Chauhan, Catley et al. 2005; Chauhan, Hideshima et al. 2006; Ruiz, Krupnik et al. 2006). A novel proteasome inhibitor (NPI-0052) has been described as suitable for anti-cancer therapy and has been shown to be more effective at inducing apoptosis *in vitro* in CLL than bortezomib (Chauhan, Catley et al. 2005; Chauhan, Hideshima et al. 2006; Ruiz, Krupnik et al. 2006). Future work should focus on investigating the use of bortezomib in combination with other therapies in CLL, or should focus on evaluating NPI-0052 for use as a single agent in CLL.

Chapter 4: The use of TRAIL Monoclonal Antibodies in CLL

4.1 Introduction: The use of TRAIL Monoclonal Antibodies in CLL.

The ability of TRAIL to signal to apoptosis via TRAIL-R1 and TRAIL-R2 in malignant cells, but induce relatively low levels of apoptosis in normal cells has suggested it may be a promising therapy for cancer (Wiley, Schooley et al. 1995; Pitti, Marsters et al. 1996; Ashkenazi, Pai et al. 1999; Griffith, Rauch et al. 1999; Walczak, Miller et al. 1999). There are currently a number of different forms of TRAIL in clinical trials (Wiley, Schooley et al. 1995; Pitti, Marsters et al. 1996; Adams, Palombella et al. 1999). Agonsitic antibodies to TRAIL-R1 and TRAIL-R2 have been developed (Wiley, Schooley et al. 1995; Pitti, Marsters et al. 1996; Georgakis, Li et al. 2003; Johnson, Huang et al. 2003; Georgakis, Li et al. 2005; Pukac, Kanakaraj et al. 2005).

CLL cells are resistant to TRAIL when treated without a sensitising agent (MacFarlane, Harper et al. 2002). Recent reports have suggested that various therapeutic agents can sensitise CLL cells to TRAIL-induced apoptosis (Johnston, Kabore et al. 2003; Inoue, MacFarlane et al. 2004; Kabore, Sun et al. 2006). Although some of the data are correlative and the mechanisms of sensitisation are not always clear, it has been hypothesised that fludarabine and bortezomib upregulate TRAIL receptor expression at the cell surface and HDAC inhibitors increase recruitment of FADD to the DISC (Johnston, Kabore et al. 2003; Inoue, MacFarlane et al. 2004; Kabore, Sun et al. 2006).

Human Genome Sciences (HGS) have developed and characterised humanised monoclonal antibodies to TRAIL-R1 and TRAIL-R2 named ETR1 and ETR2, respectively (Johnson, Huang et al. 2003; Georgakis, Li et al. 2005; Pukac, Kanakaraj et al. 2005; Zeng, Wu et al. 2006). The antibodies have been humanised to minimise immunogenicity. ETR1 and ETR2 are agonistic antibodies and are used without the need for cross-linking, making them distinct from other antibodies to TRAIL-R1 and TRAIL-R2 (Griffith, Rauch et al. 1999; Wagner, King et al. 2003; Wang, Engels et al. 2004; Georgakis, Li et al. 2005). However, ETR1 and ETR2 have not been characterised as a potential single agent therapy or in combination with other agents for use in CLL.

Chapter 4: The use of TRAIL mAbs in CLL

The aims of this study were to characterise the apoptotic activity of ETR1 and ETR2 in CLL either as single agents or in combination therapy. It was also important to compare the apoptotic activity of ETR1 and ETR2 against versions of TRAIL that are candidates for clinical trials, such as Apo2L and HIS-tagged TRAIL, to determine the best candidates for clinical trials in this disease. Four cell lines were used to characterise the apoptotic activity of ETR1 and ETR2 compared with HIS-tagged TRAIL. In addition receptor-surface expression was measured to predict the activity of ETR1 and ETR2 in each cell line. The apoptotic activity of ETR1 and ETR2 was determined in CLL with and without sensitising agents

4.2 Results

Surface expression of TRAIL-R1 and TRAIL-R2 and the activity of ETR1 and ETR2 in a panel of cell lines.

Z-138 (mantle cell lymphoma), Ramos (burkitt lymphoma), Jurkat E6.1 (T-cell lymphoblastic leukaemia) and Elijah (burkitt lymphoma) cells were treated with increasing concentrations of ETR1 and ETR2 either alone or in combination or with HIS-tagged TRAIL for up to 8 hours (Figures 4.1-4.4 A). Z-138, Ramos and Jurkat cells were sensitive to HIS-tagged TRAIL (59 ± 4.8, 75 ± 8, and 32 ± 8 % PS^+ cells, respectively) confirming the activity of HIS-tagged TRAIL through either TRAIL-R1 or TRAIL-R2 (Figures 4.1-4.3 A). Elijah cells were resistant to HIS-tagged TRAIL (Figure 4.4 A).

ETR1 induced apoptosis in Z-138 and Ramos cells in a concentration-dependent manner, reaching maximum levels of apoptosis after treatment with 250 ng/ml ETR1 (46 ± 11 and 91 ± 1 % PS^+ cells, respectively) (Figures 4.1 and 4.2 A). In contrast, ETR2 did not induced apoptosis in Z-138 or Ramos cells even at 1000 ng/ml (9 ± 4 and 13 ± 3 % PS^+ cells, respectively) (Figures 4.1 and 4.2 A). Jurkat and Elijah cells were mildly sensitive to ETR1 when it was used at 1000 ng/ml (24 ± 1 and 17 ± 3 % PS^+ cells, respectively), however ETR2, or ligand induced high levels of apoptosis in Jurkat cells but failed to induce apoptosis in Elijah cells (62 ± 6 and 8 ± 1 % PS^+ cells respectively) (Figures 4.3 and 4.4 A). Using ETR1 and ETR2 in combination did not increase levels of apoptosis in any of the cell lines tested (Figures 4.1-4.4 A)

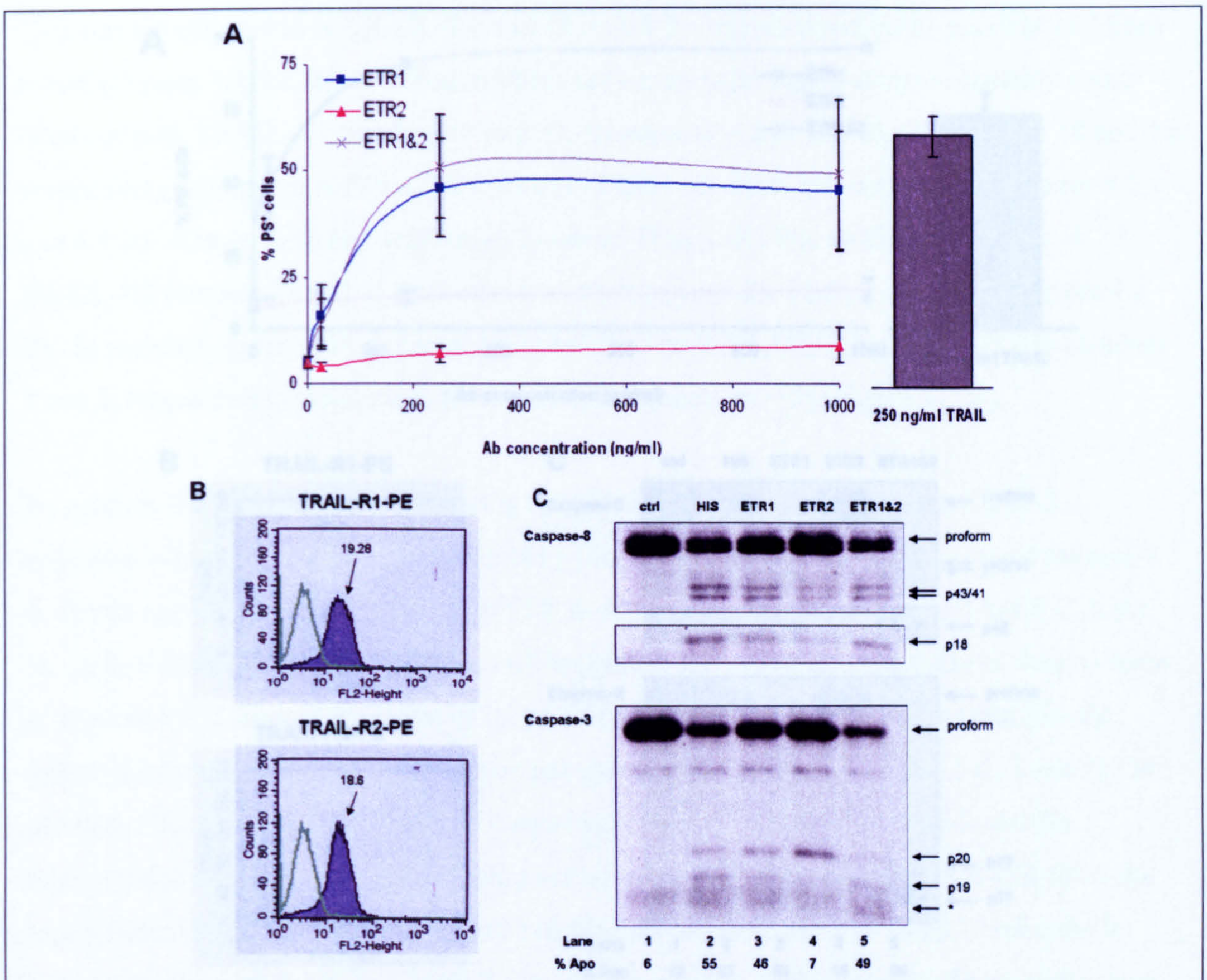

Figure 4.1: Surface expression of TRAIL-R1 and TRAIL-R2 and activity of ETR1 and ETR2 in Z-138 cells. A) Z-138 cells were treated at a density of $1x10^6$ cells per ml with HIS-tagged TRAIL (250 ng/ml) or increasing concentrations of ETR1 or ETR2 (25-1000 ng/ml) either alone or in combination for 4 hours. Control cells were treated with vehicle only (1% PBS). Cell death was quantified by measuring the percentage of PS^+ cells. Results show the mean ± SEM of at least three independent experiments. B) Z-138 cells were labelled with PE-labelled TRAIL-R1, TRAIL-R2 or IgG1 as described in Materials and Methods. Surface expression of each receptor and IgG1 were measured by flow cytometry. The green line represents the isotype control and the purple line represents the surface expression of either TRAIL-R1 or TRAIL-R2. The number in each histogram is the median of TRAIL-R1 or TRAIL-R2. Results shown are representative of three independent experiments. C) After treatment with selected concentrations of TRAIL (250 ng/ml) and TRAIL mAbs (1000 ng/ml), cell lysates were prepared and caspase-8 and -3 processing was measured by western blotting. The upper portion of the caspase-8 blot was exposed for 1 minute but the lower portion of the caspase-8 blot (showing the p18 fragment) was exposed for 5 mins. Results are representative of two independent experiments. * denotes a non-specific band.

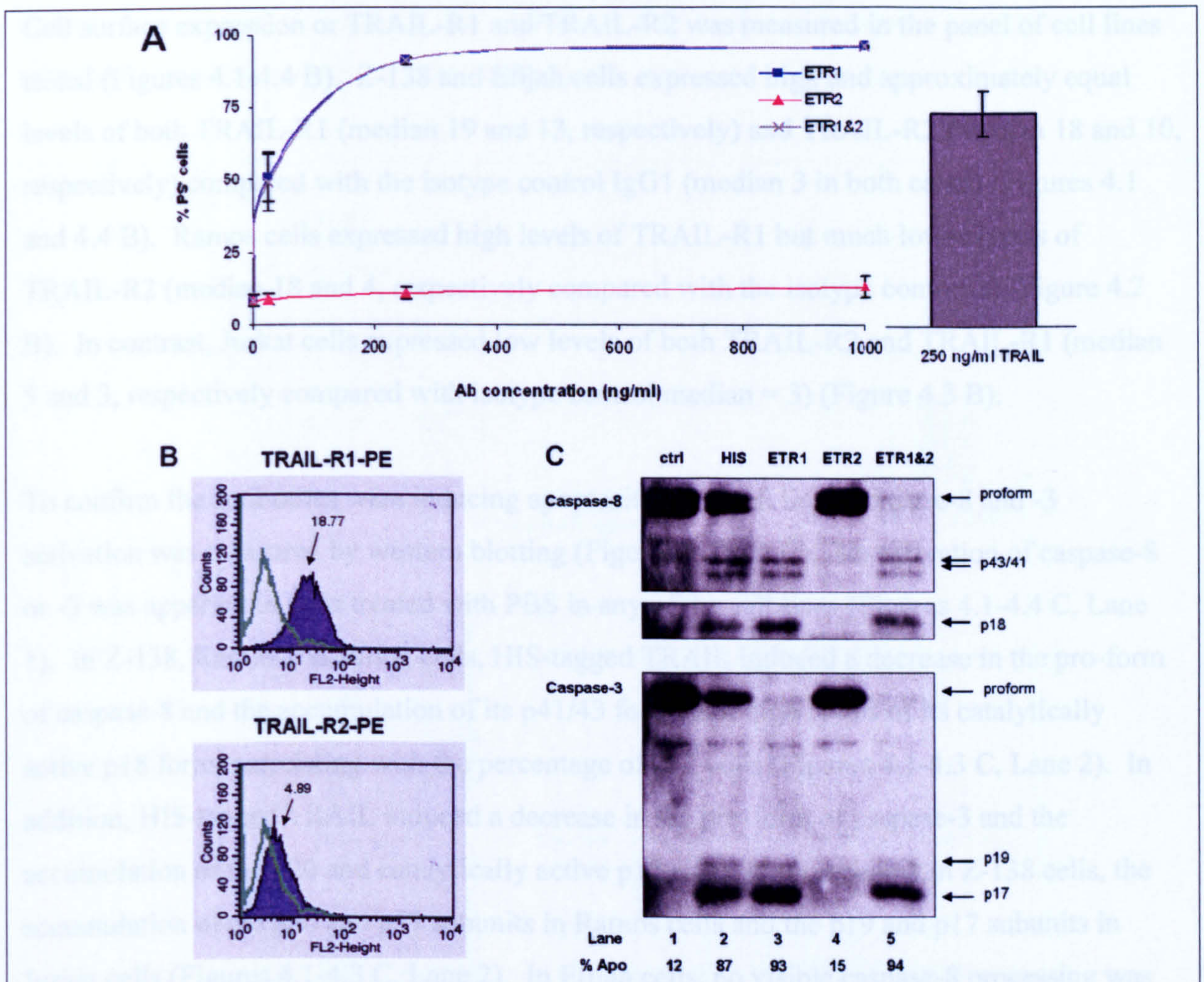

Figure 4.2: Surface expression of TRAIL-R1 and TRAIL-R2 and activity of ETR1 and ETR2 in Ramos cells. A) Ramos cells were treated at a density of $1x10^6$ cells per ml with HIS-tagged TRAIL (250 ng/ml) or increasing concentrations of ETR1 or ETR2 (25-1000 ng/ml) either alone or in combination for 4 hours. Control cells were treated with vehicle only (1 % PBS). Cell death was quantified by measuring the percentage of PS^+ cells. Results show mean ± SEM of at least three independent experiments. B) Ramos cells were labelled with PE-labelled TRAIL-R1, TRAIL-R2 or IgG1 as described in Materials and Methods. Surface expression of each receptor and isotype control was measured by flow cytometry. The green line represents the isotype control and the purple line represents the surface expression of either TRAIL-R1 or TRAIL-R2. The number in each histogram is the median of TRAIL-R1 or TRAIL-R2. Results shown are representative of three independent experiments. C) After treatment with selected concentrations of TRAIL (250 ng/ml) and TRAIL mAbs (1000 ng/ml), cell lysates were prepared and caspase-8 and -3 processing was measured by western blotting. The upper portion of the caspase-8 western blot was exposed for 5 minutes but the lower portion was exposed for 15 minutes. Results are representative of three independent experiments.

Cell surface expression or TRAIL-R1 and TRAIL-R2 was measured in the panel of cell lines tested (Figures 4.1-4.4 B). Z-138 and Elijah cells expressed high and approximately equal levels of both TRAIL-R1 (median 19 and 13, respectively) and TRAIL-R2 (median 18 and 10, respectively) compared with the isotype control IgG1 (median 3 in both cases) (Figures 4.1 and 4.4 B). Ramos cells expressed high levels of TRAIL-R1 but much lower levels of TRAIL-R2 (median 18 and 4, respectively compared with the isotype control 3) (Figure 4.2 B). In contrast, Jurkat cells expressed low levels of both TRAIL-R2 and TRAIL-R1 (median 5 and 3, respectively compared with isotype control median = 3) (Figure 4.3 B).

To confirm the antibodies were inducing apoptosis in the cell lines, caspase-8 and -3 activation was measured by western blotting (Figures 4.1-4.4 C). No activation of caspase-8 or -3 was apparent in cells treated with PBS in any of the cell lines (Figures 4.1-4.4 C, Lane 1). In Z-138, Ramos and Jurkat cells, HIS-tagged TRAIL induced a decrease in the pro-form of caspase-8 and the accumulation of its p41/43 forms and high levels of its catalytically active p18 form, correlating with the percentage of PS^+ cells (Figures 4.1-4.3 C, Lane 2). In addition, HIS-tagged TRAIL induced a decrease in the pro-form of caspase-3 and the accumulation of the p20 and catalytically active p19 subunit of caspase-3 in Z-138 cells, the accumulation of the p20 and p17 subunits in Ramos cells and the p19 and p17 subunits in Jurkat cells (Figures 4.1-4.3 C, Lane 2). In Elijah cells, no visible caspase-8 processing was apparent in samples treated with HIS-tagged TRAIL (Figure 4.4 C, Lane 2). However, there appeared to be a low level of the p20 form of caspase-3 in these cells.

After treatment with ETR1 a moderate decrease in the proforms of both caspase-8 and -3 were observed in Z-138 and Jurkat cells compared with control samples (Figure 4.1 and 4.3 C, Lanes 1 and 3). This corresponded with the appearance of both the p43/41 and the p18 forms of caspase-8 in Z-138 cells and the p43/41 forms of caspase-8 in Jurkat cells. In Jurkat cells, low levels of the p19 and p17 fragments and in Z-138 cells low levels of the p20 and p19 fragments of caspase-3 were visible after treatment with ETR1. In contrast, in Ramos cells the proforms of caspase-8 and -3 were not detectable but high levels of the p43/41 and p18 forms of caspase-8 and the p19/17 forms of caspase-3 were visible. After treatment with ETR1, Elijah cells had slightly decreased caspase-8 and -3 proforms but this may be due to unequal

loading. No processed caspase-8 was visible in ETR1-treated Elijah cells. Low levels of the p20 fragment of caspase-3 were detected.

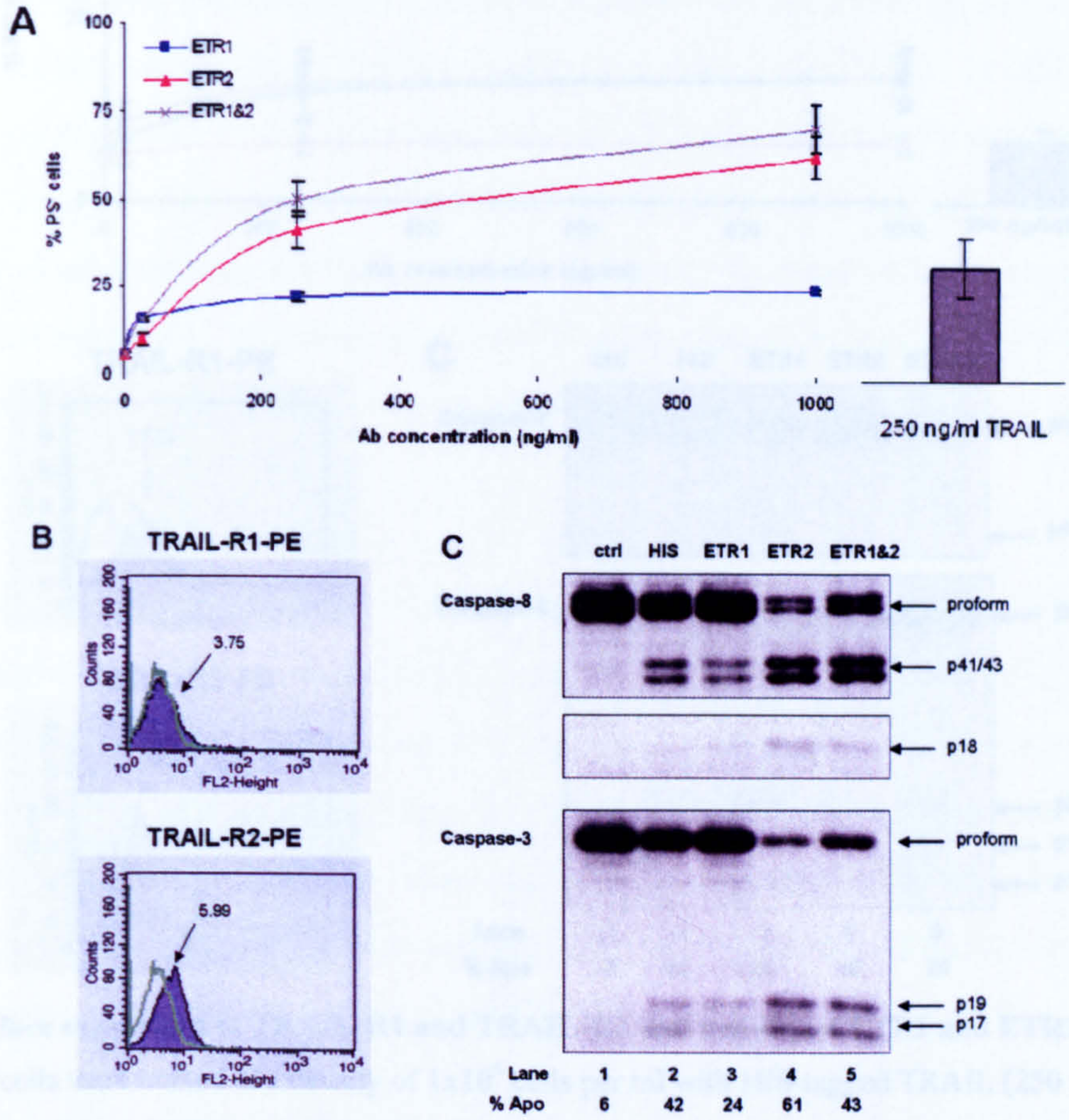

Figure 4.3: Surface expression of TRAIL-R1 and TRAIL-R2 and activity of ETR1 and ETR2 in Jurkat E6.1 cells. A) Jurkat clone E6.1 cells were treated at a density of $1x10^6$ cells per ml with HIS-tagged TRAIL (250 ng/ml) or increasing concentrations of ETR1 or ETR2 (25-1000 ng/ml) either alone or in combination for 8 hours. Control cells were treated with vehicle only (1 % PBS). Cell death was quantified by measuring the percentage of PS^+ cells. Results show the mean ± SEM of at least three independent experiments. B) Jurkat cells were labelled with PE-labelled TRAIL-R1, TRAIL-R2 or IgG1 as described in Materials and Methods. Surface expression of each receptor and IgG1 were measured by flow cytometry. The green line represents the isotype control and the purple line represents the surface expression of either TRAIL-R1 or TRAIL-R2. The number in each histogram is the median of TRAIL-R1 or TRAIL-R2. Results shown are representative of three independent experiments. C) After treatment with selected concentrations of TRAIL (250 ng/ml) and TRAIL mAbs (1000 ng/ml), cell lysates were prepared and caspase-8 and -3 processing was measured by western blotting. The upper portion of the caspase-8 western blot was exposed for 5 minutes and the lower portion was exposed for 10 minutes. Results are representative of at least three independent experiments.

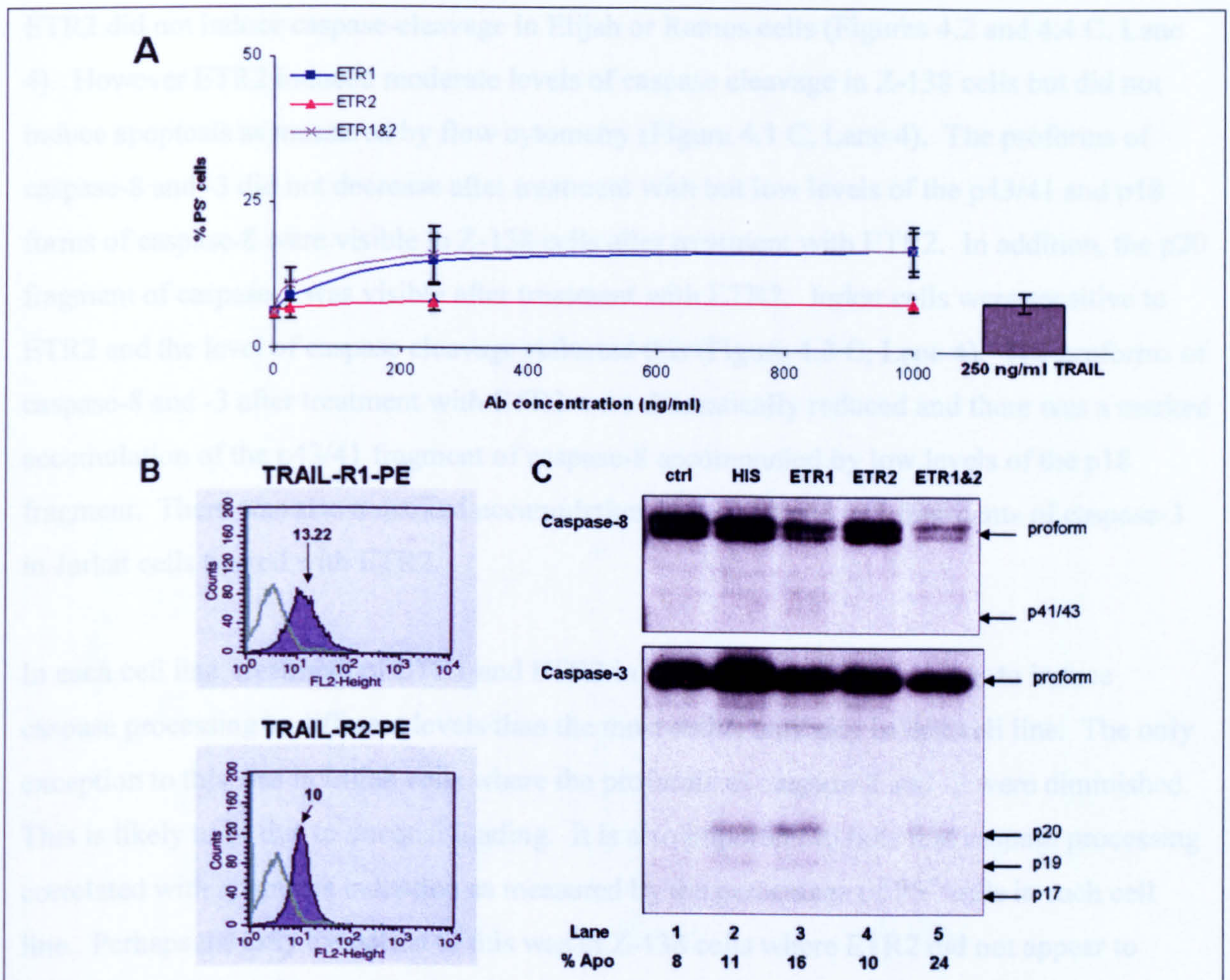

Figure 4.4: Surface expression of TRAIL-R1 and TRAIL-R2 and activity of ETR1 and ETR2 in Elijah cells. A) Elijah cells were treated at a density of $1x10^6$ cells per ml with HIS-tagged TRAIL (250 ng/ml) or increasing concentrations of ETR1 or ETR2 (25-1000 ng/ml) either alone or in combination for 8 hours. Control cells were treated with vehicle only (1% PBS). Cell death was quantified by measuring the percentage of PS^+ cells. Results show the mean ± SEM of three independent experiments. B) Elijah cells were labelled with PE-labelled TRAIL-R1, TRAIL-R2 or IgG1 as described in Materials and Methods. Surface expression of each receptor and IgG1 were measured by flow cytometry. The green line represents the isotype control and the purple line represents the surface expression of either TRAIL-R1 or TRAIL-R2. The number in each histogram is the median of TRAIL-R1 or TRAIL-R2. Results shown are representative of three independent experiments. C) After treatment with selected concentrations of TRIAL (250 ng/ml) and TRAIL Abs (1000 ng/ml), cell lysates were prepared and caspase-8 and -3 processing was measured by western blotting. Results are representative of one independent experiment.

ETR2 did not induce caspase-cleavage in Elijah or Ramos cells (Figures 4.2 and 4.4 C, Lane 4). However ETR2 induced moderate levels of caspase cleavage in Z-138 cells but did not induce apoptosis as measured by flow cytometry (Figure 4.1 C, Lane 4). The proforms of caspase-8 and -3 did not decrease after treatment with but low levels of the p43/41 and p18 forms of caspase-8 were visible in Z-138 cells after treatment with ETR2. In addition, the p20 fragment of caspase-3 was visible after treatment with ETR2. Jurkat cells were sensitive to ETR2 and the level of caspase cleavage reflected this (Figure 4.3 C, Lane 4). The proforms of caspase-8 and -3 after treatment with ETR2 were dramatically reduced and there was a marked accumulation of the p43/41 fragment of caspase-8 accompanied by low levels of the p18 fragment. There was also a marked accumulation of the p19 and p17 fragments of caspase-3 in Jurkat cells treated with ETR2.

In each cell line, treatment of ETR1 and ETR2 in combination did not appear to induce caspase processing to different levels than the most active antibody in that cell line. The only exception to this was in Elijah cells where the proforms of caspase-8 and -3 were diminished. This is likely to be due to unequal loading. It is also important to note that caspase processing correlated with apoptosis induction as measured by the percentage of PS^+ cells in each cell line. Perhaps the only exception to this was in Z-138 cells where ETR2 did not appear to induce high levels of caspase processing but induced apoptosis in 46% of cells.

Apoptosis inducing ability of ETR1 and ETR2 as single agents in CLL patient samples. CLL cells have previously been reported to be resistant to TRAIL (MacFarlane, Harper et al. 2002). To confirm this using TRAIL mAbs, CLL cells from 10 patient samples were treated with increasing concentrations of ETR1 or ETR2 (100-1000 ng/ml) or with either HIS-tagged TRAIL (100 ng/ml) or vehicle only (0.1% DMSO) for 6 hours (Figure 4.5).

Spontaneous apoptosis varied between patient samples. Overall, cells from CLL patient samples did not respond to any form of TRAIL (6 out of 10 patient samples did not respond to treatment with ETR1 or ETR2). However, there was some variation in these results. In one patient sample, treatment with ETR2 in particular but also ETR1, led to a mild concentration-dependent decrease in spontaneous apoptosis (~ 5 % decrease in spontaneous apoptosis in

patient 5). In 3 out of 10 patient samples (patients 1, 3, and 8), ETR1 induced low levels of apoptosis above control samples (~ 5-10 % apoptosis). In 2 of these patient samples the response to ETR1 was concentration-dependent (patients 3 and 8). Although ETR1 induced apoptosis in some patient samples, apoptosis induction occurred in a low percentage of cells and did not occur in the majority of patient samples.

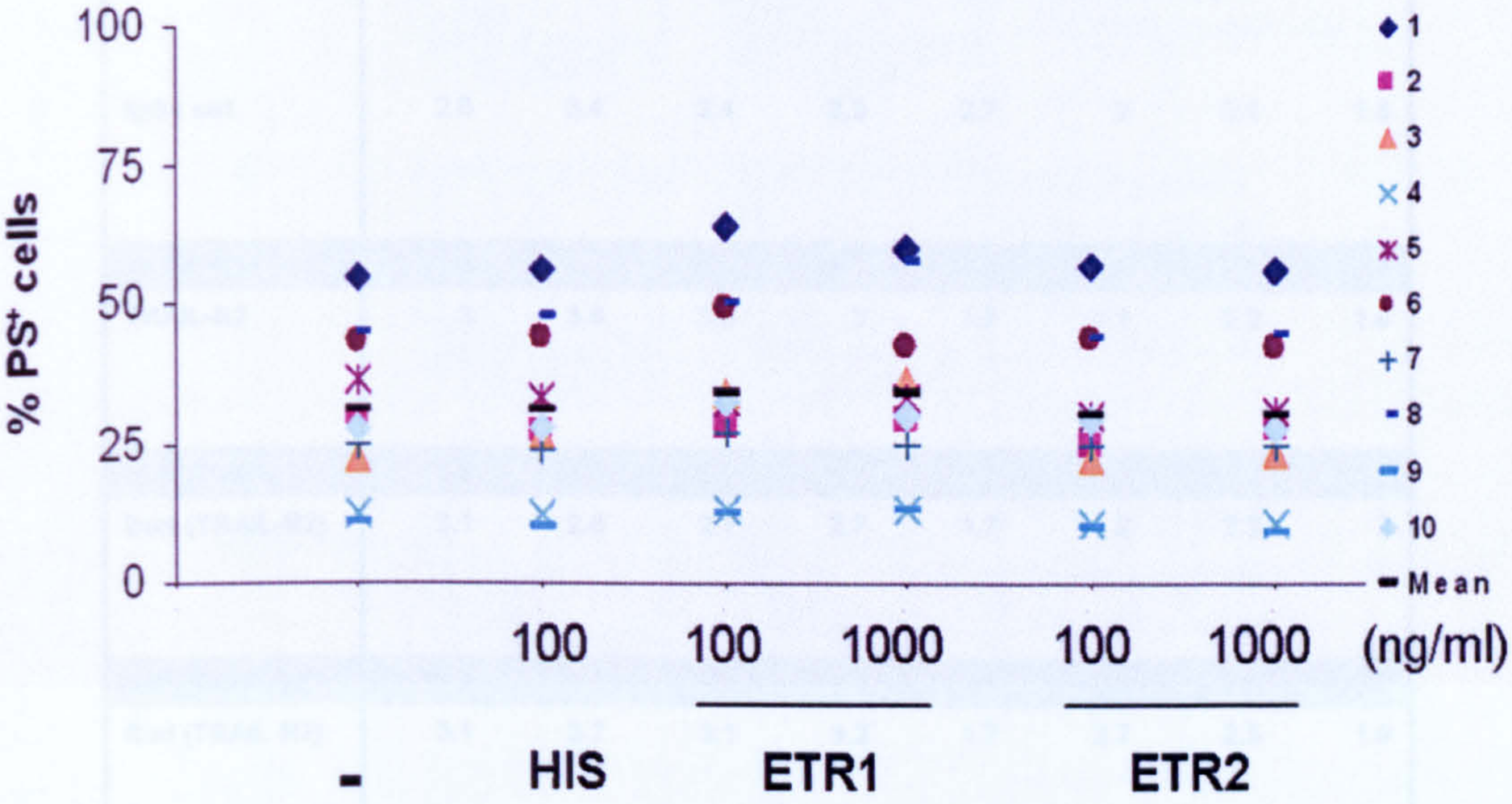

Figure 4.5: Primary CLL cells are resistant to ETR1 and ETR2 alone. CLL cells from 10 patients were purified and cultured at a density of $5x10^6$ per ml with HIS-tagged TRAIL (100 ng/ml) or increasing concentrations of ETR1 or ETR2 (100-1000 ng/ml) for 6 hours. Control cells were treated with vehicle only (1% PBS). Cell death was quantified by measuring the percentage of PS^+ cells. Each patient is depicted as a single symbol on the graph. The black bar represents the mean of all patient samples.

Changes in Surface expression of TRAIL-R1 and TRAIL-R2 in CLL patient samples after exposure to sensitising chemotherapeutic drugs

Although CLL cells are resistant to TRAIL, various drugs including fludarabine, bortezomib and HDAC inhibitors, have been shown to overcome this resistance (Johnston, Kabore et al. 2003; Inoue, MacFarlane et al. 2004; Kabore, Sun et al. 2006). Sensitisation was suggested to be through an upregulation of TRAIL-receptors (Johnston, Kabore et al. 2003; Kabore, Sun et al. 2006). Therefore, CLL cells from 8 patients were pretreated with fludarabine, bortezomib,

depsipeptide or valproate for 16 hours. After treatment, cells were measured for TRAIL-R1 and TRAIL-R2 surface expression (Figure 4.6 and Table 4.1). One patient sample was used as representative and corresponds to patient 2 in Figures 4.5, 4.7 and 4.8 and in Table 4.1. The data are also summarised in Table 4.1.

Table 4.1: Changes in TRAIL-receptor surface expression after treatment with various therapeutic agents in 8 CLL patient samples.

Patient Number	*1*	*2*	*3*	*4*	*5*	*6*	*7*	*10*
IgG1 ctrl	2.6	3.4	2.4	2.3	2.7	2	2.1	1.8
TRAIL-R1	3.5	6.1	5.5	4.4	2	2.4	2.7	3.8
TRAIL-R2	3	3.6	3.5	3	1.7	2.1	2.2	1.9
bort (TRAIL-R1)	3.9	4.4	5.2	4.1	2.3	2.6	2.3	3.3
bort (TRAIL-R2)	3.1	2.6	2.7	2.7	1.7	2	2.2	2
flud (TRAIL-R1)	3.8	6.3	4.4	3.9	2.1	2.2	2.6	3.8
flud (TRAIL-R2)	3.1	3.7	3.1	3.2	1.7	2.7	2.5	1.9
depsi (TRAIL-R1)	3.9	6.3	6.3	4.9	2.5	3.1	3.3	3.7
depsi (TRAIL-R2)	3.1	3.9	3.3	3.1	1.9	2.3	2.2	2.2
VPA (TRAIL-R1)	3.8	9	6.1	6.6	3	3.6	2.6	4.6
VPA (TRAIL-R2)	3.1	4.5	3.9	3.9	2.1	2.2	2.4	2.3

CLL samples were purified and treated with various therapeutic agents at a density of 5 x 10^6 per ml for 16 hours. After treatment cells were stained with PE-conjugated TRAIL-R1 or TRAIL-R2 as described in Materials and Methods. PE-conjugated IgG1 was used as an isotype control. Each patient number corresponds to the patient numbers in Figures 4.5, 4.7 and 4.8. The numbers shown are the median-fluorescence intensity after staining with IgG1, TRAIL-R1-PE or TRAIL-R2-PE as determined by flow cytometry. The lines containing TRAIL-R1 and TRAIL-R2 show the surface expression of TRAIL-receptors without pretreatment. Abbreviations are; bort (1 nM bortezomib), flud (10 μM fludarabine), depsi (10 nM depsipeptide) and VPA (2 mM valproate). IgG1 ctrl is the median fluorescence intensity of the isotype control.

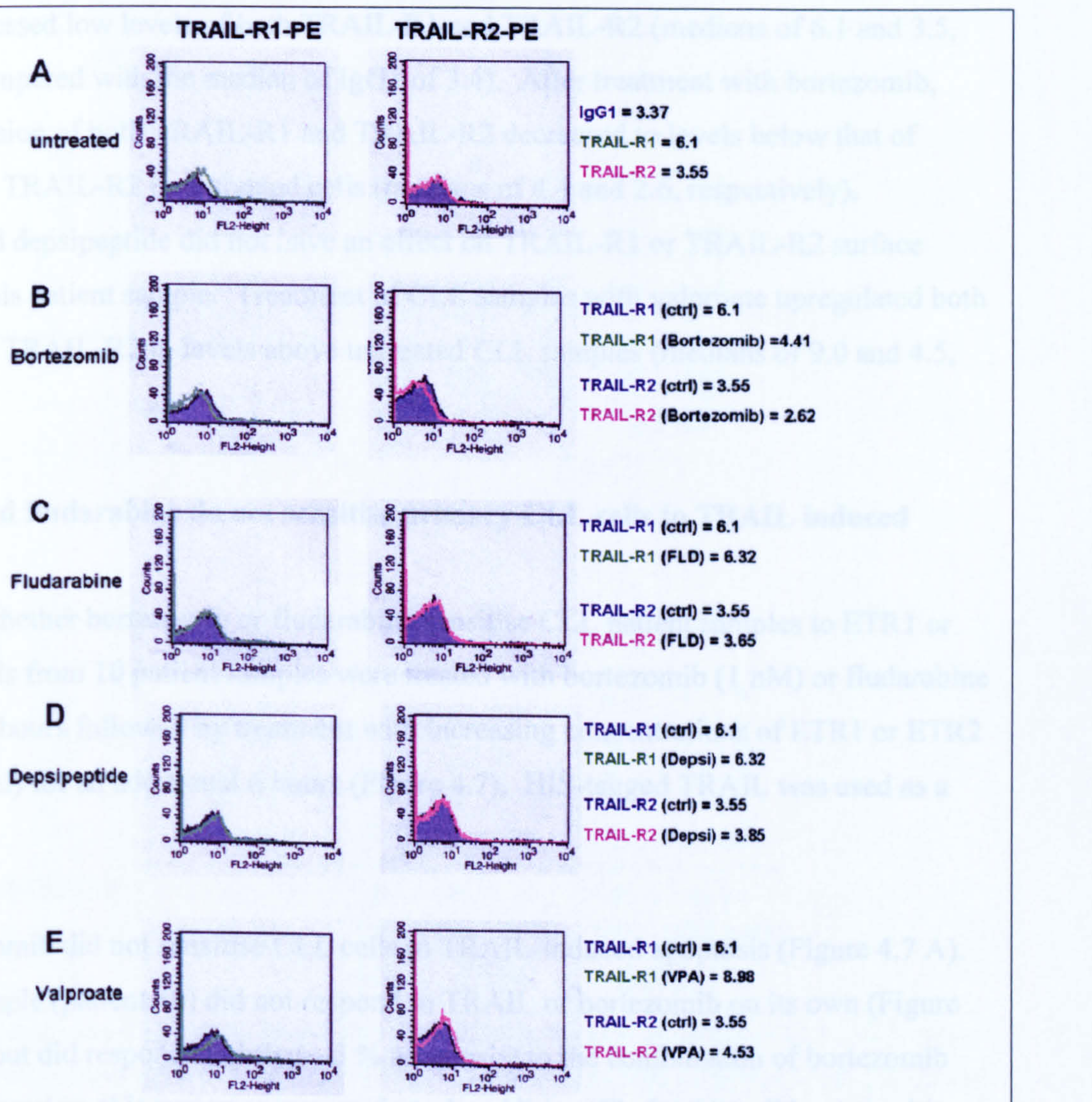

Figure 4.6: Surface expression of TRAIL-R1 and TRAIL-R2 in CLL before and after treatment with various sensitising agents. Primary CLL cells from 8 patients were cultured at a density of 5x 10^6 per ml for 16 hours with 0.1% DMSO (A), 1 nM bortezomib (B), 10 μM fludarabine (C), 10 nM depsipeptide (D) or 2 mM valproate (E). For each treatment, isotype control (IgG1), TRAIL-R1, and TRAIL-R2 surface expression was measured as described in Materials and Methods. A) The purple line represents expression of the isotype control (IgG1) and the green line represents the surface expression of TRAIL-R1 and TRAIL-R2, respectively. B-E) The purple line represents the expression of TRAIL-R1 and TRAIL-R2 in CLL cells treated with 0.1% DMSO. The green and pink lines represent the surface expression of TRAIL-R1 and TRAIL-R2, respectively in CLL cells treated with various sensitising agents. The respective medians are shown to the right of the histogram. Results shown are of one representative patient sample.

CLL cells expressed low levels of both TRAIL-R1 and TRAIL-R2 (medians of 6.1 and 3.5, respectively compared with the median of IgG1 of 3.4). After treatment with bortezomib, receptor expression of both TRAIL-R1 and TRAIL-R2 decreased to levels below that of TRAIL-R1 and TRAIL-R2 in untreated cells (medians of 4.4 and 2.6, respectively). Fludarabine and depsipeptide did not have an effect on TRAIL-R1 or TRAIL-R2 surface expression in this patient sample. Treatment of CLL samples with valproate upregulated both TRAIL-R1 and TRAIL-R2 to levels above untreated CLL samples (medians of 9.0 and 4.5, respectively).

Bortezomib and fludarabine do not sensitise primary CLL cells to TRAIL induced apoptosis.

To determine whether bortezomib or fludarabine sensitise CLL patient samples to ETR1 or ETR2, CLL cells from 10 patient samples were treated with bortezomib (1 nM) or fludarabine (10 μM) for 16 hours followed by treatment with increasing concentrations of ETR1 or ETR2 (100-1000 ng/ml) for an additional 6 hours (Figure 4.7). HIS-tagged TRAIL was used as a comparison.

Overall, bortezomib did not sensitise CLL cells to TRAIL-induced apoptosis (Figure 4.7 A). One patient sample (patient 10) did not respond to TRAIL or bortezomib on its own (Figure 4.5 and 4.7 A) but did respond slightly (~ 5 % apoptosis) to the combination of bortezomib and TRAIL. However, this response was modest. In addition, Fludarabine did not sensitise CLL cells to TRAIL-induced apoptosis overall (Figure 4.7 B). Two patients were sensitive to fludarabine on their own (patients 6 and 7) but the addition of TRAIL did not increase apoptosis above these levels in any patient samples (Figure 4.7 B).

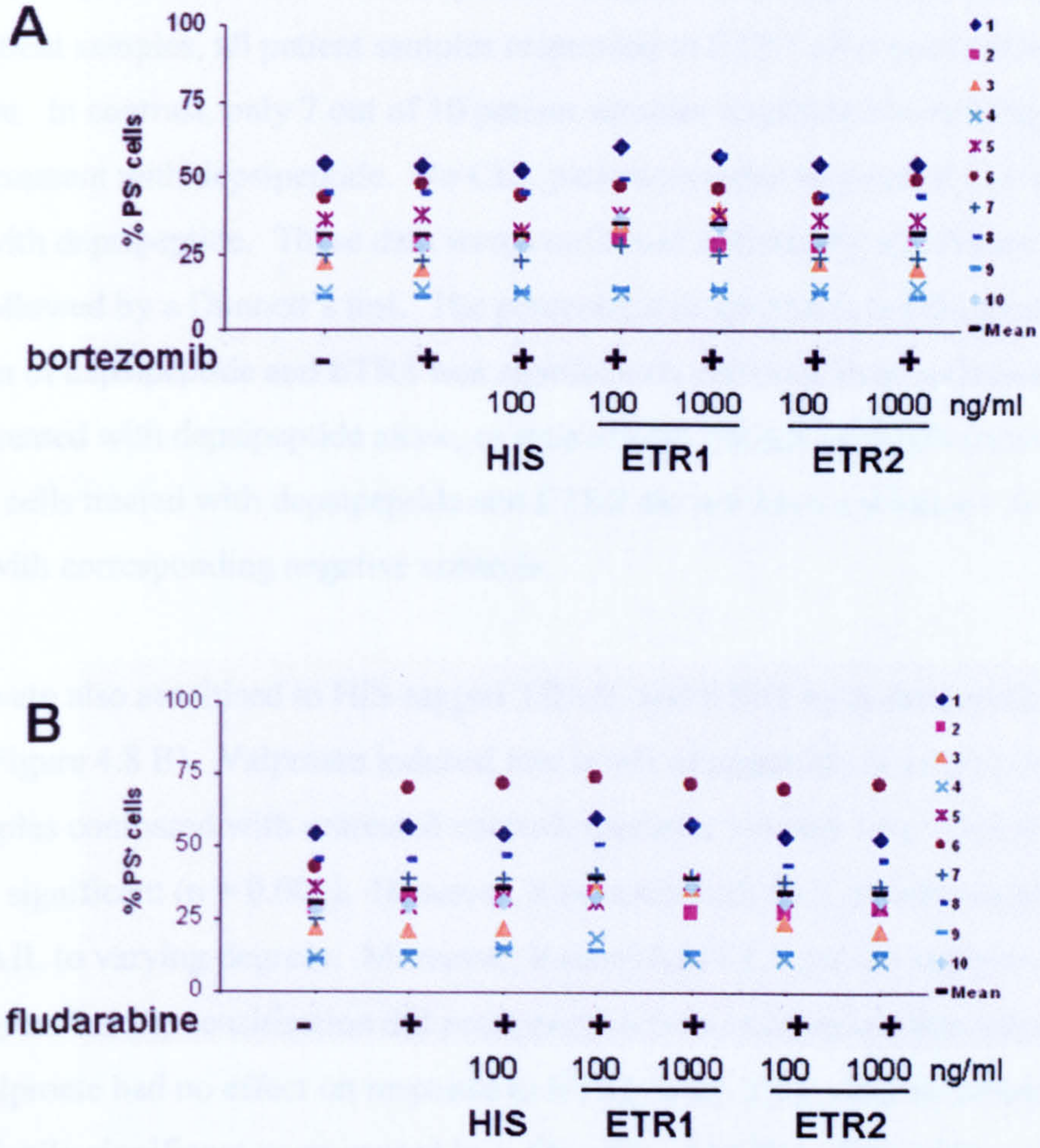

Figure 4.7: Bortezomib and fludarabine do not potentiate TRAIL-induced apoptosis in CLL. CLL cells from 10 patients were cultured at a density of $5x10^6$ cells per ml for 16 hours with 1 nM bortezomib (A), 10 μM fludarabine (B), or vehicle only control (0.1% DMSO). HIS-tagged TRAIL (100 ng/ml) or increasing concentrations of either ETR1 or ETR2 (100-1000 ng/ml) were added for an additional 6 hours. Cell death was quantified by measuring the percentage of PS^+ cells. Each patient is depicted as a single symbol on the graphs. The black line represents the mean of all patient samples.

Histone Deacetylase Inhibitors sensitise CLL patient samples to TRAIL induced apoptosis through TRAIL-R1.

CLL cells were pretreated with depsipeptide or valproate for 16 hours followed by treatment with increasing concentrations of ETR1 or ETR2 or with HIS-tagged TRAIL for an additional 6 hours (Figure 4.8 A and B). Depsipeptide sensitised CLL cells from all patient samples to ETR1 but not to ETR2 (Figure 4.8 A). Furthermore, CLL cells were sensitised to ETR1 in a

concentration-dependent manner in most patient samples. Although response to ETR1 varied between patient samples, all patient samples responded to ETR1 after pre-treatment with depsipeptide. In contrast, only 7 out of 10 patient samples responded to HIS-tagged TRAIL after pre-treatment with depsipeptide. No CLL patient samples responded to ETR2 after pre-treatment with depsipeptide. These data were confirmed statistically significant by a One Way ANOVA followed by a Dunnett's test. The percentage of apoptosis in cells treated with a combination of depsipeptide and ETR1 was significantly different then cells that were untreated, treated with depsipeptide alone, or treated with TRAIL or ETR1 alone ($p < 0.05$). In contrast, cells treated with depsipeptide and ETR2 did not have a p-value < 0.05 when compared with corresponding negative controls.

CLL cells were also sensitised to HIS-tagged TRAIL and ETR1 by pretreatment with valproate (Figure 4.8 B). Valproate induced low levels of apoptosis in its own in 7 out of 10 patient samples compared with untreated controls (patients 1-4 and 7-9). This result was statistically significant ($p = 0.003$). However, it sensitised all CLL patient samples to HIS-tagged TRAIL to varying degrees. Moreover, it sensitised CLL patient samples to ETR1 to varying degrees but the sensitisation did not appear to be concentration dependent. In contrast, valproate had no effect on response to ETR2 in any CLL patient samples. These data were statistically significant as measured by a One Way ANOVA followed by a Dunnett's test. Cells treated with valproate and TRAIL or ETR1 had a p-value < 0.05 when compared with cells that were untreated, treated with valproate alone or with TRAIL or ETR1 alone. Cells treated with valproate and ETR2 did not have p-values < 0.05 when compared with relevant negative controls.

To further determine which preparations of TRAIL can be sensitised by depsipeptide and valproate, CLL cells were incubated with 1000 ng/ml of various preparations of TRAIL including, HIS-tagged TRAIL, HIS-tagged TRAIL-Low endotoxin (Alexis Biochemicals), Apo2L (Genentech), ETR1 or ETR2 (Human Genome Sciences) and caspase-8 and -3 processing measured (Figure 4.8 C).

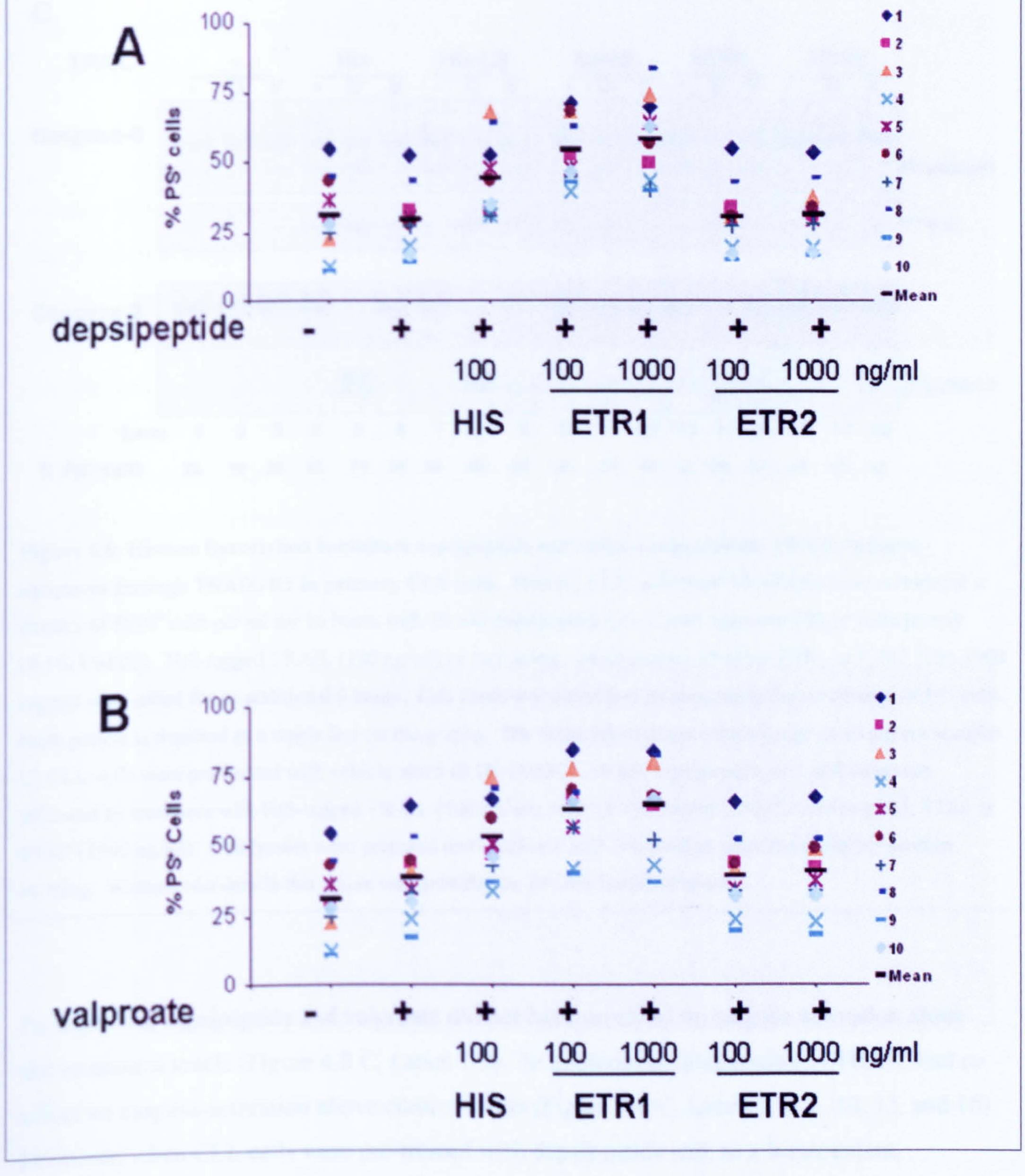
A
% PS+ cells
100
75
50
25
0
depsipeptide
-
+
+
+
+
+
+
100
100
1000
100
1000
ng/ml
HIS
ETR1
ETR2
1
2
3
4
5
6
7
8
9
10
Mean
B
% PS+ Cells
valproate
-
+
+
+
+
+
+
100
100
1000
100
1000
ng/ml
HIS
ETR1
ETR2
Mean

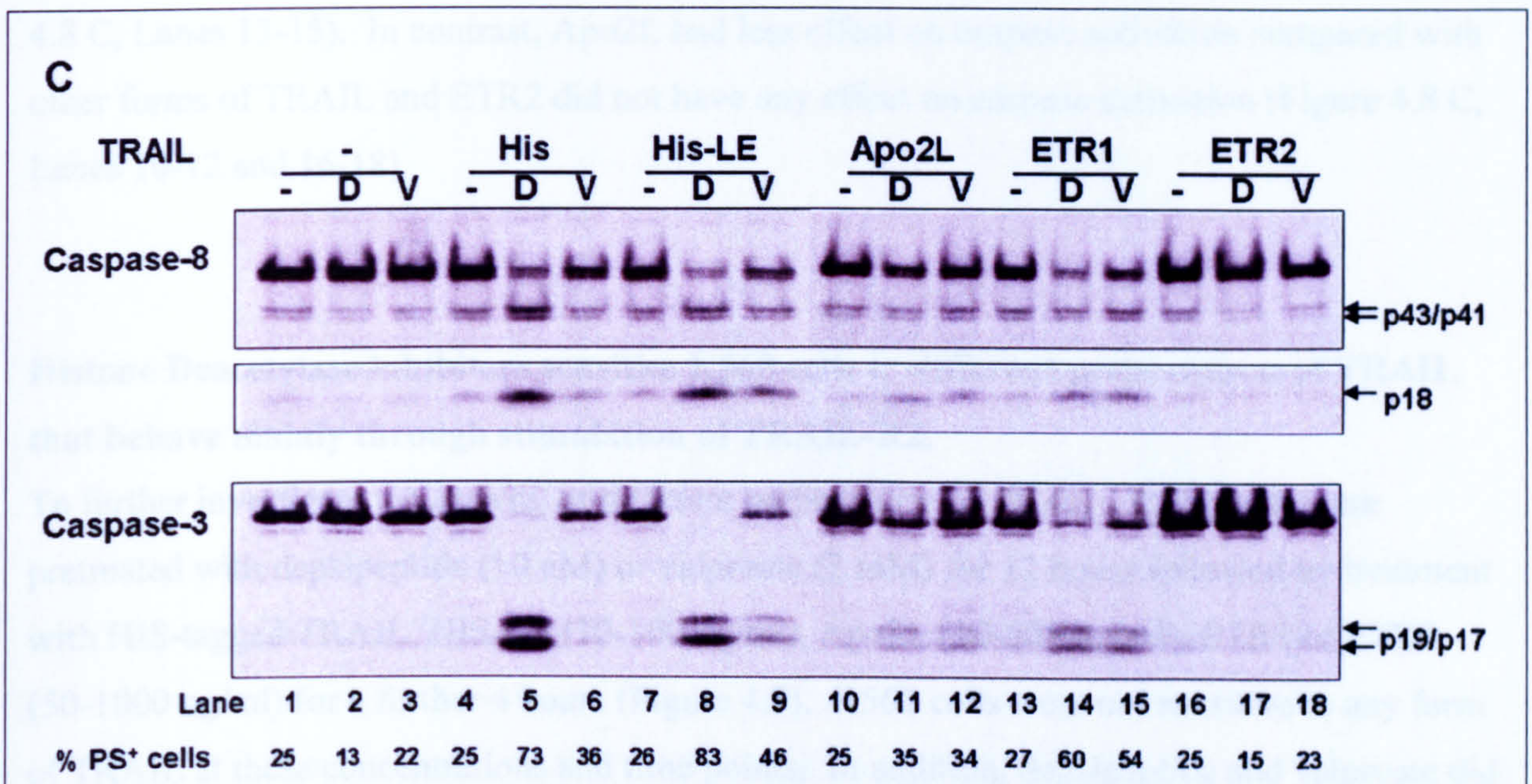

Figure 4.8: Histone Deacetylase Inhibitors depsipeptide and valproate potentiate TRAIL-induced apoptosis through TRAIL-R1 in primary CLL cells. Primary CLL cells from 10 patients were cultured at a density of $5x10^6$ cells per ml for 16 hours with 10 nM depsipeptide (A), 2 mM valproate (B), or vehicle only (0.1% DMSO). HIS-tagged TRAIL (100 ng/ml) or increasing concentrations of either ETR1 or ETR2 (100-1000 ng/ml) were added for an additional 6 hours. Cell death was quantified by measuring the percentage of PS^+ cells. Each patient is depicted as a single line on the graphs. The black line indicates the average of all patient samples. C) CLL cells were pre-treated with vehicle alone (0.1% DMSO), 10 nM depsipeptide or 2 mM valproate followed by treatment with HIS-tagged TRAIL (100 ng/ml), HIS-LE (100 ng/ml), Apo2L (100 ng/ml), ETR1 or ETR2 (1000 ng/ml). Cell lysates were prepared and caspase-8 and -3 activation were measured by western blotting. Western blot data in this figure was provided by Dr. Marion MacFarlane.

As expected, depsipeptide and valproate did not have an effect on caspase activation alone above control levels (Figure 4.8 C, Lanes 1-3). In addition, no preparation of TRAIL had an effect on caspase-activation above control levels (Figure 4.8 C, Lanes 1, 4, 7, 10, 13, and 16). However, when CLL cells were pre-treated with depsipeptide and, to a lesser extent, valproate, HIS-tagged TRAIL and HIS-LE had a similar effect on caspase-8 and -3 activation (Figure 4.8 C, Lanes 4-9). In this case the proforms of caspase-8 and -3 were decreased and the buildup of p41/43 and p18 of caspase-8 and p19/17 of caspase-3 were apparent. ETR1 had a similar effect on caspase activation after treatment with depsipeptide and valproate (Figure

4.8 C, Lanes 13-15). In contrast, Apo2L had less effect on caspase activation compared with other forms of TRAIL and ETR2 did not have any effect on caspase activation (Figure 4.8 C, Lanes 10-12 and 16-18).

Histone Deacetylase inhibitors sensitise K562 cells to different preparations of TRAIL that behave mainly through stimulation of TRAIL-R2.

To further investigate the activity of different preparations of TRAIL, K562 cells were pretreated with depsipeptide (10 nM) or valproate (2 mM) for 12 hours followed by treatment with HIS-tagged TRAIL, HIS-LE (10-100 ng/ml), Apo2L (10-500 ng/ml), ETR1 or ETR2 (50-1000 ng/ml) for a further 4 hours (Figure 4.9). K562 cells were not sensitive to any form of TRAIL at these concentrations and time points. In addition, depsipeptide and valproate did not kill K562 cells on their own. However, depsipeptide and, to a lesser extent, valproate sensitised K562 cells to HIS-tagged TRAIL and HIS-LE at high concentrations only (4-fold increase in apoptosis at 100 ng/ml TRAIL) (Figure 4.9 A).

Surprisingly, after depsipeptide treatment Apo2L was extremely active in K562 cells yielding up to an 8-fold increase in apoptosis (Figure 4.9 A). This activity was most apparent using low concentrations of Apo2L where it was not inducing apoptosis on its own. ETR2 was also surprisingly active in K562 cells after depsipeptide treatment yielding an 18-fold increase in apoptosis at 1000 ng/ml (Figure 4.9 A). In contrast, ETR1 was not active in K562 cells even after depsipeptide or valproic acid treatment failing to yield even a 2-fold increase in % PS^+ cells (Figure 4.9 A). Valproate was less effective than depsipeptide at sensitising K562 cells in these experiments.

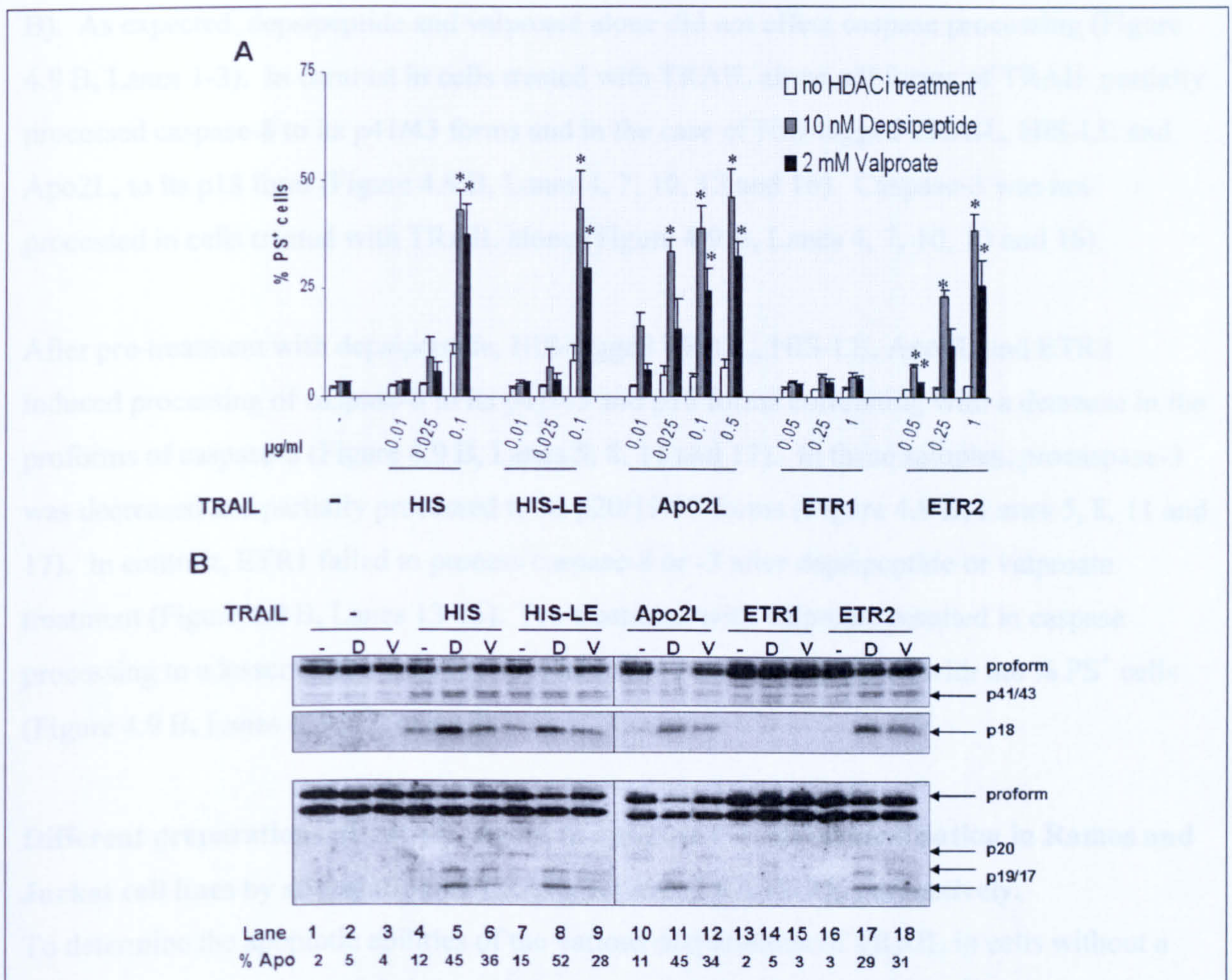

Figure 4.9: Histone Deacetylase Inhibitors potentiate TRAIL-induced apoptosis through TRAIL-R2 in K562 cells after treatment with various preparations of TRAIL. K562 cells were cultured at $0.8x10^6$ cells per ml for 12 hours with 10 nM depsipeptide, 2 mM valproate, or vehicle only control (0.1% DMSO). HIS-tagged TRAIL, HIS-LE (10-100 ng/ml), Apo2L (10-500 ng/ml), or increasing concentrations of either ETR1 (50-1000 ng/ml) or ETR2 (50-1000 ng/ml) were added either alone or in combination for an additional 4 hours. A) After TRAIL treatment, cell death was quantified by measuring the percentage of PS^+ cells. Results are shown as a mean ± SEM of at least three independent experiments. * denotes a p value < 0.05 compared with the corresponding control samples as measured by a One Way ANOVA followed by a Dunnett's test. B) Cell lysates were collected and caspase-8 and -3 activation were measured by western blotting. Western blots show one representative sample of at least three independent experiments.

To confirm the activity of different preparations of TRAIL in K562 cells, lysates were taken after treatment and caspase-8 and -3 processing were measured by western blotting (Figure 4.9

B). As expected, depsipeptide and valproate alone did not affect caspase processing (Figure 4.9 B, Lanes 1-3). In contrast in cells treated with TRAIL alone, all forms of TRAIL partially processed caspase-8 to its p41/43 forms and in the case of HIS-tagged TRAIL, HIS-LE and Apo2L, to its p18 form (Figure 4.9 B, Lanes 4, 7, 10, 13 and 16). Caspase-3 was not processed in cells treated with TRAIL alone (Figure 4.9 B, Lanes 4, 7, 10, 13 and 16).

After pre-treatment with depsipeptide, HIS-tagged TRAIL, HIS-LE, Apo2L and ETR2 induced processing of caspase-8 to its p41/43 and p18 forms correlating with a decrease in the proforms of caspase-8 (Figure 4.9 B, Lanes 5, 8, 11 and 17). In these samples, procaspase-3 was decreased and partially processed to its p20/19/17 forms (Figure 4.9 B, Lanes 5, 8, 11 and 17). In contrast, ETR1 failed to process caspase-8 or -3 after depsipeptide or valproate treatment (Figure 4.9 B, Lanes 13-16). Pre-treatment with valproate resulted in caspase processing to a lesser extent than depsipeptide; however this correlated with the % PS^+ cells (Figure 4.9 B, Lanes 6, 9, 12, and 18).

Different preparations of TRAIL signal to apoptosis without sensitisation in Ramos and Jurkat cell lines by stimulation of TRAIL-R1 and TRAIL-R2, respectively.

To determine the apoptotic abilities of the various preparations of TRAIL in cells without a sensitising agent, Ramos and Jurkat cells were treated with increasing concentrations of HIS-tagged TRAIL, HIS-LE, Apo2L (10-500 ng/ml), ETR1 or ETR2 (25-1000 ng/ml) for 4 and 8 hours, respectively (Figure 4.10).

In Ramos cells (Figure 4.10 A), HIS-tagged TRAIL induced the highest levels of apoptosis at 500 ng/ml treatment (61 ± 3% PS^+ cells). HIS-LE and ETR1 induced similar levels of apoptosis in Ramos cells at the highest concentration (51 ± 3% and 53 ± 4% PS^+ cells, respectively). Apo2L only induced moderate levels of apoptosis in Ramos cells even at 500 ng/ml (30 ± 2% PS^+ cells). As observed in Figure 4.2, ETR2 did not induce apoptosis in Ramos cells even at 1000 ng/ml (6 ± 0.5 % PS^+ cells).

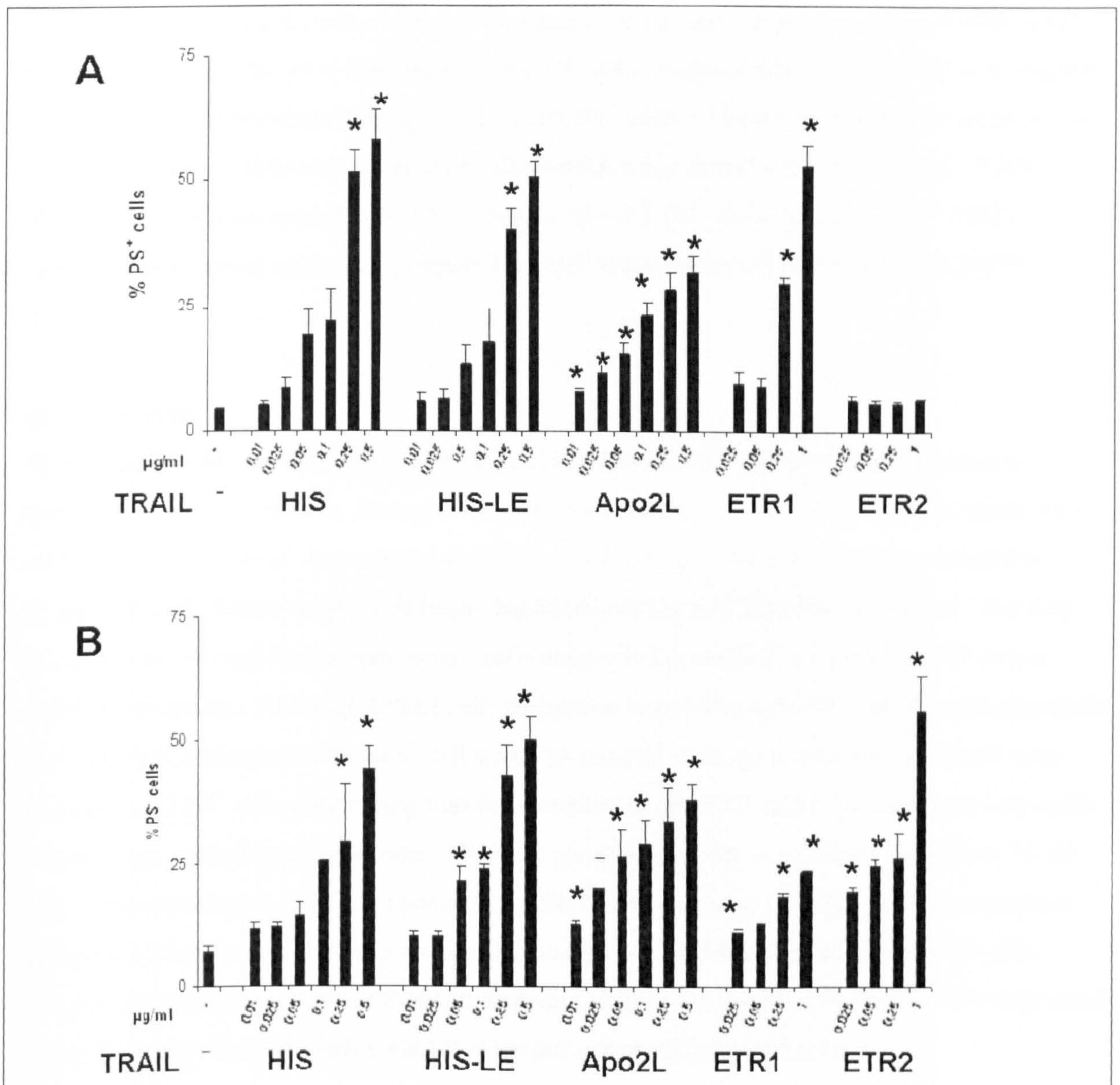

Figure 4.10: Ramos and Jurkat cells respond through TRAIL-R1 and TRAIL-R2, respectively, without sensitisation through an HDAC inhibitor after treatment with various preparations of TRAIL. Ramos and Jurkat cells were cultured at $1x10^6$ cells per ml for 4 and 8 hours, respectively with increasing concentrations of HIS, HIS-LE, Apo2L (10-500 ng/ml), or ETR1 or ETR2 (50-1000 ng/ml). A) After TRAIL treatment, Ramos cell death was quantified by measuring the percentage of PS^+ cells. Results are presented as a mean ± SEM of at least 3 independent experiments. B) After TRAIL treatment, Jurkat cell death was quantified by measuring the percentage of PS^+ cells. Results are presented as a mean ± SEM of at least 3 independent experiments. * denotes a p-value < 0.05 compared with control samples as measured by the student's t-test.

In Jurkat cells (Figure 4.10 B), ETR2, HIS-tagged TRAIL and HIS-LE induced similar levels of apoptosis (56 ± 7%, 44 ± 5% and 50 ± 5% PS^+ cells, respectively). Apo2L induced slightly lower levels of apoptosis at 500 ng/ml (37 ± 3% PS^+ cells). However at lower concentrations (25 ng/ml), Apo2L induced higher levels of apoptosis compared with HIS-tagged TRAIL and HIS-LE (20 ± 6% compared with 12 ± 1% and 10 ± 1% PS^+ cells, respectively). ETR1 induced low levels of apoptosis compared with all other forms of TRAIL (23 ± 0.2% PS^+ cells).

4.3 Discussion

Humanised TRAIL mAbs; ETR1 and ETR2, have been developed by HGS to be used as therapeutic agents (Johnson, Huang et al. 2003; Georgakis, Li et al. 2005). In this study, four cell lines were screened for response to ETR1 and ETR2 individually and in combination (Figures 4.1-4). Interestingly, cell lines responded mainly to ETR1 but not ETR2. The only exception to this was Jurkat cells where cells responded primarily to ETR2 but ETR1 to a much lesser extent. Although Elijah cells responded somewhat to ETR1, the percent apoptosis was very low compared with other cell lines. In general, caspase activation correlated with percentage of PS^+ cells confirming that the mechanism of ETR1 and ETR2-induced cell death was through induction of apoptosis. The only exception to this is in Figure 4.1 where Z-138 cells were sensitive to ETR2 as measured by the % PS^+ cells, but caspase activation was not apparent in these cells. One explanation for this is that Z-138 cells may undergo TRAIL-induced apoptosis or cell death through caspase-independent means. Further work would need to be completed to characterise TRAIL-induced cell death in Z-138 cells.

Interestingly, despite relative resistance to ETR1 and ETR2 in Elijah cells, the proform of caspase-8 and -3 was reduced in samples treated with ETR1 and a combination of ETR1 and ETR2. Although caspase-8 activation was not apparent at this exposure, caspase-3 was partially processed to its p20 fragment in samples treated with ETR1, ETR1 and ETR2 and HIS-tagged TRAIL. The mechanism of resistance to TRAIL is not clear in Elijah cells.

However, several approaches could be used to investigate TRAIL-resistance. Elijah cells could be screened for resistance to other drugs or chemicals such as etoposide to determine if

they are also resistant to chemicals. Lysates could be checked to see the balance of pro-and anti-apoptotic proteins in the cell. For example the c-FLIP to caspase-8 ratio may be the deciding factor in determining resistance to TRAIL. Another approach that may be taken is to try and sensitise Elijah cells to TRAIL-induced apoptosis through sensitising agents. This may give a clue as to the mechanism of resistance. However, tumour cell lines tend to be heavily mutated and deficient in apoptosis and therefore, the mechanism of resistance to TRAIL in tumour cell lines may vary and could be caused by a number of different factors that may reveal little about the mechanism of resistance to TRAIL in CLL cells and therefore these experiments were not pursued further.

ETR1 and ETR2 induce apoptosis in cell lines without crosslinking (in contrast to other antibodies to TRAIL receptors). However, it has been reported that crosslinking of ETR1 and ETR2 can increase apoptosis induction in resistant cell lines (Johnson, Huang et al. 2003; Georgakis, Li et al. 2005). Further work needs to be completed to see whether ETR1 and ETR2 resistance can be overcome by crosslinking both in primary CLL cells treated alone or pre-treated with a sensitising agent and in cell lines used in this study.

Using ETR1 and ETR2 in combination did not increase apoptosis compared with using them individually. This suggests that there is not cross-talk between the two receptor pathways. Furthermore, there is no therapeutic advantage of using HIS-tagged TRAIL (that can bind to all four TRAIL receptors) or any version of TRAIL that can bind both TRAIL-R1 and TRAIL-R2 (Degli-Esposti, Dougall et al. 1997; Degli-Esposti, Smolak et al. 1997; MacFarlane, Ahmad et al. 1997; Pan, Ni et al. 1997; Pan, O'Rourke et al. 1997; Walczak, Degli-Esposti et al. 1997). Targeting one receptor is sufficient to induce apoptosis provided cells are able to undergo apoptosis through that receptor.

Surprisingly, there appeared to be no correlation between TRAIL-R1 and TRAIL-R2 surface expression and response to ETR1 or ETR2, respectively (Figures 4.1-4). This is in agreement with another study that also measured surface expression of TRAIL receptors and compared this with sensitivity to ETR1 and ETR2 (Georgakis, Li et al. 2005). For example, Z-138 cells expressed high surface levels of TRAIL-R1 and TRAIL-R2 but only responded to ETR1. In

addition, Elijah cells expressed high levels of TRAIL-R1 and TRAIL-R2 but did not respond to either ETR1 or ETR2.

In contrast, Ramos and Jurkat TRAIL-receptor surface expression appeared to correlate to apoptosis induction by ETR1 and ETR2 to some degree. However, expression of high levels of one receptor does not indicate that apoptosis induction will occur through that receptor. This suggests that receptor surface expression should not be used as a predictor of sensitivity to TRAIL, ETR1 or ETR2. In addition, these data suggest that the mechanism of resistance to TRAIL is not determined by the level of receptor surface expression alone and may be attributed to a downstream event such as DISC formation or levels of c-FLIP or caspase-8 within the cell.

As expected, primary CLL cells did not respond highly to ETR1 and did not respond to ETR2 as a single agent treatment. Despite reports that bortezomib and fludarabine increase surface expression of TRAIL-R1 and TRAIL-R2 and therefore sensitise CLL cells to TRAIL-induced apoptosis, this was not the case in any of the 10 CLL cases tested in this chapter (Johnston, Kabore et al. 2003; Kabore, Sun et al. 2006). Furthermore, bortezomib actually decreased surface expression of TRAIL-R1 and TRAIL-R2 in many patient samples. However, in the two studies mentioned, upregulation of TRAIL receptors occurred only in cells that underwent apoptosis. Furthermore, no controls were carried out to check that surface expression was only measured on live cells. Therefore the upregulation of TRAIL-R1 and TRAIL-R2 surface expression may have been measured on cells that were already dead, thus undermining the conclusions taken from the experiment. It is important to note that there have been no further reports on bortezomib or fludarabine sensitisation to TRAIL in CLL cells.

HDAC inhibitors increased the surface expression of TRAIL-R1 and TRAIL-R2 and sensitised CLL cells from all patient samples to TRAIL-induced apoptosis. Recent reports have shown that this increase in receptor surface expression is not necessary for sensitisation to TRAIL-induced apoptosis (Inoue, Twiddy et al. 2006). Although the mechanism of HDAC inhibitor sensitisation to TRAIL is not clear, HDAC inhibitors were hypothesised to be important for FADD recruitment to the DISC (Inoue, MacFarlane et al. 2004). Further studies

are required to determine the mechanism of HDAC inhibitor sensitisation to TRAIL but are beyond the scope of this study.

When CLL cells were pre-treated with an HDAC inhibitor, ETR1 was able to induce apoptosis in all 10 patient samples. HIS-tagged TRAIL was slightly less effective than ETR1 at inducing apoptosis in CLL cells and ETR2 was not able to induce apoptosis in any CLL samples. Taken together, these data suggest that when CLL cells are pre-treated with an HDAC inhibitor, they respond to apoptosis through TRAIL-R1 and not TRAIL-R2. This is in contrast to recent findings suggesting that tumour cells respond to TRAIL primarily through TRAIL-R2 (Kelley, Totpal et al. 2005).

Interestingly, Apo2L was almost completely inactive in primary CLL cells and in Ramos cells (Figure 4.8 C and Figure 4.10 A). However, in K562 cells and in Jurkat cells Apo2L was very active, particularly at low concentrations (Figure 4.9 and Figure 4.10 B). In addition, data with ETR1 and ETR2 suggest that CLL cells and Ramos cells are only able to undergo apoptosis when stimulated through TRAIL-R1, but K562 cells and Jurkat cells are only able to undergo apoptosis when stimulated through TRAIL-R2 (Figures 4.8-4.10). Taken together, these data suggest that Apo2L can induce apoptosis primarily through TRAIL-R2. In contrast, HIS-tagged TRAIL and HIS-LE induced apoptosis regardless of whether cells were sensitive to ETR1 or ETR2, suggesting that these versions of TRAIL can induce apoptosis through stimulation of TRAIL-R1 or TRAIL-R2.

Possible reasons for the signalling differences between Apo2L and HIS-tagged TRAIL lie in the preparations of both ligands. Apo2L lacks exogenous sequence tags and is reported to contain an internal zinc atom and therefore maintains better trimer stability than HIS-TRAIL (Hymowitz, Christinger et al. 1999; Hymowitz, O'Connell et al. 2000; Lawrence, Shahrokh et al. 2001). Therefore, signalling through TRAIL-R1 may be facilitated partially through the exogenous Histidine tag on HIS-TRAIL.

Alternatively, signalling to apoptosis through TRAIL-R1 may be partially aided by lack of trimer stability. Apo2L has been shown to bind equally to TRAIL-R1 and TRAIL-R2 (Kelley

et al). Therefore, it is likely that the mechanism of selectivity of Apo2L is not due to differential binding affinities of TRAIL-R1 and TRAIL-R2. The reason for TRAIL-R2 selectivity is more likely to lie in the ability of Apo2L to form a more stable TRAIL-R2 complex than TRAIL-R1 complex.

It is important to note that Apo2L does not induce apoptosis solely through TRAIL-R2 but is mildly effective at inducing apoptosis in Ramos cells and in CLL cells, and therefore is only partially selective towards TRAIL-R2. Interestingly, even in Jurkat and K562 cells Apo2L was very effective at low concentrations, but less effective than HIS-tagged TRAIL at higher concentrations suggesting that Apo2L is saturated at higher concentrations. Therefore, Apo2L may not be an appropriate therapy even in cells that are sensitive to TRAIL through TRAIL-R2.

This is the first study to identify that different preparations of TRAIL can signal to apoptosis through different receptors and that, in the presence of an HDAC inhibitor, CLL cells respond to apoptosis through TRAIL-R1. To date, the majority of studies investigating sensitivity to TRAIL have been in cell lines rather than primary tumours. For this reason, it is not yet clear whether TRAIL-R1 or TRAIL-R2 is important for signalling to apoptosis in primary haematological malignancies or other tumour types including solid tumours.

A recent study using ETR1 and ETR2 has shown that many primary lymphomas respond to ETR1 and ETR2 as single agents at comparable levels. The study showed TRAIL-R1 and TRAIL-R2 to be equally important in a range of lymphomas. However, response to the mAbs in this study was modest at best (Georgakis, Li et al. 2005). In addition a recent study showed ETR1 to be very effective in vivo in a range of tumour types including colon, non-small cell lung and renal tumours (Pukac, Kanakaraj et al. 2005).

In contrast, TRAIL-R2 has been implicated to be the major receptor to signal to apoptosis in primary renal cell carcinomas and primary synovial fibroblasts (Ichikawa, Liu et al. 2003; Zeng, Wu et al. 2006). A group has also recently generated receptor-selective mutant ligands and shown the TRAIL-R2 ligand to be more important in tumour cell lines (Kelley, Totpal et

al. 2005). It would be interesting to see if CLL cells and Ramos cells respond to the TRAIL-R1 ligand generated in their study (Kelley, Totpal et al. 2005). More studies using primary tumour cells are necessary to determine whether tumour cells undergo apoptosis by stimulation of TRAIL-R1 or TRAIL-R2. Data from this chapter and the above studies clearly demonstrates the necessity for primary tumours to be evaluated for sensitivity through TRAIL-R1 or TRAIL-R2 *in vitro* prior to clinical trials to minimise the risk of toxicity and to increase the chance of successful therapy.

Combination therapy of an HDAC inhibitor with ETR1 or HIS-tagged TRAIL shows promise as a therapy in CLL. Preparations of TRAIL that induce apoptosis predominantly through TRAIL-R2 are of limited use in CLL and other tumour types that signal to apoptosis through TRAIL-R1. Furthermore, recent evidence has suggested that TRAIL may activate survival pathways in some cases (Harper, Farrow et al. 2001; Ehrhardt, Fulda et al. 2003; Di Pietro and Zauli 2004). Preparations of TRAIL such as ETR2 and Apo2L may be detrimental to CLL patients because they may activate survival pathways. In one patient sample (Figure 4.4, patient 5); incubation with all forms of TRAIL in the absence of a sensitising agent decreased spontaneous apoptosis, suggesting that survival signals may have been activated in this patient sample. Moreover, after incubation with depsipeptide, that same patient sample had a decreased spontaneous apoptosis in cells treated with ETR2 compared with cells treated with depsipeptide alone (Figure 4.5 A, patient 5).

Another possible danger of treating CLL patients with Apo2L, HIS-tagged TRAIL or ETR2 is the potential of unwanted liver toxicity. There have been reports of hepatotoxicity as a possible unwanted effect of treatment with TRAIL (Jo, Kim et al. 2000). There is particularly concern of potential toxicity of combination therapies using TRAIL that may produce unanticipated toxicities. Although Apo2L is reported to be less toxic to hepatocytes than HIS-tagged TRAIL (Lawrence, Shahrokh et al. 2001), the literature on TRAIL-induced hepatotoxicity is somewhat contradictory (Jo, Kim et al. 2000). Some versions of TRAIL are reportedly more toxic to hepatocytes than others, and this may depend the exogenous tag that TRAIL is labelled with or its method of purification (Lawrence, Shahrokh et al. 2001; Ganten, Koschny et al. 2006).

Several reports using blocking antibodies and monoclonal antibodies have suggested that primary human hepatocytes may undergo apoptosis through stimulation of both TRAIL-R1 and TRAIL-R2 (Mori, Thomas et al. 2004; Ganten, Koschny et al. 2006). By treating CLL cells with a version of TRAIL that only targets one receptor, liver toxicity may be significantly reduced. However, there has been no comparative study investigating the effects of HIS-tagged TRAIL, Apo2L, ETR1 and ETR2 on hepatocytes either alone or in combination with an HDAC inhibitor. This type of study may clarify the literature on TRAIL-induced hepatocyte toxicity and aid in determining what combinations of therapy may yield good results without causing unmanageable hepatotoxicity.

To summarize, TRAIL remains a good candidate for therapy in CLL provided an appropriate version of TRAIL is used with an appropriate sensitising agent. Although several studies have pointed to bortezomib and fludarabine as being good potential sensitising agents for use with TRAIL in CLL, this study showed no such promise for these agents in combination with TRAIL. HDAC inhibitors such as depsipeptide and valproate remain good candidates for use in CLL in combination with TRAIL. Valproate is already approved and being used as an anti-convulsant and therefore remains the most promising candidate for treatment with TRAIL in CLL (Zaccara, Messori et al. 1988).

Data in this study have indicated that versions of TRAIL that signal through TRAIL-R1 are essential for promising therapeutic results in CLL. Therefore, ETR2 and Apo2L are not ideal candidates for combination therapy in CLL. Although HIS-tagged TRAIL can signal through TRAIL-R1 and has been shown to be effective in CLL, it can bind to all four TRAIL receptors and may activate survival pathways or cause unwanted toxicity. For this reason ETR1 remains the most promising candidate for combination therapy with an HDAC inhibitor for clinical trials in CLL.

Chapter 5: The Generation and Characterisation of TRAIL Receptor-Selective Mutants

5.1 Introduction: The Generation and Characterisation of TRAIL Receptor-Selective Mutants

A novel approach allowing phage display of trimeric protein was recently used to develop TRAIL receptor-selective mutant ligands to investigate various tumour cell lines for their capacity to undergo apoptosis *via* either TRAIL-R1 or TRAIL-R2 (Kelley, Totpal et al. 2005). The study indicated that the resulting TRAIL-R2 mutant ligand was extremely active in most cell lines tested, including the T-cell lymphoblastic leukaemia cell line Jurkat, the colon carcinoma cell line Colo-205 and the breast carcinoma cell line MDA-MB-231. In contrast, the TRAIL-R1 mutant ligand was found to be inactive in all cell lines tested. The primary conclusion was that tumour cells signal primarily through TRAIL-R2 and that TRAIL-R1 is of little importance in apoptotic signalling in tumour cells and therefore has little value for tumour therapy.

Data obtained in Chapter 4 using agonistic TRAIL mAbs suggests that CLL cells signal to apoptosis primarily through TRAIL-R1 when sensitised with HDAC inhibitors. Possible reasons for the discrepancy described in the previous paragraph are; a TRAIL-R1-signalling cell line was not represented in the panel of cell lines tested and therefore the TRAIL-R1 mutant ligand was not active in cell lines signalling through TRAIL-R2, or one or several of the six mutations in the TRAIL-R1 mutant ligand was causing inactivity.

The aims of this project were to develop TRAIL receptor-selective mutant ligands based on previous published work (Kelley, Totpal et al. 2005). TRAIL-R1 and TRAIL-R2-specific mutant ligands were developed and characterised. Jurkat and Ramos cells were used as cell lines that signal to apoptosis primarily through TRAIL-R1 and TRAIL-R2 and blocking and neutralising antibodies to TRAIL-R1 and R2, respectively, to verify the specificity of the mutant ligands.

In agreement with previous findings, the TRAIL-R1 mutant ligand with 6 mutations was found to be inactive, even in cells that have been shown to respond through TRAIL-R1. The mutation thought to be responsible for this lack of activity was Tyr189Ala. Upon removal of this mutation, the TRAIL-R1 ligand became active and specific to TRAIL-R1. Furthermore, the TRAIL-R1 mutant, but not the TRAIL-R2 mutant, was found to be active in primary CLL cells after sensitisation with depsipeptide. This, taken together with data

using TRAIL mAbs, confirms that CLL cells respond to TRAIL through TRAIL-R1 and not TRAIL-R2 when sensitised with an HDAC inhibitor.

5.2 Results

Various TRAIL mutants display different levels of apoptotic activity and specificity.

In order to characterise the apoptotic activity of TRAIL mutants generated by Kelley et al 2005, TRAIL.R1-6 and TRAIL.R2-6 were expressed in E.coli and purified in the same manner as HIS-tagged TRAIL as described in Materials and Methods. Jurkat and Ramos cells had previously been shown in Chapter 4 to signal to apoptosis through TRAIL-R1 and TRAIL-R2, respectively and were used as receptor specific cell lines to determine the apoptotic activity and specificity of each mutant generated (Table 5.1 and Figures 5.1 and 5.2).

As expected, TRAIL.R2-6 (the mutant specific for TRAIL-R2) was extremely active in Jurkat cells (Table 5.1 and Figure 5.1). Despite this marked activity in Jurkat cells, it was entirely inactive in Ramos cells (Table 5.1 and Figure 5.2). The activity in a cell line that acts predominantly through TRAIL-R2 (Jurkat cells) and inactivity in a TRAIL-R1 specific cell line (Ramos cells) suggested that TRAIL.R2-6 specifically acts through TRAIL-R2. These data are in agreement with previous findings (Kelley, Totpal et al. 2005).

In contrast, TRAIL.R1-6 was inactive even in Ramos cells (Table 5.1 and Figures 5.1 and 5.2). It was clear that one or several of the six mutations in this ligand were causing this inactivity. Therefore, it was necessary to generate intermediate mutants with only some of the changes from wt TRAIL to TRAIL.R1-6. The aim of this was to determine which mutations were causing this marked decrease in activity of TRAIL.R1-6 compared with wild type TRAIL and, if possible, to find a mutant that displayed selectivity towards TRAIL-R1 but no loss of activity.

The first intermediate TRAIL mutant to be developed was TRAIL.R1-2 (Table 5.1). The two amino acid substitutions, Tyr213Trp and Ser215Asp, were originally thought to be specific to TRAIL-R1 as they have a similar affinity as wt TRAIL to TRAIL-R1-Fc but have a 10-fold lower affinity to TRAIL-R2-Fc (Kelley, Totpal et al. 2005). Despite a reduced affinity to TRAIL-R2-Fc, TRAIL.R1-2 had a similar activity to wt TRAIL in

Ramos and Jurkat cells (Table 5.1 and Figures 5.1 and 5.2). The activity of this mutant did not differ from the activity of wt TRAIL in Jurkat cells, suggesting that it did not act specifically through TRAIL-R1.

Table 5.1 Apoptosis inducing abilities of various TRAIL variants

											% PS$^+$ cells [c]	
His-TRAIL Variant [a]	**Amino acid changes [b]**										**Ramos**	**Jurkat**
- (control)											9.3 ± 1.3	5.7 ± 0.4
wild type	189 Tyr	191 Arg	193 Gln	199 Asn	201 Lys	213 Tyr	215 Ser	264 His	266 Ile	267 Asp	41.8 ± 5.2	45.5 ± 4.1
TRAIL.R1-6	**Ala**	Arg	**Ser**	**Val**	**Arg**	**Trp**	**Asp**	His	Ile	Asp	13. 7 ± 1.3	6.4 ± 0.8
TRAIL.R1-2	Tyr	Arg	Gln	Asn	Lys	**Trp**	**Asp**	His	Ile	Asp	42.2 ± 3.1	46.6 ± 3.1
TRAIL.R1-4	Tyr	Arg	Gln	**Val**	**Arg**	**Trp**	**Asp**	His	Ile	Asp	43.5 ± 2.5	25.0 ± 2.6
TRAIL.R1-5a	**Ala**	Arg	Gln	**Val**	**Arg**	**Trp**	**Asp**	His	Ile	Asp	18.9 ± 0.7	6.6 ± 0.4
TRAIL.R1-1	**Ala**	Arg	Gln	Asn	Lys	Tyr	Asp	His	Ile	Asp	30.6 ± 2.9	24.9 ± 2.2
TRAIL.R1-5	Tyr	Arg	**Ser**	**Val**	**Arg**	**Trp**	**Asp**	His	Ile	Asp	35.9 ± 6.4	20.0 ± 2.3
TRAIL.R2-6	**Gln**	**Lys**	**Arg**	Asn	Lys	Tyr	Asp	**Arg**	**Leu**	**Gln**	9.4 ± 1.6	58.4 ± 11.6

[a] Variants were produced from His-tagged TRAIL (95-281). The last number of the variant indicates the number of amino acid substitutions compared to wt TRAIL

[b] Amino acid changes are relative to the wild type TRAIL and shown in bold.

[c] Apoptosis was measured in the indicated cell type by phosphatidylserine (PS) externalization after exposure for 4 h to TRAIL or its variant (500 ng ml^{-1}). The results are expressed as Mean ± SEM of at least three separate determinations.

Next, TRAIL.R1-4 was synthesised and tested against wt TRAIL (Table 5.1). This mutant contained the two amino acid substitutions from TRAIL.R1-2 and also had two further amino acid substitutions, Asn199Val and Lys201Arg. TRAIL.R1-4 retained activity similar to wt TRAIL in Ramos cells but lost much of its activity in Jurkat cells (Table 5.1). These data suggest that TRAIL.R1-4 is selective to TRAIL-R1 to a certain degree. However, there appeared to be a residual signal to Jurkat cells above that of ETR1. Therefore, it was necessary to determine whether further mutations could increase selectivity to TRAIL-R1 without losing activity.

The next mutant to be developed contained all the mutations in TRAIL.R1-4 and an additional mutation, Tyr198Ala, to make TRAIL.R1-5a (Table 5.1). This combination of mutations resulted in a marked loss of activity in Ramos and Jurkat cells compared with wt TRAIL (Table 5.1). This suggested that Tyr198Ala was responsible for the loss of activity originally reported in the complete TRAIL-R1 mutant, TRAIL.R1-6. To confirm this, TRAIL.R1-1, was generated (Table 5.1). As expected, the single mutation Tyr198Ala caused a marked reduction of activity in both Ramos and Jurkat cells suggesting that this single mutation, at least in part, caused the reduction in activity of TRAIL.R1-6 (Table 5.1).

Therefore the final mutant made was TRAIL.R1-5, which lacked the Tyr189Ala mutation (Table 5.1). As shown in Figures 5.1 and 5.2, this mutant caused a significant reduction in activity of Jurkat cells though still displayed activity in Ramos cells. Although TRAIL.R1-5 displayed some activity in Jurkat cells, this did not increase above the level of apoptosis cause by ETR1. Therefore, this reported activity in Jurkat cells could be due to a residual TRAIL-R1 signal in that specific cell line. In addition, there was very little reduction of activity in Ramos cells, suggesting that TRAIL.R1-5 was specific to TRAIL-R1 (Table 5.1 and Figure 5.2).

Receptor-selective mutant ligands to TRAIL-R1 and TRAIL-R2 induce apoptosis in Jurkat cells.

To test the specificity of TRAIL.R1-5 and the apoptotic activity of TRAIL.R2-6, Jurkat cells were treated with increasing concentrations of various forms of TRAIL or ETR1 or ETR2 (Figure 5.1).

HIS-TRAIL, TRAIL.R1-5 and TRAIL.R2-6 induced apoptosis in Jurkat cells in a concentration-dependent manner (Figure 5.1 A). TRAIL.R2-6 induced the highest levels of apoptosis reaching 68 ± 6% at 1000 ng/ml compared with 6 ± 0.5% in untreated cells. Wt TRAIL had less apoptotic activity in Jurkat cells compared with TRAIL.R2-6. The highest concentration of wt TRAIL (1000 ng/ml) induced 51 ± 1.2% apoptosis in agreement with previous findings in Chapter 4. In comparison, 1000 ng/ml of TRAIL.R1-5 induced a concentration-dependent increase in apoptosis, resulting in 25 ± 2% PS^+ cells.

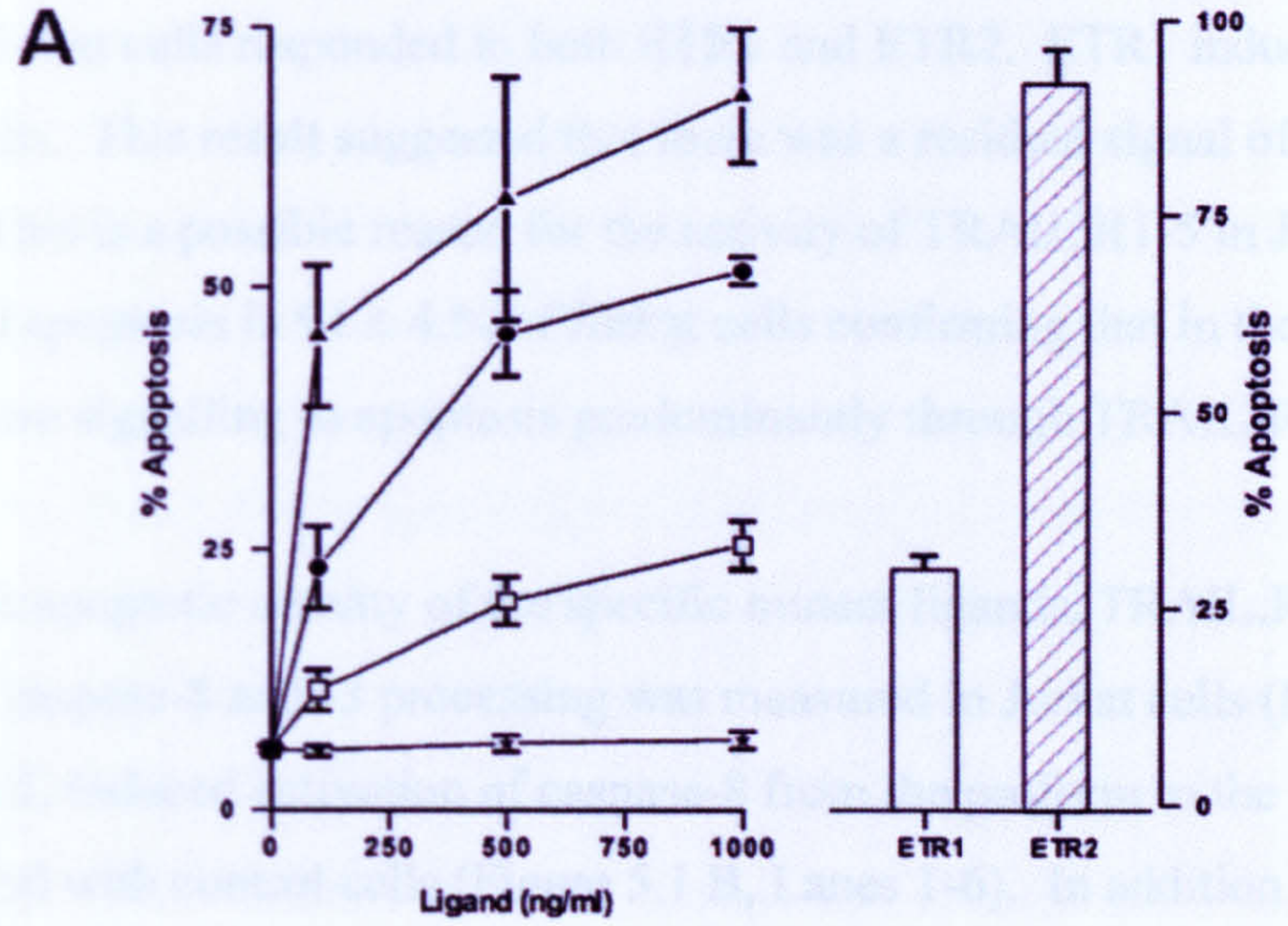

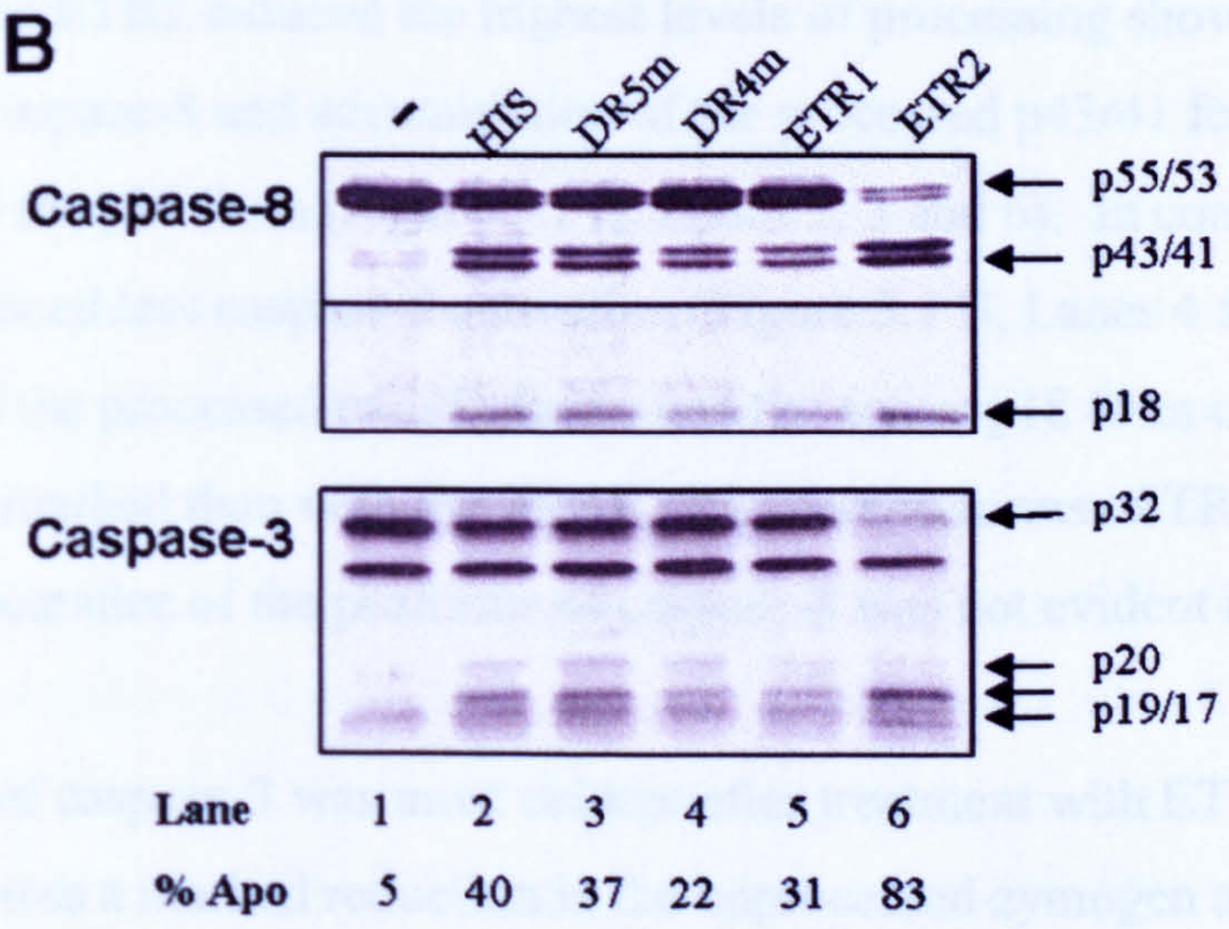

Figure 5.1: TRAIL mutants induce varying levels of apoptosis in Jurkat cells. A) Jurkat cells were cultured at $1x10^6$ cells per ml and treated with increasing concentrations of wt TRAIL (circles), TRAIL.R1-5 (squares), TRAIL.R1-6 (stars) or TRAIL.R2-6 (triangles) (100-1000 ng/ml), or treated with 1000 ng/ml ETR1 or ETR2 for 4 hours. Control cells were cultured with 1% PBS. Apoptosis was assessed by flow cytometry and determined by the percentage of PS^+ cells. Results are shown as mean ± SEM of at least three individual experiments. The student's t-test was used to determine significance of results. All concentrations of TRAIL.R1-6 and 100 ng/ml of TRAIL.R1-5 had a p-value > 0.05. All other data points were statistically significant as compared with the control ($p < 0.05$). B) Jurkat cells were treated with 500 ng/ml of wt TRAIL, TRAIL.R1-5 or TRAIL.R2-6, or treated with 1000 ng/ml ETR1 or ETR2 for 4 hours. Cell lysates were collected and caspase-8 and -3 processing was measured by western blotting. Results are representative of two independent experiments. DR4m is TRAIL.R1-5 and DR5m is TRAIL.R2-6.

In contrast, TRAIL.R1-6 was entirely inactive in Jurkat cells. ETR1 and ETR2 were used as a measure for the ability of Jurkat cells to respond to TRAIL through TRAIL-R1 or TRAIL-R2. Jurkat cells responded to both ETR1 and ETR2. ETR1 induced apoptosis in 30 ± 2% of cells. This result suggested that there was a residual signal of TRAIL-R1 in Jurkat cells. This is a possible reason for the activity of TRAIL.R1-5 in Jurkat cells. ETR2 induced apoptosis in 91 ± 4.% of Jurkat cells confirming that in these experiments Jurkat cells were signalling to apoptosis predominantly through TRAIL-R2.

To confirm the apoptotic activity of the specific mutant ligands, TRAIL.R2-6 and TRAIL.R1-5, caspase-8 and -3 processing was measured in Jurkat cells (Figure 5.1 B). All forms of TRAIL induced activation of caspase-8 from the proform to the processed p43/41 forms compared with control cells (Figure 5.1 B, Lanes 1-6). In addition, the catalytically active p18 subunit was also detected in all TRAIL treated samples. Wild type TRAIL, TRAIL.R2-6, and ETR2 induced the highest levels of processing shown by a reduction of the proform of caspase-8 and accumulation of the processed p43/41 forms and also the accumulation of the p18 form (Figure 5.1 B, Lanes 2, 3 and 6). In comparison, TRAIL.R1-5 and ETR1 induced less caspase-8 activation (Figure 5.1 B, Lanes 4 and 5). The accumulation of the processed p43/41 forms and the active p18 form of caspase-8 was evident but less marked than with the TRAIL-R2 specific forms of TRAIL and wt TRAIL. Also, the disappearance of the proforms of caspase-8 was not evident in these samples.

The processing of caspase-3 was most evident after treatment with ETR2 (Figure 5.1 B, Lane 6). There was a marked reduction in the unprocessed zymogen and an accumulation of the processed and catalytically active p19/17 fragments. In addition, wt TRAIL and TRAIL.R2-6 induced a small reduction in the presence of the proform of caspase 3 and an accumulation of p19/17 fragments (Figure 5.1 B, Lanes 2 and 3). In comparison, treatment with TRAIL.R1-5 and ETR1 corresponded with a small accumulation of the catalytically active p19/17 subunits of caspase-3 (Figure 5.1 B, Lanes 4 and 5). Processing of caspase-8 and -3 correlated with the induction of apoptosis as measured by PS externalisation.

The receptor-selective mutant ligand to TRAIL-R1 induces apoptosis in Ramos cells. To determine the specificity of TRAIL.R2-6, and the apoptotic activity of TRAIL.R1-5, Ramos cells were treated with increasing concentrations of various forms of TRAIL or ETR1 or ETR2 (Figure 5.2).

Wild type TRAIL and TRAIL.R1-5 induced apoptosis in a concentration-dependent manner. There appeared to be no difference in induction of apoptosis between wt TRAIL and TRAIL.R1-5, 49 ± 6% and 42 ± 5%, respectively. In comparison, TRAIL.R1-6 induced very little apoptosis in Ramos cells even when used at the highest concentration (17 ± 1%). As expected, TRAIL.R2-6 displayed no activity in Ramos cells suggesting that it acts through TRAIL-R2 alone. The TRAIL receptor specific antibodies ETR1 and ETR2 were used as a measure for the specificity of Ramos cells to signal to apoptosis through TRAIL-R1. As expected, ETR1 was extremely active in Ramos cells inducing 88 ± 0.1% apoptosis at 4 hours. In contrast, ETR2 induced 14 ± 3 % apoptosis suggesting that Ramos cells were responding to TRAIL specifically through TRAIL-R1 in these experiments.

Caspase-8 and -3 activation were used to confirm the ability of the TRAIL to induce apoptosis in Ramos cells (Figure 5.2 B). Only wt TRAIL, TRAIL.R1-5 and ETR1 induced processing of the caspase-8 proforms to its p43/41 forms and the catalytically active p18 form (Figure 5.2 B). ETR1 induced the highest level of caspase processing corresponding with induction of apoptosis (Figure 5.2 B, Lane 5). Levels of the proforms of caspase-8 were greatly reduced corresponding with the appearance of the processed forms p43/41 and, most notably, the marked accumulation of the p18 fragment. In comparison, wt TRAIL and TRAIL.R1-5 induced cleavage of the proforms to their p43/41 processed forms and accumulation of the catalytically active p18 form (Figure 5.2 B, Lanes 2 and 4). However, the accumulation of cleaved forms of caspase-8 were less evident in wt TRAIL and TRAIL.R1-5 treated cells compared with cells treated with ETR1. As expected, ETR2 and TRAIL.R2-6 did not induce caspase-8 cleavage (Figure 5.2 B, Lanes 3 and 6).

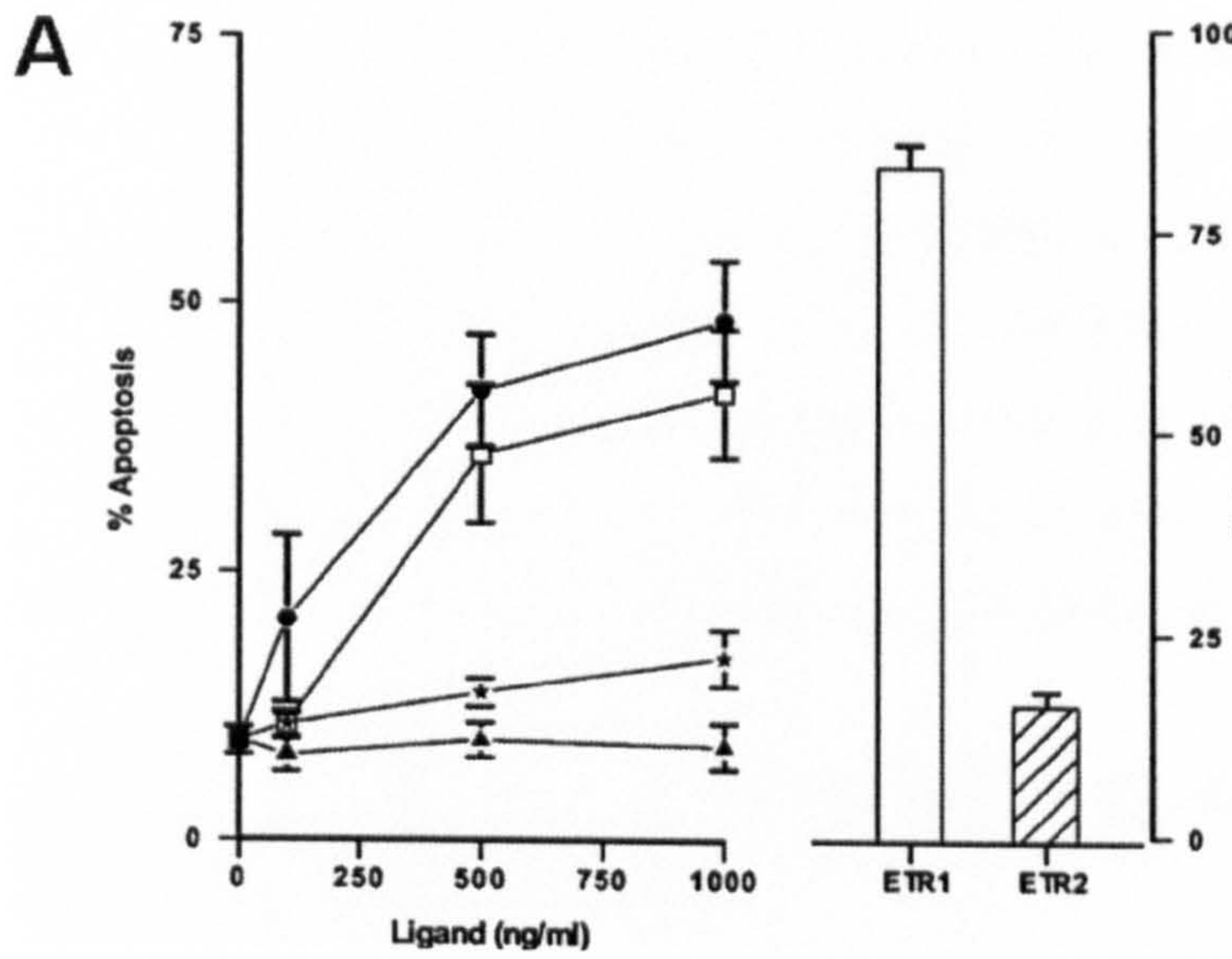

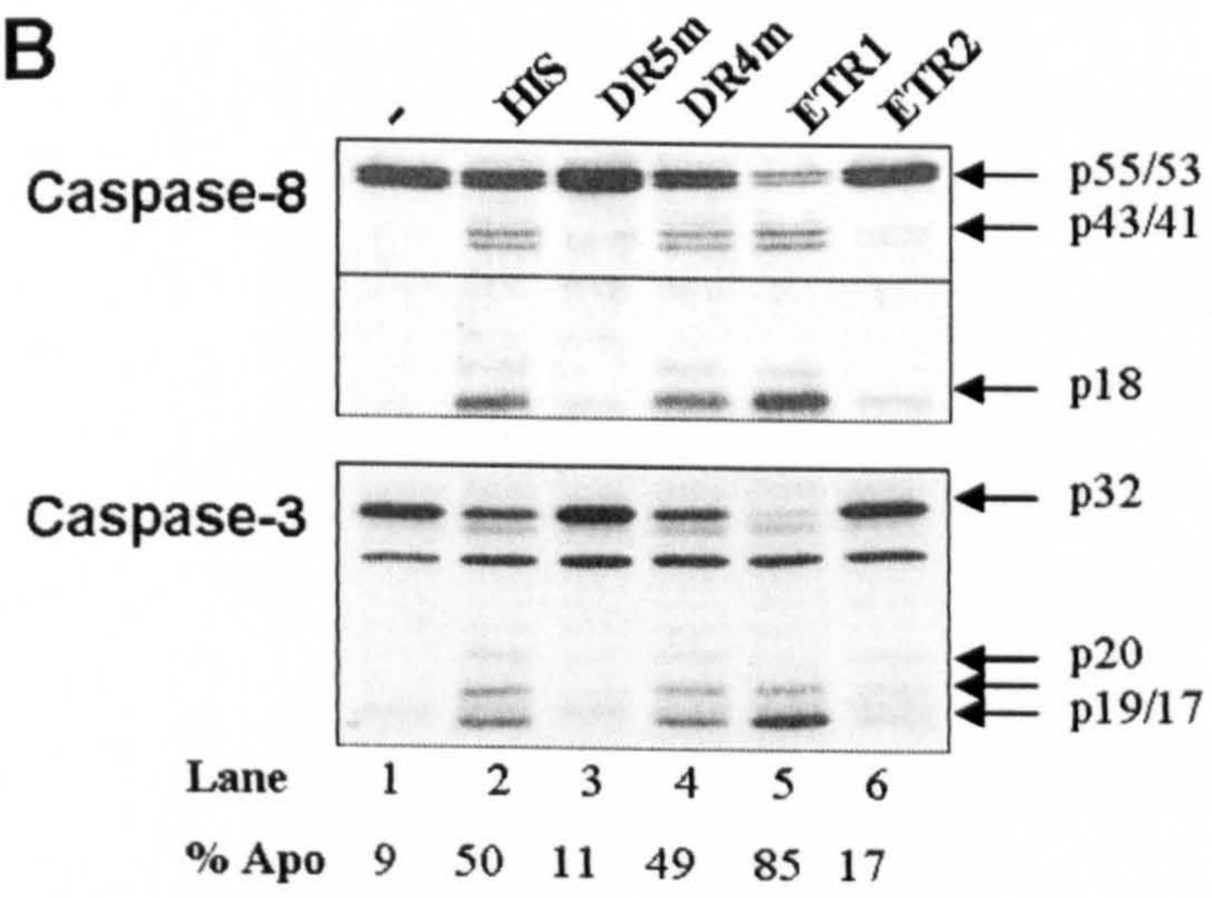

Figure 5.2: TRAIL mutants induce varying levels of apoptosis in Ramos cells. A) Ramos cells were cultured at $1x10^6$ cells per ml and treated with increasing concentrations of wt TRAIL (circles), TRAIL.R1-5 (squares), TRAIL.R1-6 (stars) or TRAIL.R2-6 (triangles) (100-1000 ng/ml), or treated with 1000 ng/ml ETR1 or ETR2 for 4 hours. Control cells were cultured with 1% PBS. Apoptosis was assessed by flow cytometry and determined by the percentage of PS^+ cells. Results are shown as mean ± SEM of at least three individual experiments. A t-test was carried out to determine statistical significance. All data points were statistically significant with the exception of 100 ng/ml wt TRAIL and TRAIL.R1-5 and all data points relating to TRAIL.R2-6 and TRAIL.R1-6 and ETR1 ($p > 0.05$). B) Ramos cells were treated with 500 ng/ml wt TRAIL, TRAIL.R1-5 or TRAIL.R2-6 or 1000 ng/ml ETR1 or ETR2 for 4 hours. Cell lysates were collected and caspase-8 and -3 processing was measured by western blotting. Results are representative of two individual experiments. DR4m is TRAIL.R1-5 and DR5m is TRAIL.R2-6.

Caspase-3 cleavage in Ramos cells correlated with caspase-8 cleavage. ETR1, wt TRAIL and TRAIL.R1-5 induced caspase-3 cleavage from its proform to its p20/19/17 forms (Figure 5.2 B). ETR1 induced the highest level of caspase-3 cleavage with almost a complete disappearance of the proform to a marked accumulation of its catalytically active p17 and p19 forms (Figure 5.2 B lane 5). Also, wt TRAIL and TRAIL.R1-5 induced a less apparent reduction in procaspase-3 and an accumulation of the p17, p19, and low levels of the p20 subunits (Figure 5.2 B lanes 2 and 4). The R2 specific forms of TRAIL did not induce detectable levels of caspase-3 cleavage (Figure 5.2 B lanes 3 and 6).

Blocking and Neutralising antibodies to TRAIL-R1 and TRAIL-R2, respectively, confirm the specificity of the mutant ligands.

To verify specificity of TRAIL.R1-5 in Ramos cells, a blocking antibody to TRAIL-R1 was used to block the apoptotic activity of various forms of TRAIL (Figure 5.3 A). The TRAIL-R1 blocking antibody alone induced apoptosis slightly above control levels. The TRAIL-R2 neutralising antibody induced low levels of apoptosis. All forms of TRAIL induced high levels of apoptosis (> 45%). The TRAIL-R1 blocking antibody inhibited apoptosis of wt TRAIL, TRAIL.R1-5 and ETR1 to some extent. Almost 50% of the apoptotic activity of wt TRAIL and ETR1 was blocked by the TRAIL-R1 blocking antibody. Similarly, greater than 50% of the apoptotic activity of TRAIL.R1-5 was inhibited by the TRAIL-R1 blocking antibody. In contrast, the TRAIL-R2 neutralising antibody did not block the apoptotic activity of any forms of TRAIL in Ramos cells.

To verify the specificity of TRAIL.R1-5 and TRAIL.R2-6 in Jurkat cells, blocking and neutralising antibodies were used as described above (Figure 5.3 B). The TRAIL-R1 blocking antibody induced no apoptosis on its own in Jurkat cells. In contrast, the TRAIL-R2 neutralising induced 20% apoptosis in Jurkat cells on its own. TRAIL.R2-6 and ETR2 induced > 50% apoptosis alone. The induction of apoptosis was not blocked by the TRAIL-R1 blocking antibody. The TRAIL-R2 neutralising antibody inhibited apoptosis to its baseline level of 20% in cells treated with TRAIL.R2-6 and ETR2.

TRAIL.R1-5 and ETR1 induced 25-30% apoptosis in Jurkat cells on their own. The TRAIL-R1 blocking antibody inhibited apoptosis induced by TRAIL.R1-5 and ETR1 to less than 10% apoptosis. The TRAIL-R2 neutralising antibody induced low levels of

apoptosis on its own and therefore was not used to block TRAIL.R1-5 or ETR1. Blocking TRAIL-R1 in Jurkat cells inhibits the activity of TRAIL.R1-5 and ETR1.

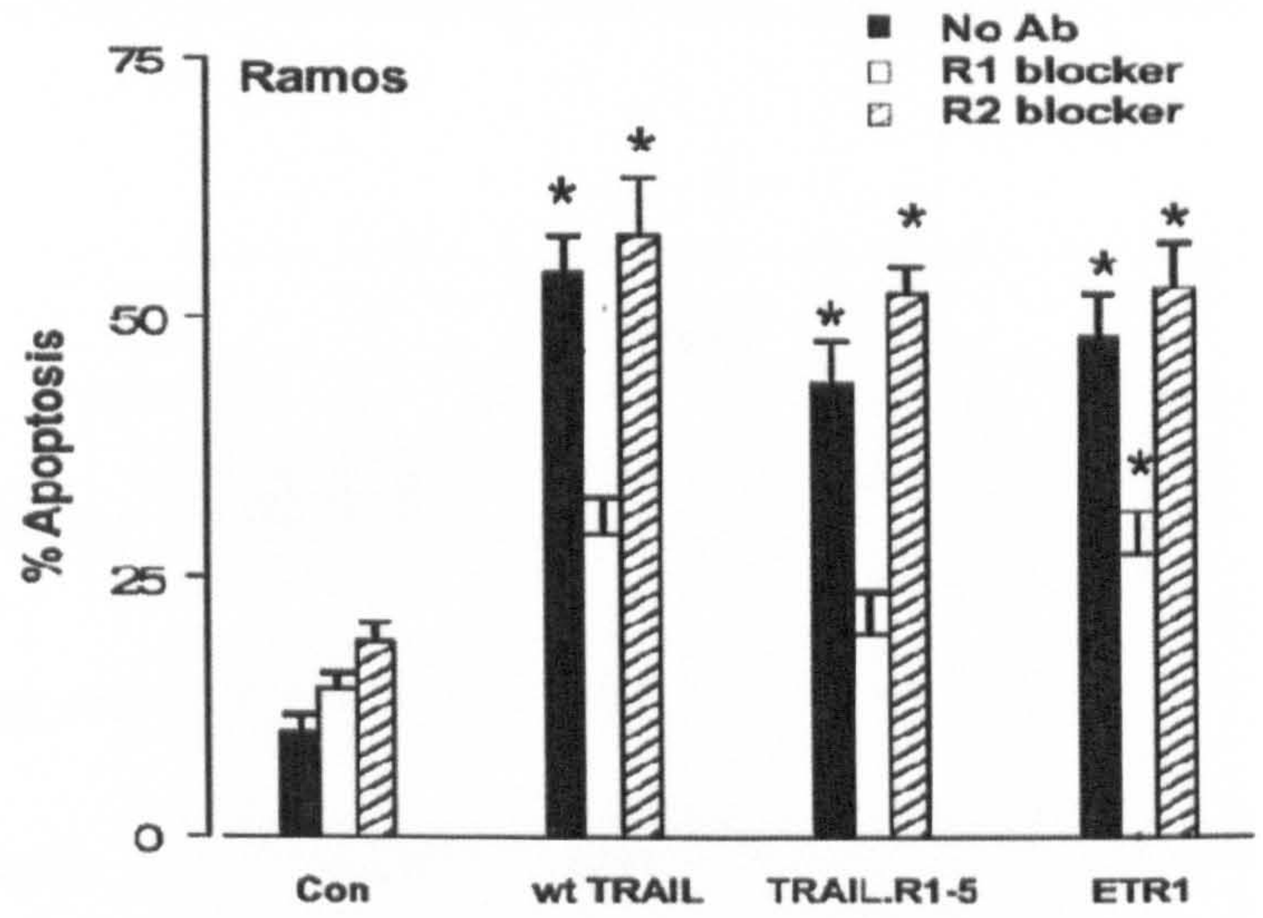

Figure 5.3: The activity of TRAIL mutants is selectively blocked in Ramos and Jurkat cells by blocking/neutralising antibodies. A) Ramos cells were cultured at $1x10^6$ cells per ml and pre-treated for 30 mins at 37°C either alone or with TRAIL-R1 blocking Ab (1 μg/ml) or TRAIL-R2 neutralising Ab (5 μg/ml) followed by 4 hours treatement with wt TRAIL (500 ng/ml), TRAIL.R1-5 (500 ng/ml) or ETR1 (1000 ng/ml). B) Jurkat cells were cultured at $1x10^6$ cells per ml and pre-treated for 30 min at 37°C either alone or with TRAIL-R1 blocking Ab (1 μg/ml) or TRAIL-R2 neutralising Ab (5 μg/ml). Cells were subsequently treated with either TRAIL.R2-6 (250 ng/ml), TRAIL.R1-5 (1000 ng/ml), ETR1 (1000 ng/ml) or ETR2 (1000 ng/ml) for 4 hours. Control cells were cultured with 1% PBS. Cell death was quantified by measuring the percentage of PS^+ cells. Results are shown as a Mean ± SEM of three individual experiments. * denotes a p-value < 0.05 compared with the corresponding control samples as determined by a One Way ANOVA followed by a Dunnett's test.

TRAIL-induced formation of a DISC in Ramos and Jurkat cells.

Biotin-labelled forms of the ligands were used to assess the formation of a DISC in Ramos and Jurkat cells (Figure 5.4). Thirty million Ramos cells and fifty million Jurkat cells were incubated with 500 ng/ml of biotin-labelled, wt TRAIL, TRAIL.R1-5, TRAIL.R1-6, or TRAIL.R2-6.

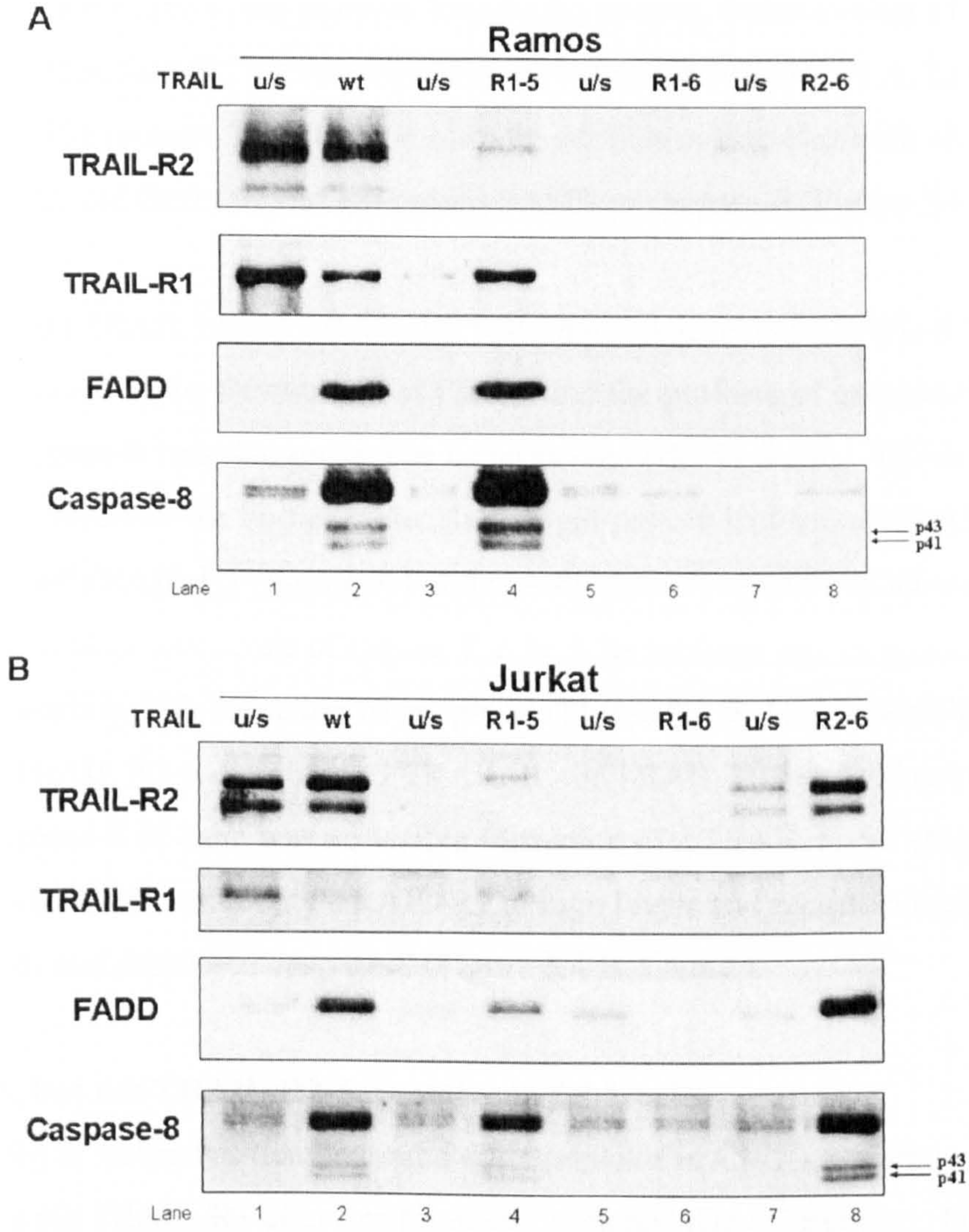

Figure 5.4: TRAIL mutants selectively induce DISC formation in Ramos and Jurkat cells. A) Ramos cells (30×10^6) were treated with biotinylated wt TRAIL, TRAIL.R1-5 or TRAIL.R2-6 (500 ng/ml) for 25 mins at 37°C. B) Jurkat cells (50×10^6) were treated with biotinylated wt TRAIL, TRAIL.R1-5 or TRAIL.R2-6 for 25 mins at 37°C. The collection and elution of DISC proteins was completed as described in Materials and Methods. The presence of TRAIL-R2, TRAIL-R1, FADD and caspase-8 were measured by western blotting. Results shown are representative of at least three individual experiments. Unstimulated lanes indicate the presence of components of the DISC pulled with biotinylated TRAIL in whole cell lysates. This figure was completed in collaboration with Dr. Marion MacFarlane.

In Ramos cells, wt TRAIL bound both TRAIL-R1 and TRAIL-R2 (Figure 5.4A Lane 2), and recruited FADD (Figure 5.4 A, Lane 2) and caspase-8 to the DISC. Caspase-8 was processed to its p43/41 forms (Figure 5.4 A, Lane 2). TRAIL.R1-5 bound TRAIL-R1 and very low levels of TRAIL-R2 (Figure 5.4 A, Lane 4). Only the high molecular weight band of TRAIL-R2 bound to TRAIL.R1-5. In addition, FADD and both the proform and processed p43/41 fragments of caspase-8 were recruited to the DISC (Figure 5.4 A, Lane 4). In contrast TRAIL.R1-6, the inactive TRAIL-R1 mutant, failed to bind TRAIL-R1 or TRAIL-R2 and therefore did not recruit FADD or caspase-8 (Figure 5.4 A, Lane 6). The TRAIL-R2 specific mutant, TRAIL.R2-6 also did not form a complex with either TRAIL-R1 or TRAIL-R2 and therefore did not recruit FADD or caspase-8 (Figure 5.4 A, Lane 8).

In Jurkat cells, wt TRAIL bound TRAIL-R2 and very low levels of TRAIL-R1 (Figure 5.4 B, Lane 2). This led to the recruitment of FADD and the proform of caspase-8 (Figure 5.4 B, Lane 2). Caspase-8 was also present in its processed p43/41 forms. TRAIL.R1-5 bound only low levels of the higher molecular weight protein isoform of TRAIL-R2 and also low levels of TRAIL-R1 (Figure 5.4 B, Lane 4). Low levels of FADD were recruited to the DISC as well as low levels of capase-8 in both its proform and its processed p43/41 forms, corresponding with induction of apoptosis (Figure 5.4 B, Lane 4 and Figure 5.2). As expected, TRAIL.R1-6 did not bind TRAIL-R1 or TRAIL-R2, and did not recruit FADD and caspase-8 as there was no visible formation of a TRAIL DISC (Figure 5.4 B, Lane 6). TRAIL.R2-6 bound only TRAIL-R2 at high levels and recruited high levels of FADD and pro- and processed caspase-8 (Figure 5.4 B, Lane 8).

TRAIL.R1-5, but not TRAIL.R2-6, is active in CLL cells.

Work with TRAIL mAbs has demonstrated that apoptosis in CLL is induced predominantly *via* TRAIL-R1 after pre-treatment with an HDAC inhibitor. To confirm this, CLL cells from 10 patients were pre-treated with 10 nM depsipeptide followed by treatment with ligands specific to TRAIL-R1 and TRAIL-R2 (Figure 5.5).

Depsipeptide alone and TRAIL alone did not induce apoptosis in any CLL patient samples (Figure 5.5 and data not shown). As expected, wt TRAIL, TRAIL.R1-5 and ETR1 induced apoptosis in depsipeptide-treated CLL cells to various degrees depending upon the patient sample with patients 3 and 8 being the most pronounced. Apoptosis induction was statistically significant in CLL cells that had been treated with depsipeptide followed by

treatment with TRAIL.R1-5 or ETR1 compared with cells that were untreated, treated with depsipeptide alone or treated with TRAIL.R1-5 or ETR1 alone ($p < 0.05$ as measured by a One Way ANOVA followed by a Dunnett's test). TRAIL.R2-6 and ETR2 did not significantly induce apoptosis in any CLL patient samples pre-treated with depsipeptide.

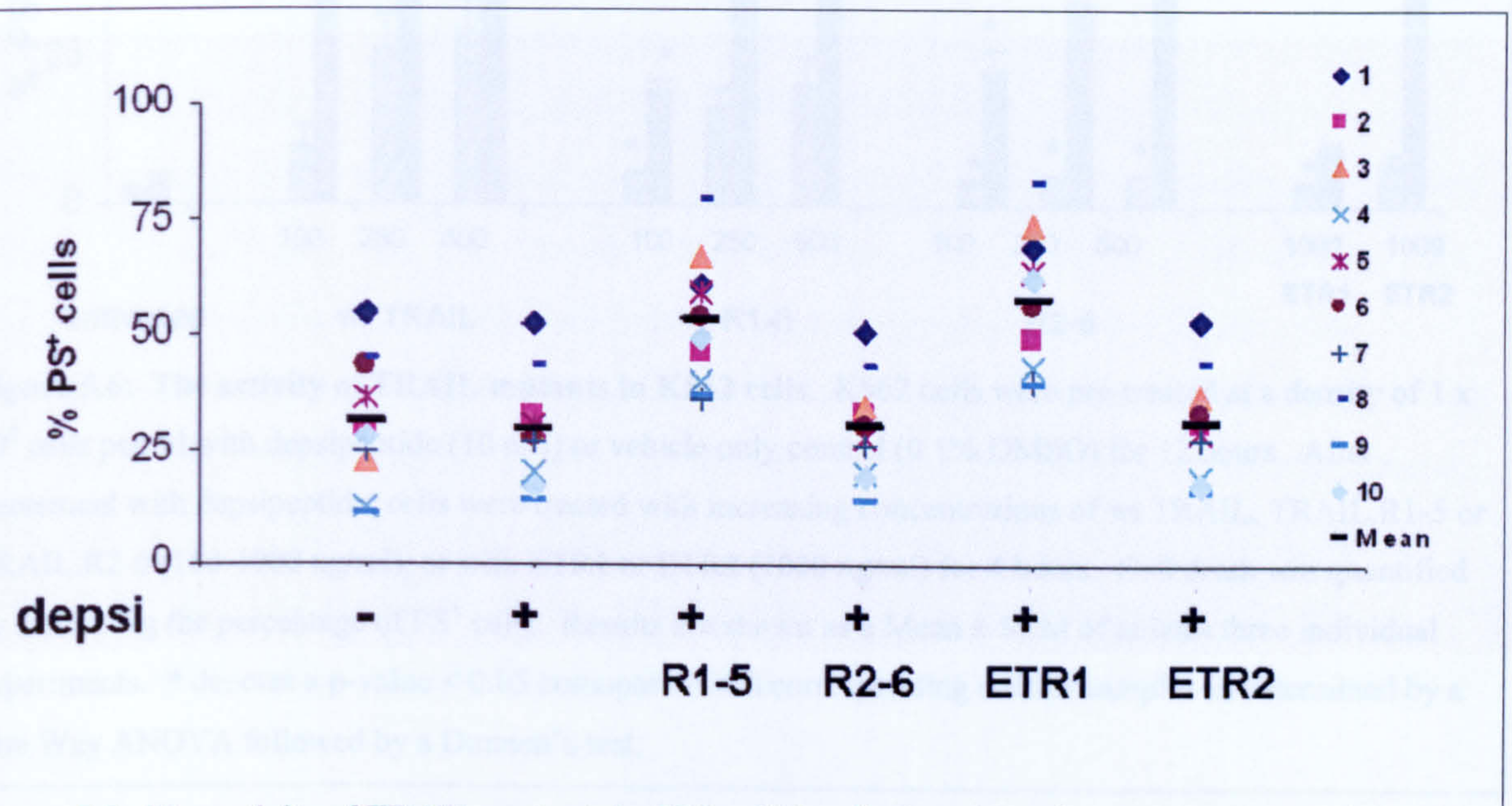

Figure 5.5: The activity of TRAIL mutants in CLL. CLL cells from 10 patients were pre-treated at a density of 5×10^6 cells per ml with depsipeptide (10 nM) or vehicle only control (0.1% DMSO) for 16 hours. After treatment with depsipeptide, cells were treated with wt TRAIL (100 ng/ml), TRAIL-R1-5 (1000 ng/ml), TRAIL-R2-6 (1000 ng/ml), ETR1 (1000 ng/ml) or ETR2 (1000 ng/ml) for 6 hours. Cell death was quantified by measuring the percentage of PS^+ cells. Each symbol represents one patient. The black line represents the mean for each treatment of all ten patient samples. Results with a p value < 0.05 according to a One Way ANOVA followed by a Dunnett's test were considered statistically significant.

TRAIL induces apoptosis in K562 cells via TRAIL-R1 and TRAIL-R2.

K562 cells are resistant to low concentrations of TRAIL in the absence of a sensitising agent (work in Chapter 4). However, in the presence of an HDAC inhibitor such as depsipeptide, work with TRAIL mAbs and various other preparations of TRAIL, such as Apo2L, suggests that K562 cells respond to TRAIL induced apoptosis primarily through TRAIL-R2 (work in Chapter 4). To confirm this result, K562 cells were treated with depsipeptide (10 nM) for 12 hours followed by treatment with increasing concentrations of wt TRAIL, TRAIL.R1-5 or TRAIL.R2-6, or ETR1 and ETR2 for 4 hours (Figure 5.6).

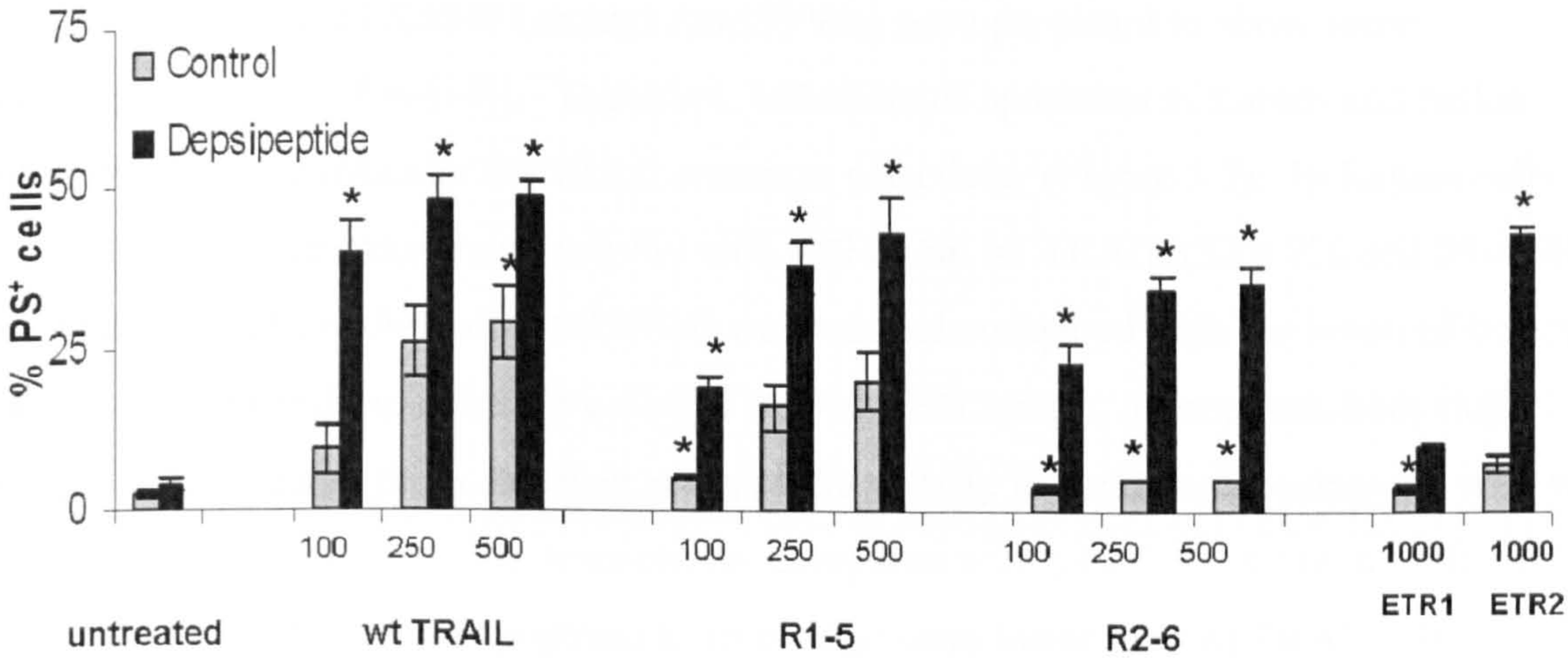

Figure 5.6: The activity of TRAIL mutants in K562 cells. K562 cells were pre-treated at a density of 1 x 10^6 cells per ml with depsipeptide (10 nM) or vehicle only control (0.1% DMSO) for 12 hours. After treatement with depsipeptide, cells were treated with increasing concentrations of wt TRAIL, TRAIL.R1-5 or TRAIL.R2-6 (100-1000 ng/ml), or with ETR1 or ETR2 (1000 ng/ml) for 4 hours. Cell death was quantified by measuring the percentage of PS^+ cells. Results are shown as a Mean ± SEM of at least three individual experiments. * denotes a p-value < 0.05 comopared with corresponding control samples as determined by a One Way ANOVA followed by a Dunnett's test.

Surprisingly, K562 cells responded to wt TRAIL and TRAIL.R1-5 alone at high concentrations of 500 and 1000 ng/ml (Figure 5.6 grey bars). Wild type TRAIL (1000 ng/ml) induced 29 ± 6% apoptosis in K562 cells after 4 hours of treatment. In comparison, the same concentration of TRAIL.R1-5 induced 20 ± 4% apoptosis in these cells at 4 hours. K562 cells did not undergo apoptosis when treated with TRAIL.R2-6, ETR1, or ETR2 as single agents.

In the presence of depsipeptide (Figure 5.6 black bars), K562 cells were further sensitised to wt TRAIL and TRAIL.R1-5. K562 cells were also sensitised to TRAIL.R2-6 and ETR2 in the presence of depsipeptide but remained resistant to ETR1 in agreement with findings in Chapter 4. Wild type TRAIL induced the highest levels of apoptosis (49 ± 3%) followed by ETR 2 (43 ± 1%) and TRAIL.R2-6 (36 ± 3%). TRAIL.R1-5 induced comparable levels of apoptosis (43 ± 6%). ETR1 induced very little apoptosis after treatment with depsipeptide (10 ± 1%).

Mutants with one amino acid change show some selectivity to TRAIL-R1.

Two TRAIL mutants (Ala191Leu and Asn199Val) were predicted to show some selectivity towards TRAIL-R1. Therefore, induction of apoptosis in Ramos and Jurkat cells was used as a measure for TRAIL-receptor selectivity (Figure 5.7). In Ramos cells Ala191Leu showed comparable activity with 500 ng/ml wt TRAIL (52 ± 7% and 59 ± 4%, respectively). The activity of Asn199Val was reduced compared with the levels of both wt TRAIL and Ala191Leu in Ramos cells (37 ± 2% at 500 ng/ml). In contrast, both single change mutants displayed a decrease in apoptotic activity in Jurkat cells compared with wt TRAIL (22 ± 5% and 19 ± 7%, respectively compared with 54 ± 10% at 500 ng/ml). The Asn199Val mutant induced apoptosis to levels that were lower than wt TRAIL. In contrast, the Ala191Leu mutant did not induce levels of apoptosis that were different from wt TRAIL at the same concentration. The activity of the single change mutants was below that of wt TRAIL, but was above that of ETR1 (12 ± 1%). Monoclonal Antibodies to TRAIL-R1 and TRAIL-R2 confirmed that apoptosis induction in Ramos cells was occurring specifically through TRAIL-R1 and in Jurkat cells was occurring predominantly through TRAIL-R2.

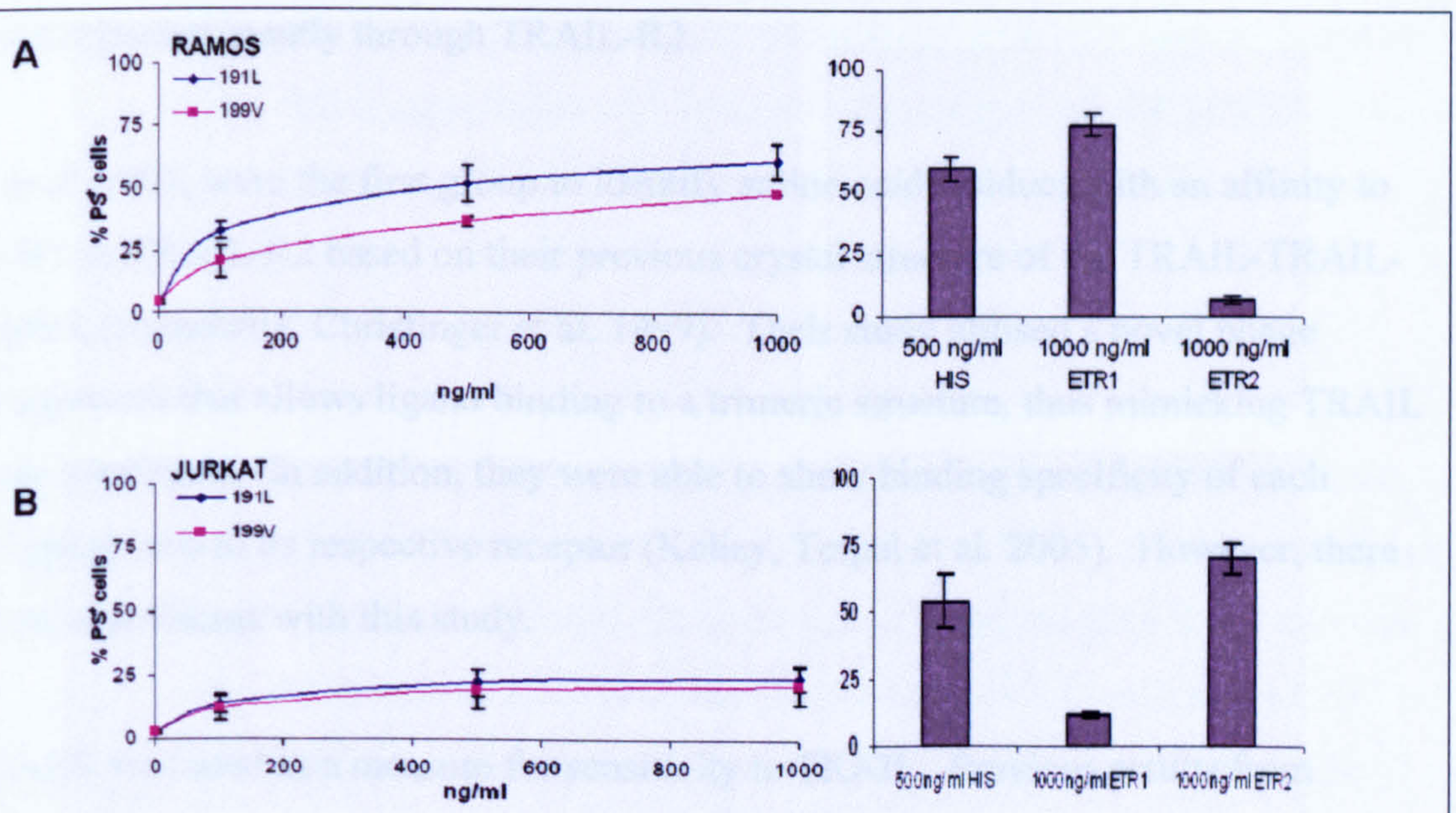

Figure 5.7: Single amino acid mutation results in selectivity towards TRAIL-R1. A) Ramos and B) Jurkat cells were cultured at a density of 1 x 10^6 cells per ml with increasing concentrations of Arg191Leu or Asn199Val (100-1000 ng/ml) or wt TRAIL (500 ng/ml), ETR1 or ETR2 (1000 ng/ml) for 4 hours. Apoptosis was measured by quantifying the % PS^+ cells and results are shown as Mean ± SEM of three independent experiments. Results were considered statistically significant from the control if they had a p value < 0.05 according to the student's t-test.

5.3 Discussion

TRAIL receptor-selective mutant ligands not only provide a possible therapy in CLL or other tumour models, but they also have the ability to provide mechanistic insight into the signalling patterns of each TRAIL-receptor individually. In this study, CLL cells were found to be sensitive to TRAIL.R1-5 as well as ETR1 after sensitisation with depsipeptide. These results confirm that CLL cells pretreated with depsipeptide respond to TRAIL via TRAIL-R1 and treating CLL cells with preparations of TRAIL that induce apoptosis primarily through TRAIL-R2 (ETR2 and Apo2L) may be ineffective.

Kelley et al. 2005, designed mutant ligands to bind to trimeric TRAIL-R1 and TRAIL-R2. After designing several mutants to TRAIL-R1 and TRAIL-R2 (including TRAIL.R1-6 and TRAIL.R2-6) they tested the mutants for apoptotic induction in a panel of cell lines that had been sensitive or resistant to Apo2L. In addition, they tested the binding affinity of each ligand to all four TRAIL receptors by a Biacore assay. The study found that although each of the TRAIL mutants bound to its respective receptor with a higher affinity than the other TRAIL receptors, only the TRAIL-R2 mutants killed tumour cell lines that respond to Apo2L. The primary conclusion drawn from this study was that cancer cell lines signal to apoptosis predominantly through TRAIL-R2.

Kelley et al. 2005, were the first group to identify amino acid residues with an affinity to TRAIL-R1 or TRAIL-R2 based on their previous crystal structure of the TRAIL-TRAIL-R2 complex (Hymowitz, Christinger et al. 1999). Their study utilised a novel phage display approach that allows ligand binding to a trimeric structure, thus mimicking TRAIL signalling conditions. In addition, they were able to show binding specificity of each mutant ligand used to its respective receptor (Kelley, Totpal et al. 2005). However, there were several problems with this study.

First, Apo2L was used as a measure for sensitivity to TRAIL. Previous results from Chapter 4 in this thesis have suggested that Apo2L induces apoptosis predominantly through stimulation of TRAIL-R2. Therefore, Kelley et al. 2005, were selecting for sensitivity to TRAIL-R2 and any cell line that is sensitive primarily through TRAIL-R1 would not be included in the panel of cell lines tested. Data in this chapter has not only compared the efficacy of the mutant ligands generated with that of wt TRAIL, but has also

utilised agonistic mAbs to TRAIL to determine what percentage of apoptosis in each cell type is through TRAIL-R1 and TRAIL-R2, respectively.

Second, after determining that the TRAIL-R1 mutants were inactive in the panel of cell lines tested, Kelley et al. 2005, concluded the reason was because cancer cells signal to apoptosis predominantly through TRAIL-R2. However, there could be several reasons why the TRAIL-R1 mutant was inactive in their study. The panel of cell lines used may not have signalled to apoptosis through TRAIL-R1, or one of the six amino acid mutations in the TRAIL-R1 mutants was causing a lack of activity rather than an increased affinity to TRAIL-R1. However, these issues were not addressed in the Kelley et al. 2005, study.

In this study, two mutants TRAIL.R1-6 and TRAIL.R2-6 (DR4-8 and DR5-8 in Kelley et al.2005, respectively) were produced and tested against wt TRAIL, ETR1 and ETR2 in Jurkat and Ramos cell lines. These cell lines were shown to signal to apoptosis in Chapter 4 through TRAIL-R2 and TRAIL-R1, respectively.

In agreement with previous findings, TRAIL.R2-6 induced high levels of apoptosis in Jurkat cells but no apoptosis in Ramos cells and this correlated with both caspase-8 and -3 processing, suggesting that it signalled to apoptosis specifically through TRAIL-R2 (Figure 5.1 and 5.2). In addition, TRAIL.R2-6 activity in Jurkat cells was blocked by a TRAIL-R2 neutralizing antibody, but not affected by a TRAIL-R1 blocking antibody, further confirming specificity through TRAIL-R2 (Figure 5.3B).

Although TRAIL.R2-6 pulled low levels of TRAIL-R2 in unstimulated cells in a Ramos DISC, in live cells TRAIL.R2-6 failed to form a stable complex (Figure 5.4 A, Lanes 7 and 8). In contrast, TRAIL.R2-6 bound TRAIL-R2 in Jurkat cells but not TRAIL-R1 and was able to recruit FADD and caspase-8 (including the processed p41/43 forms) to the DISC at higher levels than wt TRAIL, suggesting that apoptosis caused by TRAIL.R2-6 in Jurkat cells was purely through TRAIL-R2 (Figure 5.4 B). After sensitization with depsipeptide, TRAIL.R2-6 failed to induce apoptosis above vehicle controls in all patient samples tested (Figure 5.5). Taken together with data from Chapter 4, this suggests that TRAIL.R2-6 is not able to signal to apoptosis through TRAIL-R1.

TRAIL.R1-6 was inactive in both Ramos and Jurkat cells suggesting that one or more of the amino acid mutations was responsible for this lack of activity (Figure 5.1 and 5.2 and Table 5.1). Although binding of TRAIL.R1-6 to TRAIL-R1 was demonstrated in a previous publication (Kelley, Totpal et al. 2005), DISCs in Ramos and Jurkat cells demonstrate that TRAIL.R1-6 does not bind TRAIL-R1 or TRAIL-R2 in live cells or under unstimulated conditions, suggesting that TRAIL.R1-6 does not bind TRAIL-R1 and does not form a stable complex in live cells (Figure 5.4, Lanes 5 and 6). Therefore intermediate mutants were produced in order to pinpoint the residues responsible for this lack of activity (Table 5.1).

As shown in Table 5.1, amino acid mutations at residues 213 and 215 (TRAIL.R1-2) had no effect on the activity of TRAIL and behaved in the same way as wt TRAIL. These mutations had been incorporated in all of the TRAIL-R1 mutants in the original TRAIL mutant paper as it was suggested that these substitutions decreased binding of TRAIL to TRAIL-R2 by 10-fold (data not shown in Kelley et al. 2005). No work has been done to determine whether or not this is the case. However these mutations alone do not have an effect on the activity or specificity of TRAIL towards either receptor.

The addition of two residue switches, Asn199Val and Lys201Arg (TRAIL.R1-4), did not alter the activity of TRAIL in Ramos cells suggesting that it allowed signalling to apoptosis through TRAIL-R1. In contrast, the activity of TRAIL.R1-4 was partially reduced in Jurkat cells, suggesting that amino acid switches at 199 or 201 or both were responsible for a reduced signalling through TRAIL-R2. Despite a partial selectivity, it appeared that TRAIL.R1-4 signalled to apoptosis at a higher level than ETR1, suggesting that some of the apoptosis caused by TRAIL.R1-4 was because of a partial signal to TRAIL-R2. Therefore, an additional mutation was added at residue 189.

The addition of one amino acid switch reduced the activity of TRAIL in both Ramos and Jurkat cells (Tyr189Ala, TRAIL.R1-5a) suggesting that it was perhaps responsible for the lack of activity of the original TRAIL.R1-6 mutant. Therefore, wt TRAIL was mutated at 189 for a single amino acid switch and activity of this mutant (TRAIL.R1-1) was tested in Jurkat and Ramos cells. Although activity of TRAIL.R1-1 was higher in Ramos and Jurkat cells than both the TRAIL.R1-6 and TRAIL.R1-5a mutants, the addition of just one amino acid mutation did reduce activity of TRAIL compared with wt activity. This suggests that

the Tyr189Ala switch was partially causing a lack of activity in the TRAIL.R1-6 and TRAIL.R1-5a mutants however, a combination of this switch with one or more of the other five amino acid changes were probably causing full inactivity. In order to clarify the exact combination of amino acid changes necessary to cause lack of activity, a detailed study would need to be completed where different combinations of amino acid switches were tested.

Dr. Mike Sutcliffe (University of Manchester) modelled the structure of the TRAIL-TRAIL-R1 complex (Hymowitz, Christinger et al. 1999), based on the TRAIL-TRAIL-R2 crystal structure shown in the Appendix (Figure A.3) and provided two possible reasons for why the Tyr189Ala substitution may decrease the activity of TRAIL. Based on this structural model, the Tyr189 forms a hydrogen bond to a conserved Glu in both TRAIL-R1 and TRAIL-R2 (Figure A.3 A). The Tyr189A substitution to a small, non-polar residue removes this hydrogen bond in both the TRAIL-TRAIL-R1 and TRAIL-TRAIL-R2 complexes. This substitution also results in the removal of hydrophobic interactions with Arg191, Asp267, Ala272 and Lys224 which may change the folding patterns of the TRAIL protein. This explains why the addition of this as a single mutation decreases the activity of TRAIL both in Ramos and Jurkat cells.

The final mutant synthesised was TRAIL.R1-5 and it was lacking the 189 amino acid switch and had a switch at 193 instead. As seen in Table 5.1 and in Figures 5.1 and 5.2, TRAIL.R1-5 retained most of the original activity of wt TRAIL in Ramos cells, but lost much of its activity in Jurkat cells, suggesting that it was signalling purely through TRAIL-R1 (Figure 5.1 and 5.2). TRAIL.R1-5-induced caspase-8 and -3 activation correlated with induction of apoptosis in both Ramos and Jurkat cells, confirming the induction of apoptosis in these cells (Figure 5.1 and 5.2). In addition, depsipeptide sensitised CLL cells in all patient samples (to varying degrees) to TRAIL.R1-5, suggesting that it can behave through TRAIL-R1 (Figure 5.5). A blocking antibody to TRAIL-R1 was able to block the activity of TRAIL.R1-5 but a neutralising antibody to TRAIL-R2 did not have an effect on TRAIL.R1-5 activity further confirming specificity through TRAIL-R1 (Figure 5.3 A).

TRAIL.R1-5 was able to form DISC complexes in both Ramos and Jurkat cells (Figure 5.4). TRAIL.R1-5 bound TRAIL-R1 but not TRAIL-R2 in unstimulated Ramos cells but pulled low levels of TRAIL-R2 in live cells. This suggests that either TRAIL.R1-5 can

pull TRAIL-R1/TRAIL-R2 heterocomplexes, as well as pure complexes, or the TRAIL-R2 antibody can detect low level of TRAIL-R1. Interestingly, in unstimulated lanes, both TRAIL.R1-5 and TRAIL.R2-6 pulled less of their respective receptor than wt TRAIL despite pulling more FADD and caspase-8 in live cells (Figure 5.4). One possible reason for this is that the TRAIL mutants were designed to bind to a trimeric structure, and therefore may have been selected not to pull free TRAIL-receptors whereas wt TRAIL was identified for its similarities with other TNF-family members but not by its ablility to bind to a trimeric structure (Wiley, Schooley et al. 1995; Pitti, Marsters et al. 1996; Kelley, Alkan et al. 2004).

K562 cells have previously been shown to be resistant to TRAIL at low concentrations but sensitised after treatment with depsipeptide (Inoue, MacFarlane et al. 2004). In Chapter 4, K562 cells were shown to signal primarily through TRAIL-R2 and were resistant to ETR1 before and after treatment with depsipeptide.

Wild type TRAIL and TRAIL.R1-5 induced low levels of apoptosis in K562 cells at high concentrations on their own (Figure 5.6). This was surprising given that K562 cell had previously been shown to be resistant to ETR1 both with and without depsipeptide (Chapter 4). Pre-treatment with depsipeptide further sensitised K562 cells to wt TRAIL and TRAIL.R1-5 and also sensitised cells to TRAIL.R2-6 and ETR2. In keeping with previous results, K562 cells remained resistant to ETR1. This result suggests that there could be signalling differences between antibodies and ligand; it is not clear whether sensitising agents can exaggerate these differences. Analysis of DISC proteins using each mutant ligand may help to identify possible signalling differences between the mutants. However, further investigation of the signalling differences between ligands and antibodies would require a large panel of cell lines and different preparations of TRAIL and TRAIL mAbs and is beyond the scope of this investigation.

Work with these mutants suggests that very few amino acid mutations are required for specificity through TRAIL-R1 or TRAIL-R2. It remains to be determined which mutations are necessary for the ability of TRAIL to selectively function through TRAIL-R1. A structural model of the TRAIL-TRAIL-R1 complex (completed by Mike Sutcliffe based on the TRAIL-TRAIL-R2 crystal structure (Hymowitz, Christinger et al. 1999)) has suggested two possible sites for mutation that, with a single amino acid switch, could

improve the ability of TRAIL to selectively function through TRAIL-R1 by disrupting TRAIL-TRAIL-R2 interactions.

First, Asn199Val is predicted to cause a loss of two hydrogen bonds in the TRAIL-TRAIL-R2 complex, but only one of these affected residues is conserved in TRAIL-R1, therefore only one hydrogen bond is lost in the TRAIL-TRAIL-R1 complex (Figure A.3 A). As a single mutant, this residue may provide some specificity to TRAIL-R1 although it may reduce the activity of TRAIL in both a TRAIL-R1 cell type and a TRAIL-R2 cell type because hydrogen bonds are lost in both the TRAIL-TRAIL-R1 and the TRAIL-TRAIL-R2 complexes.

Second, Arg191 is predicted to form protein-protein interactions in the TRAIL-TRAIL-R2 complex but not the TRAIL-TRAIL-R1 complex. Therefore, disrupting these interactions either by a hydrophobic residue (Leucine) or a charge reversal (Glutamine) should increase specificity to TRAIL-R1 without altering the activity of TRAIL in a TRAIL-R1 signalling cell. Interestingly, Arg191 was mutated in TRAIL.R2-6 to a Lysine to increase binding to TRAIL-R2.

To test this theory, Arg191Leu and Asn199Val were generated as single change mutants and tested in Ramos and Jurkat cells (Figure 5.7). As predicted, Arg191Leu retained the same apoptotic activity as wt TRAIL in Ramos cells, but this activity was reduced in Jurkat cells. In contrast, the activity of Asn199Val was reduced in both Ramos and Jurkat cells compared with the activity of wt TRAIL. However the reduction in apoptosis was more apparent in Jurkat cells, suggesting that the TRAIL-TRAIL-R2 complex was more disrupted than the TRAIL-TRAIL-R1 complex as predicted. Both mutants provide a degree of specificity however levels of apoptosis induced by each mutant in Jurkat cells exceed those induced by ETR1 suggesting the partial involvement of TRAIL-R2 in apoptosis induction by these mutants. DISC analysis would need to be completed to form more concrete conclusions about signalling differences between ligand and mAb.

A recent publication has designed novel TRAIL-R2-selective mutants with 1 or 2 amino acid changes (van der Sloot, Tur et al. 2006). They modelled the TRAIL-TRAIL-receptor complexes (TRAIL-R1, TRAIL-R2, TRAIL-R3 and TRAIL-R4) and considered mutating residues that were in the TRAIL-TRAIL-receptor interface but were not conserved among

all four TRAIL-receptors. Interestingly, many of the same residues that were mutated both in TRAIL.R1-6 and TRAIL.R2-6 were considered in this study (van der Sloot, Tur et al. 2006). However, final mutations were the single mutant Asp269His and the double mutants Asn269His and Glu195Arg, and Asp269His and Tyr214Arg. Binding to TRAIL-R2 was increased compared with wt TRAIL in all mutants. In addition, binding to TRAIL-R1 was decreased compared with wt TRAIL in all mutants. The biological activity of the mutants was compared in a panel of cell lines and the activity of each mutant was successfully blocked with a neutralizing antibody to TRAIL-R2, but not by a TRAIL-R1 neutralising antibody. It is important to note that TRAIL-R1 receptor-selective mutants were not addressed in this study (van der Sloot, Tur et al. 2006).

The fewer mutations introduced into the TRAIL sequence, the less likely protein misfolding will occur. Therefore, ligands need to be designed for specificity but also contain as few amino acid changes as possible. TRAIL.R1-5 has 5 amino acid changes and some of these may be unnecessary. It is clear from intermediate mutants generated, that Tyr213Trp and Ser215Asp do not provide specificity to TRAIL-R1 and therefore are not necessary. In addition, when comparing TRAIL.R1-4 with Asn199Val, there appears to be no difference in apoptotic ability of the two mutants and no difference in specificity. Therefore, Lys201Arg may not be required in a TRAIL-R1-selective mutant. TRAIL.R1-5 was used as a final TRAIL-R1 mutant; however Gln193Ser reduces the activity of TRAIL both in Ramos and Jurkat cells and may not enhance specificity. Therefore a double mutant Arg191Leu and Asn199Val may provide specificity to TRAIL-R1 without compromising activity. To further identify potential mutants, combinations of double switches should be tested on Jurkat and Ramos cells.

Chapter 6: An Investigation into TRAIL internalisation patterns

6.1 Introduction: TRAIL internalisation patterns

K562 cells were found to signal to apoptosis through both TRAIL-R1 and TRAIL-R2 when treated with receptor-selective mutant ligands in the presence of an HDAC inhibitor (Chapter 5). This was a surprising result given that treatment with TRAIL mAbs suggested that K562 cells signal primarily through TRAIL-R2 when pre-treated with an HDAC inhibitor (data in Chapter 4). In this Chapter, K562 DISC formation was analysed in the presence and absence of depsipeptide using wt TRAIL and mutant ligands. Interestingly, when TRAIL was used at high concentrations in the presence of depsipeptide, less FADD was detected in the DISC than in cells treated with TRAIL in the absence of depsipeptide. One possible explanation for this was that the DISC complex was being internalised and dissociated from TRAIL more rapidly when TRAIL was used at higher concentrations. Therefore internalisation patterns of TRAIL were investigated.

Endocytosis is an important process to maintain the correct balance of nutrients and chemicals within a cell (Polo and Di Fiore 2006). Many forms of endocytosis have been identified and new pathways continue to be identified. However the majority of proteins are thought to be internalised by clathrin-mediated endocytosis (Polo and Di Fiore 2006). The role of endocytosis in apoptosis has not been studied thoroughly. There have been several contradictory reports identifying the role of endocytosis in Death Receptor-induced apoptosis (Algeciras-Schimnich, Shen et al. 2002; Schneider-Brachert, Tchikov et al. 2004; Austin, Lawrence et al. 2006; Lee, Feig et al. 2006). However, the importance of internalisation to TRAIL-induced apoptosis is not yet clear.

One paper concluded that endocytosis was necessary for CD95-induced apoptosis in type I cells (Lee, Feig et al. 2006). Another paper stated that TNFR1 DISC formation and endocytosis into receptosomes were inseparable events (Schneider-Brachert, Tchikov et al. 2004). While the same has not been indicated for TRAIL-induced apoptosis, the question is pertinent to work done with TRAIL, particularly when considering mechanisms of resistance to TRAIL. In this chapter, BJAB cells were primarily used to study TRAIL internalisation.

TRAIL was found to rapidly internalise in BJAB cells. In addition, endocytosis was not required for DISC formation in either BJAB or HeLa cells. HeLa cells expressing the K44A dominant negative dynamin-1 protein were used as a tool to investigate the mechanisms of TRAIL internalisation. The K44A dynamin had no effect on TRAIL-induced apoptosis or DISC formation at 4°C. In addition, dynamin was not required for TRAIL internalisation in HeLa cells suggesting that, in the absence of dynamin, a pathway other than clathrin-mediated endocytosis may be employed.

Work from this chapter raises several questions that warrant further study. What effect does inhibition of TRAIL internalisation have on TRAIL-induced apoptosis? Is a defect in endocytosis a possible mechanism for resistance to TRAIL and can sensitisation to TRAIL-induced apoptosis overcome this block? What is the mechanism of TRAIL internalisation? All of these questions can be addressed with the right approaches and may lead to further avenues of investigation in future.

6.2 Results

TRAIL mutants form a DISC in K562 cells.

To characterise signalling differences between wt TRAIL, TRAIL.R1-5, and TRAIL.R2-6, analysis of the DISC proteins pulled from each ligand after 30 mins of treatment with TRAIL was undertaken as described in Materials and Methods (Figure 6.1). As expected, wt TRAIL pulled high levels of both TRAIL-R1 and TRAIL-R2 (Figure 6.1, Lane 2). High levels of FADD and caspase-8 were pulled corresponding to levels of apoptosis. In addition, caspase-8 was partially processed to its p43/41 forms at this time. Cells that were treated with wt TRAIL after lysis (Figure 6.1, Lane 1) pulled both TRAIL-R1 and TRAIL-R2 but not FADD or caspase-8 demonstrating that wt TRAIL can bind to both TRAIL-R1 and TRAIL-R2.

TRAIL.R1-5 formed a stable DISC complex in K562 cells (Figure 6.1, Lane 4). Unexpectedly, both TRAIL-R1 and TRAIL-R2 (particularly the high molecular weight band) bound to TRAIL.R1-5. High levels of FADD and both the proforms and processed p43/41

forms of caspase-8 were visible in the DISC complex at this time point. Cells that were treated with TRAIL.R1-5 after lysis (Figure 6.1, Lane 3) only bound to TRAIL-R1.

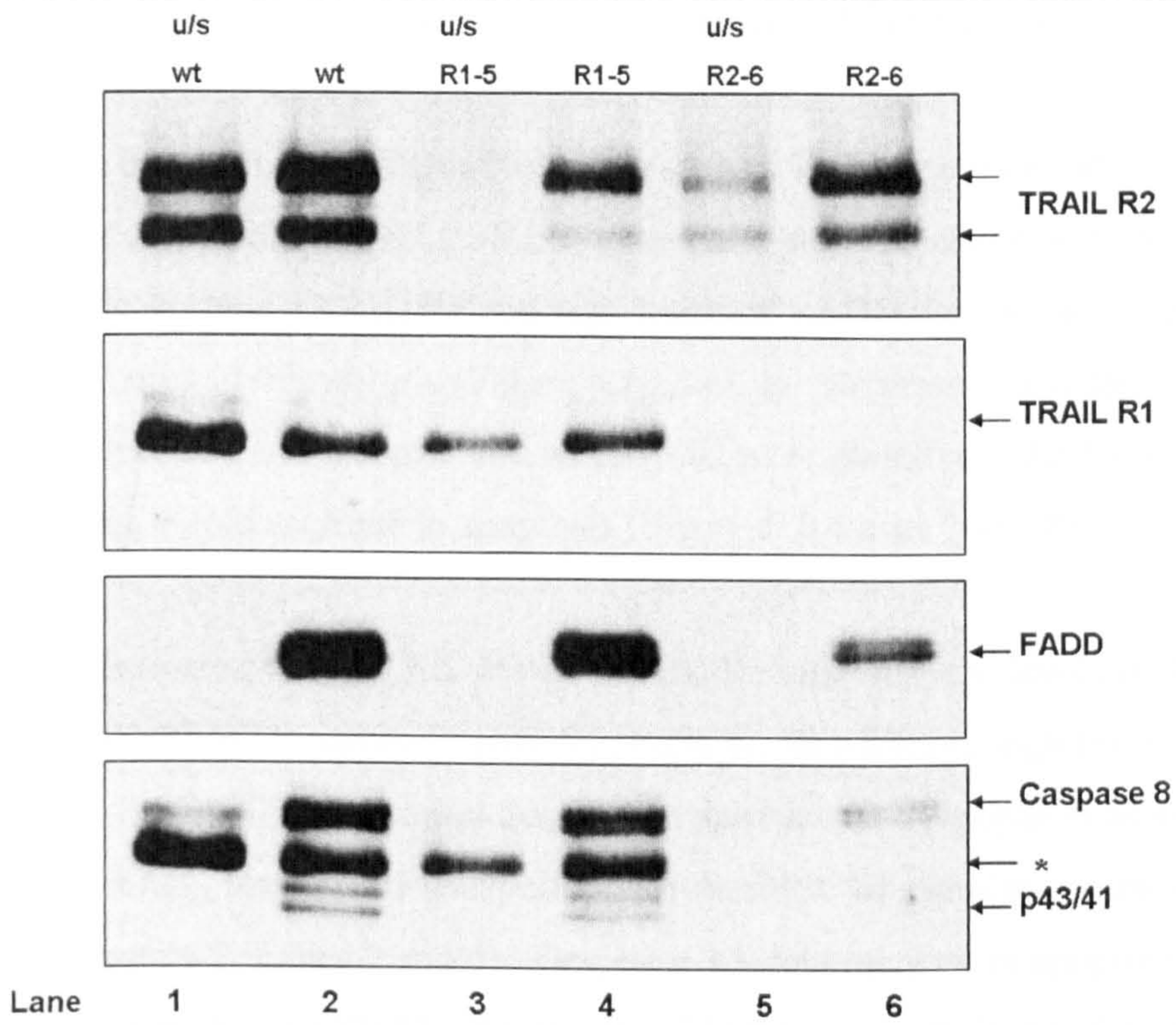

Figure 6.1: TRAIL receptor-selective mutants induce DISC formation in K562 cells. K562 cells were either left unstimulated or treated with biotinylated wt TRAIL, TRAIL.R1-5 or TRAIL.R2-6 (500 ng/ml) for 30 minutes at 37°C. The collection and analysis of DISC proteins was completed as described in Materials and Methods. TRAIL-R1, TRAIL-R2, FADD, and caspase-8 were detected using western blotting. Results shown are representative of at least three individual experiments. Unstimulated (u/s) lanes indicate the presence of components of the DISC pulled with biotinylated TRAIL in whole cell lysates. * Denotes TRAIL-R1 from a re-probed membrane.

TRAIL.R2-6 formed a smaller DISC complex in K562 cells (Figure 6.1, Lane 6). TRAIL.R2-6 only pulled TRAIL-R2 and recruited low levels of FADD and procaspase-8. No processed caspase-8 was visible in the DISC at this time. Cells that were treated with TRAIL.R2-6 after lysis (Figure 6.1, Lane 5) only bound TRAIL-R2. Ligand-induced DISC formation correlated with apoptosis induction in all cases.

TRAIL-induced DISC formation in the presence of Depsipeptide in K562 cells.

Thirty million K562 cells were pre-treated with and without Depsipeptide (10 nM) for 12 hours followed by treatment with; wt TRAIL, TRAIL.R1-5 or TRAIL.R2-6 (500 ng/ml) for 30 mins. Analysis of DISC proteins was carried out as described in Materials and Methods.

As shown by unstimulated lanes (Figure 6.2, Lanes 1 and 7) depsipeptide induced an increase in TRAIL-R2 and a decrease in TRAIL-R1 as expected. In the control situation, wt TRAIL bound both TRAIL-R1 and TRAIL-R2 and high levels of FADD despite only inducing 10% apoptosis at four hours in this sample (Figure 6.2, Lane 2). However when samples were pre-treated with depsipeptide less receptor and less FADD were pulled into the DISC complex despite a more than 4-fold increase in apoptosis (Figure 6.2, Lanes 2 and 8).

In control samples treated with TRAIL.R1-5, TRAIL-R1 and very low levels of TRAIL-R2 were pulled into the DISC complex (Figure 6.2, Lane 4). In addition, high levels of FADD were recruited to the DISC complex but despite the same levels of apoptosis as samples treated with wt TRAIL, less FADD was pulled into the DISC of samples treated with TRAIL.R1-5 (Figure 6.2, Lanes 2 and 4). Despite a 3.5-fold increase in apoptosis in samples treated with depsipeptide, less TRAIL-R1 and less FADD were recruited to the DISC in this situation (Figure 6.2, Lanes 4 and 10). No TRAIL-R2 was visible at the DISC in this sample (Figure 6.2, Lane 10).

As expected, TRAIL.R2-6 pulled low levels of TRAIL-R2 but no TRAIL-R1 in the control situation (Figure 6.2, Lane 6). Also, correlating with the induction of apoptosis, very little FADD was pulled into the DISC (Figure 6.2, Lane 6). Depsipeptide increased binding of TRAIL.R2-6 to TRAIL-R2 but the level of FADD remained approximately the same despite a 4-fold increase in apoptosis (Figure 6.2, Lanes 6 and 12).

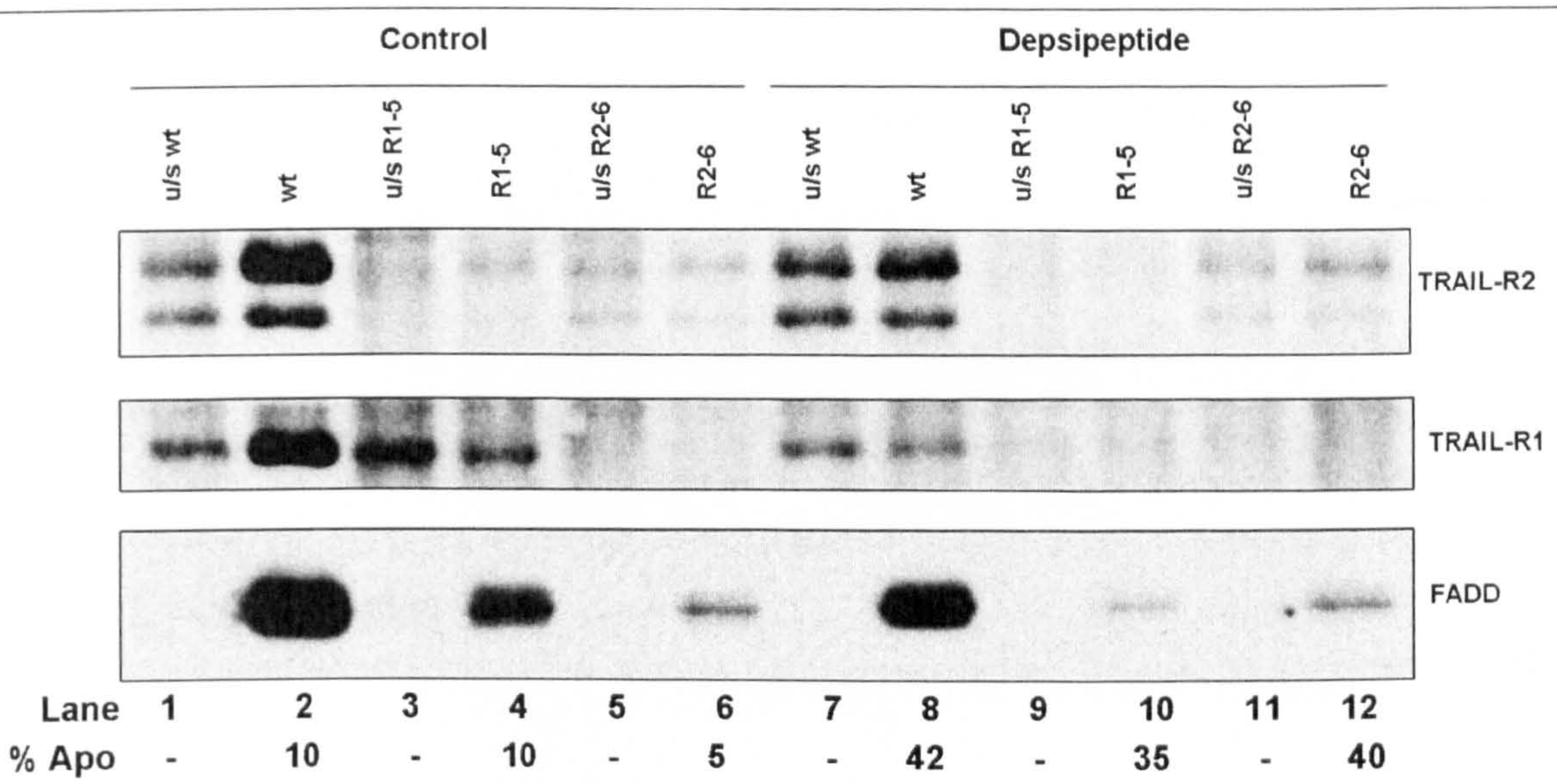

Figure 6.2: TRAIL receptor-selective mutants induce DISC formation in K562 cells in the presence of depsipeptide. K562 cells were treated with or without 10 nM depsipeptide for 12 hours followed by treatment with either biotinylated wt TRAIL, TRAIL.R1-5 or TRAIL.R2-6 for 25 mins at 37°C. The collection and analysis of DISC proteins was completed as described in Materials and Methods. TRAIL-R1, TRAIL-R2 and FADD were detected using western blotting. Results are shown as one experiment representative of at least three. Unstimulated lanes indicate the presence of components of the DISC pulled with biotinylated TRAIL in whole cell lysates.

Caspase-8 processing in K562 lysates correlates with TRAIL-induces apoptosis.

To confirm that caspase-8 processing in whole cell lysates correlates with TRAIL-induced apoptosis in K562 cells, K562 cells were pre-treated with or without depsipeptide followed by treatment with various forms of TRAIL for up to 8 hours. Untreated cells did not appear to have processed caspase-8 in the lysate (Figure 6.3 A and B, Lane 1). In contrast, cells treated with depsipeptide had low levels of the p43/41 forms of caspase-8 in the lysates (Figure 6.3 B, Lane 2). In cells that were not pre-treated with depsipeptide, wt TRAIL and TRAIL.R1-5 accumulated a build-up of similar levels of the p43/41 and the p18 fragments of caspase-8 over time reaching maximum levels after 4 hours of treatment (Figure 6.3 A, Lanes 2-9). The build-up of processed caspase-8 was much less apparent in samples treated with TRAIL.R2-6 with only low levels of the p43/41 forms of caspase-8 visible (Figure 6.3 A, Lanes 10-13). These data correlated with levels of apoptosis induction.

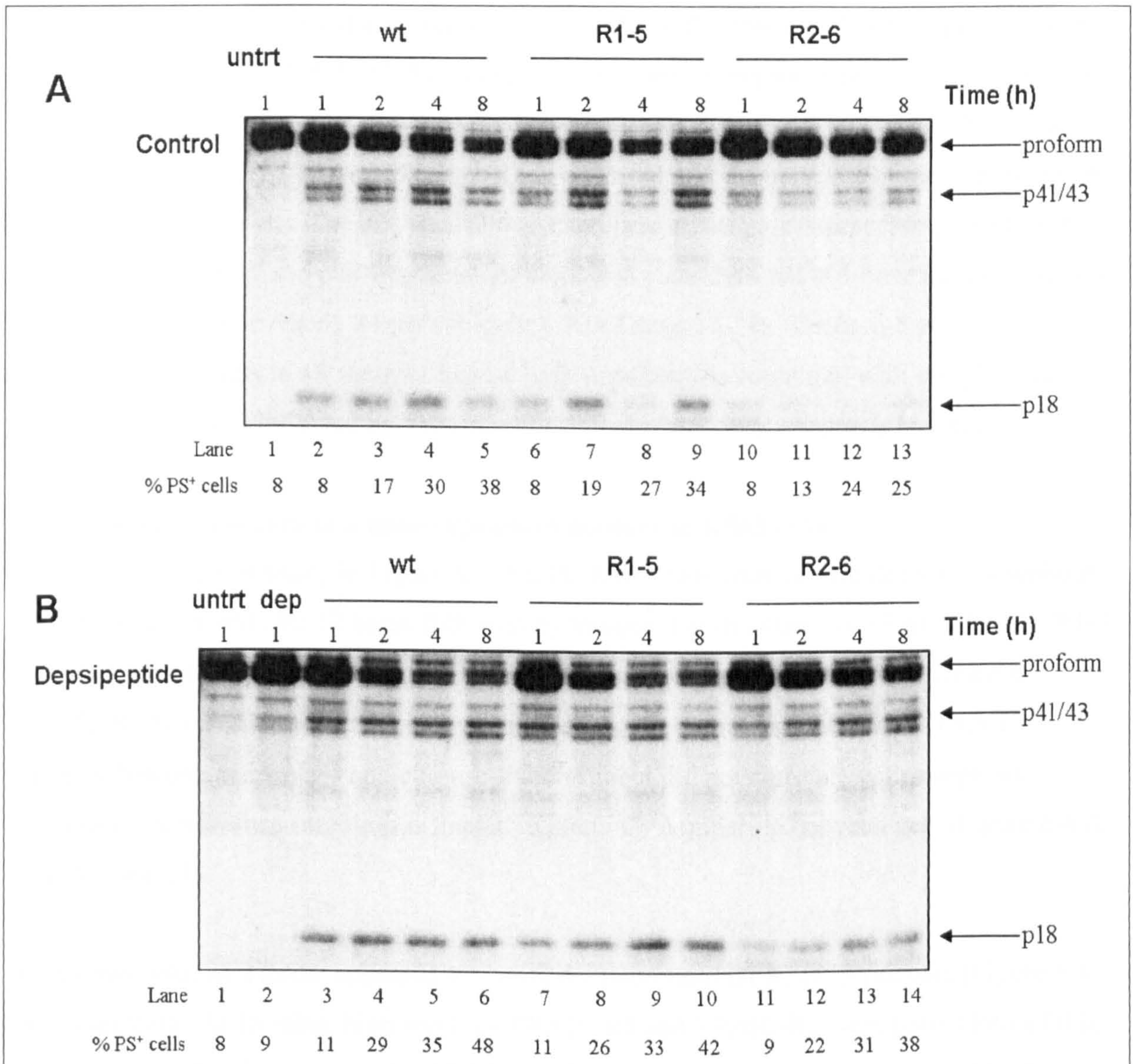

Figure 6.3: TRAIL receptor-selective mutants induce a time-dependent processing of caspase-8 in K562 cells. A) K562 cells were treated with biotinylated wt TRAIL, TRAIL.R1-5 or TRAIL.R2-6 (500 ng/ml) for 1, 2, 4 or 8 hours at 37°C. Cell lysates were collected and caspase-8 activation was assessed by western blotting. B) K562 cells were pretreated with Depsipeptide (10 nM) for 12 hours followed by treatment with biotinylated wt TRAIL, TRAIL.R1-5 or TRAIL.R2-6 (500 ng/ml) for 1, 2, 4 or 8 hours at 37°C. Caspase-8 activation was assessed by western blotting. Apoptosis was measured by determining the percentage of PS^+ cells. Results shown are one experiment only.

Samples pre-treated with depsipeptide followed by treatment with TRAIL accumulated more processed caspase-8 than samples treated with TRAIL in the absence of depsipeptide (Figure 6.3). Wt TRAIL and TRAIL.R1-5 induced similar levels of caspase-8 processing in samples pre-treated with depsipeptide in a time dependent manner (Figure 6.3 B, Lanes 3-10). The p43/41 and p18 fragments were clearly visible at 1 hour and the presence of the p18 fragment increased up to 8 hours. The TRAIL.R2-6 mutant induced caspase-8 processing to a lesser extent but the p43/41 and p18 fragments of caspase-8 were detected at 1 hour and accumulated to reach maximum levels by 8 hours (Figure 6.3 B, Lanes 11-14). Caspase-8 processing reached higher levels in all samples treated with depsipeptide compared with samples treated with vehicle control followed by TRAIL and also correlated with apoptosis induction.

DISC formation occurs in a time-dependent manner in K562 cells.

To address the discrepancy in Figure 6.2, 3 x 10^7 K562 cells were pre-treated with or without depsipeptide (10 nM) for 12 hours followed by treatment with either; wt TRAIL, TRAIL.R1-5 or TRAIL.R2-6 (500 ng/ml) for 15, 30, or 60 mins. Depsipeptide induced a decrease in TRAIL-R1 but did not induce an increase in TRAIL-R2 in these experiments. TRAIL-receptor binding and FADD and caspase-8 recruitment did not correlate with apoptosis induction. A reference sample was loaded to allow for comparing between gels (Figure 6.4 A and B, Lane 11).

In control cells, wt TRAIL appeared to recruit the maximum DISC at 15 minutes (Figure 6.4 A, Lanes 2-4). At 15 mins, high levels of TRAIL-R1 and TRAIL-R2 were pulled into a DISC complex as well as large amounts of FADD and both the proform and processed p41/43 fragments of caspase-8 (Figure 6.4 A, Lane 2). At 30 mins wt TRAIL treatment, the levels of TRAIL-R1 and TRAIL-R2 were slightly reduced compared with the 15 min time point, however, FADD levels remained approximately equal to the 15 minute time point (Figure 6.4 A, Lanes 2 and 3). Levels of the proform of caspase-8 were reduced but the p41/43 fragments remained the same as the 15 minute time point (Figure 6.4 A, Lanes 2 and 3). At 60 mins wt TRAIL treatment the DISC appeared to have mainly dissociated (Figure 6.4 A, Lane 4). No TRAIL-R1 or TRAIL-R2 was visible at the DISC (Figure 6.4 A, Lane 4). Levels of FADD and caspase-8 were dramatically reduced (Figure 6.4 A, Lane 4).

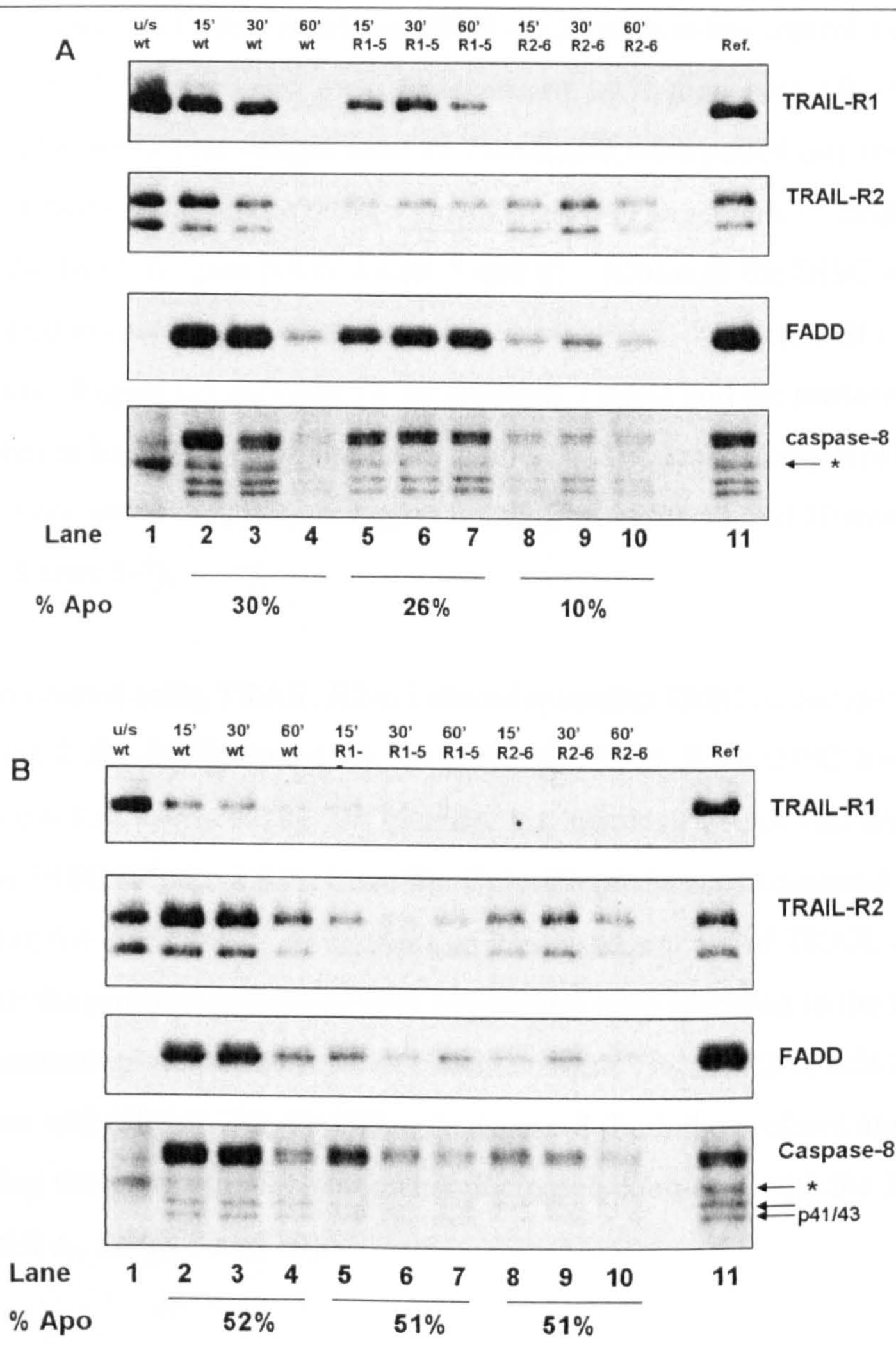

Figure 6.4: TRAIL receptor-selective mutants induce a time-dependent DISC formation in K562 cells. A) K562 cells were treated with biotinylated wt TRAIL, TRAIL.R1-5 or TRAIL.R2-6 (500 ng/ml) for 15, 30, or 60 mins at 37°C. B) K562 cells were pre-treated with depsipeptide (10 nM) for 12 hours followed by treatment with biotinylated wt TRAIL, TRAIL.R1-5 or TRAIL.R2-6 for 15, 30 or 60 mins at 37°C. The collection and analysis of DISC proteins was completed as described in Materials and Methods. TRAIL-R1, TRAIL-R2, FADD and caspase-8 were detected using western blotting. Results are shown as one experiment representative of at least three. Unstimulated lanes indicate the presence of DISC proteins pulled with biotinylated TRAIL in whole cell lysates. * denotes the presence of TRAIL-R1 from a re-probed membrane.

TRAIL.R1-5 appeared to form a maximum DISC at 30 mins in the control situation (Figure 6.4 A, Lanes 5-7). At 15 mins and, to a greater extent, at 30 mins both TRAIL-R1 and low levels of the higher molecular weight band of TRAIL-R2 were pulled into the DISC complex. High levels of FADD and both the proform and the p41/43 fragments of caspase-8 were recruited into the DISC (Figure 6.4 A, Lanes 5 and 6). Although the DISC was formed to a lesser extent at 60 mins, TRAIL-R1 and low levels of TRAIL-R2 were still recruited to the DISC at this time (Figure 6.4 A, Lane 7). In addition, FADD and the proform of caspase-8 were still present at high levels (Figure 6.4 A, Lane 7). The processed p41/43 forms of caspase-8 were present at the DISC at higher levels than in the 15 and 30 min time points (Figure 6.4 A, Lanes 5-7).

As expected in control cells, TRAIL.R2-6 induced a smaller DISC as compared with wt TRAIL and TRAIL.R1-5 (Figure 6.4 A). In addition, TRAIL.R2-6 DISC formation peaked at 30 mins (Figure 6.4 A, Lanes 8-10). At 15 mins, low levels of TRAIL-R2 and FADD were recruited to the DISC (Figure 6.4 A, Lane 8). Only the proform of caspase-8 was visible at this time (Figure 6.4 A, Lane 8). At 30 mins an increased amount of TRAIL-R2, FADD and caspase-8 (both the proform and the p41/43 fragments) were recruited to the DISC (Figure 6.4 A, Lane 9). Interestingly, after 60 mins of treatment with TRAIL.R2-6, K562 cells still had DISC formation with TRAIL-R2, FADD and caspase-8 (both the proform and the p41/43 fragments) being detected although somewhat decreased compared with the 30 minute time point (Figure 6.4 A, Lanes 9 and 10).

In K562 cells that were pre-treated with depsipeptide, the DISC formed by wt TRAIL appeared to reach a maximum between 15 and 30 mins and was not dismantled by 60 mins (Figure 6.4 A and B, Lanes 2-4). In these samples, TRAIL-R1 was not recruited to the wt DISC to the same extent as the control samples (Figure 6.4 A and B Lanes 2-4). In contrast, more TRAIL-R2 was recruited in the depsipeptide pre-treated samples compared with the control samples at all time points (Figure 6.4 A and B, Lanes 2-4). Despite an increase in TRAIL-R2 recruitment to the DISC, FADD recruitment was decreased at the earlier time points in the samples pre-treated with depsipeptide at 15 and 30 mins (Figure 6.4 A and B,

Lanes 2 and 3). In contrast, more FADD appeared to be recruited at the DISC at 60 mins in the depsipeptide-treated samples as compared with the same time-point of the control samples (Figure 6.4 A and B, Lane 4). There was an increased recruitment of procaspase-8 to the DISC in all depsipeptide treated samples compared with control wt TRAIL samples (Figure 6.4 A and B, Lanes 2-4). However, the accumulation of processed caspase-8 was decreased in all of these samples with the exception of the 60 minute time point where it was approximately equal to that of the control samples (Figure 6.4 A and B, Lanes 2-4).

In samples pre-treated with depsipeptide followed by treatment with TRAIL.R1-5, the DISC appeared to reach a maximum at 15 mins (Figure 6.4 B, Lanes 5-7). At 15 mins, less TRAIL-R1 was recruited to the DISC but there was an increase in TRAIL-R2 recruitment (Figure 6.4 A and B, Lane 5). However at 30 and 60 mins in depsipeptide-treated samples, TRAIL-R1 was not visible and the presence of TRAIL-R2 was decreased compared with the corresponding control samples (Figure 6.4 A and B, Lanes 6 and 7). FADD recruitment was decreased in all depsipeptide-treated samples compared with samples treated with TRAIL.R1-5 alone (Figure 6.4 A and B, Lanes 5-7). However, procaspase-8 recruitment to the DISC was increased in the depsipeptide treated TRAIL.R1-5 sample at 15 mins despite a decrease in the processed p41/43 fragments of caspase-8 compared with control samples (Figure 6.4 A and B, Lane 5). In contrast, at 30 and 60 mins, caspase-8 recruitment was decreased in the depsipeptide-treated samples compared with control samples (Figure 6.4 A and B, Lanes 6 and 7).

In samples pre-treated with depsipeptide followed by treatment with TRAIL.R2-6, DISC formation reached a maximum at 30 mins (Figure 6.4 B, Lanes 8-10). As expected, TRAIL-R1 was not recruited to the DISC. However, more TRAIL-R2 was recruited to the DISC in depsipeptide-treated samples at all time points compared with samples treated only with TRAIL.R2-6 (Figure 6.4 A and B, Lanes 8-10). Despite this, FADD recruitment was decreased in depsipeptide treated samples compared with TRAIL.R2-6 control samples (Figure 6.4 A and B, Lanes 8-10). At 15 and 30 mins, in depsipeptide-treated samples, more procaspase-8 was recruited to the DISC but less processed caspase-8 was evident in the DISC at these times compared with control samples (Figure 6.4 A and B, Lanes 8 and 9). Caspase-8

recruitment at 60 mins was the same in depsipeptide-treated and control samples (Figure 6.4 A and B, Lane 10).

K562 DISC formation is concentration-dependent in K562 cells.

To address the lack of correlation between DISC formation and the percent apoptosis in K562 cells with and without depsipeptide, a concentration-response using wt TRAIL and TRAIL.R2-6 was completed. K562 cells were treated with or without depsipeptide followed by treatment with increasing concentrations of wt TRAIL or TRAIL.R2-6 (100-500 ng/ml) for 30 minutes (Figure 6.5). DISC proteins were analysed as described in Materials and Methods. Unstimulated lanes indicate that in this experiment there was a dramatic decrease in TRAIL-R1 after depsipeptide treatment, which is consistent with previous results (Figure 6.5, Lanes 1 and 9). However these lanes also indicate a decrease in TRAIL-R2 after depsipeptide treatment which is inconsistent with previous experiments and must be taken into consideration when analysing the results (Figure 6.5, Lanes 1 and 9). A reference sample was loaded to allow for comparing between two different gels (Figure 6.5, Lanes 8 and 16).

In control samples, a maximum DISC formation occurred at 500 ng/ml wt TRAIL treatment (Figure 6.5, Lanes 2-4). 100 ng/ml wt TRAIL was not sufficient to induce DISC formation (Figure 6.5, Lane 2). In this sample, low levels of TRAIL-R1 and FADD were pulled into the DISC (Figure 6.5, Lane 2). TRAIL-R2 and caspase-8 were not visible in this sample (Figure 6.5, Lane 2). Increasing the concentration of wt TRAIL to 250 ng/ml formed a small DISC (Figure 6.5, Lane 3). Low levels of TRAIL-R1 and TRAIL-R2 were visible in this DISC as well as FADD (Figure 6.5, Lane 3). Caspase-8 was not detected in this sample. 500 ng/ml of wt TRAIL recruited high levels of TRAIL-R1, TRAIL-R2, FADD and caspase-8 (Figure 6.5, Lane 4). In this sample caspase-8 was processed to its p41/43 forms (Figure 6.5, Lane 4). In control cells, wt TRAIL DISC formation correlated with apoptosis induction as observed previously.

After pre-treatment with depsipeptide, wt TRAIL formed a DISC at all concentrations (Figure 6.5, Lanes 10-12). Less TRAIL-R1 was pulled into all of the depsipeptide-treated cells, corresponding to a decrease in TRAIL-R1 levels (Figure 6.5, Lanes 10-12). In the 100 and

250 ng/ml wt TRAIL DISCs, more TRAIL-R2, FADD and caspase-8 were pulled into the depsipeptide-treated DISCs compared with control DISCs (Figure 6.5, Lanes 2-3 and 10-11). In the case of depsipeptide-treated samples, more caspase-8 was pulled into the 250 ng/ml DISC than the 100 ng/ml DISC. The caspase-8 pulled into the 250 ng/ml DISC was partially processed into its p41/43 forms (Figure 6.5, Lanes 10 and 11). In samples treated with 500 ng/ml wt TRAIL, no TRAIL-R1 and less TRAIL-R2, FADD and caspase-8 were recruited to the DISC in the depsipeptide-treated sample compared with the corresponding control sample (Figure 6.5, Lanes 4 and 12). Less caspase-8 was recruited to the DISC in depsipeptide-treated cells that were treated with 500 ng/ml wt TRAIL than cells treated with lower concentrations (Figure 6.5, Lanes 10-12).

DISC formation at 100 and 250 ng/ml correlated with apoptosis induction in control and depsipeptide-treated samples (Figure 6.5, Lanes 2-3 and 10-11). However at 500 ng/ml wt TRAIL treatment apoptosis induction did not correlate with DISC formation as previously observed (Figure 6.5, Lanes 4 and 12).

All samples treated with TRAIL.R2-6 did not pull TRAIL-R1 into the DISC, in agreement with previous results (Figure 6.5, Lanes 5-7 and 13-15). In control samples 100 ng/ml was not sufficient to form a visible DISC (Figure 6.5, Lane 5). Increasing the concentration of TRAIL.R2-6 to 250 or 500 ng/ml increased recruitment of TRAIL-R2 (particularly the higher molecular weight band) and FADD in a concentration dependent manner, however caspase-8 recruitment to either DISC was not visible in these samples (Figure 6.5, Lanes 6 and 7).

In depsipeptide-treated samples, the TRAIL.R2-6 DISC appeared to reach a maximum at 250 ng/ml; however DISC formation was evident in all samples (Figure 6.5, Lanes 13-15). At 100 ng/ml, low levels of the high molecular weight band of TRAIL-R2, FADD and procaspase-8 were recruited into the DISC (Figure 6.5, Lane 13). Increasing the concentration of TRAIL.R2-6 to 250 ng/ml increased levels of TRAIL-R2, FADD and procaspase-8 recruited to the DISC (Figure 6.5, Lane 14). When cells were treated with 500 ng/ml TRAIL.R2-6, less TRAIL-R2, FADD and pro-caspase-8 were recruited to the DISC compared with 250 ng/ml TRAIL.R2-6 treatment (Figure 6.5, Lanes 14 and 15). Although depsipeptide increased

formation of a TRAIL.R2-6 DISC at 500 ng/ml compared with control cells, this increase was less dramatic than observed using lower concentrations of TRAIL.R2-6.

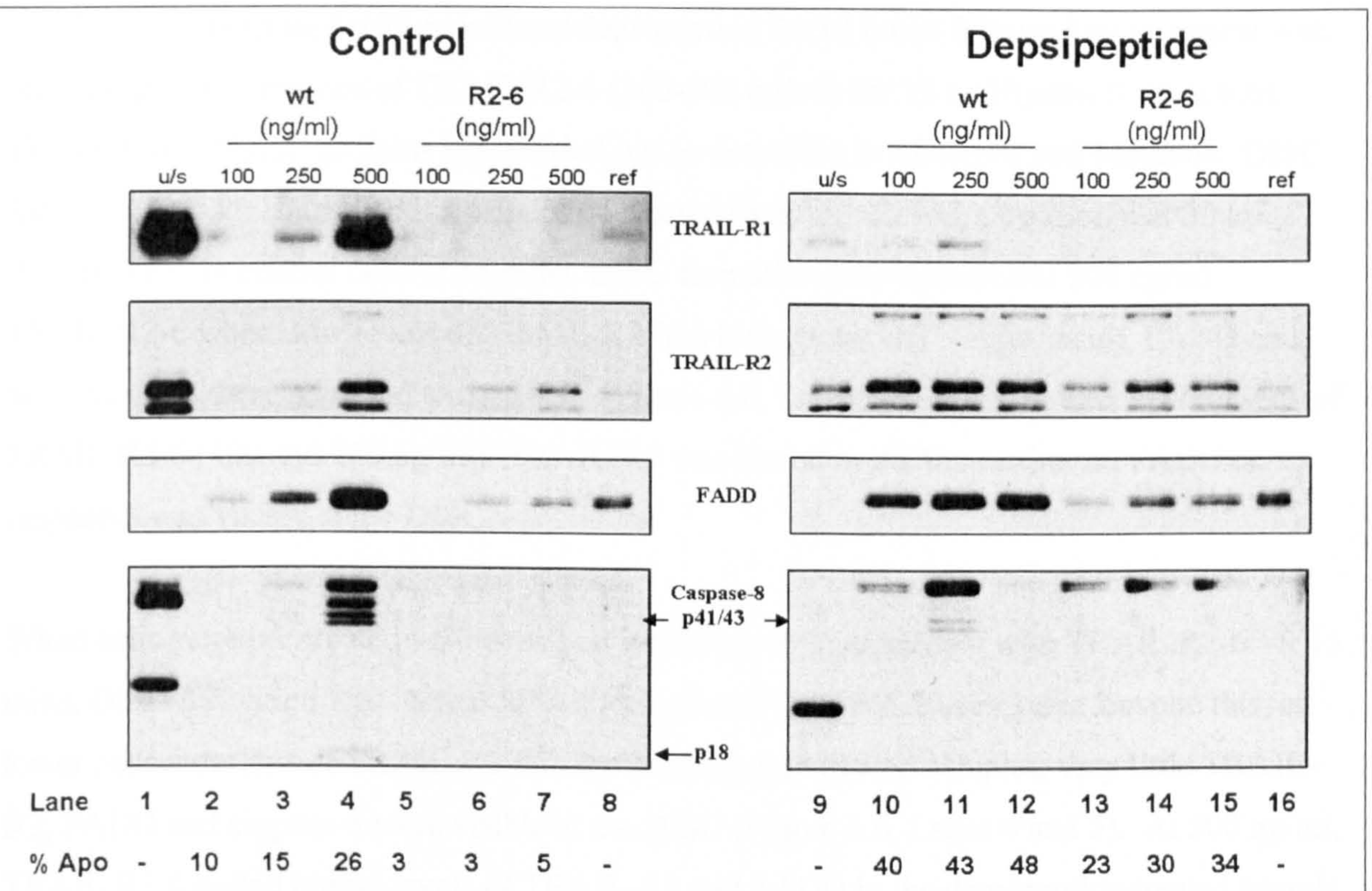

Figure 6.5: wt TRAIL and TRAIL.R2-6 induce a concentration-dependent DISC formation in K562 cells after depsipeptide treatment. K562 cells were treated with or without depsipeptide (10 nM) for 12 hours followed by treatment with biotinylated wt TRAIL or TRAIL.R2-6 (100-500 ng/ml) for 30 mins at 37°C. The collection and elution of DISC proteins was completed as described in Materials and Methods. TRAIL-R1, TRAIL-R2, FADD and caspase-8 were detected using western blotting. Results are shown as one experiment representative of two. Unstimulated lanes indicate the presence of DISC proteins pulled with biotinylated TRAIL in whole cell lysates.

Compared with control samples treated with corresponding concentrations of TRAIL.R2-6, samples treated with depsipeptide followed by treatment with TRAIL.R2-6 had an increase in FADD and caspase-8 recruitment to the DISC. With the exception of samples treated with 250 and 500 ng/ml of TRAIL.R2-6, DISC formation in all other TRAIL.R2-6-treated samples correlated with apoptosis induction (Figure 6.5, Lanes 5-7 and 13-15).

TRAIL.R2-6 forms a DISC in K562 cells in a concentration- and time-dependent manner in the presence of depsipeptide.

K562 cells were treated with or without depsipeptide for 12 hours followed by treatment with increasing concentrations of TRAIL.R2-6 (100-500 ng/ml) for 15 or 30 mins (Figure 6.6). The analysis of DISC proteins was carried out as described in Materials and Methods. DISC formation in both control and depsipeptide-treated samples reached a maximum at 30 mins (Figure 6.6). In control cells at 15 mins, DISC formation only occurred at 500 ng/ml TRAIL.R2-6 where low levels of TRAIL-R2 (the high molecular weight band), FADD and pro-caspase-8 were recruited to the DISC (Figure 6.6, Lane 3). Using lower concentrations of TRAIL.R2-6 (100 and 250 ng/ml), TRAIL-R2 was bound to the ligand, but no FADD or caspase-8 was visible at the DISC.

When cells were pre-treated with depsipeptide followed by treatment with TRAIL.R2-6 for 15 mins, DISC formation was increased in all samples (Figure 6.6, Lanes 1-6). Despite this, at lower concentrations of TRAIL.R2-6 in the depsipeptide-treated samples, very little TRAIL-R2, FADD and caspase-8 were visible at the DISC (Figure 6.6, Lanes 4 and 5). At 500 ng/ml, TRAIL.R2-6 pulled higher levels of TRAIL-R2 and FADD in the depsipeptide-treated sample compared with the control sample (Figure 6.6, Lanes 3 and 6). However, the same amount of procaspase-8 was pulled into the DISC in the depsipeptide-treated sample compared with the corresponding control sample (Figure 6.6, Lanes 3 and 6).

A visible DISC was formed in all samples treated with TRAIL.R2-6 for 30 mins (Figure 6.6, Lanes 7-12). As observed in Figure 6.5, DISC formation in the control samples increased with concentration (Figure 6.6, Lanes 7-9). The lowest concentrations of TRAIL.R2-6 (100 and 250 ng/ml) pulled both TRAIL-R2 and low levels of FADD as well as procaspase-8 in a concentration-dependent manner (Figure 6.6, Lanes 7 and 8). The highest concentration of TRAIL.R2-6 (500 ng/ml) formed a large DISC pulling TRAIL-R2, FADD and high levels of pro-caspase-8 (Figure 6.6, Lane 9).

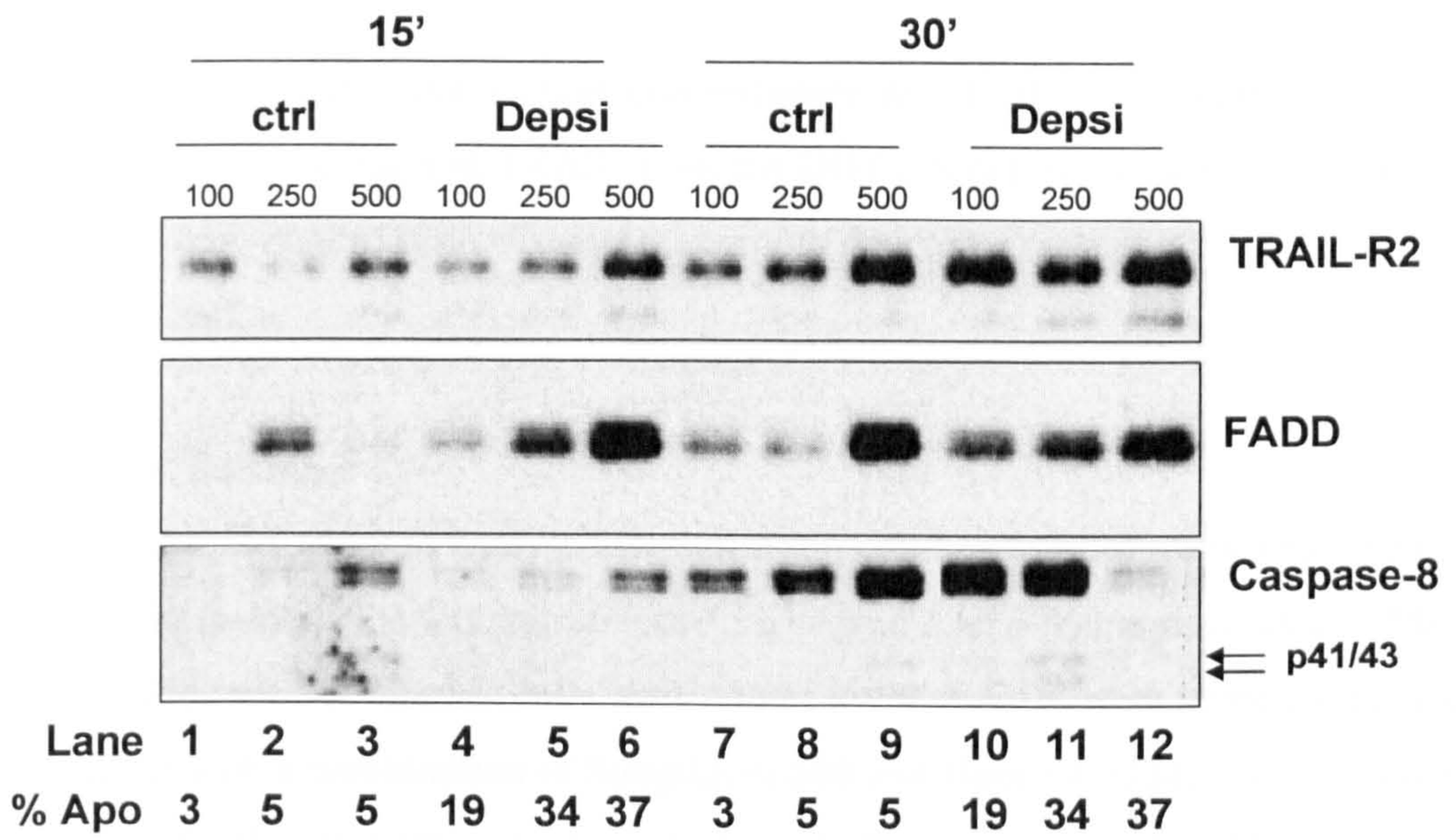

Figure 6.6: TRAIL.R2-6 induces a concentration- and time- dependent DISC formation in K562 cells. K562 cells were treated with or without Depsipeptide (10 nM) for 12 hours followed by treatment with TRAIL.R2-6 (100-500 ng/ml) for 15 or 30 mins at 37°C. The collection and elution of DISC proteins was carried out as described in Materials and Methods. TRAIL-R2, FADD and caspase-8 were detected using western blotting. Results shown are of one experiment.

In samples pre-treated with depsipeptide followed by 30 mins treatment with TRAIL.R2-6 DISC formation was approximately equal in all samples with the exception of recruitment of FADD (Figure 6.6, Lanes 10-12). All samples recruited high levels of TRAIL-R2 and pro-caspase-8 (Figure 6.6, Lanes 10-12). Caspase-8 was partially processed at the highest concentration of TRAIL.R2-6 (Figure 6.6, Lane 12). FADD recruitment increased with the concentration of TRAIL.R2-6 reaching the highest levels at 500 ng/ml TRAIL.R2-6 (Figure 6.6, Lanes 10-12).

At the lowest concentrations of TRAIL.R2-6 (100 and 250 ng/ml), depsipeptide-treated samples recruited higher levels of DISC protein than corresponding control samples (Figure 6.6, Lanes 7-8 and 10-11). In contrast, TRAIL.R2-6 (500 ng/ml) recruited more DISC proteins in control samples when compared with depsipeptide-treated samples in accordance with previous observations (Figure 6.6, Lanes 9 and 12).

Chapter 6: Internalisation patterns of TRAIL

It remained a possibility that using a high concentration of TRAIL induced rapid internalisation and dissociation of TRAIL from the DISC. Since analysis of DISC proteins only provides a snap-shot of time, it was necessary to develop a real-time assay to visualise TRAIL internalisation.

K562 cells auto fluoresce

To develop a real-time assay to analyse internalisation patterns in K562 cells, cells were labelled with biotinylated TRAIL and Streptavidin-tagged Alexa-568 as described in Materials and Methods (Figure 6.7). Control cells were either; left untreated, were treated with Hoechst-33342 or treated with a combination of Strepdavin-568 and Hoechst-33342. Samples were analysed by confocal microscopy. Unexpectedly, auto fluorescence in the 563 and 405 channels was observed in control cells that were untreated and cells treated with Hoechst-33342 only. In cells treated with TRAIL, no signal was observed when gain was reduced to levels where auto fluorescence was not detected (data not shown). Therefore, K562 cells were not used for further confocal studies.

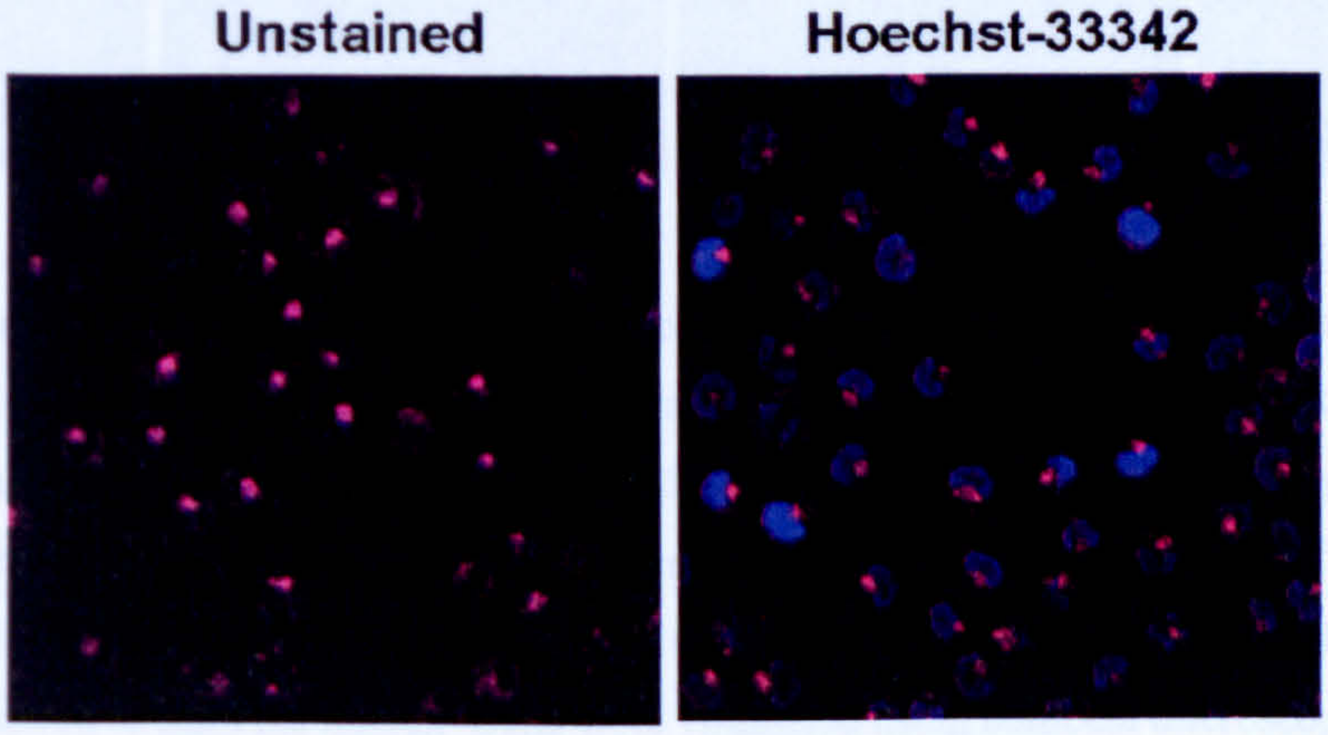

Figure 6.7:K562 cells auto fluoresce. K562 cells were chilled to 4°C for up to 1 hour followed by treatment with either Streptavidin-labelled Alexa-568 or PBS only. Cells were fixed in 4% paraformaldehyde and washed three times in PBS. Cells were either left unstained or treated with Hoechst-33342. This experiment was completed on two separate occasions.

TRAIL internalisation rapidly occurs in BJAB cells

BJAB cells were labelled with wt TRAIL and Alexa-568 as described in Materials and Methods. After labelling, live cells were either fixed with 4% paraformaldehyde for 10 mins at room temperature or released to 37°C for up to 30 mins followed by fixation at room temperature (Figure 6.8). Cells were also labelled with Hoechst-33342 to stain the nucleus. Control cells were labelled with streptavidin-568 alone and Hoechst-33342.

Treating BJAB cells with streptavidin-568 alone did not stain the cells. After treatment at 4°C without releasing the cells up to 37°C, there appeared to be a diffuse ring-like staining on the surface of the cells. There was no detectable TRAIL within the cells. At 5 mins marked internalisation began to occur, although TRAIL still remained in the ring structure observed at 4°C. By 15-30 mins, internalisation of TRAIL was apparent.

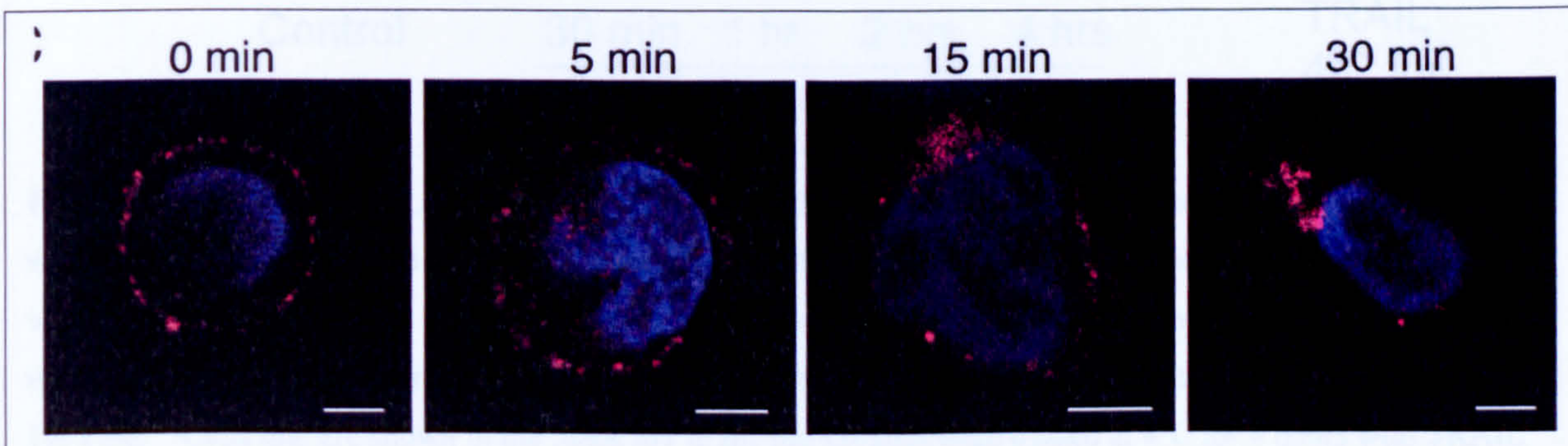

Figure 6.8: Pre-loaded TRAIL internalises in BJAB cells after release to 37°C. BJAB cells (1 x 10^6 per sample) were chilled to 4°C for 1 hour followed by treatment with 500 ng/ml biotinylated TRAIL for 45 mins at 4°C. TRAIL was washed away three times with cold PBS. Cells were then treated with Streptavidin labelled Alexa-568 for 1 hour at 4°C. Cells were either fixed after 4°C treatment or released up to 37°C for 5, 15 and 30 mins fixed in 4% paraformaldehyde for 10 mins at room temperature. Cells were treated with Hoechst-33342 for up to 5 mins after fixation to stain the nuclei. Cells were visualised using confocal microscopy. The white bar represents 5 μm. Results shown are of one representative cell from each time point of more than 50 images taken. This experiment was completed independently at least three times.

Pre-loading does not have an effect on the kinetics of TRAIL-induced apoptosis.

To determine whether pre-loading has an effect on the kinetics of apoptosis in BJAB cells, cells were either pre-loaded with wt TRAIL at 4°C, washed and then released to 37°C for up to 4 hours or were treated at 37°C without pre-loading for up to 4 hours (Figure 6.9). Cells were treated with 500 ng/ml TRAIL.

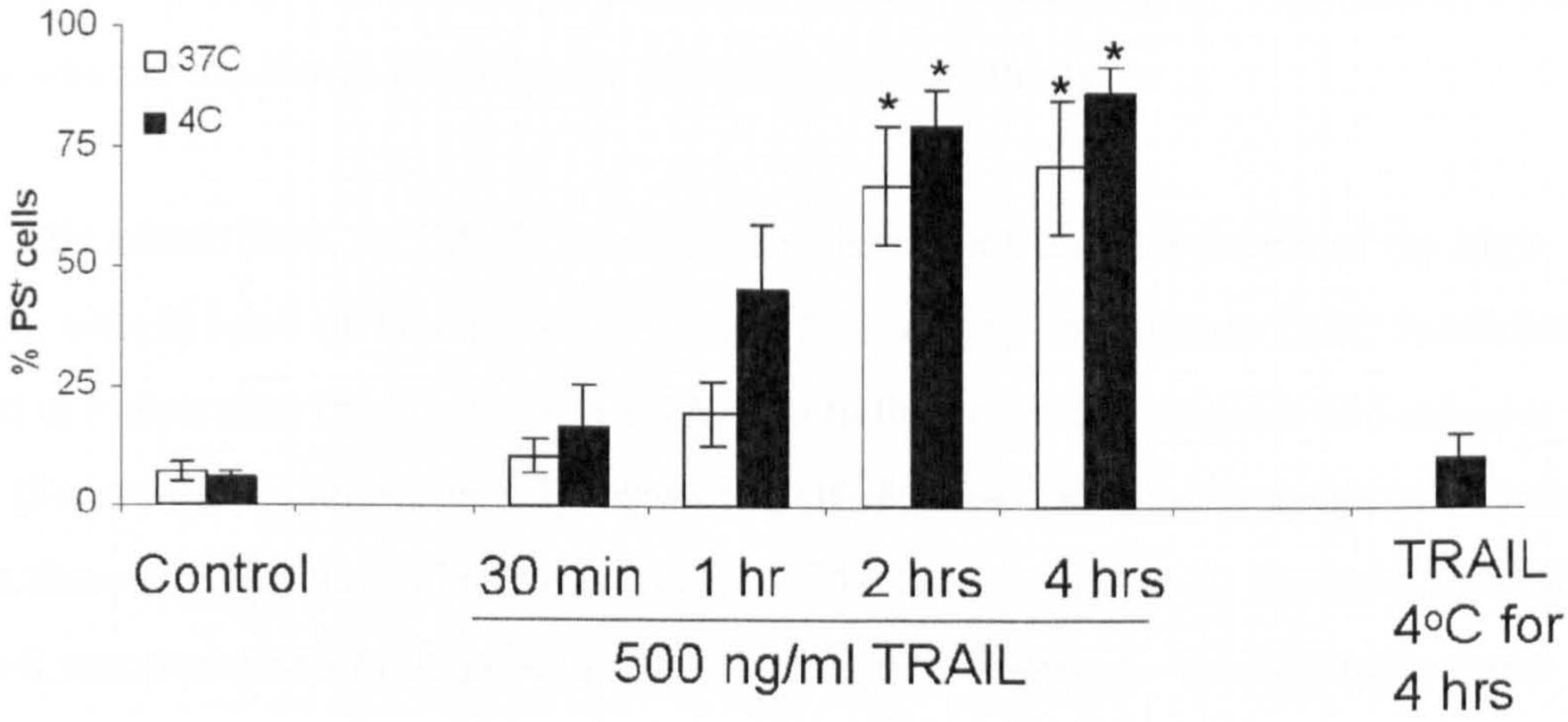

Figure 6.9: Pre-loading TRAIL causes an induction of apoptosis in BJAB cells to levels similar to treating without pre-loading. BJAB cells were either pre-loaded with wt TRAIL as described in Figure 6.8, or treated with TRAIL at 37°C without pre-loading. Cells that were pre-loaded were washed and released up to 37°C for the indicated time. Cells were treated with 500 ng/ml TRAIL for up to 4 hours. Control cells were treated with 1% PBS. Cells that are shown in the black bar in the last column were treated at 4°C for 4 hours with TRAIL without an increase in temperature to 37°C. Apoptosis was measured by determining the % PS^+ cells. Results shown are mean ± SEM of three independent experiments. * indicates a p value of <0.05 in samples that were compared with the control as determined by a One Way ANOVA followed by a Dunnett's test.

BJAB cells that were pre-loaded with TRAIL underwent apoptosis in a time-dependent manner starting at 1 hour (45 ± 13.9% at 1 hour compared with 5 ± 1.5% in control samples) (Figure 6.9, Black bars). The percent apoptosis increased reaching a maximum at 4 hours (86 ± 5.7% at 4 hours) (Figure 6.9, Black bars). Cells that were not pre-loaded with TRAIL began undergoing apoptosis within 2 hours of treatment and reached maximum levels of apoptosis within 4 hours (67 ± 12.5 and 71 ± 14%, respectively compared with 7 ± 2% in control samples) (Figure 6.9, White bars). There were no statistically significant differences between

cells that were pre-loaded with TRAIL and cells treated at 37°C without pre-loading as determined by a One Way ANOVA followed by a Dunnett's test.

A comparison of TRAIL-induced DISC formation with and without pre-loading

To determine the effects of pre-loading on DISC formation in BJAB cells, cells were pre-loaded with biotinylated TRAIL for 45 mins, washed and released up to 37°C for increasing amounts of time, or treated at 37°C without pre-loading (Figure 6.10). Analysis of DISC proteins was carried out as described in Materials and Methods.

In the unstimulated lane, wt TRAIL bound both TRAIL-R1 and low levels of the high molecular weight band of TRAIL-R2 (Figure 6.10, Lane 1). Maximum DISC formation occurred at 5mins after treatment with TRAIL in both pre-loaded samples and samples treated at 37°C (Figure 6.10, Lanes 2 and 7). Both TRAIL-R1 and TRAIL-R2 were pulled into the DISC in these samples as well as high levels of FADD and caspase-8. As early as 5 mins, caspase-8 was processed to its p43/41 forms and its p18 fragment. Interestingly, more caspase-8 processing occurred in samples pre-loaded with TRAIL. This was particularly the case with the catalytically active p18 fragment of caspase-8 (Figure 6.10, Lanes 2 and 7).

In samples that were not pre-loaded with TRAIL, TRAIL-R1 and TRAIL-R2 binding and FADD and caspase-8 recruitment were reduced in a time-dependent manner reaching the lowest levels at 60 mins (Figure 6.10, Lanes 2-5). Caspase-8 processing also reached lower levels at later time points in these samples. However the pro-form of caspase-8 was consistently present in all samples treated with TRAIL in the absence of pre-loading (Figure 6.10, Lanes 2-5).

In BJAB cells that were pre-loaded with TRAIL, DISC formation was reduced after reaching a maximum at 5 mins (Figure 6.10, Lanes 7-10). The binding of TRAIL to TRAIL-R1 and TRAIL-R2 and the recruitment of FADD and caspase-8 was also reduced in samples treated with TRAIL up to 60 mins. Interestingly, the proform of caspase-8 was reduced in a time-dependent manner in samples pre-loaded with TRAIL. By 30 and 60 mins treatment with TRAIL, the proform of caspase-8 was not visible but the p43/41 and p18 fragments were

visible in these samples (Figure 6.10, Lanes 7-10). Surprisingly, TRAIL bound to both TRAIL-R1, TRAIL-R2 and recruited FADD and caspase-8 to the DISC in BJAB cells treated at 4°C alone for 45 mins without subsequent treatment at 37°C (Figure 6.10, Lane 6).

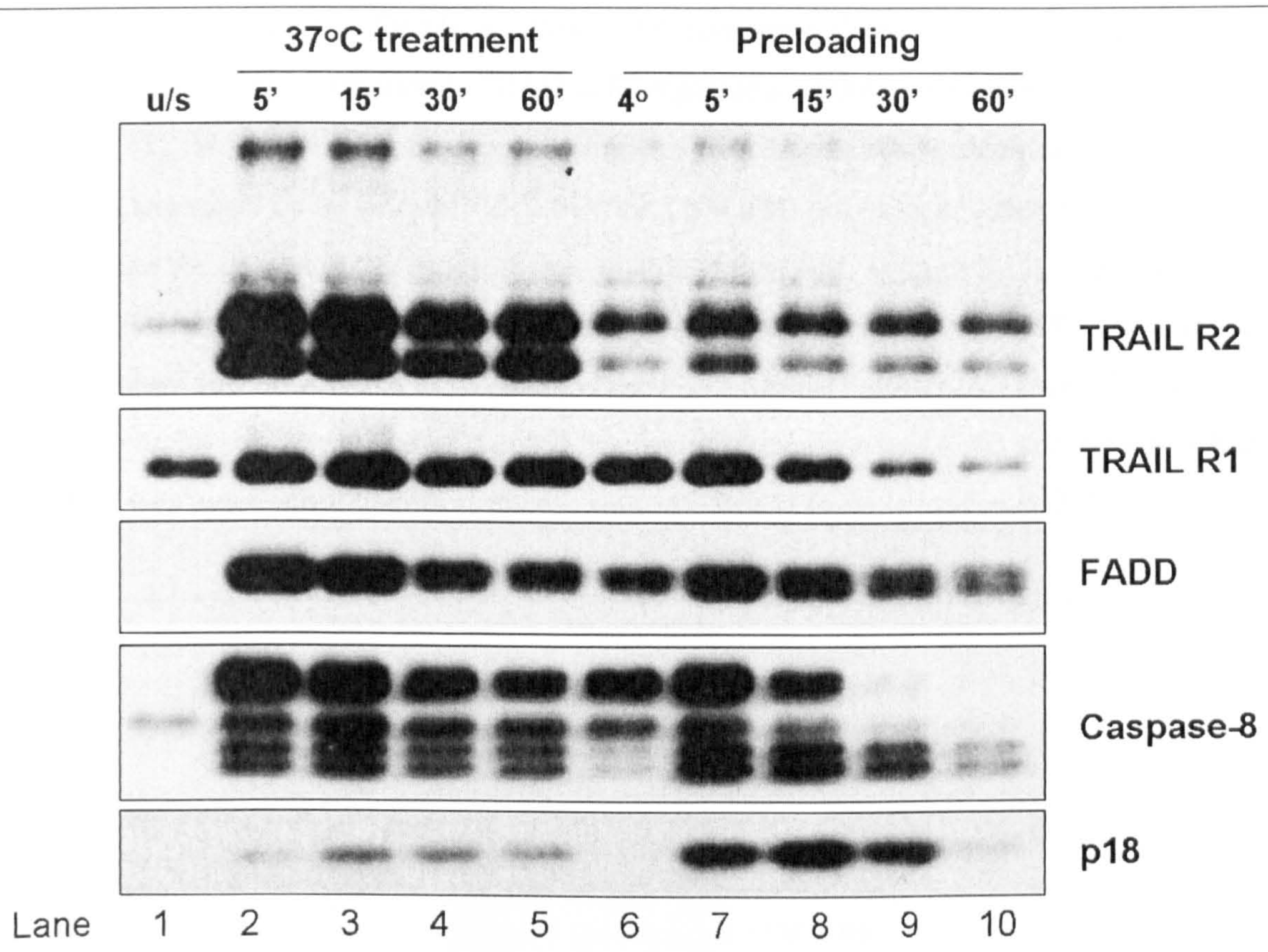

Figure 6.10: Pre-loading TRAIL induces DISC formation in a time-dependent manner. 2.5 x 10^7 BJAB cells were either pre-loaded with biotinylated wt TRAIL at 4°C as described in Figure 6.9 or were washed in PBS and the temperature was raised to 37°C for the indicated time, or were treated with TRAIL at 37°C for the indicated time and then washed and lysed. Analysis of DISC proteins was carried out as described in Materials and Methods. Control cells for pre-loading consisted of treatment with 500 ng/ml biotinylated TRAIL for 45 mins at 4°C without raising the temperature up to 37°C. Unstimulated cells were lysed and then treated with TRAIL to measure binding of the ligand to each receptor. Results shown are representative of three independent experiments

Z-VAD.fmk inhibits caspase-8 activation within the DISC.

Caspase-8 activation has been hypothesised to be necessary for CD95 receptor aggregation and internalisation (Algeciras-Schimnich, Shen et al. 2002). Therefore, BJAB cells were pre-treated with increasing concentrations of the pan-caspase inhibitor z-VAD.fmk followed by treatment with biotinylated TRAIL to allow DISC formation (Figure 6.11). As expected, TRAIL induced DISC formation in BJAB cells regardless of the presence of z-VAD.fmk (Figure 6.11). However, caspase-8 processing was decreased as the concentration of z-VAD.fmk increased up to 300 μM. Z-VAD.fmk (100 μM) only blocked caspase-8 processing partially and the p18 band of caspase-8 was visible at the DISC (Figure 6.11, Lane 2). In contrast, 200 and 300 μM z-VAD.fmk blocked caspase-8 processing to its p18 form, but did not fully block the cleavage of caspase-8 to its p43/41 forms (Figure 6.11, Lanes 3 and 4). Interestingly, all concentrations of z-VAD.fmk induced changes in FADD and the upper band of FADD was much more visible at these concentrations (Figure 6.11, Lanes 2-4).

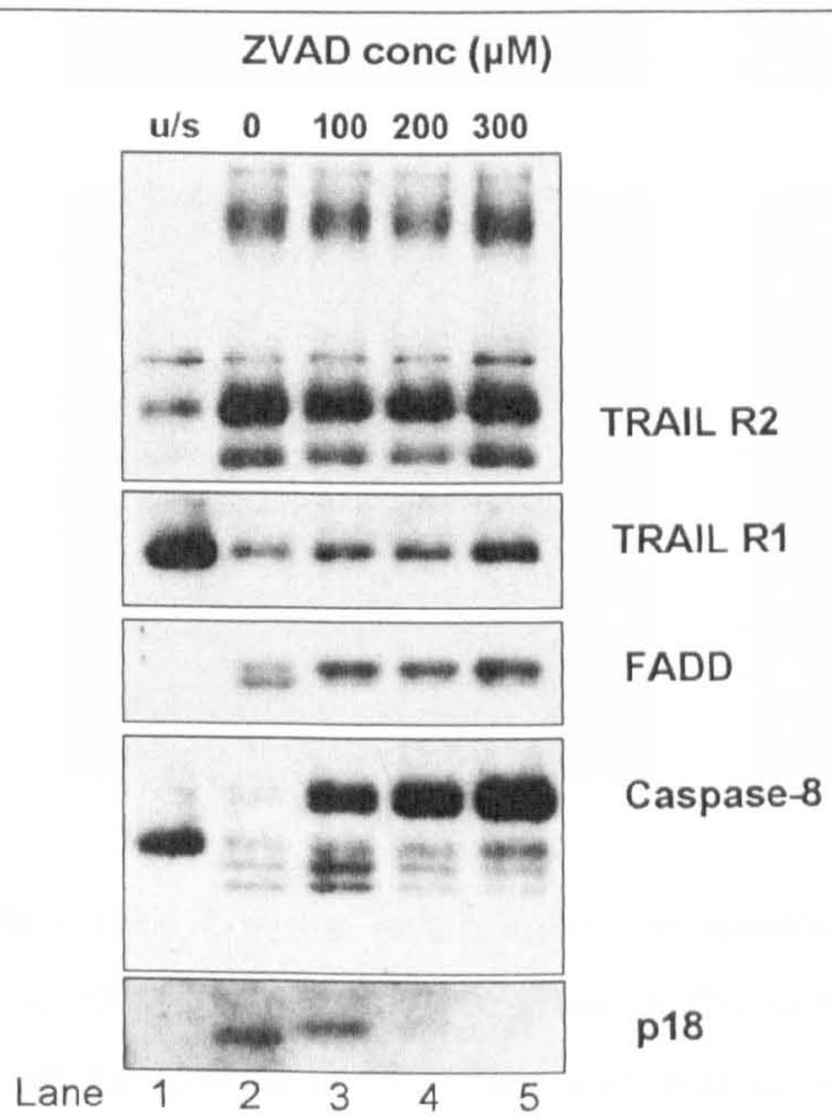

Figure 6.11: Z-VAD.fmk inhibits caspase-8 activation within a TRAIL-induced DISC in BJAB cells in a concentration-dependent manner. 25 x 10^7 BJAB cells were treated with increasing concentration of z-VAD.fmk (0-300 μM) for 30 mins at 37°C followed by treatment with biotinylated TRAIL (500 ng/ml) for 30 mins at 37°C. Cells were washed in ice cold PBS and analysis of DISC proteins was carried out at described in Materials and Methods. Unstimulated cells were treated with biotinylated TRAIL after lysis. Results shown are of one experiment.

Z-VAD.fmk blocks the formation of visible structures in BJAB cells.

To confirm whether Z-VAD.fmk blocks internalisation of TRAIL signal, BJAB cells were pre-treated with 200 μM z-VAD.fmk and pre-loaded with biotinylated TRAIL and [illegible] streptavidin-568. As expected, internalisation occurred in samples that were not treated with z-VAD.fmk (Figure 6.12). However, pre-treatment with z-VAD.fmk reduced the signal and reduced capping (Figure 6.12).

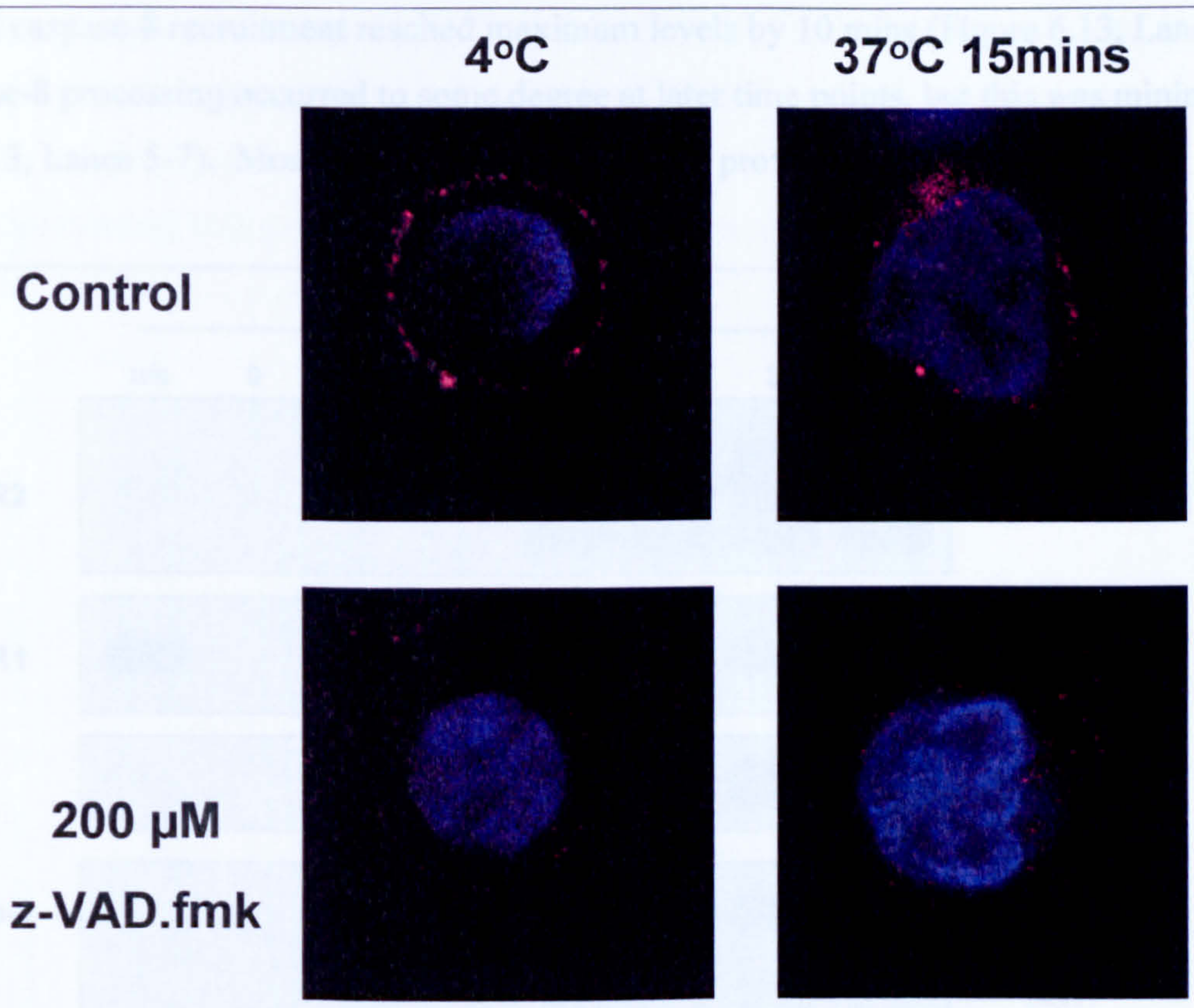

Figure 6.12: Z-VAD.fmk inhibits a TRAIL signal on confocal microscopy. BJAB cells were pre-treated with z-VAD.fmk (200 μM) for 30 mins at 37°C. Cells were then chilled to 4°C for up to 1 hour followed by treatment with biotinylated TRAIL (500 ng/ml) for 45 mins at 4°C. Cells were washed in cold PBS and treated with Streptavidin labelled Alexa-568 for 1 hour at 4°C. Cells were washed and either fixed in 4% paraformaldehyde or the temperature was rapidly shifted to 37°C for 15 mins. Cells were then fixed in 4% paraformaldehyde and stained with Hoechst-33342 for up to 5 mins. Control cells were treated with streptavidin-labelled Alexa-568 alone. The data shown is of one experiment only. Results shown are of one cell that is representative of several images taken.

TRAIL-induced DISC formation in BJAB cells does not require internalisation

Internalisation can be blocked at 4°C (Borle and Loveday 1968). To further investigate the kinetics of DISC formation at 4°C, BJAB cells were pre-chilled on ice for 1 hour followed by treatment with biotinylated wt TRAIL for up to 45 mins at 4°C (Figure 6.13). Analysis of DISC proteins was carried out as described in Materials and Methods. Interestingly, DISC formation began at 5 mins after TRAIL was added and TRAIL-R1 and TRAIL-R2 binding and FADD and caspase-8 recruitment reached maximum levels by 10 mins (Figure 6.13, Lanes 4-7). Caspase-8 processing occurred to some degree at later time points, but this was minimal (Figure 6.13, Lanes 5-7). Most caspase-8 remained in its proform.

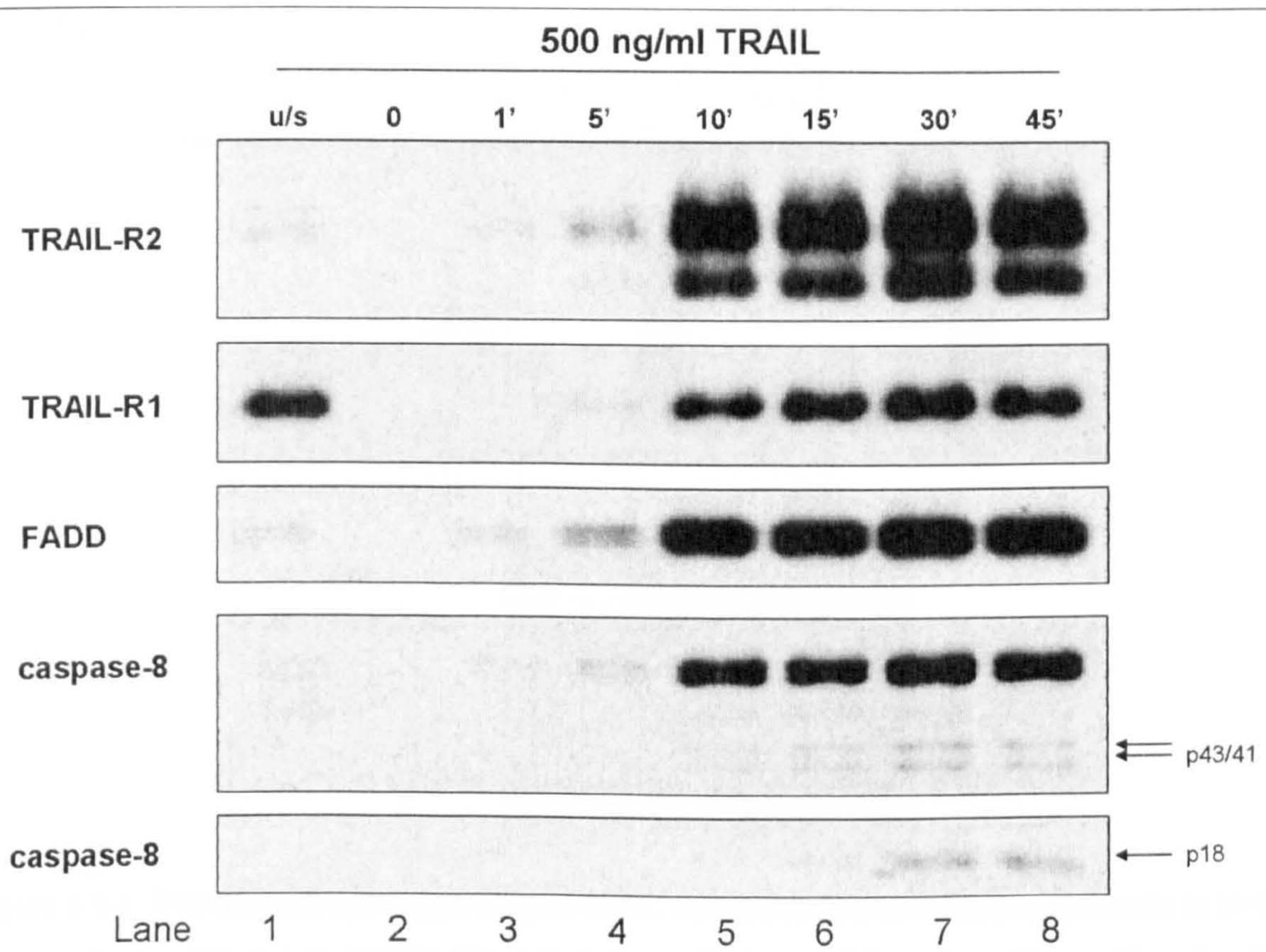

Figure 6.13: TRAIL-induced DISC formation in BJAB cells does not require internalisation. 25 x 10^6 BJAB cells were pre-chilled to 4°C for up to 1 hour followed by treatment with biotinylated TRAIL at 4°C for up to 45 mins. Cells were then washed and lysed. Analysis of DISC proteins was carried out as described in Materials and Methods. Unstimulated cells were treated with biotinylated TRAIL after lysis. Negative control cells were not treated with biotinylated TRAIL.

TRAIL-induced apoptosis and DISC formation does not require dynamin in HeLa cells

HeLa cells have previously been stably transfected with the dominant negative K44A dynamin mutation in a tetracycline off system (Altschuler, Barbas et al. 1998). To determine the importance of dynamin in DISC formation and TRAIL-induced apoptosis, tetracycline was either withdrawn from HeLa cells expressing wt or K44A dynamin-1 for 48 hours (Figure 6.14 A). The cells were subsequently treated with TRAIL for 4 hours and apoptosis was measured by flow cytometry (Figure 6.14 A). TRAIL induced similar and high levels of apoptosis in both dynamin deficient and HeLa cells with functional dynamin (73 ± 4.1 and 74 ± 5.5%, respectively compared with control levels of 7.7 ± 1.2 and 4.7 ± 1.5%, respectively). There was no statistical difference between HeLa cells carrying the dominant negative dynamin mutation and HeLa cells carrying the wt dynamin as measured by the student's t-test ($p=0.74$).

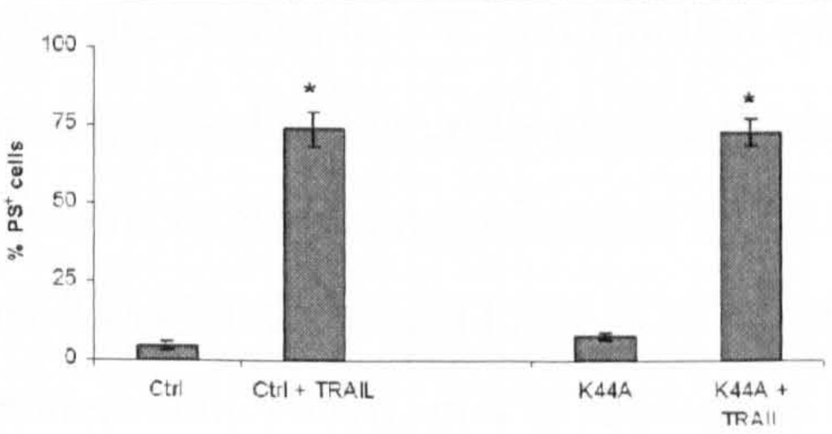

Figure 6.14: TRAIL-induced apoptosis and DISC formation does not require dynamin in HeLa cells.

HeLa cells were cultured as described in Materials and Methods. HeLa cells stably transfected with wt or K44A dynamin-1 were plated out at a density of 0.25×10^6 per ml and left to grow in the absence of tetracycline for 48 hours. A) HeLa cells were treated with 500 ng/ml TRAIL for 6 hours. Control cells were treated with 1% PBS. Apoptosis was assessed by determining the % PS^+ cells as described in Materials and Methods. B) HeLa cells were chilled to 4°C followed by treatment with 500 ng/ml biotinylated TRAIL for 15 and 45 mins. Cells were then washed and lysed. Analysis of DISC proteins was carried out as described in Materials and Methods. Unstimulated lanes represent cells that have been treated with TRAIL after lysis.

To determine whether dynamin has an effect on DISC formation in HeLa cells at 4°C, tetracycline was withdrawn from HeLa cells expressing wt or K44A dynamin-1 for 48 hours (Figure 6.14 B). HeLa cells were pre-cooled to 4°C and biotinylated TRAIL was added to the cells for up to 45 mins at 4°C (Figure 6.14 B). Analysis of DISC proteins was carried out as described in Materials and Methods. TRAIL-R1 and TRAIL-R2 bound biotinylated TRAIL and FADD and caspase-8 were recruited to the DISC at 45 mins in HeLa cells regardless of dynamin expression (Figure 6.14 B). There was no apparent difference in DISC formation between the two cell types. In each sample, dynamin function was determined by transferrin uptake as shown in Figure 6.15 B.

TRAIL internalisation does not require dynamin in HeLa cells

To determine whether dynamin was required for TRAIL internalisation in HeLa cells stably transfected with wt or K44A dynamin-1, tetracycline was withdrawn from the growing medium for 48 hours. Cells were pre-cooled to 4°C and labelled with biotinylated TRAIL followed by streptavidin-568 as described in Materials and Methods. After labelling, cells were released up to 37°C for 10 mins to allow internalisation of TRAIL (Figure 6.15 A). Cells were also labelled with Hoechst-33342 and cholera toxin B as nuclear and cell surface markers, respectively. Cells treated with TRAIL at 4°C showed no internalisation of TRAIL and a very low signal. Internalisation of TRAIL occurred in cells containing the wt dynamin proteins and in cells containing the dominant negative K44A dynamin mutation when treated at 37°C for 15 mins.

To confirm that the K44A mutation was inhibiting dynamin function in HeLa cells, cells were labelled at 4°C with Transferrin-633 and fixed or released up to 37°C for 30 mins to allow internalisation (Figure 6.15 B). Cells that were treated at 4°C without a temperature shift to 37°C, labelled with Transferrin on the cell surface only (Figure 6.15 B). At 37°C the dominant negative K44A dynamin HeLa cells mostly failed to internalise transferrin and therefore transferrin remained on the surface of these cells (Figure 6.15 B). In contrast, HeLa cells with wt dynamin allowed internalisation of transferrin and very little was observed on the surface of these cells when treated at 37°C for 30 mins (Figure 6.15 B). These data confirm that the

K44A mutation of dynamin was successfully blocking clathrin-mediated endocytosis in these experiments.

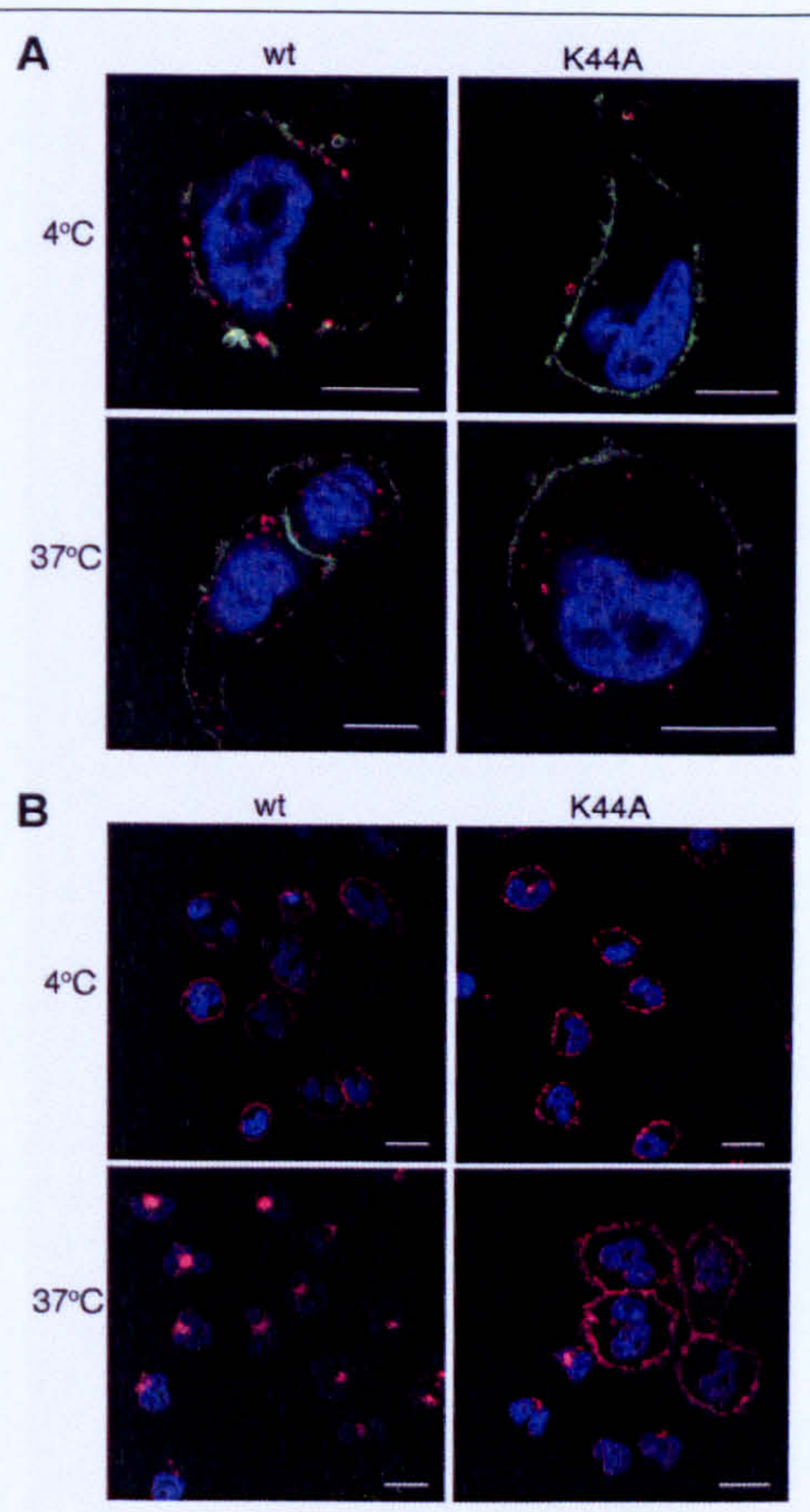

Figure 6.15: TRAIL internalisation does not require dynamin in HeLa cells but transferrin internalisation does require dynamin. HeLa cells were cultured and plated on coverslips in the absence of tetracycline as described in Materials and Methods. A) HeLa cells were chilled to 4°C for up to 1 hour followed by treatment with 500 ng/ml biotinylated TRAIL for 45 mins. Cells were washed in cold PBS and treated with Streptavidin-labelled Alexa-568 for 1 hour followed by PBS washes at 4°C. Cells were either fixed in 4% paraformaldehyde or released up to 37°C for 15 mins followed by fixation at room temperature. Cells were stained at room temperature with cholera toxin B labelled with Alexa-488 and Hoechst-33342 as described in Materials and Methods. Images were collected by confocal microscopy. The white bar represents 5 μm. B) HeLa cells were chilled to 4°C for up to 1 hour followed by treatment with 5 μg/ml transferring-633 for 45 mins at 4°C. Cells were washed in cold PBS and either fixed with 4% paraformaldehyde or released up to 37°C for 30 mins followed by fixation at room temperature. Cells were counterstained with Hoechst-33342 and images were collected as described above. The white bar represents 5 μm. Results shown are of one representative image of many images taken. These experiments were completed independently at least three times.

6.3 Discussion

Results in Chapters 4 and 5 regarding K562 cells appeared to be somewhat contradictory. In Chapter 4 using TRAIL mAbs, K562 cells were found to respond to TRAIL primarily through TRAIL-R2 when treated in the presence of depsipeptide. In contrast, the TRAIL.R1-5 mutant generated in Chapter 5 not only induced low levels of apoptosis on its own in K562 cells, but also induced apoptosis in K562 cells that had been pre-treated with depsipeptide. This was a discrepancy that needed to be addressed.

To further investigate signalling differences between mutant ligands, DISC proteins were pulled using biotinylated ligand in the absence of depsipeptide (Figure 6.1). FADD and caspase-8 recruitment correlated with the ability of TRAIL to induce apoptosis. Surprisingly, TRAIL.R1-5 pulled both TRAIL-R1 and TRAIL-R2 into the DISC at approximately equal levels. The presence of both the high and lower molecular weight band of TRAIL-R2 suggested that this was not non-specific recognition of TRAIL-R1 by the TRAIL-R2 antibody. The lack of TRAIL-R2 in the unstimulated lanes also suggested that TRAIL.R1-5 was unable to bind to TRAIL-R2 directly and therefore TRAIL-R2 was more likely being pulled into the DISC by forming heterocomplexes with TRAIL-R1. In addition, wt TRAIL was also likely to be able to form both homocomplexes and heterocomplexes because it binds to both TRAIL-R1 and TRAIL-R2. In contrast, TRAIL.R2-6 did not appear to bind to TRAIL-R1 and therefore probably only formed pure TRAIL-R2 complexes. Taken together, these data suggested that heterocomplexes may be important for the induction of apoptosis in K562 cells in the absence of a sensitising agent. However further study is required to prove this hypothesis.

Although TRAIL-induced FADD and caspase-8 recruitment correlated with apoptosis in the absence of depsipeptide in K562 cells, this was not the case in the presence of depsipeptide (Figure 6.2). Pre-treatment of K562 cells with depsipeptide decreased the levels of FADD recruited to the DISC by wt TRAIL and TRAIL.R1-5 and levels of FADD remained the same after treatment with TRAIL.R2-6. This was surprising and in contrast to what has been observed with wt TRAIL in the past in K562 cells (Inoue, MacFarlane et al. 2004). It is also

well known that caspase-8 and FADD recruitment to the DISC are required for TRAIL-induced apoptosis at least through TRAIL-R2 (Sprick, Weigand et al. 2000). In these experiments, it appeared that levels of apoptosis did not correlate with FADD recruitment to the DISC. It was evident from figure 6.3 that caspase-8 activation in whole cell lysates correlated with induction of apoptosis with each ligand. Therefore, a problem with detecting FADD and caspase-8 recruitment was supposed.

There are several limitations to measuring DISC proteins at specific time points. Measuring DISC proteins only takes a snap shot in time and therefore measurements in real time is not possible and receptor, FADD and caspase-8 recycling cannot be accounted for. The total amount of FADD and caspase-8 being recruited and dissociated from the DISC cannot be measure by one time point. One possible reason for the discrepancy observed between FADD recruitment and apoptosis induction in K562 cells was that depsipeptide caused a more rapid dissociation of the DISC complex with ligand compared with treatment with wt TRAIL in control cells. Thus at 30 mins TRAIL treatment, little FADD and caspase-8 were evident in the DISC, however this cannot account for the total amount of FADD and caspase-8 recruited and dissociated from the DISC by this time. Therefore a time course with and without depsipeptide treatment was completed with each ligand to address this issue (Figure 6.4).

Caspase-8 recruitment to the DISC varied, although procaspase-8 recruitment increased after depsipeptide treatment, but the p41/43 fragments decreased in all samples after depsipeptide treatment. There are two possible explanations for this, that less caspase-8 is processed in the DISC in depsipeptide-treated samples, or that caspase-8 is rapidly processed and removed from the DISC complex and procaspase-8 is then recruited back into the DISC complex. Cell lysates taken from K562 cells treated with each ligand before and after depsipeptide treatment would suggest that caspase-8 activation is increased in depsipeptide treated samples compared with control samples (Figure 6.4). Therefore it is more likely that depsipeptide induces a more rapid turnover of caspase-8 in K562 cells.

Although the results in Figure 6.4 do not address the discrepancy between FADD recruitment and induction of apoptosis, they do indicate some interesting differences between

homotrimeric and heterotrimeric receptor complexes. In control cells, it appeared as though TRAIL.R1-5 and TRAIL.R2-6 are signalling primarily through homotrimers (based on the ratios of TRAIL-R1 and TRAIL-R2 observed in the DISC). In contrast, wt TRAIL could be signalling through heterocomplexes and pure homocomplexes as it can bind both TRAIL-R1 and TRAIL-R2. It is clear from control samples that wt TRAIL peaks earlier than both mutant ligands and dissociates from the DISC more quickly.

In samples pre-treated with depsipeptide TRAIL-R1 expression was reduced. Based on the ratio of TRAIL-R1 and TRAIL-R2 in the DISC, it appears that wt TRAIL signals mainly through TRAIL-R2 pure trimers in this case. However TRAIL.R1-5 appears to signal through heterotrimeric complexes pulling roughly equal levels of both TRAIL-R1 and TRAIL-R2 at 15 mins. TRAIL.R2-6 signals through pure TRAIL-R2 complexes as observed in control samples. In this case, TRAIL.R1-5 appears to peak at 15 mins and the DISC appears to dissociate rapidly after that. The kinetics of TRAIL.R2-6 dissociation remains the same with and without depsipeptide pre-treatment.

In contrast, in depsipeptide pre-treated samples, the wt TRAIL DISC appeared to peak at a later time than in control samples, and the DISC appears to stabilise and is visible at 60 mins. These data suggest that TRAIL dissociates more quickly from heterotrimers in the K562 DISC than in pure TRAIL-R1 or pure TRAIL-R2 complexes. Further studies should be undertaken to address the stability of pure receptor complexes compared with heterotrimeric complexes and could be completed using tools such as the mutant ligands generated in Chapter 5 and cells deficient in TRAIL-R2 (Thomas, Henson et al. 2004). The biological significance of more rapid TRAIL-DISC dissociation has not been determined.

To further address the discrepancy between induction of apoptosis and levels of FADD and caspase-8 recruitment by TRAIL before and after treatment with depsipeptide, K562 cells were treated with increasing concentrations of TRAIL with and without depsipeptide (Figures 6.5 and 6.6). Lower concentrations of both wt TRAIL and TRAIL.R2-6 failed to form a DISC in K562 cells without pre-treatment with depsipeptide. Treatment with depsipeptide facilitated TRAIL-TRAIL-R2 binding, FADD and caspase-8 recruitment. DISC formation

correlated with apoptosis induction at lower concentrations of TRAIL; however at 500 ng/ml of TRAIL, apoptosis induction and DISC recruitment did correlate.

These data suggest that depsipeptide facilitates rapid dissociation or turnover of DISC components when cells are treated with high concentrations of TRAIL. However, when TRAIL is added at lower concentrations, this process appears to be slowed and therefore induction of apoptosis and the accumulation of DISC components appear to correlate. TRAIL.R2-6 pulls less receptor, FADD and caspase-8 than wt TRAIL. This is probably because wt TRAIL can bind both TRAIL-R1 homotrimeric complexes, TRAIL-R2 homotrimeric complexes and possibly heterotrimeric complexes and potentially more than three times the amount of protein as TRAIL.R2-6 (that can only form a DISC with TRAIL-R2 complexes).

In light of these data and recent papers regarding endocytosis in the death receptor family, internalisation became an obvious topic to investigate further (Algeciras-Schimnich, Shen et al. 2002; Schneider-Brachert, Tchikov et al. 2004; Austin, Lawrence et al. 2006; Lee, Feig et al. 2006). Confocal microscopy was employed with the aim of developing a real time assay as a measure of internalisation. Unfortunately, K562 cells were found to auto fluoresce and because of this determined unsuitable for confocal microscopy studies (Figure 6.7). BJAB cells were used as an alternative for several reasons.

First, BJAB cells have been used by a number of groups investigating internalisation in the death receptor family. In terms of CD95, they are widely considered a type I cell and the mechanism of cell death has been well characterised (Algeciras-Schimnich, Shen et al. 2002; Lee, Feig et al. 2006). Also, BJAB cells express high levels of both TRAIL-R1 and TRAIL-R2 and undergo apoptosis through both receptors as determined by ETR1 and ETR2 (Appendix Figure A.4). In addition to this, BJAB cells are able to undergo TRAIL-induced apoptosis without a sensitising agent. Although this does not mimic K562 cells exactly, it removes a layer of complexity from experiments.

To maximise the signal, TRAIL was pre-loaded onto the BJAB cells at 4°C. This technique has been used previously to visualize the movements of TNF and is thought to synchronise the ligand-receptor complex at the cell surface to provide a stronger signal (Schneider-Brachert, Tchikov et al. 2004). It is unclear whether this method can promote internalisation. With this technique, TRAIL was rapidly internalised into BJAB cells upon release to 37°C but did not appear to localize with the nucleus. It is important to note that contrary to previous reports investigating TNF-R1, the levels and timing of TRAIL-induced apoptosis were not significantly altered by pre-loading the cells with TRAIL and releasing them up to 37°C compared with cells treated without pre-loading (Figure 6.9). Data from Figure 6.9 shows single cells that are representative of more than 50 images taken, however due to space restraints, single cells were shown. Ideally, statistics should be carried out to determine what percentage of cells internalised TRAIL at each time point, however this is above the scope of these experiments.

Despite this, there were some slight differences with DISC formation when cells were pre-loaded with TRAIL compared with when they were treated at 37°C in BJAB cells. It appeared that pre-loading cells with TRAIL discouraged rapid dissociation of the DISC and also discouraged constant recruitment of procaspase-8 into the DISC. It is not clear whether internalisation blocks recruitment of procaspase-8 to the DISC as these data would suggest. Therefore a preliminary experiment was completed and the results are shown in the Appendix (Figure A.5). In this figure TRAIL was pre-loaded onto BJAB cells and allowed to form a DISC. Cells were taken up to 37°C to allow for internalisation and then rapidly chilled back to 4°C to prevent further movement of the DISC complex.

Results from this study were inconclusive. At early times, no further caspase-8 was recruited into the DISC at 4°C compared with cells treated and lysed at 37°C. However, at later times (30 mins) some caspase-8 did appear to be recruited back into the DISC at 4°C. The reason why the results are inconclusive is that the levels of caspase-8 recruited to the DISC at 4°C are low and only occur at later time points. Thirty minutes is sufficient for receptors to be recycled back to the cell surface and therefore recruitment of caspase-8 back to recycled

receptors cannot be ruled out as a possibility. Further studies addressing this question were not pursued due to the difficulty of ruling out receptor recycling as a possibility.

One report has highlighted that caspase-8 activation is a requirement for DISC aggregation and internalisation in the case of CD95 (Algeciras-Schimnich, Shen et al. 2002). Some preliminary studies were carried out to investigate whether this was the case for TRAIL and are shown in Figures 6.11 and 6.12. Pre-treatment of BJAB cells with up to 300 μM of z-VAD.fmk did not inhibit the formation of a DISC (Figure 6.11). However, when confocal studies were carried out to measure internalisation of TRAIL in the presence of z-VAD.fmk relatively little signal was detected compared with cells treated with TRAIL alone (Figure 6.12). Taken together, these data support the theory that caspase-8 activation is required for aggregation of the DISC but does not affect DISC formation, in concurrence with the previous publication concerning CD95 (Algeciras-Schimnich, Shen et al. 2002). However, it is important to note that these studies were only carried out on one occasion and would need to be repeated several times in parallel with other experiments in order to make the claims stated above.

One recent paper set out to investigate the internalisation patterns of TNFR1 (Schneider-Brachert, Tchikov et al. 2004). The study suggested that TNFR1 endocytosis and DISC formation were inseparable events and that endocytosis was required for DISC formation (Schneider-Brachert, Tchikov et al. 2004). Data in this chapter would suggest that the same is not the case with TRAIL. DISC formation was found to occur at 4°C in BJAB cells within 10 mins of TRAIL treatment and within 45 mins of TRAIL treatment in HeLa cells (Figures 6.13 and 6.14). However, at 4°C endocytosis will not occur as confirmed by experiments using confocal microscopy.

These data demonstrate that DISC formation occurs at the plasma membrane prior to endocytosis in TRAIL-induced apoptosis. Although this is not direct evidence that internalisation of the TRAIL DISC is not required for TRAIL induced apoptosis it does support the idea that DISC formation is a very separate event from DISC internalisation.

Work completed by Dr. Xiao Ming Sun set out to investigate the role of TRAIL and receptor-internalisation in TRAIL-induced apoptosis (Figure A.6). In this figure, TRAIL-receptor internalisation is blocked by pre-treatment of BJAB cells with hyperosmotic solution. After blocking internalisation by this method, he set out to determine the effects in the block of internalisation of TRAIL-induced apoptosis. Despite reports that internalisation is required for CD95 and TNFR1-mediated DISC formation and apoptosis (Schneider-Brachert, Tchikov et al. 2004; Lee, Feig et al. 2006), Figure A.6 shows that blocking internalisation through pre-treatment with hyperosmotic solution sensitises BJAB cells to TRAIL-induced apoptosis. This suggests that internalisation may be a mechanism to dampen TRAIL-induced apoptosis, not the other way around.

A very recent paper suggested that clathrin-mediated endocytosis was probably the mechanism by which the TRAIL DISC was internalised (Austin, Lawrence et al. 2006). HeLa cells expressing the K44A dominant negative mutation in dynamin-1 were used as an attempt to block internalisation and to determine whether TRAIL-induced apoptosis was affected. The uptake of transferrin was used as a measure for the function of dynamin and was mostly blocked in the dominant negative HeLa cells but not blocked in wt HeLa cells confirming the loss of function of dynamin (Figure 6.15 B). However, in the absence of a functional dynamin, TRAIL internalisation was not inhibited suggesting the employment of one of the many other defined endocytic pathways (Figure 6.15 A). Unsurprisingly, TRAIL-induced apoptosis and DISC formation was also not affected by the absence of a functional dynamin (Figure 6.14).

It is a well known phenomenon that when one endocytic pathway is not functioning, other pathways may compensate and be used in its place (Polo and Di Fiore 2006). The data in Figures 6.14 and 6.15 do not disprove the involvement of the clathrin-mediated endocytic pathway, but instead suggest that TRAIL may internalise via other pathways in its absence. Further work would be required to pin-point the exact mechanism by which TRAIL can internalise. Several clathrin-independent endocytic pathways have been identified and dominant negative proteins have been developed by various groups and may play an important part in identifying which pathway is relevant to TRAIL internalisation (Altschuler, Barbas et

al. 1998; Shi, Faundez et al. 1998; Nesterov, Carter et al. 1999; Glebov, Bright et al. 2006). Studies looking at colocalisation of TRAIL with other well defined proteins such as transferrin may also be useful in determining which pathways are important. One important point is that although internalisation inhibitors have been widely used in the past, they are increasingly being considered by the endocytosis field as less useful due to their non-specific nature. Therefore, it is not recommended that they should be used in future studies concerning TRAIL.

The experiments completed in this chapter raise several questions. What is the mechanism of TRAIL capping and is it caspase-dependent? What is the mechanism of TRAIL internalisation and does TRAIL internalise with DISC proteins? Is TRAIL internalisation important for TRAIL-induced apoptosis? If not, is TRAIL receptor internalisation important for apoptosis? Are there differences in TRAIL-R1 and TRAIL-R2 internalisation and, if so, do they have an impact on the way cells respond to receptor-selective versions of TRAIL? Is failure to internalise TRAIL a mechanism of resistance in some cell types?

There are a number of straightforward approaches that could be used to answer many of these questions. For example, the used of dominant negative proteins that are important in internalisation may be a good approach to looking at the mechanism of TRAIL internalisation. Mutant ligands could be used to look at differential internalisation of TRAIL-R1 and TRAIL-R2 complexes. Looking at colocalisation of TRAIL with DISC proteins may be a good approach to investigate receptor and DISC internalisation.

One thing to keep in mind is that many of the well known methods used for investigating endocytosis can stress cells and are even known to induce apoptosis on their own. If this occurs, results obtained from many experiments can become meaningless. So far, melding of the two fields has proved to be problematic for this reason. It is therefore important to execute caution when investigating the significance of endocytosis in relation TRAIL-induced apoptosis, or other forms of apoptosis.

Chapter 7: Discussion and Future Work

7.1 Discussion and Future Work

Work in this thesis has aimed to determine the mechanism of action (or resistance) of various therapeutic agents for use in CLL and to further the understanding of several potential therapies.

7.2 Bortezomib

Work in Chapter 3 aimed at identifying the underlying reason for the discrepancy between promising *in vitro* and discouraging *in vivo* data for bortezomib therapy of CLL. In the presence of various components of whole blood, it was shown that RBCs interfere with the activity of bortezomib, but not MG132, in CLL cells. Further *in vivo* studies suggested that the mechanism of interference by RBCs was preferential uptake of bortezomib by RBCs thus limiting the availability of bortezomib to lymphocyte cells *in vivo*. This not only has implications for the dosing schedules and administration of bortezomib in CLL, but also in a range of other haematological malignancies and solid tumours. These data suggest that bortezomib may not be an ideal single agent therapy in CLL, but may be useful in combination with other therapeutic agents provided it is used at a sub-toxic dose.

No work has currently been undertaken to investigate the mechanism of preferential uptake by RBCs or the structural properties of bortezomib that mediate its uptake in RBCs. Studies on the mechanism of bortezomib uptake may provide some clues as to what structural properties proteasome inhibitors need in order to avoid interference by RBCs. Furthermore, it could potentially provide novel ways of overcoming RBC uptake of bortezomib by revealing pathways that could be blocked to prevent uptake and sensitise CLL cells to bortezomib-induced apoptosis *in vivo*.

The whole blood apoptosis assays developed in Chapter 3 have opened a new range of opportunities in terms of pre-clinical testing in patient samples. Data in Chapter 3 demonstrated that it is not sufficient to culture and treat primary tumour cells *in vitro* and expect them to react the same way to therapeutic agents *in vivo*. There are many environmental signals not present in *in vitro* testing using purified CLL cells, but may contribute to resistance to therapies *in vivo* (Jones, Ganeshaguru et al. 2003; Flinn, Byrd et al.

2005). For example, the AKT survival signalling pathway was activated by human serum and caused resistance to fludarabine in CLL cells (Jones, Ganeshaguru et al. 2003). In addition, the microenvironment is thought to be important in maintaining the survival of CLL cells (Kipps 2000; Pedersen, Kitada et al. 2002; Tsukada, Burger et al. 2002), but it is not clear what survival pathways are activated *in vivo* that are switched off in the absence of the bone marrow microenvironment.

All pre-clinical testing in CLL should include samples where cells have been treated on stromal layers or in the presence of cytokines such as IL-4, IFNα, IFNγ, IL-8 or IL-13 (to mimic effects of the bone marrow microenvironment) and in the presence of whole blood (to mimic effects of whole blood components).

7.3 Mechanisms of TRAIL-induced apoptosis

In Chapter 4, TRAIL mAbs ETR1 and ETR2 were screened for apoptosis-inducing ability on a panel of 4 lymphoma cell lines and on CLL cells. CLL cells were sensitised with an HDAC inhibitor, to ETR1 and other forms of TRAIL that can induce apoptosis through stimulation of TRAIL-R1, but were resistant to ETR2 and Apo2L. This was surprising given the number of studies suggesting that TRAIL-R2 is the key receptor in apoptosis induction of tumour cells (MacFarlane, Ahmad et al. 1997; Truneh, Sharma et al. 2000; Kelley, Totpal et al. 2005).

Further work in Chapter 5, using mAbs and mutant ligands confirmed that CLL cells, when pre-treated with an HDAC inhibitor, undergo apoptosis through stimulation of TRAIL-R1. Other candidates that had previously been reported to sensitise CLL cells to TRAIL-induced apoptosis failed to sensitise CLL to TRAIL mAbs or wt TRAIL (Johnston, Kabore et al. 2003; Kabore, Sun et al. 2006). Therefore, it was not possible to determine whether CLL cells are able to undergo apoptosis through stimulation of TRAIL-R2 using different sensitising agents. Further investigation is required to determine the general importance of TRAIL-R1 in CLL cells with and without many different sensitising agents.

In addition, the function of TRAIL-R2 has not been defined in CLL cells. TRAIL has been known to activate survival pathways, including the NF-κB pathway, and induce proliferation

in various cell types, particularly in the absence of caspase-activation (Harper, Farrow et al. 2001; Ehrhardt, Fulda et al. 2003). Further work should be carried out to determine if survival pathways are activated in CLL in response to preparations of TRAIL that induce apoptosis through TRAIL-R2.

Crosslinking antibodies are used to stimulate receptor aggregation and formation of higher order structures by linking several receptor complexes together on the cell surface. Crosslinking was shown to improve the efficacy of many versions of TRAIL, including Apo2L, ETR1 and ETR2 in resistant cell lines (Georgakis, Li et al. 2005; Kelley, Totpal et al. 2005). Crosslinking antibodies were not used in experiments in Chapters 4 or 5, but may have yielded different results. Crosslinking may improve apoptosis-inducing ability of Apo2L, TRAIL.R2-6 or ETR2 in CLL *in vitro*, which would suggest that formation of higher order structures may be important for TRAIL-induced apoptosis. This would also suggest that distribution patterns of TRAIL-R1 and TRAIL-R2 on the surface of CLL cells may be different. For example, distribution of TRAIL-R1 may be more localised than that of TRAIL-R2 and not require crosslinking. This could be a possible mechanism of resistance to TRAIL, not only in CLL cells, but perhaps in other tumour types. Further work should be carried out to determine the effects of crosslinking on TRAIL-induced apoptosis using the different versions of TRAIL from this study.

Studies completed using Apo2L and TRAIL mutants in tumour cell lines have suggested that TRAIL-R2 may be the key receptor for apoptosis induction in most tumour types (Kelley, Totpal et al. 2005). However, data from Chapters 4 and 5 show otherwise in the case of CLL. This study and others demonstrate the importance of using primary cells for pre-clinical evaluation of TRAIL or its mAbs (Kurbanov, Geilen et al. 2005). Many subsequent studies have evaluated the importance of each TRAIL-receptor in primary tumour cells and surprisingly, given the prior literature, TRAIL-R1 appears to be of major importance in a number of tumour types (Strater, Hinz et al. 2002; Georgakis, Li et al. 2005; Kurbanov, Geilen et al. 2005; Menoret, Gomez-Bougie et al. 2006; Zeng, Wu et al. 2006). Table 7.1 shows several studies that have suggested the importance of one TRAIL receptor over the other in primary tumour cells. Studies using cell lines were omitted from the table.

Table 7.1: The importance of TRAIL-R1 and TRAIL-R2 for apoptosis induction in various tumours.

Tumour Type	Important receptor for apoptosis induction	Summary	Reference
colon carcinoma	TRAIL-R1	Measured immunohistochemistry of TRAIL-Receptor expression against disease-free survival and found that survival is associated with increased expression of TRAIL-R1, but not TRAIL-R2	Strater, Walczak et al 2002
myeloma cells	TRAIL-R1	Used ETR1 and ETR2 in primary myeloma cells and found that ETR1 killed cells to a higher extent than ETR2. ETR1 also killed medullary and extra medullary myeloma from patients after relapse.	Menoret, Gomez-Bougie et al 2006
renal cell carcinoma	TRAIL-R2	Used the antibody TRM-1 and found it to be effective, but the effects were more pronounced after crosslinking. In vivo administration suppressed tumour growth of renal cell carcinoma in xenografts in immunodeficient mice	Zeng, Wu et al 2006
melanoma cells	TRAIL-R1	Used blocking antibodies to show that TRAIL-R1 was important for signalling to apoptosis in TRAIL-R1 expressing cell lines and that primary cells express high levels of TRAIL-R1, suggesting that it may be a promising therapeutic target in melanoma	Kurbanov, Geilen et al 2005
Non-Hodgkin lymphoma	TRAIL-R1 and TRAIL-R2	Used ETR1 and ETR2 in primary samples and found that both antibodies were able to induce low levels of apoptosis in the majority of samples. This is in contrast to findings in Chapter 4 suggesting that CLL cells are resistant to ETR1 and ETR2 on their own. Differences could be due to varying incubation times and concentrations used.	Georgakis, Younes et al 2005

One study in particular commented on the discrepancy between results in primary melanoma cultures and cell lines derived from patient samples (Kurbanov, Geilen et al. 2005). Very little emphasis has been placed on the importance to TRAIL-R1 in melanoma because cell lines express little of it compared with TRAIL-R2 (2 out of 7 cell lines expressed TRAIL-R1 at moderate levels) (Kurbanov, Geilen et al. 2005). These authors looked at sensitivity of TRAIL-R1 expressing cell lines using blocking antibodies to TRAIL-R1 and TRAIL-R2 and found that TRAIL-R1 was predominantly responsible for signalling to apoptosis in those cell lines (Kurbanov, Geilen et al. 2005). Using immunohistochemistry, they showed TRAIL-R1 expression in primary cells, but all cell lines (apart from 1) had a higher TRAIL-R2 expression compared with TRAIL-R1 (Kurbanov, Geilen et al. 2005). This study demonstrates that cell lines are not representative and are not a sufficient replacement for primary tumour cells (Kurbanov, Geilen et al. 2005).

As shown in Table 7.1, only one tumour type (renal cell carcinoma) appeared to signal to apoptosis through TRAIL-R2, using the TRAIL-R2 antibody TRM-1 as a marker for

sensitivity (Zeng, Wu et al. 2006). In contrast, TRAIL-R1 appears to be important for the induction of apoptosis in a range of primary tumour types (Strater, Hinz et al. 2002; Georgakis, Li et al. 2005; Kurbanov, Geilen et al. 2005; Menoret, Gomez-Bougie et al. 2006). These studies have used both blocking antibodies to TRAIL-R1 and TRAIL-R2 and using ETR1 and ETR2 as direct activators of the apoptotic pathways of TRAIL-R1 and TRAIL-R2. Future work should focus on using a range on agonistic antibodies (not only ETR1 and ETR2) and mutant ligands to evaluate apoptotic induction in primary tumour cells because it is important to note that using different forms of TRAIL in primary tumours may yield different results.

Work in Chapter 4 also showed that ETR1 and ETR2 do not synergise in a panel of cell lines, suggesting that there is no crosstalk between the two receptor pathways. In addition, most of the literature using ETR1 and ETR2 as agonistic antibodies has suggested that one receptor is predominant over the other. Thus, it was surprising that mutants signalling to TRAIL-R1 and TRAIL-R2 (TRAIL.R1-5 and TRAIL.R2-6, respectively) both induced apoptosis in the chronic myeloid leukaemia cell line K562 after pre-treatment with depsipeptide. On further investigation, TRAIL.R1-5, the TRAIL-R1 signalling mutant, pulled both TRAIL-R1 and TRAIL-R2 into heterocomplexes within the DISC. This has been previously described in studies using overexpression of TRAIL-R1 and TRAIL-R2, but the biological significance of this was not described (Kischkel, Lawrence et al. 2000; Sprick, Weigand et al. 2000). Work in this thesis has shown that heterocomplexes can be formed and can signal to apoptosis in K562 cells. Presumably, ETR1 and ETR2 cannot form heterocomplexes of TRAIL-R1 and TRAIL-R2, which may be the underlying reason for differences in apoptotic induction by mAb and ligand.

Interestingly, TRAIL.R2-6 did not pull heterocomplexes under any circumstances, suggesting that the ligand is specific to TRAIL-R2 only. These data indicate that TRAIL.R1-5 may not contain the exact mutations necessary for selectivity towards TRAIL-R1 homotrimers and would need further improvement to reach ideal specificity. An alternative explanation is that upon stimulation with TRAIL, TRAIL-R1 may pull TRAIL-R2 into a complex. The latter suggestion would indicate that, in contrast to findings from Chapter 4 (using mAbs), in certain

cell types (or in cell types stimulated with ligand that may form heterotrimers) TRAIL-R1 and TRAIL-R2 signalling are interlinked. In addition, it would imply that the connection between the two receptors can only be initiated through stimulation of TRAIL-R1 suggesting that TRAIL-R1/-R2 receptor complexes are not pre-formed. It is not clear whether this may be the case with "decoy" receptors upon ligand binding, but TRAIL mutants remain a good tool to investigate the signalling between TRAIL-R1 and TRAIL-R2 complexes and possibly heterocomplexes.

Chapter 6 highlighted the discrepancy between FADD and caspase-8 recruitment to the TRAIL DISC prior to and after treatment with depsipeptide in K562 cells. Apoptosis induction did not correlate with FADD recruitment and this was surprising. After time courses and concentration-responses it was evident that DISC components were being disassembled upon treatment with higher concentrations of TRAIL, which was causing the discrepancy described above. One explanation was that upon treatment of K562 cells with a high concentration of ligand, TRAIL, along with its receptors and DISC components, was being internalised rapidly into a low pH compartment and dissociating from the DISC.

During the course of this study, a paper was published suggesting that Fas internalisation was required for formation and activation of the DISC, and that survival signalling pathways were activated at the plasma membrane (Lee, Feig et al. 2006). Taken together with a study completed with TNF that suggested TNFR1 signalling occurs in a receptosome complex within the cell and internalisation is required for formation of the DISC implied that the same may be true for TRAIL (Schneider-Brachert, Tchikov et al. 2004). Therefore studies were undertaken to identify the role of internalisation in TRAIL-induced apoptosis. It is particularly difficult to carry out such studies as many common methods used to inhibit internalisation, such as using chemical inhibitors and transfecting cells with dominant negative proteins, can cause stress, thus leading to apoptosis. Therefore novel methods to measure internalisation were required in the studies highlighted in Chapter 6.

Although internalisation appeared to occur rapidly in BJAB and HeLa cells, it was not a prerequisite for DISC formation, as the DISC formed readily at 4°C. These data

unequivocally demonstrate, in contrast to Fas and TNF, that TRAIL DISC formation occurs at the plasma membrane. In addition, when TRAIL signalling was synchronised by pre-loading at 4°C followed by a washout, caspase-8 was not further recruited to the DISC, suggesting that FADD and caspase-8 are recruited to the TRAIL DISC only at the plasma membrane. Furthermore, data completed by Dr. Xiao Ming Sun (Figure A.6) suggested that blocking internalisation using hyperosmotic solution, did not block TRAIL-induced apoptosis, but actually sensitised BJAB cells to TRAIL confirming that internalisation is not important for DISC formation or apoptosis induction in these cells. These data suggest that DISC formation is the requisite step in TRAIL-induced apoptosis and that this occurs at the plasma membrane.

Data from Chapter 6 are in agreement with a recently published study that showed caspase-8 to rapidly cleave clathrin adaptor proteins upon binding with TRAIL in BJAB cells (Austin, Lawrence et al. 2006). The study implied that TRAIL internalisation was not required for TRAIL-induced apoptosis and that cleavage of the clathrin-mediated endocytic machinery was a mechanism to amplify the TRAIL signal, presumably through synchronisation of TRAIL-receptor complexes at the surface of the cells (Austin, Lawrence et al. 2006). However, the study did not demonstrate the mechanism of TRAIL or receptor internalisation (Austin, Lawrence et al. 2006). Work in Chapter 6, using inducible dominant negative dynamin-1 expressing HeLa cells, demonstrates that in the absence of clathrin-mediated endocytosis, TRAIL is still able to internalise, indicating that clathrin-mediated endocytosis is not necessary for TRAIL internalisation.

These studies, taken together, indicate that TRAIL is rapidly internalised in BJAB and HeLa cells, but that TRAIL internalisation is not necessary for DISC formation or TRAIL-induced apoptosis. In addition, TRAIL can be internalised via both clathrin-dependent and independent means. These studies suggest that internalisation may dampen the TRAIL signal, thus mediating resistance to TRAIL in certain cell types.

Because CLL has low surface expression of both TRAIL receptors, it was not possible to carry out studies in Chapter 6 using CLL cells. However, internalisation patterns of TRAIL and their implications may apply to CLL. Increasing availability of FADD and caspase-8 to the

DISC appears to be an important step in sensitising CLL cells to TRAIL-induced apoptosis using HDAC inhibitors (Inoue, MacFarlane et al. 2004). It may be possible that rapid internalisation of TRAIL, prior to DISC formation, blocks FADD and caspase-8 association with the receptors. Blocking internalisation or slowing it may sensitise CLL cells to TRAIL-induced apoptosis by allowing FADD and caspase-8 to form a DISC at the plasma membrane. Further work should be carried out to determine the mechanism of action of depsipeptide in relation to internalisation and TRAIL-induced apoptosis in CLL.

This thesis has also demonstrated that TRAIL-R1 and TRAIL-R2 may have different signalling patterns. This was demonstrated in Chapter 6 using K562 cells. Mutant ligands have provided a tool to investigate signalling and internalisation patterns of TRAIL-R1 and TRAIL-R2. Further work should be carried out to investigate different internalisation patterns of TRAIL-R1 and TRAIL-R2 using the specific mutant ligands generated in Chapter 5 based on methodology developed in Chapter 6.

Appendix

Annexin V Binding Buffer

10 mM Hepes/NaOH (pH 7.4)

150 mM NaCl

5 mM KCl

1 mM $MgCl_2$

1.8 mM $CaCl_2$

dH_2O (up to 500 ml)

1 x SDS Sample Buffer

1.5M Tris

15% Glycerol (v/v)

2% SDS (v/v)

25 mg Bromophenol Blue

pH to 6.8 in 50ml dH_2O

5% β-mercaptoethanol added immediately prior to use

DISC Lysis Buffer

30 mM Tris/HCl (pH 7.5)

150 mM NaCl

10% Glycerol (w/v)

1% Triton-X-100 (v/v)

1 complete mini protease inhibitor tablet per 10 ml lysis buffer (added immediately prior to use)

Running Buffer

3.03 g Tris

14.4 g Glycine

10% SDS (v/v)

dH_2O (up to 1 L)

Transfer Buffer

3.03 g Tris

14.4 g Glycine

200 ml Methanol

dH_2O (up to 1 L)

Tris Buffered Saline (TBS) 10x

20 mM Tris

137 mM NaCl

HCl (to pH 7.6)

dH_2O (up to 1 L)

Coomasie Stain

400 ml Methanol

100 ml Acetic Acid

2.5 g Bromophenol Blue

500 ml dH_2O

Filtered with Whatman paper

Coomasie Destain

400 ml Methanol

100 ml Acetic Acid

500 ml dH_2O

LB Broth (2 x NaCl)

10 g Tryptone

5 g Yeast

10 g NaCl

1 L dH_2O

Autoclaved

Figure A.1: Some common recipes used in this thesis.

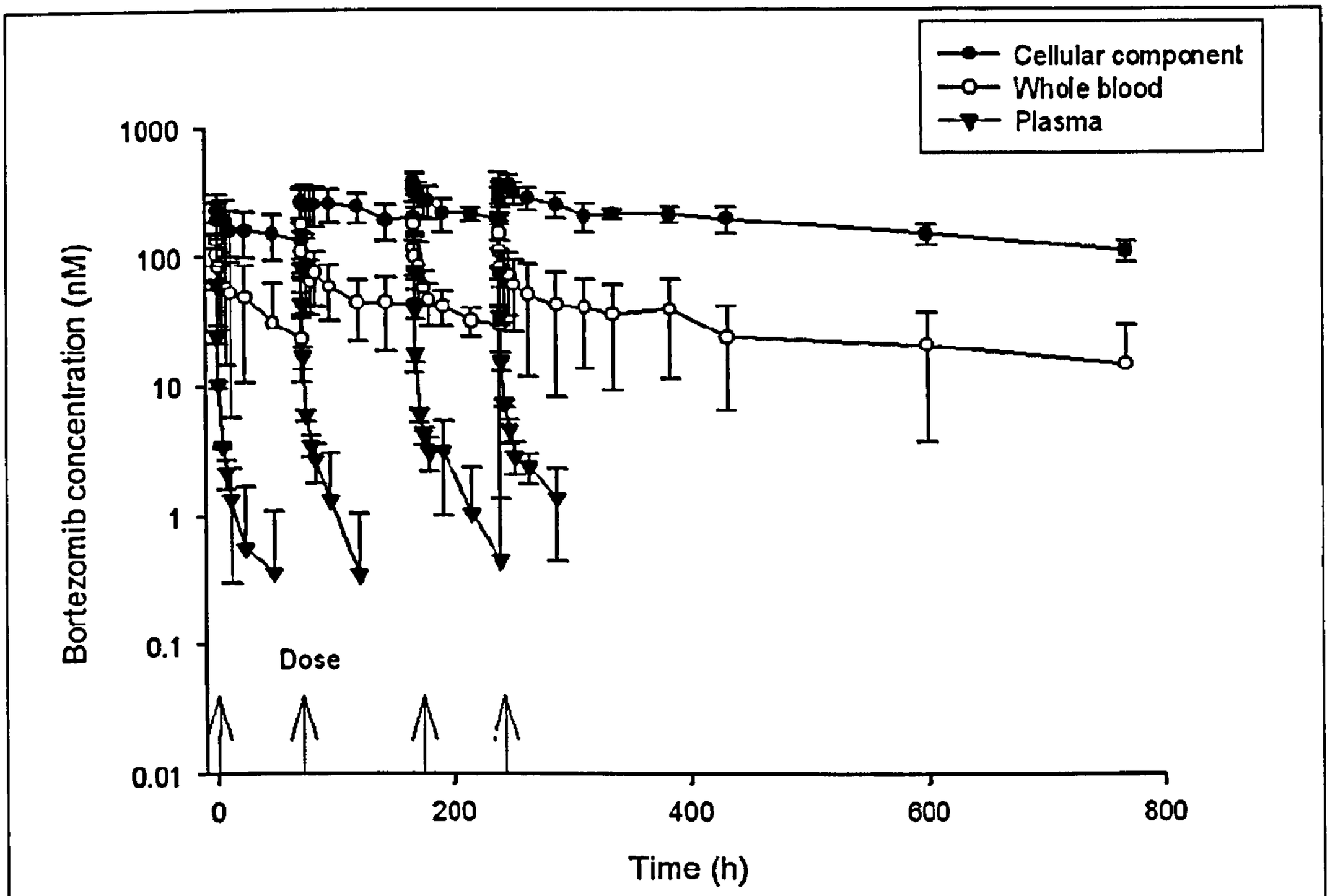

Figure A.2: Bortezomib is preferentially distributed to the red blood cell fraction in vivo. Intravenous dosing of bortezomib (0.1 mg/kg) was carried out on days 1, 4, 8, and 11. Following each dose administration, blood samples were obtained at 0.17, 0.5, 1, 2, 4, 24, 48, and 72 hours. In addition, pre-dose samples were taken before the first and third doses, and at 114 and 192 hours after the fourth dose. After each consecutive bolus dose, the concentrations of bortezomib in plasma, whole blood, and the cellular component of whole blood were determined. This figure was provided by Johan Monbaliu and Roland De Coster at Johnson and Johnson (Beerse, Belgium).

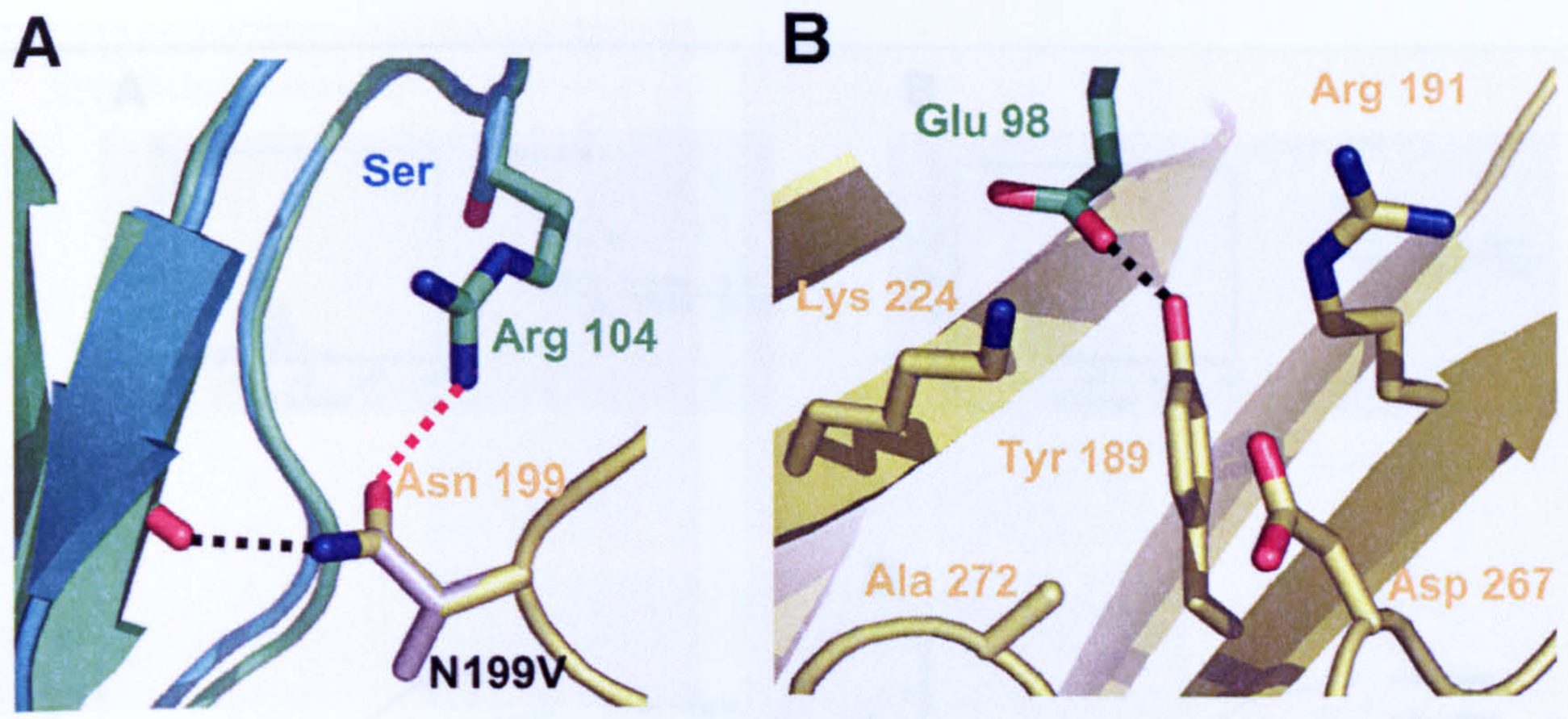

Figure A.3: Model of TRAIL/TRAIL-R1 complex and crystal structure of TRAIL/TRAIL-R2 complex. A) Role of TRAIL Asn199 in TRAIL (yellow)/TRAIL-R1 (cyan)/TRAIL-R2 (green) interactions. The hydrogen bond present with both TRAIL-R1 and TRAIL-R2 is shown as a black dashed line and that present with only TRAIL-R2 as a red dashed line. The loss of these hydrogen bonds with the TRAIL substitution Asn199Val is also illustrated. B) Role of TRAIL Tyr189 in TRAIL (yellow)/TRAIL-R/R2 (green) interactions. The hydrogen bond from this tyrosine to the conserved glutamine in TRAIL-R1/R2 is shown as a dashed line. Residues in TRAIL involved in hydrophobic interactions with Tyr 189, interactions lost in Tyr189Ala substituted TRAIL are also shown. This figure was provided by Dr. Mike Sutcliffe (University of Manchester).

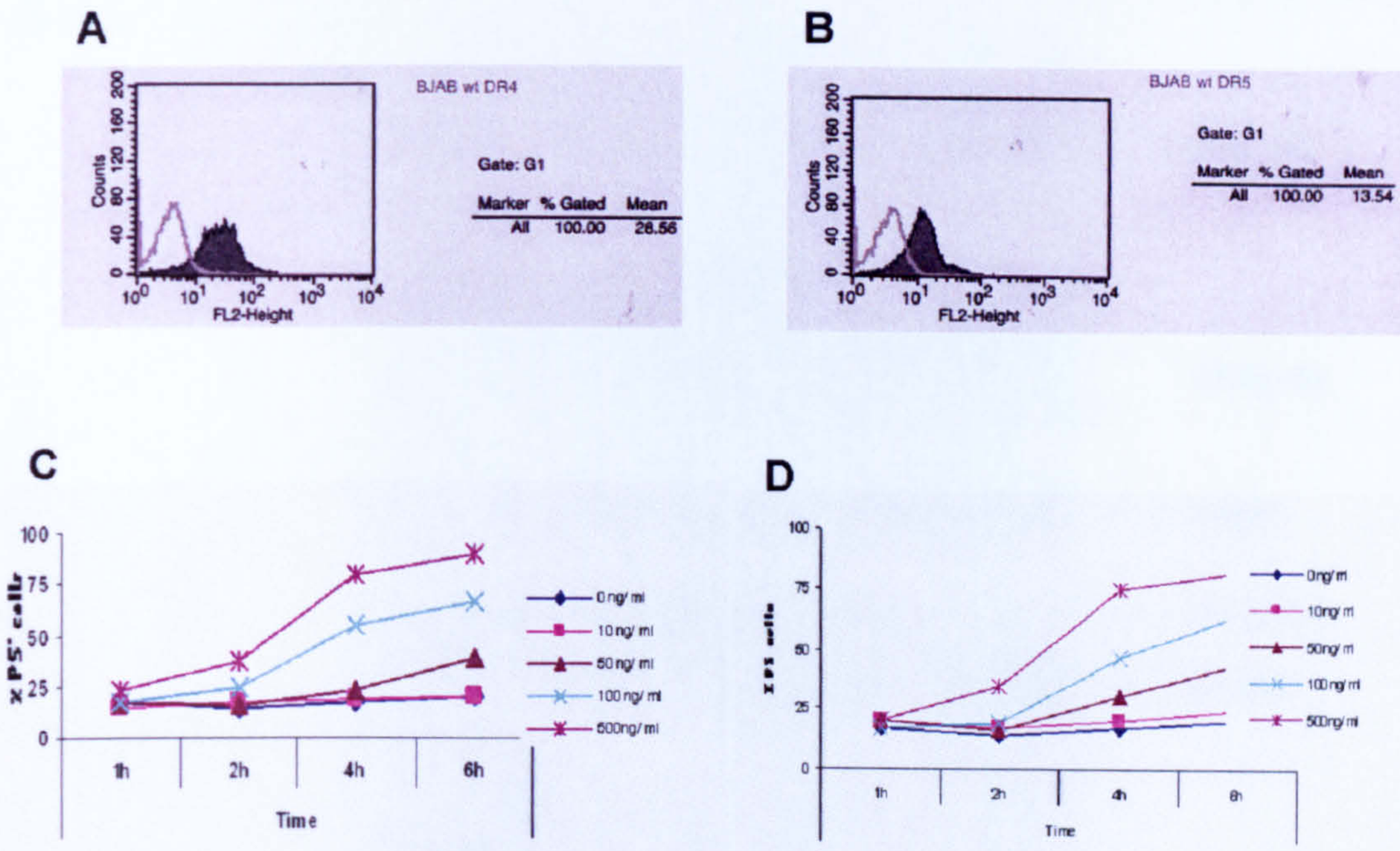

Figure A.4: Surface expression of TRAIL-R1 and TRAIL-R2 and sensitivity to ETR1 and ETR2 in BJAB cells. A) BJAB cells were stained for surface expression IgG1 (grey line) or TRAIL-R1 (filled in line) as described in Materials and Methods. The mean-fluorescence intensity of TRAIL-R1 stained cells was 28 compared with 3 for IgG1 stained cells. B) BJAB cells were stained for surface expression of IgG1 (grey line) or TRAIL-R2 (filled in line) as described in Materials and Methods. The mean-fluorescence intensity of TRAIL-R2 stained cells was 13 compared with IgG1 stained cells (3). C) BJAB cells were treated with increasing concentrations of ETR1 (0-500 ng/ml) for up to 6 hrs. Apoptosis was assessed by determining the % PS^+ cells by flow cytometry. D) BJAB cells were treated with increasing concentrations of ETR2 (0-500 ng/ml) for up to 6 hrs. Apoptosis was assessed by determining the % PS^+ cells by flow cytometry.

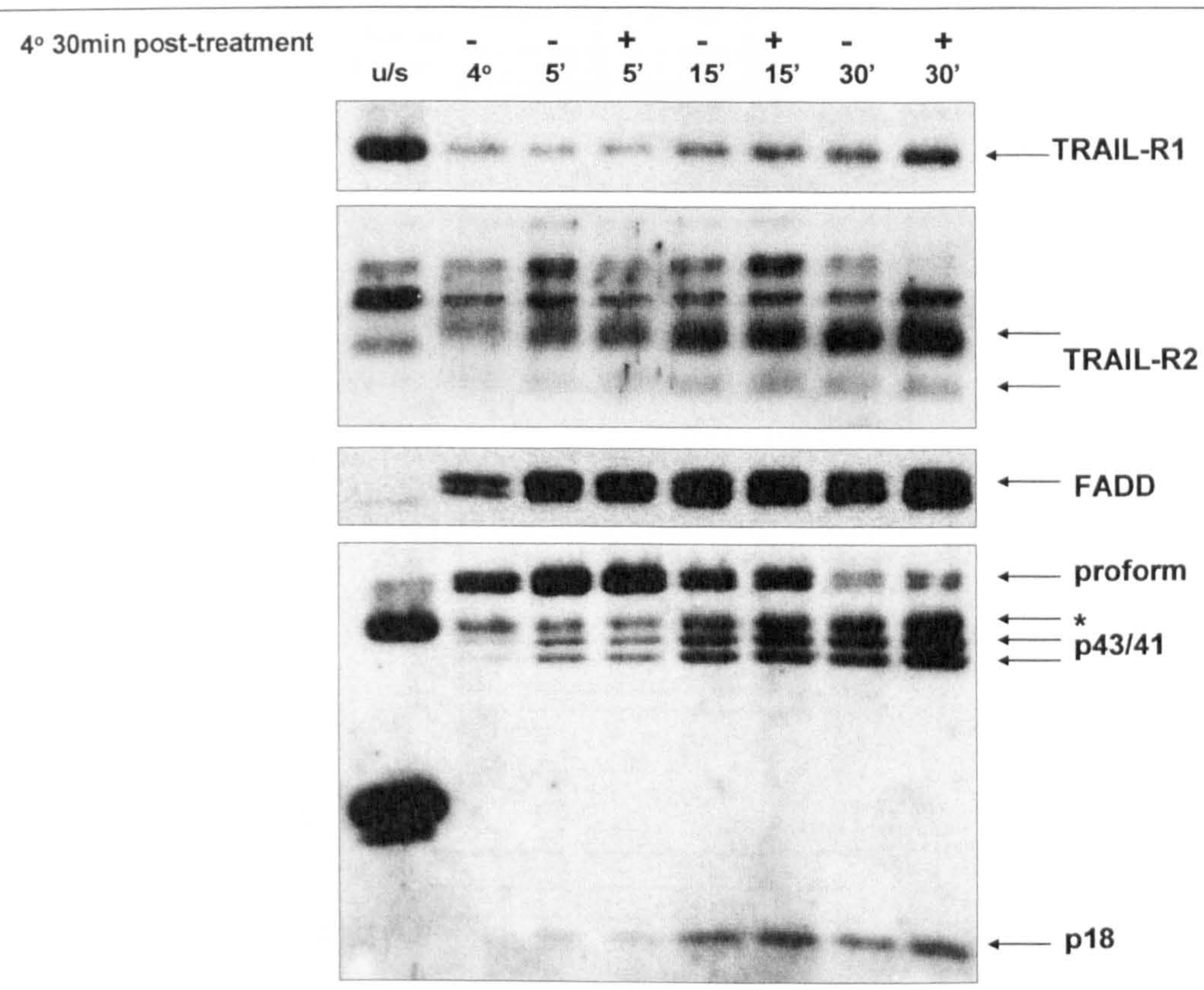

Figure A.5. TRAIL DISC formation in BJAB cells after pre-loading at 4°C, releasing up to 37°C for a set time and cooling back to 4°C 30 mins post-release. BJAB cells were pre-cooled to 4°C for 1 hour followed by pre-loading with biotinylated TRAIL for 45 mins at 4°C. Cells were washed in ice cold PBS and released up to 37°C for the indicated time and lysed, or rapidly cooled back down to 4°C by resuspending in pre-cooled media for 30 mins followed by lysis. Analysis of the DISC proteins was carried out as described in Materials and Methods. A + at the top of the lane indicates that cells were re-cooled to 4°C prior to lysis. U/s cells indicate that cells were treated with biotinylated TRAIL post-lysis. * indicates the presence of TRAIL-R1 from a re-probed membrane. Results shown are of one experiment.

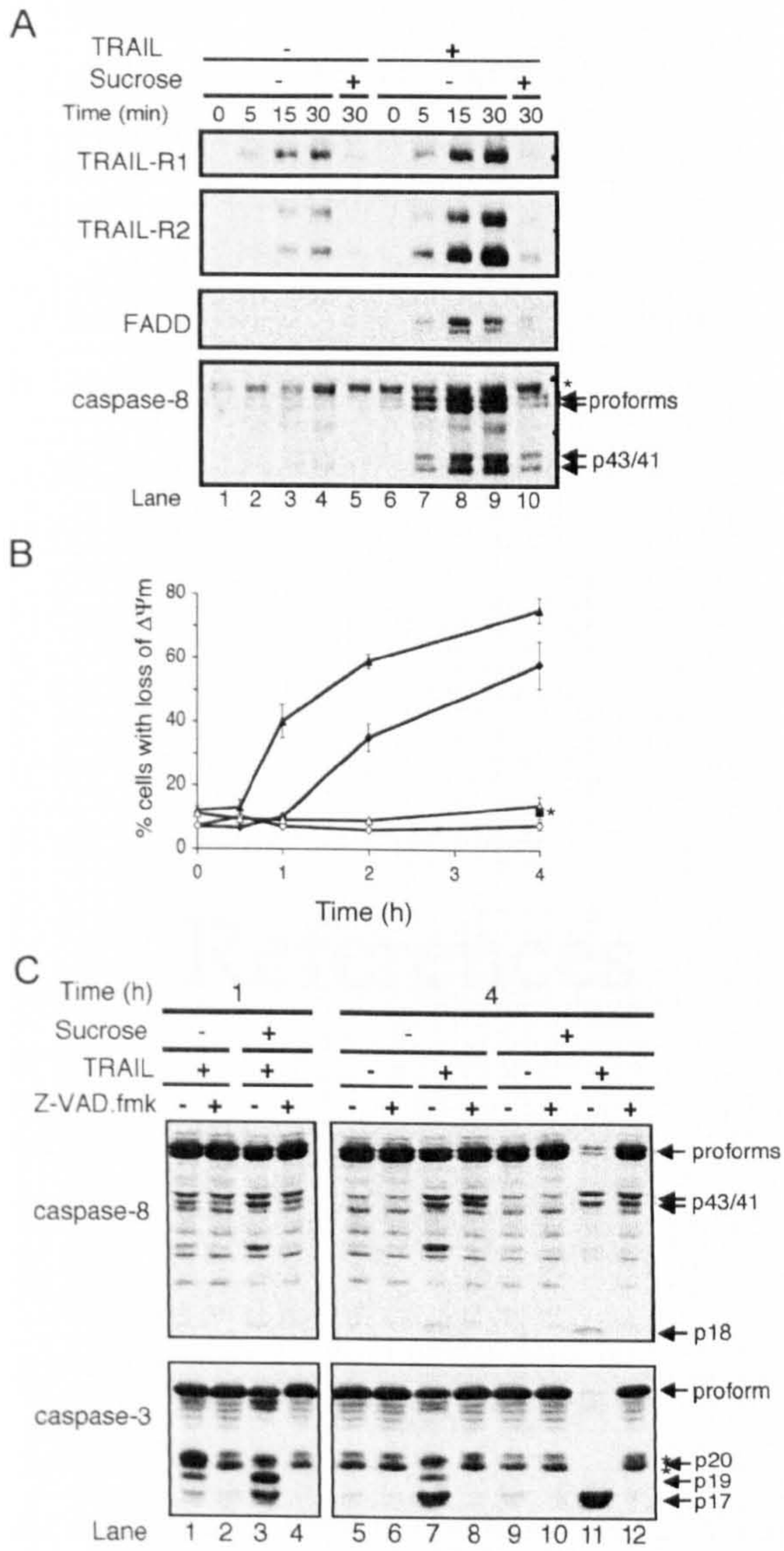

Figure A.6: TRAIL-R1 and TRAIL-R2 internalisation is not required for apoptosis. A) BJAB cells were pre-labelled with cleavable biotin and receptors were allowed to internalise at 37°C in the absence (lanes 1-5) or presence (lanes 6-10) of TRAIL (1 μg/106 cells). Sucrose (250 mM) was included in the treatment of some cells (lanes 5 and 10) prior to biotin labelling, during ligand binding and receptor internalisation. Biotinylated proteins were pulled down by neutrAvidin beads. Internalised TRAIL-R1 and TRAIL-R2 and associated FADD or caspase-8 was detected by western blot analysis. B) BJAB cells were incubated in normal (diamonds) or hyperosmotic medium (triangles) for 30 mins prior to treatment with TRAIL (1 μg/10^6 cells) in the absence (closed symbols) or presence (open symbols) of z-VAD.fmk (10 μM) for the indicated times. Apoptosis was assessed by TMRE, showing loss of mitochondrial membrane potential. As an additional control, cells were also treated with hyperosmotic medium in the absence of TRAIL for 4 h (Closed squares with an asterisk). Results shown are Mean ± SEM of 3 experiments. C) Cells obtained from the experiments shown in panel B of this Figure were subjected to western blot analysis. Arrows indicate proforms of caspase-8 or -3 and their related processed forms. Asterisks indicate un-identified and non-specific proteins. This figure was provided by Dr. Xiao Ming Sun.

References

Adams, J. (2002). "Development of the proteasome inhibitor PS-341." Oncologist 7(1): 9-16.

Adams, J. (2003). "The proteasome: structure, function, and role in the cell." Cancer Treat Rev **29 Suppl 1**: 3-9.

Adams, J. (2004). "The development of proteasome inhibitors as anticancer drugs." Cancer Cell **5**(5): 417-21.

Adams, J. (2004). "The proteasome: a suitable antineoplastic target." Nat Rev Cancer **4**(5): 349-60.

Adams, J. and M. Kauffman (2004). "Development of the proteasome inhibitor Velcade (Bortezomib)." Cancer Invest **22**(2): 304-11.

Adams, J., V. J. Palombella, et al. (1999). "Proteasome inhibitors: a novel class of potent and effective antitumor agents." Cancer Res **59**(11): 2615-22.

Aghajanian, C., S. Soignet, et al. (2002). "A phase I trial of the novel proteasome inhibitor PS341 in advanced solid tumor malignancies." Clin Cancer Res **8**(8): 2505-11.

Agterof, M. J. and D. H. Biesma (2005). "Images in clinical Medicine. Bortezomib-induced skin lesions." N Engl J Med **352**(24): 2534.

Algeciras-Schimnich, A., L. Shen, et al. (2002). "Molecular ordering of the initial signaling events of CD95." Mol Cell Biol **22**(1): 207-20.

Almond, J. B. and G. M. Cohen (2002). "The proteasome: a novel target for cancer chemotherapy." Leukemia **16**(4): 433-43.

Almond, J. B., R. T. Snowden, et al. (2001). "Proteasome inhibitor-induced apoptosis of B-chronic lymphocytic leukaemia cells involves cytochrome c release and caspase activation, accompanied by formation of an approximately 700 kDa Apaf-1 containing apoptosome complex." Leukemia **15**(9): 1388-97.

Amyere, M., M. Mettlen, et al. (2002). "Origin, originality, functions, subversions and molecular signalling of macropinocytosis." Int J Med Microbiol **291**(6-7): 487-94.

An, J., Y. Sun, et al. (2004). "Maximal apoptosis of renal cell carcinoma by the proteasome inhibitor bortezomib is nuclear factor-kappaB dependent." Mol Cancer Ther **3**(6): 727-36.

Ashkenazi, A. and V. M. Dixit (1999). "Apoptosis control by death and decoy receptors." Curr Opin Cell Biol **11**(2): 255-60.

Ashkenazi, A., R. C. Pai, et al. (1999). "Safety and antitumor activity of recombinant soluble Apo2 ligand." J Clin Invest **104**(2): 155-62.

Austen, B., J. E. Powell, et al. (2005). "Mutations in the ATM gene lead to impaired overall and treatment-free survival that is independent of IGVH mutation status in patients with B-CLL." Blood **106**(9): 3175-82.

Austin, C. D., D. A. Lawrence, et al. (2006). "Death-receptor activation halts clathrin-dependent endocytosis." Proc Natl Acad Sci U S A **103**(27): 10283-8.

Bellosillo, B., N. Villamor, et al. (2002). "Spontaneous and drug-induced apoptosis is mediated by conformational changes of Bax and Bak in B-cell chronic lymphocytic leukemia." Blood **100**(5): 1810-6.

Berenson, J. R., S. Jagannath, et al. (2005). "Safety of prolonged therapy with bortezomib in relapsed or refractory multiple myeloma." Cancer **104**(10): 2141-8.

Binet, J. L., A. Auquier, et al. (1981). "A new prognostic classification of chronic lymphocytic leukemia derived from a multivariate survival analysis." Cancer **48**(1): 198-206.

Bishop, N. E. (2003). "Dynamics of endosomal sorting." Int Rev Cytol **232**: 1-57.

Bogner, C., F. Schneller, et al. (2003). "Cycling B-CLL cells are highly susceptible to inhibition of the proteasome: involvement of p27, early D-type cyclins, Bax, and caspase-dependent and -independent pathways." Exp Hematol **31**(3): 218-25.

Bolden, J. E., M. J. Peart, et al. (2006). "Anticancer activities of histone deacetylase inhibitors." Nat Rev Drug Discov **5**(9): 769-84.

Boldin, M. P., T. M. Goncharov, et al. (1996). "Involvement of MACH, a novel MORT1/FADD-interacting protease, in Fas/APO-1- and TNF receptor-induced cell death." Cell **85**(6): 803-15.

Borle, A. B. and J. Loveday (1968). "Effects of temperature, potassium, and calcium on the electrical potential difference in HeLa cells." Cancer Res **28**(12): 2401-5.

Bottom, K. S., D. M. Adams, et al. (1997). "Trilineage hematopoietic toxicity associated with valproic acid therapy." J Pediatr Hematol Oncol **19**(1): 73-6.

Bradford, M. M. (1976). "A rapid and sensitive method for the quantitation of microgram quantities of protein utilizing the principle of protein-dye binding." Anal Biochem **72**: 248-54.

Brandt, L. (1985). "Environmental factors and leukaemia." Med Oncol Tumor Pharmacother **2**(1): 7-10.

Burger, J. A., N. Tsukada, et al. (2000). "Blood-derived nurse-like cells protect chronic lymphocytic leukemia B cells from spontaneous apoptosis through stromal cell-derived factor-1." Blood **96**(8): 2655-63.

Butler, L. M., V. Liapis, et al. (2006). "The histone deacetylase inhibitor, suberoylanilide hydroxamic acid, overcomes resistance of human breast cancer cells to Apo2L/TRAIL." Int J Cancer **119**(4): 944-54.

Cain, K., D. G. Brown, et al. (1999). "Caspase activation involves the formation of the aposome, a large (approximately 700 kDa) caspase-activating complex." J Biol Chem **274**(32): 22686-92.

Caligaris-Cappio, F. and T. J. Hamblin (1999). "B-cell chronic lymphocytic leukemia: a bird of a different feather." J Clin Oncol **17**(1): 399-408.

Caravita, T., P. de Fabritiis, et al. (2006). "Bortezomib: efficacy comparisons in solid tumors and hematologic malignancies." Nat Clin Pract Oncol **3**(7): 374-87.

Carter, A., K. Lin, et al. (2006). "Imperfect correlation between p53 dysfunction and deletion of TP53 and ATM in chronic lymphocytic leukaemia." Leukemia **20**(4): 737-40.

Cavo, M. (2006). "Proteasome inhibitor bortezomib for the treatment of multiple myeloma." Leukemia **20**(8): 1341-52.

Chan, F. K., H. J. Chun, et al. (2000). "A domain in TNF receptors that mediates ligand-independent receptor assembly and signaling." Science **288**(5475): 2351-4.

Chandra, J., I. Niemer, et al. (1998). "Proteasome inhibitors induce apoptosis in glucocorticoid-resistant chronic lymphocytic leukemic lymphocytes." Blood **92**(11): 4220-9.

Chang, D. W., Z. Xing, et al. (2002). "c-FLIP(L) is a dual function regulator for caspase-8 activation and CD95-mediated apoptosis." Embo J **21**(14): 3704-14.

Chauhan, D., L. Catley, et al. (2005). "A novel orally active proteasome inhibitor induces apoptosis in multiple myeloma cells with mechanisms distinct from Bortezomib." Cancer Cell **8**(5): 407-19.

Chauhan, D., T. Hideshima, et al. (2006). "A novel proteasome inhibitor NPI-0052 as an anticancer therapy." Br J Cancer **95**(8): 961-5.

Chawla-Sarkar, M., S. I. Bae, et al. (2004). "Downregulation of Bcl-2, FLIP or IAPs (XIAP and survivin) by siRNAs sensitizes resistant melanoma cells to Apo2L/TRAIL-induced apoptosis." Cell Death Differ **11**(8): 915-23.

Cheng, Z. J., R. D. Singh, et al. (2006). "Membrane microdomains, caveolae, and caveolar endocytosis of sphingolipids." Mol Membr Biol **23**(1): 101-10.

Cheung, H. H., N. Lynn Kelly, et al. (2006). "Involvement of caspase-2 and caspase-9 in endoplasmic reticulum stress-induced apoptosis: a role for the IAPs." Exp Cell Res **312**(12): 2347-57.

Chim, C. S., G. C. Ooi, et al. (2005). "Side effects and good effects from new chemotherapeutic agents. Case 3. Bortezomib in primary refractory plasmacytoma." J Clin Oncol **23**(10): 2426-8.

Chinnaiyan, A. M., K. O'Rourke, et al. (1996). "Signal transduction by DR3, a death domain-containing receptor related to TNFR-1 and CD95." Science **274**(5289): 990-2.

Chiorazzi, N., K. R. Rai, et al. (2005). "Chronic lymphocytic leukemia." N Engl J Med **352**(8): 804-15.

Ciechanover, A. (2003). "The ubiquitin proteolytic system and pathogenesis of human diseases: a novel platform for mechanism-based drug targeting." Biochem Soc Trans **31**(2): 474-81.

Clancy, L., K. Mruk, et al. (2005). "Preligand assembly domain-mediated ligand-independent association between TRAIL receptor 4 (TR4) and TR2 regulates TRAIL-induced apoptosis." Proc Natl Acad Sci U S A **102**(50): 18099-104.

Collins, R. J., L. A. Verschuer, et al. (1989). "Spontaneous programmed death (apoptosis) of B-chronic lymphocytic leukaemia cells following their culture in vitro." Br J Haematol **71**(3): 343-50.

Creagh, E. M., H. Conroy, et al. (2003). "Caspase-activation pathways in apoptosis and immunity." Immunol Rev **193**: 10-21.

Damke, H., T. Baba, et al. (1994). "Induction of mutant dynamin specifically blocks endocytic coated vesicle formation." J Cell Biol **127**(4): 915-34.

Damle, R. N., T. Wasil, et al. (1999). "Ig V gene mutation status and CD38 expression as novel prognostic indicators in chronic lymphocytic leukemia." Blood **94**(6): 1840-7.

Degli-Esposti, M. A., W. C. Dougall, et al. (1997). "The novel receptor TRAIL-R4 induces NF-kappaB and protects against TRAIL-mediated apoptosis, yet retains an incomplete death domain." Immunity **7**(6): 813-20.

Degli-Esposti, M. A., P. J. Smolak, et al. (1997). "Cloning and characterization of TRAIL-R3, a novel member of the emerging TRAIL receptor family." J Exp Med **186**(7): 1165-70.

Dewson, G., R. T. Snowden, et al. (2003). "Conformational change and mitochondrial translocation of Bax accompany proteasome inhibitor-induced apoptosis of chronic lymphocytic leukemic cells." Oncogene **22**(17): 2643-54.

Di Pietro, R. and G. Zauli (2004). "Emerging non-apoptotic functions of tumor necrosis factor-related apoptosis-inducing ligand (TRAIL)/Apo2L." J Cell Physiol **201**(3): 331-40.

Dohner, H., S. Stilgenbauer, et al. (2000). "Genomic aberrations and survival in chronic lymphocytic leukemia." N Engl J Med **343**(26): 1910-6.

Dreger, P. and E. Montserrat (2002). "Autologous and allogeneic stem cell transplantation for chronic lymphocytic leukemia." Leukemia **16**(6): 985-92.

Duechler, M., M. Shehata, et al. (2005). "Induction of apoptosis by proteasome inhibitors in B-CLL cells is associated with downregulation of CD23 and inactivation of Notch2." Leukemia **19**(2): 260-7.

Duiker, E. W., C. H. Mom, et al. (2006). "The clinical trail of TRAIL." Eur J Cancer **42**(14): 2233-40.

Ehrhardt, H., S. Fulda, et al. (2003). "TRAIL induced survival and proliferation in cancer cells resistant towards TRAIL-induced apoptosis mediated by NF-kappaB." Oncogene **22**(25): 3842-52.

Elter, T., M. Hallek, et al. (2006). "Fludarabine in chronic lymphocytic leukaemia." Expert Opin Pharmacother **7**(12): 1641-51.

Engelhardt, M., A. M. Muller, et al. (2005). "Severe irreversible bilateral hearing loss after bortezomib (VELCADE) therapy in a multiple myeloma (MM) patient." Leukemia **19**(5): 869-70.

Estrov, Z., M. Talpaz, et al. (1998). "Z-138: a new mature B-cell acute lymphoblastic leukemia cell line from a patient with transformed chronic lymphocytic leukemia." Leuk Res **22**(4): 341-53.

Faderl, S., K. Rai, et al. (2006). "Phase II study of single-agent bortezomib for the treatment of patients with fludarabine-refractory B-cell chronic lymphocytic leukemia." Cancer **107**(5): 916-24.

Fadok, V. A., D. L. Bratton, et al. (1998). "The role of phosphatidylserine in recognition of apoptotic cells by phagocytes." Cell Death Differ **5**(7): 551-62.

Feinberg, B., R. Kurzrock, et al. (1988). "A phase I trial of intravenously-administered recombinant tumor necrosis factor-alpha in cancer patients." J Clin Oncol **6**(8): 1328-34.

Fernandez, V., E. Hartmann, et al. (2005). "Pathogenesis of mantle-cell lymphoma: all oncogenic roads lead to dysregulation of cell cycle and DNA damage response pathways." J Clin Oncol **23**(26): 6364-9.

Fiegl, M., A. Falkner, et al. (2006). "Routine clinical use of alemtuzumab in patients with heavily pretreated B-cell chronic lymphocytic leukemia: a nation-wide retrospective study in Austria." Cancer **107**(10): 2408-16.

Flinn, I. W., J. C. Byrd, et al. (2005). "Flavopiridol administered as a 24-hour continuous infusion in chronic lymphocytic leukemia lacks clinical activity." Leuk Res **29**(11): 1253-7.

Fribley, A. and C. Y. Wang (2006). "Proteasome inhibitor induces apoptosis through induction of endoplasmic reticulum stress." Cancer Biol Ther **5**(7): 745-8.

Fribley, A., Q. Zeng, et al. (2004). "Proteasome inhibitor PS-341 induces apoptosis through induction of endoplasmic reticulum stress-reactive oxygen species in head and neck squamous cell carcinoma cells." Mol Cell Biol **24**(22): 9695-704.

Fribley, A. M., B. Evenchik, et al. (2006). "Proteasome inhibitor PS-341 induces apoptosis in cisplatin-resistant squamous cell carcinoma cells by induction of Noxa." J Biol Chem **281**(42): 31440-7.

Fuentes-Prior, P. and G. S. Salvesen (2004). "The protein structures that shape caspase activity, specificity, activation and inhibition." Biochem J **384**(Pt 2): 201-32.

Fulda, S. and K. M. Debatin (2006). "Extrinsic versus intrinsic apoptosis pathways in anticancer chemotherapy." Oncogene **25**(34): 4798-811.

Ganten, T. M., R. Koschny, et al. (2006). "Preclinical differentiation between apparently safe and potentially hepatotoxic applications of TRAIL either alone or in combination with chemotherapeutic drugs." Clin Cancer Res **12**(8): 2640-6.

Gaur, U. and B. B. Aggarwal (2003). "Regulation of proliferation, survival and apoptosis by members of the TNF superfamily." Biochem Pharmacol **66**(8): 1403-8.

Georgakis, G. V., Y. Li, et al. (2005). "Activity of selective fully human agonistic antibodies to the TRAIL death receptors TRAIL-R1 and TRAIL-R2 in primary and cultured lymphoma cells: induction of apoptosis and enhancement of doxorubicin- and bortezomib-induced cell death." Br J Haematol **130**(4): 501-10.

Gillespie, S., J. Borrow, et al. (2006). "Bim plays a crucial role in synergistic induction of apoptosis by the histone deacetylase inhibitor SBHA and TRAIL in melanoma cells." Apoptosis **11**(12): 2251-65.

Glebov, O. O., N. A. Bright, et al. (2006). "Flotillin-1 defines a clathrin-independent endocytic pathway in mammalian cells." Nat Cell Biol **8**(1): 46-54.

Glickman, M. H. and A. Ciechanover (2002). "The ubiquitin-proteasome proteolytic pathway: destruction for the sake of construction." Physiol Rev **82**(2): 373-428.

Goy, A., A. Younes, et al. (2005). "Phase II study of proteasome inhibitor bortezomib in relapsed or refractory B-cell non-Hodgkin's lymphoma." J Clin Oncol **23**(4): 667-75.

Green, D. R. (2005). "Apoptotic pathways: ten minutes to dead." Cell **121**(5): 671-4.

Griffith, T. S., C. T. Rauch, et al. (1999). "Functional analysis of TRAIL receptors using monoclonal antibodies." J Immunol **162**(5): 2597-605.

Gupta, S., A. Pagliuca, et al. (2006). "Life-threatening motor neurotoxicity in association with bortezomib." Haematologica **91**(7): 1001.

Hamblin, T. (2002). "Is chronic lymphocytic leukemia one disease?" Haematologica **87**(12): 1235-8.

Han, D. K., P. M. Chaudhary, et al. (1997). "MRIT, a novel death-effector domain-containing protein, interacts with caspases and BclXL and initiates cell death." Proc Natl Acad Sci U S A **94**(21): 11333-8.

Hanada, M., D. Delia, et al. (1993). "bcl-2 gene hypomethylation and high-level expression in B-cell chronic lymphocytic leukemia." Blood **82**(6): 1820-8.

Harper, N., S. N. Farrow, et al. (2001). "Modulation of tumor necrosis factor apoptosis-inducing ligand- induced NF-kappa B activation by inhibition of apical caspases." J Biol Chem **276**(37): 34743-52.

Hehlgans, T. and K. Pfeffer (2005). "The intriguing biology of the tumour necrosis factor/tumour necrosis factor receptor superfamily: players, rules and the games." Immunology **115**(1): 1-20.

Held, J. and K. Schulze-Osthoff (2001). "Potential and caveats of TRAIL in cancer therapy." Drug Resist Updat **4**(4): 243-52.

Hitomi, J., T. Katayama, et al. (2004). "Involvement of caspase-4 in endoplasmic reticulum stress-induced apoptosis and Abeta-induced cell death." J Cell Biol **165**(3): 347-56.

Hu, S., C. Vincenz, et al. (1997). "I-FLICE, a novel inhibitor of tumor necrosis factor receptor-1- and CD-95-induced apoptosis." J Biol Chem **272**(28): 17255-7.

Hymowitz, S. G., H. W. Christinger, et al. (1999). "Triggering cell death: the crystal structure of Apo2L/TRAIL in a complex with death receptor 5." Mol Cell **4**(4): 563-71.

Hymowitz, S. G., M. P. O'Connell, et al. (2000). "A unique zinc-binding site revealed by a high-resolution X-ray structure of homotrimeric Apo2L/TRAIL." Biochemistry **39**(4): 633-40.

Ichikawa, K., W. Liu, et al. (2003). "TRAIL-R2 (DR5) mediates apoptosis of synovial fibroblasts in rheumatoid arthritis." J Immunol **171**(2): 1061-9.

Inoue, S., M. MacFarlane, et al. (2004). "Histone deacetylase inhibitors potentiate TNF-related apoptosis-inducing ligand (TRAIL)-induced apoptosis in lymphoid malignancies." Cell Death Differ **11 Suppl 2**: S193-206.

Inoue, S., A. Mai, et al. (2006). "Inhibition of histone deacetylase class I but not class II is critical for the sensitization of leukemic cells to tumor necrosis factor-related apoptosis-inducing ligand-induced apoptosis." Cancer Res **66**(13): 6785-92.

Inoue, S., R. T. Snowden, et al. (2004). "CDDO induces apoptosis via the intrinsic pathway in lymphoid cells." Leukemia **18**(5): 948-52.

Inoue, S., D. Twiddy, et al. (2006). "Upregulation of TRAIL-R2 is not involved in HDACi mediated sensitization to TRAIL-induced apoptosis." Cell Death Differ **13**(12): 2160-2.

Irmler, M., M. Thome, et al. (1997). "Inhibition of death receptor signals by cellular FLIP." Nature **388**(6638): 190-5.

Jackson, G., H. Einsele, et al. (2005). "Bortezomib, a novel proteasome inhibitor, in the treatment of hematologic malignancies." Cancer Treat Rev **31**(8): 591-602.

Jahrsdorfer, B., J. E. Wooldridge, et al. (2005). "Good prognosis cytogenetics in B-cell chronic lymphocytic leukemia is associated in vitro with low susceptibility to apoptosis and enhanced immunogenicity." Leukemia **19**(5): 759-66.

Jaskiewicz, A. D., J. D. Herrington, et al. (2005). "Tumor lysis syndrome after bortezomib therapy for plasma cell leukemia." Pharmacotherapy **25**(12): 1820-5.

Jeremias, I., C. Kupatt, et al. (1998). "Inhibition of nuclear factor kappaB activation attenuates apoptosis resistance in lymphoid cells." Blood **91**(12): 4624-31.

Jewell, A. P., P. M. Lydyard, et al. (1995). "Growth factors can protect B-chronic lymphocytic leukaemia cells against programmed cell death without stimulating proliferation." Leuk Lymphoma **18**(1-2): 159-62.

Jo, M., T. H. Kim, et al. (2000). "Apoptosis induced in normal human hepatocytes by tumor necrosis factor-related apoptosis-inducing ligand." Nat Med **6**(5): 564-7.

Johnston, J. B., A. F. Kabore, et al. (2003). "Role of the TRAIL/APO2-L death receptors in chlorambucil- and fludarabine-induced apoptosis in chronic lymphocytic leukemia." Oncogene **22**(51): 8356-69.

Jones, D. T., K. Ganeshaguru, et al. (2003). "Albumin activates the AKT signaling pathway and protects B-chronic lymphocytic leukemia cells from chlorambucil- and radiation-induced apoptosis." Blood **101**(8): 3174-80.

Kabore, A. F., J. Sun, et al. (2006). "The TRAIL apoptotic pathway mediates proteasome inhibitor induced apoptosis in primary chronic lymphocytic leukemia cells." Apoptosis **11**(7): 1175-93.

Kane, R. C., A. T. Farrell, et al. (2006). "United States Food and Drug Administration approval summary: bortezomib for the treatment of progressive multiple myeloma after one prior therapy." Clin Cancer Res **12**(10): 2955-60.

Keating, M. J., S. O'Brien, et al. (2005). "Early results of a chemoimmunotherapy regimen of fludarabine, cyclophosphamide, and rituximab as initial therapy for chronic lymphocytic leukemia." J Clin Oncol **23**(18): 4079-88.

Kelley, R. F., K. Totpal, et al. (2005). "Receptor-selective mutants of apoptosis-inducing ligand 2/tumor necrosis factor-related apoptosis-inducing ligand reveal a greater contribution of death receptor (DR) 5 than DR4 to apoptosis signaling." J Biol Chem **280**(3): 2205-12.

Kelley, S. K., L. A. Harris, et al. (2001). "Preclinical studies to predict the disposition of Apo2L/tumor necrosis factor-related apoptosis-inducing ligand in humans: characterization of in vivo efficacy, pharmacokinetics, and safety." J Pharmacol Exp Ther **299**(1): 31-8.

Kelley, T. W., S. Alkan, et al. (2004). "Treatment of human chronic lymphocytic leukemia cells with the proteasome inhibitor bortezomib promotes apoptosis." Leuk Res **28**(8): 845-50.

Kerr, J. F., A. H. Wyllie, et al. (1972). "Apoptosis: a basic biological phenomenon with wide-ranging implications in tissue kinetics." Br J Cancer **26**(4): 239-57.

Keutgens, A., I. Robert, et al. (2006). "Deregulated NF-kappaB activity in haematological malignancies." Biochem Pharmacol **72**(9): 1069-80.

Kim, Y., N. Suh, et al. (2002). "An inducible pathway for degradation of FLIP protein sensitizes tumor cells to TRAIL-induced apoptosis." J Biol Chem **277**(25): 22320-9.

Kipps, T. J. (2000). "Chronic lymphocytic leukemia." Curr Opin Hematol **7**(4): 223-34.

Kirkham, M. and R. G. Parton (2005). "Clathrin-independent endocytosis: new insights into caveolae and non-caveolar lipid raft carriers." Biochim Biophys Acta **1745**(3): 273-86.

Kischkel, F. C., S. Hellbardt, et al. (1995). "Cytotoxicity-dependent APO-1 (Fas/CD95)-associated proteins form a death-inducing signaling complex (DISC) with the receptor." Embo J **14**(22): 5579-88.

Kischkel, F. C., D. A. Lawrence, et al. (2000). "Apo2L/TRAIL-dependent recruitment of endogenous FADD and caspase-8 to death receptors 4 and 5." Immunity **12**(6): 611-20.

Kitada, S. and J. C. Reed (2004). "MCL-1 promoter insertions dial-up aggressiveness of chronic leukemia." J Natl Cancer Inst **96**(9): 642-3.

Klein, G., B. Giovanella, et al. (1975). "An EBV-genome-negative cell line established from an American Burkitt lymphoma; receptor characteristics. EBV infectibility and permanent conversion into EBV-positive sublines by in vitro infection." Intervirology **5**(6): 319-34.

Knoops, L., A. Jacquemain, et al. (2005). "Bortezomib-induced Sweet syndrome." Br J Haematol **131**(2): 142.

Kostova, Z. and D. H. Wolf (2003). "For whom the bell tolls: protein quality control of the endoplasmic reticulum and the ubiquitin-proteasome connection." Embo J **22**(10): 2309-17.

Kovalenko, A. and D. Wallach (2006). "If the prophet does not come to the mountain: dynamics of signaling complexes in NF-kappaB activation." Mol Cell **22**(4): 433-6.

Krober, A., T. Seiler, et al. (2002). "V(H) mutation status, CD38 expression level, genomic aberrations, and survival in chronic lymphocytic leukemia." Blood **100**(4): 1410-6.

Kurbanov, B. M., C. C. Geilen, et al. (2005). "Efficient TRAIL-R1/DR4-mediated apoptosis in melanoma cells by tumor necrosis factor-related apoptosis-inducing ligand (TRAIL)." J Invest Dermatol **125**(5): 1010-9.

Lawrence, D., Z. Shahrokh, et al. (2001). "Differential hepatocyte toxicity of recombinant Apo2L/TRAIL versions." Nat Med **7**(4): 383-5.

Le Borgne, R., A. Bardin, et al. (2005). "The roles of receptor and ligand endocytosis in regulating Notch signaling." Development **132**(8): 1751-62.

LeBlanc, H., D. Lawrence, et al. (2002). "Tumor-cell resistance to death receptor--induced apoptosis through mutational inactivation of the proapoptotic Bcl-2 homolog Bax." Nat Med **8**(3): 274-81.

Lee, K. H., C. Feig, et al. (2006). "The role of receptor internalization in CD95 signaling." Embo J **25**(5): 1009-23.

Li, P., D. Nijhawan, et al. (1997). "Cytochrome c and dATP-dependent formation of Apaf-1/caspase-9 complex initiates an apoptotic protease cascade." Cell **91**(4): 479-89.

Lonial, S., E. K. Waller, et al. (2005). "Risk factors and kinetics of thrombocytopenia associated with bortezomib for relapsed, refractory multiple myeloma." Blood **106**(12): 3777-84.

Lozzio, B. B. and C. B. Lozzio (1977). "Properties of the K562 cell line derived from a patient with chronic myeloid leukemia." Int J Cancer **19**(1): 136.

Ludwig, D. L., D. S. Pereira, et al. (2003). "Monoclonal antibody therapeutics and apoptosis." Oncogene **22**(56): 9097-106.

Luo, J. L., H. Kamata, et al. (2005). "IKK/NF-kappaB signaling: balancing life and death--a new approach to cancer therapy." J Clin Invest **115**(10): 2625-32.

MacFarlane, M., M. Ahmad, et al. (1997). "Identification and molecular cloning of two novel receptors for the cytotoxic ligand TRAIL." J Biol Chem **272**(41): 25417-20.

MacFarlane, M., N. Harper, et al. (2002). "Mechanisms of resistance to TRAIL-induced apoptosis in primary B cell chronic lymphocytic leukaemia." Oncogene **21**(44): 6809-18.

Marsden, V. S. and A. Strasser (2003). "Control of apoptosis in the immune system: Bcl-2, BH3-only proteins and more." Annu Rev Immunol **21**: 71-105.

Masdehors, P., H. Merle-Beral, et al. (2000). "Deregulation of the ubiquitin system and p53 proteolysis modify the apoptotic response in B-CLL lymphocytes." Blood **96**(1): 269-74.

Masdehors, P., S. Omura, et al. (1999). "Increased sensitivity of CLL-derived lymphocytes to apoptotic death activation by the proteasome-specific inhibitor lactacystin." Br J Haematol **105**(3): 752-7.

Medema, J. P., C. Scaffidi, et al. (1997). "FLICE is activated by association with the CD95 death-inducing signaling complex (DISC)." Embo J **16**(10): 2794-804.

Menezes, J., W. Leibold, et al. (1975). "Establishment and characterization of an Epstein-Barr virus (EBC)-negative lymphoblastoid B cell line (BJA-B) from an exceptional, EBV-genome-negative African Burkitt's lymphoma." Biomedicine **22**(4): 276-84.

Menoret, E., P. Gomez-Bougie, et al. (2006). "Mcl-1L cleavage is involved in TRAIL-R1- and TRAIL-R2-mediated apoptosis induced by HGS-ETR1 and HGS-ETR2 human mAbs in myeloma cells." Blood **108**(4): 1346-52.

Merup, M., G. Juliusson, et al. (1997). "Amplification of multiple regions of chromosome 12, including 12q13-15, in chronic lymphocytic leukaemia." Eur J Haematol **58**(3): 174-80.

Mirandola, P., I. Sponzilli, et al. (2006). "Anticancer agents sensitize osteosarcoma cells to TNF-related apoptosis-inducing ligand downmodulating IAP family proteins." Int J Oncol **28**(1): 127-33.

Mitsiades, C. S., N. Mitsiades, et al. (2006). "Proteasome inhibition as a new therapeutic principle in hematological malignancies." Curr Drug Targets **7**(10): 1341-7.

Miyakoshi, S., M. Kami, et al. (2006). "Severe pulmonary complications in Japanese patients after bortezomib treatment for refractory multiple myeloma." Blood **107**(9): 3492-4.

Mori, E., M. Thomas, et al. (2004). "Human normal hepatocytes are susceptible to apoptosis signal mediated by both TRAIL-R1 and TRAIL-R2." Cell Death Differ **11**(2): 203-7.

Mousavi, S. A., L. Malerod, et al. (2004). "Clathrin-dependent endocytosis." Biochem J **377**(Pt 1): 1-16.

Muzio, M., A. M. Chinnaiyan, et al. (1996). "FLICE, a novel FADD-homologous ICE/CED-3-like protease, is recruited to the CD95 (Fas/APO-1) death--inducing signaling complex." Cell **85**(6): 817-27.

Nawrocki, S. T., J. S. Carew, et al. (2005). "Bortezomib inhibits PKR-like endoplasmic reticulum (ER) kinase and induces apoptosis via ER stress in human pancreatic cancer cells." Cancer Res **65**(24): 11510-9.

Nesterov, A., R. E. Carter, et al. (1999). "Inhibition of the receptor-binding function of clathrin adaptor protein AP-2 by dominant-negative mutant mu2 subunit and its effects on endocytosis." Embo J **18**(9): 2489-99.

Neuzil, J., E. Swettenham, et al. (2004). "Sensitization of mesothelioma to TRAIL apoptosis by inhibition of histone deacetylase: role of Bcl-xL down-regulation." Biochem Biophys Res Commun **314**(1): 186-91.

Nicholson, D. W. (1999). "Caspase structure, proteolytic substrates, and function during apoptotic cell death." Cell Death Differ **6**(11): 1028-42.

Nikrad, M., T. Johnson, et al. (2005). "The proteasome inhibitor bortezomib sensitizes cells to killing by death receptor ligand TRAIL via BH3-only proteins Bik and Bim." Mol Cancer Ther 4(3): 443-9.

O'Connor, O. A. (2005). "Marked clinical activity of the proteasome inhibitor bortezomib in patients with follicular and mantle-cell lymphoma." Clin Lymphoma Myeloma 6(3): 191-9.

O'Connor, O. A., J. Wright, et al. (2005). "Phase II clinical experience with the novel proteasome inhibitor bortezomib in patients with indolent non-Hodgkin's lymphoma and mantle cell lymphoma." J Clin Oncol **23**(4): 676-84.

Obeng, E. A., L. M. Carlson, et al. (2006). "Proteasome inhibitors induce a terminal unfolded protein response in multiple myeloma cells." Blood **107**(12): 4907-16.

Ogasawara, J., R. Watanabe-Fukunaga, et al. (1993). "Lethal effect of the anti-Fas antibody in mice." Nature **364**(6440): 806-9.

Orth, J. D., E. W. Krueger, et al. (2006). "A novel endocytic mechanism of epidermal growth factor receptor sequestration and internalization." Cancer Res **66**(7): 3603-10.

Oscier, D. G., A. C. Gardiner, et al. (2002). "Multivariate analysis of prognostic factors in CLL: clinical stage, IGVH gene mutational status, and loss or mutation of the p53 gene are independent prognostic factors." Blood **100**(4): 1177-84.

Pacifico, F. and A. Leonardi (2006). "NF-kappaB in solid tumors." Biochem Pharmacol **72**(9): 1142-52.

Packham, G. and F. K. Stevenson (2005). "Bodyguards and assassins: Bcl-2 family proteins and apoptosis control in chronic lymphocytic leukaemia." Immunology **114**(4): 441-9.

Pahler, J. C., S. Ruiz, et al. (2003). "Effects of the proteasome inhibitor, bortezomib, on apoptosis in isolated lymphocytes obtained from patients with chronic lymphocytic leukemia." Clin Cancer Res 9(12): 4570-7.

Pai, S. I., G. S. Wu, et al. (1998). "Rare loss-of-function mutation of a death receptor gene in head and neck cancer." Cancer Res **58**(16): 3513-8.

Pan, G., J. Ni, et al. (1997). "An antagonist decoy receptor and a death domain-containing receptor for TRAIL." Science **277**(5327): 815-8.

Pan, G., K. O'Rourke, et al. (1997). "The receptor for the cytotoxic ligand TRAIL." Science **276**(5309): 111-3.

Panayiotidis, P., D. Jones, et al. (1996). "Human bone marrow stromal cells prevent apoptosis and support the survival of chronic lymphocytic leukaemia cells in vitro." Br J Haematol **92**(1): 97-103.

Pedersen, I. M., S. Kitada, et al. (2002). "Protection of CLL B cells by a follicular dendritic cell line is dependent on induction of Mcl-1." Blood **100**(5): 1795-801.

Perez-Galan, P., G. Roue, et al. (2006). "The proteasome inhibitor bortezomib induces apoptosis in mantle-cell lymphoma through generation of ROS and Noxa activation independent of p53 status." Blood **107**(1): 257-64.

Peter, M. E., P. Legembre, et al. (2005). "Does CD95 have tumor promoting activities?" Biochim Biophys Acta **1755**(1): 25-36.

Pitti, R. M., S. A. Marsters, et al. (1996). "Induction of apoptosis by Apo-2 ligand, a new member of the tumor necrosis factor cytokine family." J Biol Chem **271**(22): 12687-90.

Polo, S. and P. P. Di Fiore (2006). "*Endocytosis conducts the cell signaling orchestra.*" Cell **124**(5): 897-900.

Popat, R., S. Joel, et al. (2006). "Bortezomib for multiple myeloma." Expert Opin Pharmacother **7**(10): 1337-46.

Pour, L., R. Hajek, et al. (2005). "Skin lesions induced by bortezomib." Haematologica **90**(12 Suppl): ECR44.

Pukac, L., P. Kanakaraj, et al. (2005). "HGS-ETR1, a fully human TRAIL-receptor 1 monoclonal antibody, induces cell death in multiple tumour types in vitro and in vivo." Br J Cancer **92**(8): 1430-41.

Qin, J. Z., J. Ziffra, et al. (2005). "Proteasome inhibitors trigger NOXA-mediated apoptosis in melanoma and myeloma cells." Cancer Res **65**(14): 6282-93.

Rai, K. R. and E. Montserrat (1987). "Prognostic factors in chronic lymphocytic leukemia." Semin Hematol **24**(4): 252-6.

Richardson, P. G., B. Barlogie, et al. (2005). "Clinical factors predictive of outcome with bortezomib in patients with relapsed, refractory multiple myeloma." Blood **106**(9): 2977-81.

Richardson, P. G., H. Briemberg, et al. (2006). "Frequency, characteristics, and reversibility of peripheral neuropathy during treatment of advanced multiple myeloma with bortezomib." J Clin Oncol **24**(19): 3113-20.

Richardson, P. G., C. Mitsiades, et al. (2006). "Bortezomib: proteasome inhibition as an effective anticancer therapy." Annu Rev Med **57**: 33-47.

Rosenwald, A., A. A. Alizadeh, et al. (2001). "Relation of gene expression phenotype to immunoglobulin mutation genotype in B cell chronic lymphocytic leukemia." J Exp Med **194**(11): 1639-47.

Rowe, M., C. M. Rooney, et al. (1985). "Distinctions between endemic and sporadic forms of Epstein-Barr virus-positive Burkitt's lymphoma." Int J Cancer **35**(4): 435-41.

Rudek, M. A., K. S. Bauer, Jr., et al. (2003). "Clinical pharmacology of flavopiridol following a 72-hour continuous infusion." Ann Pharmacother **37**(10): 1369-74.

Ruiz, S., Y. Krupnik, et al. (2006). "The proteasome inhibitor NPI-0052 is a more effective inducer of apoptosis than bortezomib in lymphocytes from patients with chronic lymphocytic leukemia." Mol Cancer Ther **5**(7): 1836-43.

Sartorius, U., I. Schmitz, et al. (2001). "Molecular mechanisms of death-receptor-mediated apoptosis." Chembiochem **2**(1): 20-9.

Scaffidi, C., I. Schmitz, et al. (1999). "Differential modulation of apoptosis sensitivity in CD95 type I and type II cells." J Biol Chem **274**(32): 22532-8.

Schmid, C. and P. G. Isaacson (1994). "Proliferation centres in B-cell malignant lymphoma, lymphocytic (B-CLL): an immunophenotypic study." Histopathology **24**(5): 445-51.

Schneider-Brachert, W., V. Tchikov, et al. (2004). "Compartmentalization of TNF receptor 1 signaling: internalized TNF receptosomes as death signaling vesicles." Immunity **21**(3): 415-28.

Schwartz, A. L. and A. Ciechanover (1999). "The ubiquitin-proteasome pathway and pathogenesis of human diseases." Annu Rev Med **50**: 57-74.

Sellick, G. S., D. Catovsky, et al. (2006). "Familial chronic lymphocytic leukemia." Semin Oncol **33**(2): 195-201.

Shah, M. H., P. Binkley, et al. (2006). "Cardiotoxicity of histone deacetylase inhibitor depsipeptide in patients with metastatic neuroendocrine tumors." Clin Cancer Res **12**(13): 3997-4003.

Shankar, S., T. R. Singh, et al. (2005). "Interactive effects of histone deacetylase inhibitors and TRAIL on apoptosis in human leukemia cells: involvement of both death receptor and mitochondrial pathways." Int J Mol Med **16**(6): 1125-38.

Shaw, A. S. (2006). "Lipid rafts: now you see them, now you don't." Nat Immunol **7**(11): 1139-42.

Sheridan, J. P., S. A. Marsters, et al. (1997). "Control of TRAIL-induced apoptosis by a family of signaling and decoy receptors." Science **277**(5327): 818-21.

Shi, G., V. Faundez, et al. (1998). "Neuroendocrine synaptic vesicles are formed in vitro by both clathrin-dependent and clathrin-independent pathways." J Cell Biol **143**(4): 947-55.

Shi, Y. (2006). "Mechanical aspects of apoptosome assembly." Curr Opin Cell Biol **18**(6): 677-84.

Shin, M. S., H. S. Kim, et al. (2001). "Mutations of tumor necrosis factor-related apoptosis-inducing ligand receptor 1 (TRAIL-R1) and receptor 2 (TRAIL-R2) genes in metastatic breast cancers." Cancer Res **61**(13): 4942-6.

Shu, H. B., D. R. Halpin, et al. (1997). "Casper is a FADD- and caspase-related inducer of apoptosis." Immunity **6**(6): 751-63.

Sigismund, S., T. Woelk, et al. (2005). "Clathrin-independent endocytosis of ubiquitinated cargos." Proc Natl Acad Sci U S A **102**(8): 2760-5.

Slee, E. A., M. T. Harte, et al. (1999). "Ordering the cytochrome c-initiated caspase cascade: hierarchical activation of caspases-2, -3, -6, -7, -8, and -10 in a caspase-9-dependent manner." J Cell Biol **144**(2): 281-92.

Sprick, M. R., M. A. Weigand, et al. (2000). "FADD/MORT1 and caspase-8 are recruited to TRAIL receptors 1 and 2 and are essential for apoptosis mediated by TRAIL receptor 2." Immunity **12**(6): 599-609.

Srinivasula, S. M., M. Ahmad, et al. (1997). "FLAME-1, a novel FADD-like anti-apoptotic molecule that regulates Fas/TNFR1-induced apoptosis." J Biol Chem **272**(30): 18542-5.

Starostik, P., T. Manshouri, et al. (1998). "Deficiency of the ATM protein expression defines an aggressive subgroup of B-cell chronic lymphocytic leukemia." Cancer Res **58**(20): 4552-7.

Starostik, P., S. O'Brien, et al. (1999). "The prognostic significance of 13q14 deletions in chronic lymphocytic leukemia." Leuk Res **23**(9): 795-801.

Strater, J., U. Hinz, et al. (2002). "Expression of TRAIL and TRAIL receptors in colon carcinoma: TRAIL-R1 is an independent prognostic parameter." Clin Cancer Res **8**(12): 3734-40.

Stubblefield, M. D., S. Slovin, et al. (2006). "An electrodiagnostic evaluation of the effect of pre-existing peripheral nervous system disorders in patients treated with the novel proteasome inhibitor bortezomib." Clin Oncol (R Coll Radiol) **18**(5): 410-8.

Sunwoo, J. B., Z. Chen, et al. (2001). "Novel proteasome inhibitor PS-341 inhibits activation of nuclear factor-kappa B, cell survival, tumor growth, and angiogenesis in squamous cell carcinoma." Clin Cancer Res 7(5): 1419-28.

Takei, K., V. Haucke, et al. (1998). "Generation of coated intermediates of clathrin-mediated endocytosis on protein-free liposomes." Cell 94(1): 131-41.

Takei, K., Y. Yoshida, et al. (2005). "Regulatory mechanisms of dynamin-dependent endocytosis." J Biochem (Tokyo) 137(3): 243-7.

Thomas, L. R., A. Henson, et al. (2004). "Direct binding of Fas-associated death domain (FADD) to the tumor necrosis factor-related apoptosis-inducing ligand receptor DR5 is regulated by the death effector domain of FADD." J Biol Chem 279(31): 32780-5.

Truneh, A., S. Sharma, et al. (2000). "Temperature-sensitive differential affinity of TRAIL for its receptors. DR5 is the highest affinity receptor." J Biol Chem 275(30): 23319-25.

Tsubuki, S., Y. Saito, et al. (1996). "Differential inhibition of calpain and proteasome activities by peptidyl aldehydes of di-leucine and tri-leucine." J Biochem (Tokyo) 119(3): 572-6.

Tsukada, N., J. A. Burger, et al. (2002). "Distinctive features of "nurselike" cells that differentiate in the context of chronic lymphocytic leukemia." Blood 99(3): 1030-7.

van der Sloot, A. M., V. Tur, et al. (2006). "Designed tumor necrosis factor-related apoptosis-inducing ligand variants initiating apoptosis exclusively via the DR5 receptor." Proc Natl Acad Sci U S A 103(23): 8634-9.

Van Regenmortel, N., K. Van de Voorde, et al. (2005). "Bortezomib-induced Sweet's syndrome." Haematologica 90(12 Suppl): ECR43.

Vanoosten, R. L., J. M. Moore, et al. (2005). "Depsipeptide (FR901228) enhances the cytotoxic activity of TRAIL by redistributing TRAIL receptor to membrane lipid rafts." Mol Ther 11(4): 542-52.

Varfolomeev, E., H. Maecker, et al. (2005). "Molecular determinants of kinase pathway activation by Apo2 ligand/tumor necrosis factor-related apoptosis-inducing ligand." J Biol Chem 280(49): 40599-608.

Vermes, I., C. Haanen, et al. (1995). "A novel assay for apoptosis. Flow cytometric detection of phosphatidylserine expression on early apoptotic cells using fluorescein labelled Annexin V." J Immunol Methods 184(1): 39-51.

Voorhees, P. M., E. C. Dees, et al. (2003). "The proteasome as a target for cancer therapy." Clin Cancer Res **9**(17): 6316-25.

Voortman, J. and G. Giaccone (2006). "Severe reversible cardiac failure after bortezomib treatment combined with chemotherapy in a non-small cell lung cancer patient: a case report." BMC Cancer **6**: 129.

Wagner, K. W., F. King, et al. (2003). "Activation and suppression of the TRAIL death-receptor pathway in chemotherapy sensitive and resistant follicular lymphoma cells." Cancer Biol Ther **2**(5): 534-40.

Walczak, H., M. A. Degli-Esposti, et al. (1997). "TRAIL-R2: a novel apoptosis-mediating receptor for TRAIL." Embo J **16**(17): 5386-97.

Walczak, H., R. E. Miller, et al. (1999). "Tumoricidal activity of tumor necrosis factor-related apoptosis-inducing ligand in vivo." Nat Med **5**(2): 157-63.

Wallach, D., E. E. Varfolomeev, et al. (1999). "Tumor necrosis factor receptor and Fas signaling mechanisms." Annu Rev Immunol **17**: 331-67.

Wang, Y., I. H. Engels, et al. (2004). "Synthetic lethal targeting of MYC by activation of the DR5 death receptor pathway." Cancer Cell **5**(5): 501-12.

Waterhouse, N. J., J. E. Ricci, et al. (2002). "And all of a sudden it's over: mitochondrial outer-membrane permeabilization in apoptosis." Biochimie **84**(2-3): 113-21.

Weiss, A., R. L. Wiskocil, et al. (1984). "The role of T3 surface molecules in the activation of human T cells: a two-stimulus requirement for IL 2 production reflects events occurring at a pre-translational level." J Immunol **133**(1): 123-8.

Wiestner, A., A. Rosenwald, et al. (2003). "ZAP-70 expression identifies a chronic lymphocytic leukemia subtype with unmutated immunoglobulin genes, inferior clinical outcome, and distinct gene expression profile." Blood **101**(12): 4944-51.

Wiley, S. R., K. Schooley, et al. (1995). "Identification and characterization of a new member of the TNF family that induces apoptosis." Immunity **3**(6): 673-82.

Willis, S. N. and J. M. Adams (2005). "Life in the balance: how BH3-only proteins induce apoptosis." Curr Opin Cell Biol **17**(6): 617-25.

Willis, S. N., L. Chen, et al. (2005). "Proapoptotic Bak is sequestered by Mcl-1 and Bcl-xL, but not Bcl-2, until displaced by BH3-only proteins." Genes Dev **19**(11): 1294-305.

Wu, K. L., W. van Wieringen, et al. (2005). "Analysis of the efficacy and toxicity of bortezomib for treatment of relapsed or refractory multiple myeloma in community practice." Haematologica **90**(7): 996-7.

References

Wyllie, A. H., J. F. Kerr, et al. (1972). "Cellular events in the adrenal cortex following ACTH deprivation." J Pathol **106**(1): Pix.

Yao, C. P., G. G. Mather, et al. (1999). "Cytotoxicity induced by the combination of valproic acid and tumor necrosis factor-alpha: implication for valproic acid-associated hepatotoxicity syndrome." Biochem Pharmacol **58**(3): 455-9.

Yuan, J., S. Shaham, et al. (1993). "The C. elegans cell death gene ced-3 encodes a protein similar to mammalian interleukin-1 beta-converting enzyme." Cell **75**(4): 641-52.

Yuille, M. R., E. Matutes, et al. (2000). "Familial chronic lymphocytic leukaemia: a survey and review of published studies." Br J Haematol **109**(4): 794-9.

Zaccara, G., A. Messori, et al. (1988). "Clinical pharmacokinetics of valproic acid--1988." Clin Pharmacokinet **15**(6): 367-89.

Zeng, Y., X. X. Wu, et al. (2006). "Monoclonal antibody to tumor necrosis factor-related apoptosis-inducing ligand receptor 2 (TRAIL-R2) induces apoptosis in primary renal cell carcinoma cells in vitro and inhibits tumor growth in vivo." Int J Oncol **28**(2): 421-30.

Zheng, B., G. V. Georgakis, et al. (2004). "Induction of cell cycle arrest and apoptosis by the proteasome inhibitor PS-341 in Hodgkin disease cell lines is independent of inhibitor of nuclear factor-kappaB mutations or activation of the CD30, CD40, and RANK receptors." Clin Cancer Res **10**(9): 3207-15.

Zhu, H., L. Zhang, et al. (2005). "Bik/NBK accumulation correlates with apoptosis-induction by bortezomib (PS-341, Velcade) and other proteasome inhibitors." Oncogene **24**(31): 4993-9.

Zou, H., Y. Li, et al. (1999). "An APAF-1.cytochrome c multimeric complex is a functional apoptosome that activates procaspase-9." J Biol Chem **274**(17): 11549-56.

Publications arising from this work

Kohlhaas, S.L., A. Craxton, et al."Receptor-mediated endocytosis in not required for TRIAL-induced apoptosis." Submitted to Journal of Biological Chemistry Jan 2007

MacFarlane, M., S. Inoue, et al. (2005). "Chronic lymphocytic leukemic cells exhibit apoptotic signaling via TRAIL-R1." Cell Death Differ **12**(7): 773-82.

MacFarlane, M., S. L. Kohlhaas, et al. (2005). "TRAIL receptor-selective mutants signal to apoptosis via TRAIL-R1 in primary lymphoid malignancies." Cancer Res **65**(24): 11265-70.

Wheat, L. M., S. L. Kohlhaas, et al. (2006). "Inhibition of bortezomib-induced apoptosis by red blood cell uptake." Leukemia **20**(9): 1646-9.

Presentations of this work

Kohlhaas S.L., L. M. C. Wheat, J. Monbaliu, R. De Coster, G. M. Cohen and M. J. S. Dyer. "Inhibition of Bortezomib-induced Apoptosis induction in Chronic Lymphocytic Leukemia by Red Blood Cell uptake" *Abstract and poster presentation at the 5th European Workshop on Cell Death* May 2006

Susan L. Kohlhaas, Marion MacFarlane, Satoshi Inoue, Mike Sutcliffe, Martin J. S. Dyer, Gerald M. Cohen
Shortlisted for the CLL Forum Young Investigators Prize, November 2006
Gave a 10 minute presentation
Submitted and abstract entitled
"TRAIL therapy of CLL: Induction of apoptosis through TRAIL-R1 but not TRAIL-R2"